Institut für Nutzpflanzenwissenschaften und Ressourcenschutz (INRES)

Nachwachsende Rohstoffe

---

# Phenotypic evaluation of wild *Silphium perfoliatum* L. accessions to create a breeding basis for material use

**Dissertation**

zur Erlangung des Grades

Doktor der Agrarwissenschaften (Dr. agr.)

der Landwirtschafltichen Fakultät

der Rheinischen Friedrich-Wilhelms-Universität Bonn

von

Christoph Anton Conrad Korte

aus

Bückeburg

Bonn, 2024

Referent: Prof. Dr. Ralf Pude

Korreferent: Prof. Dr. Annaliese Mason

Tag der mündlichen Prüfung: 28.10.2024

Angefertigt mit Genehmigung der Landwirtschaftlichen Fakultät der Universität Bonn

# Abstract

Cup plant (*Silphium perfoliatum* L.) is a promising herbaceous perennial for biomass production. In Germany, *S. perfoliatum* is mainly grown as a substrate for biogas reactors. Aside from the plant being useful for generating energy, interest in material use of the plant is increasing, especially regarding harvesting biomass at a late stage. Recent studies have shown that harvesting perennials during the growing season lowers their nutrient use efficiencies. The past few years have seen optimization of cup plant cultivation, such as crop establishment by sowing and yield improvements through crop management (plant density, fertilization level and plant protection), with the aim of making cup plant suitable for practical use and maximizing yield and quality of biomass. However, the biomass production of cup plant still cannot completely keep up with that of its competitors. There are several publications declaring a need for breeding improvements of *S. perfoliatum*. Due to the limited variation in the available plant material only a few studies mention actual breeding intentions. To increase the available variations in *S. perfoliatum,* seeds of wild plants were collected from its natural habitat. This collection and the material use of late harvested *Silphium* biomass are the foundation of this thesis. The new *Silphium* collection expands the variation of plant material available in Europe in nearly all phenotype plant traits. In most cases this expansion is directed towards more and less trait expression. The recorded plant traits include dry matter yields, yield- and quality-determining traits (plant height, shoot width, shoot number, flowering progress, cellulose and lignin content as well as lodging), *Sclerotinia* susceptibility, seed yield traits (seed number per flower head and seed weight), seed geometric traits (achene area, achene length, achene width and achene eccentricity) and seed oil traits (oil content, portions of the fatty acids 14:0, 16:0, 18:0, 18:1 and 18:2). In addition, the collection of wild *Silphium* accessions revealed previously unknown differences in cup formation, which were investigated too. In terms of biomass production, several wild accessions already outperform the available plant material in Europe. Through selection, further yield improvements are expected. Long-term breeding goals may include increased quality of biomass, pathogen resistances, achene size and cup formation (impact of cup formation on the crop still needs to be determined). Moreover, a BBCH-scale was generated, allowing for the detection of developmental stages as a plant trait and to set standards in plant breeding and crop management. Furthermore, new material use of senescent harvested biomass and of seed oil have been investigated, such as using milled cup plant biomass as an additive for paper production and as a substitute in bonded leveling compound. Both applications offer a sustainable alternative to conventional methods. *Silphium* oil needs modifications to fit material purposes, but these modifications should be accessible through plant breeding.

# Zusammenfassung

Die Durchwachsene Silphie (*Silphium perfoliatum* L.) ist ein vielversprechende mehrjährige Biomassepflanze. In Deutschland wird *S. perfoliatum* hauptsächlich als Substrat für Biogasanlagen angebaut. Neben der energetischen Nutzung, steigt auch das Interesse an seneszent geernteter Biomasse zur stofflichen Nutzung. In den letzten Jahren wurde der Anbau von *S. perfoliatum*, unter anderem durch Entwicklung eines Aussatverfahrens, Verbesserung der Erträge sowie der Bestandsführung optimiert. Bislang erreicht die Durchwachsene Silphie jedoch nicht das Ertragsniveau herkömmlicher Biomassepflanzen. Die Notwendigkeit der züchterischen Verbesserung von *S. perfoliatum* wird in aktuellen Studien thematisiert. Im Gegensatz dazu, werden nur in wenigen Veröffentlichungen tatsächliche Züchtungsabsichten erwähnt. Der Grund hierfür ist die begrenzte Vielfalt des verfügbaren Pflanzenmaterials. Um die Vielfalt im verfügbaren Pflanzenmaterial zu erhöhen, wurden Samen wilder *S. perfoliatum*-Populationen im natürlichen Verbreitungsgebiet gesammelt. Diese Sammlung und die stoffliche Nutzung seneszenter Biomasse sind die Grundlage dieser Arbeit. Die neue *Silphium*-Sammlung erweitert die Variationen des in Europa verfügbaren Pflanzenmaterials in fast allen phänotypischen Eigenschaften. Zu den erfassten Pflanzenmerkmalen gehören Trockenmasseerträge, Biomassequalität (Cellulose- und Ligningehalt), Ertragsstrukturparameter (Wuchshöhe, Triebbreite, Triebanzahl, Blütefortschritt und Lageranfälligkeit), *Sclerotinia*-Suszeptibilität, Samenertragsmerkmale (Samenanzahl und Samengewicht), Samengeometriemerkmale (Achänenfläche, Achänenlänge, Achänenbreite und Exzentrizität) und Samenölmerkmale (Ölgehalt und Fettsäuremuster). Des Weiteren wurden in der neuen Sammlung von *Silphium*-Akzessionen bislang unbekannte Unterschiede in der Ausprägung der charakteristischen Becher festgestellt und erfasst. In Bezug auf die Biomasseproduktion übertreffen bereits mehrere Akzessionen aus dem natürlichen Verbreitungsgebiet die Erträge des in Europa verfügbaren Pflanzenmaterials. Durch Selektion sind weitere Ertragssteigerungen zu erwarten. Langfristige Zuchtziele können eine höhere Biomassequalität, Resistenzen gegen Krankheitserreger, die Größe der Achäne und die Becherausprägung sein. Zusätzlich wurde eine BBCH-Skala entwickelt, mit dessen Hilfe Entwicklungsstadien als Pflanzenmerkmal erfassbar werden. Zudem trägt sie zur Standardisierung weiterer Arbeiten bei. Darüber hinaus wurden stoffliche Verwendungsmöglichkeiten von seneszent geernteter *Silphium*-Biomasse sowie des Samenöls untersucht. Die Verwendung der Biomasse als Additiv bei der Papierherstellung sowie die Verwendung als Substitut für Styropor bieten nachhaltige Alternativen zu herkömmlichen Methoden. Wohingegen das Öl ungeeignet zur Anwendung ist. Modifikationen des Öls sollten allerdings durch Pflanzenzüchtung möglich sein.

# Contents

# List of Publications

2023

Greve, M., **Korte, C. A. C.**, Entrup, J., Altrogge, H., Bischoff, P., Elfers, J., Wever, C., & Pude, R. (2023). Evaluation of the Intra- and Interspecific Development of Different Accessions of *Silphium perfoliatum* L. and *Silphium integrifolium* Michx. *Agronomy*, *13*(6). https://doi.org/10.3390/agronomy13061601

2022

Moll, L., Höller, M., Hubert, C., **Korte, C. A. C.**, Völkering, G., Wever, C., & Pude, R. (2022). Cup Plant (*Silphium perfoliatum* L.) Biomass as Substitute for Expanded Polystyrene in Bonded Leveling Compounds. *Agronomy*, *12*(1). https://doi.org/10.3390/agronomy12010178

2020

**Korte, C. A. C.**, Wever, C., Greve, M., Elfers, J., Völkering, G., Becker, L., Höller, M., Westhoff, P., Pestsova, E., Pude, R. (2020). Laying a cornerstone for cup plant breeding – agriculturally evaluation of native *Silphium* populations. Poster Presentation. Digital Breeding: International Symposium of the Society for Plant Breeding e.V. (GPZ). 11–13 February 2020. Tulln, Austria.

# List of Figures

# List of Tables

# List of Abbreviations

| | |
|---|---|
| % | Percent |
| °C | Degree Celsius |
| µl | Microliter(s) |
| µm | Micrometer(s) |
| 14:0 | Myristic acid |
| 15:0 | Pentadecanoic acid |
| 16:0 | Palmitic acid |
| 18:0 | Stearic acid |
| 18:1 | Oleic acid |
| 18:2 | Linoleic acid |
| AA | Achene area |
| AIR | Alcohol-insoluble residue |
| AL | Achene length |
| AW | Achene width |
| BLC | Bonded leveling compound |
| cm | Centimeter(s) |
| $CO_2$ | Carbon dioxide |
| CP | Cup plant |
| DAS | Days after sowing |
| DM | Dry matter |
| DMY | Dry matter yield |
| EPS | Expanded polystyrene |
| FAME | Fatty acid methyl ester |
| FeMax | Length according to Feret |
| FeMin | Width according to Feret |
| FP1 | Flowering progress mid-July |
| FP2 | Flowering progress mid/end-August |
| g | Gram(s); G-force (chapter 5.2.3) |
| GA3 | Gibberellic acid |

| | |
|---|---|
| GC-FID | Gas-chromatograph with flame ionization detector |
| h | Hour(s) |
| $H_2O$ | Water |
| ha | Hectare(s) |
| HCL | Hydrochloric acid |
| Hz | Hertz |
| K | Kelvin |
| kV | Kilovolt(s) |
| L | Liter(s) |
| LS | Lodging susceptibility |
| m | Meter(s) |
| M | Molarity |
| Mg | Megagram(s) |
| mg | Milligram(s) |
| min | Minute(s) |
| ml | Milliliter(s) |
| mm | Millimeter(s) |
| mW | Milliwatt(s) |
| N | Nitrogen (chapter 6); Newton (chapter 7) |
| n | Sample size |
| NaCl | Sodium chloride |
| NaOH | Sodium hydroxide |
| OC | Oil content |
| Pa | Pascal |
| PC | Principal Component |
| PCA | Principal Component Analysis |
| PDA | Potato dextrose agar |
| PDB | Potato dextrose broth |
| PH | plant height |
| Q | Aggregate size as cumulative share |
| r | Correlation coefficient |

| | |
|---|---|
| RNLA | Relative necrotic leaf area |
| s | Second(s) |
| SEM | Scanning electron microscopy |
| SHN | Shoot number |
| SHW | Shoot width |
| Sii | *Silphium integrifolium* from the western part of the natural range |
| Sil | *Silphium integrifolium* from the southern part of the natural range |
| SN | Seed number per flower head |
| SPHT | Sphericity index |
| SPN | *Silphium pefoliatum* accession from the northern part of the natural range |
| SPS | *Silphium pefoliatum* accession from the southern part of the natural range |
| SW | Seed weight per flower head |
| TLL | Thüringer Landesanstalt für Landwirtschaft |
| TLLLR | Thüringer Landesanstalt für Landwirtschaft und Ländlichen Raum |
| v/v | Volume/volume percent |
| vol% | Volume percent |
| $V_{tot}$ | total volume |
| w/c | Water cement ratio |
| w/l | Width to length ratio |
| wt% | Weight percent |
| Xarea | Radius of an equivalent circle |
| y | Year(s) |

# 1 General Introduction

As plant biomass is one of the few sustainable carbon stocks, it is part of the solution of substituting fossil carbon resources. It can be used for energy production or material applications. The production of energy releases the carbon previously bound in the plants, whereas material use of plant biomass allows withholding the carbon in the product during its lifespan. Further increase in sustainability might be addressed to plant biomass production. Cultivating perennials has been proven to have a better ratio of input to output energy, due to omitted annual soil preparations and sowing of new crops, as well as better nutrient use efficiencies, due to extensive root systems (Crews et al., 2018; Ruf & Emmerling, 2021). Beyond that, diversity in the agricultural landscape lets each crop contribute to ecosystem services and fill ecological niches (Werling et al., 2014). There are various species that fit these requirements (Wever et al., 2020), one of which being cup plant (*Silphium perfoliatum* L.).

Cup plant is a perennial member of the Asteraceae family and a close relative to sunflower (*Helianthus annuus* L.; Clevinger und Panero, 2000). *S. perfoliatum* is native to North America and mostly found in the central and eastern USA as well as eastern Canada (USDA Plants Database, 2024). In the first year of cultivation, cup plant forms a soilborne rosette with 12–14 leaves. In the subsequent years, *S. perfoliatum* develops quadrangular shoots with heights up to 3 m due to vernalization of the rhizome. At each node, a leaf pair is set up. Both petioles are grown together with leaf surface surrounding the whole node, forming the cups around the shoot to which the plant owes its name. During the flowering period (July–September), new buds and flower heads are set up continuously in further blooming orders. Each flower head has a diameter of 4–8 cm and consists of male tubular florets and female ligulate ray florets (summarized in Gansberger et al., 2015; Peni et al., 2020). They produce 20–30 grains with a thousand seed weight of 15–23 g, an achene length of 9–15 mm an achene width of 6–9 mm and a thickness of 1–2 mm (Schäfer et al., 2017; Assefa et al., 2015; Gansberger, 2016; summarized in Stanford, 1990).

In the 1930s and 40s, *Silphium perfoliatum* (and other species of the genus) were recognized for their variety of stress tolerances (summarized in Van Tassel et al., 2017). First agricultural publications about cup plant suggest that had been under investigation in Russia as a forage crop since 1957 (summarized in Stanford, 1990). Today, several thousand hectares in Central Europe are dedicated to growing the cup plant for biomass purposes (around 10,000 hectares in Germany alone; FNR, 2023). In practical agriculture, *Silphium perfoliatum* is sown directly on the field (Schäfer et al., 2016), mostly in intercropping systems with maize (*Zea mays* L.), in order to overcome the lack of biomass in the first year of cultivation due to the non-yielding rosette that *Silphium* forms (Biertümpfel et al., 2018). For the next 15 years, cup plant is the only crop on the field, producing dry matter yields that can exceed 20 Mg per hectare (summarized in Gansberger et al., 2015; Peni et al., 2020). The biomass is harvested between August and September, at which time it contains 25–27 % of dry matter, making it favorable for ensiling (Biertümpfel et al., 2013). Aside from its yield, *Silphium* has a number of ecological benefits and ecosystem services: a long flowering period (July–September) while producing pollen and nectar, no requirements of soil preparation due to 10–15 years as period of use and an extensive regenerative root system, having positive effects on water and nutrient absorption, on $CO_2$ sequestration, on soil erosion as well as on pollinators and ground-dwelling fauna (summarized in Gansberger et al., 2015; Peni et al., 2020).

There is only little information about current cup plant breeding successes available in the literature. The findings of Wever et al. (2019) may explain this lack of breeding activities. Five cup plant accessions of different breeders in Europe, Russia and USA were investigated, but after a genetical analysis only one of these accessions formed its own clade in between the other accessions. This indicates generally low genetic variation of plant material between breeders that might be the result of an early bottleneck. To make more variation accessible and to thus lay a cornerstone for cup plant breeding, a plant hunting trip through the native range of *S. perfoliatum* was performed, where seeds of wild plants were collected (Wever et al., 2019; Van Tassel et al., 2017). The first establishment of these accessions in a field trial was in 2017 at Campus Klein-Altendorf, near Bonn, Germany. This field trial is the basis for data collection of this work. Results of the enhanced *Silphium perfoliatum* collection are found in Chapter 2–5. In Chapter 2, dry matter yields of both the summer and winter harvest as well as cellulose and lignin contents are investigated. Until today, cup plant cannot keep up with its competitors concerning dry matter yield as well as biomass quality (Wever et al., 2019; summarized in Gansberger et al., 2015; Peni et al., 2020). Yield improvements are needed to close this yield gap and to keep up with further breeding successes. The same applies to the quality of biomass. The morphological plant traits plant height, shoot width, shoot number, flowering progress and lodging are analyzed in chapter 3. These are meaningful to uncover possible correlations to each other and thus to identify the ideotype of cup plant as a biomass crop. Additionally, after discovering previously unknown differences in the wild *Silphium* collection, the cup formation was investigated, including the creation and application of a cup formation scale, as well as phenotyping the leaves to develop a data base for leave traits of *Silphium perfoliatum*. Chapter 4 contains the results of a first screening for *Sclerotinia* susceptibility. *Sclerotinia* spp. are the main pathogens in European *Silphium* cultivation. In order to stop a *Sclerotinia* infestation and prevent further spread and formation of the so-called sclerotia, it is recommended to immediately harvest the biomass (Biertümpfel et al., 2018). There are no registered pesticides against any pathogen for *Silphium*. What is more, due to its growth height, cup plant fields are not accessible for large scale pesticide applications. To secure yield stability and biomass quality, increasing the resistance of cup plant against pathogens is indispensable. Chapter 5 provides and investigation of seed yield traits, seed geometric traits and seed oil traits. As has been the case for most of the crops, seed sizes are increasing through domestication (Fuller, 2007). It has already been shown that achene size has an effect on emergence rates and vigor of cup plant seedlings (Assefa et al., 2015; Schäfer et al., 2018). Furthermore, achene shapes have been reported to affect the singling process in seeders (Schäfer et al., 2018). In this regard, an analysis of achene area, achene length, achene width, eccentricity (measure of circularity), seeds per flower head and seed weight is provided in chapter 5. In addition, these traits, as well as oil content and portion of myristic acid (14:0), palmitic acid (16:0), stearic acid (18:0), oleic acid (18:1) and linoleic acid (18:2) were investigated to assess the potential of cup plant as an oil crop. Currently, several working groups in North and South America are involved in silflower (*Silphium integrifolium* Michx.) breeding. Silflower is one of the closest relatives of cup plant and is considered to become an oil crop in the future (Clevinger & Panero, 2000; Van Tassel et al., 2017, Vilela et al., 2018; Reinert et al., 2019). As for cup plant, a collection of wild *S. integrifoilum* accessions is available for this purpose. Through shared experiences and results as well as the fact that interspecific hybrids of *S. integrifolium* and *S. perfoliatum* are fertile, breeding programs of each species can benefit from each other (Reinert et al., 2020b). In general, cup plant is further away from being an oil crop than being a biomass crop. In any case, interest in oil of *S. perfoliatum* is justified by possible favorable properties for silflower breeding.

The main use of cup plant biomass in Germany is as a substrate for biogas reactors. Interest is growing in dual usage of silage *Silphium* since a procedure has been presented that allows to extract the fibers of the biomass before using it as an energy source. For this, fibers are extracted out of the biomass using steam explosion. The fibers can then be used in the pulp and paper industry (Neis-Beeckmann, 2021). In addition, pharmaceutical applications are described (Lunze, 2021). All mentioned uses can be performed with green biomass harvested in summer, but cup plant can be harvested in winter as well. Senescent harvested biomass has already been used for chemical pulping, making it into a possible feedstock for the paper industry (Höller et al., 2021). In this thesis, milled late harvested biomass of *Silphium perfoliatum* was used as an additive for pulp for the first time (chapter 2). In comparison to chemical pulping, *Silphium* as an additive is more cost and energy efficient, but might lower paper quality. Later harvests in general are more nutrient efficient while offering new properties of the biomass (Ruf & Emmerling, 2021; Höller, 2022).

Specifically, the parenchyma becomes similar to expanded polystyrene. Chapter 7 contains a report of using cup plant biomass as a substitute for expanded polystyrene in bonded leveling compound. Additionally, the oil of cup plant was analyzed for its potential material application as a platform chemical in the future (chapter 5).

The aim of this thesis is to assess and evaluate the variation between the newly gathered wild *Silphium perfoliatum* accessions and the previously available plant material in Europe (from now on referred to as European accessions) to guide future breeding activities. This is accomplished by analyzing phenotypic data of wild and European accessions in field trials of several years. Furthermore, harvested biomass and collected seeds from these trials were used for further experiments in the lab and greenhouse (chapter 2–5). Phenotypic data were used to create a valuable BBCH-scale that describes the developmental stages of cup plant and silflower (chapter 6). Additionally, new ways for cup plant biomass use were performed and analyzed to increase the sustainability of products and the potential for value stability of cup plant biomass as well as to formulate further breeding goals (chapter 2, 5 and 7). The results of all experiments are part of this cumulative thesis as six publications and manuscripts (chapter 2–7). To reach the previously mentioned aims the following research questions have been addressed:

I Does the new collection of wild *Silphium perfoliatum* L. accessions expands the diversity of the available European plant material?

II Is the new collection of wild *Silphium perfoliatum* L. accessions suitable for upcoming plant breeding programs?

III Can *Silphium perfoliatum* biomass harvested in winter be utilized for material use?

# 2 Harnessing natural variation in *Silphium perfoliatum* L. accessions as a resource to enhance biomass quality and quantity for paper production

This manuscript has been submitted to the journal “Industrial Crops and Products” and is currently under review:

**Christoph A. C. Korte**, Niklas Frase, Christian Wever, Martin Greve, Martin Höller, Murali Dama, Jasmin Denise Mombeck, Markus Pauly and Ralf Pude (2024). Harnessing natural variation in *Silphium perfoliatum* L. accessions as a resource to enhance biomass quality and quantity for paper production. Unpublished manuscript.

## 2.1 Introduction

Current forecasts for paper demand indicate that paper consumption will increase in the coming decades (Lamberg et al., 2012). For paper production, cellulose fibers out of lignocellulosic biomass are needed. The lignocellulosic biomass mainly consists of cellulose, hemicelluloses and lignin, which are separated by pulping processes (Pauly & Keegstra, 2008; Taherzadeh & Karimi, 2008; Kumar et al., 2009). There are different pulping processes (e.g. thermo-chemical pulping, mechanical pulping), mainly varying in cost and energy requirements as well as the quality of the resulting pulp (Biermann, 1993). Furthermore, mechanically processed biomass can be used as a filler material for paper, as described in patent EP 2 825 699 B1 “Faserstoffzusammensetzung” (D’Agnone, 2016).

The most valuable resource of lignocellulosic biomass are trees. However, as deforestation causes ecological damage and supply bottlenecks, non-wooden fibrous resources present a paper and pulp feedstock alternative (Kamoga et al., 2013). Straw as a former alternative pulp resource, was introduced into the industry in 1802 (Franklin Inst., 1835). Current promising non-wood paper and pulp feedstock plants are perennial biomass plants like Virginia mallow (*Ripariosida hermaphrodita* (L.) Weakley & D. B. Poind), flax (*Linum usitatissimum* L.), hemp (*Cannabis sativa* L.), meadow grass (several members of the *Poaceae*) and the species analyzed in this study, cup plant (*Silphium perfoliatum* L.; Höller et al., 2021; Kamoga et al., 2013; Medvedev, 1940; Mejouyo et al., 2020).

The genus *Silphium* contains two species, that have a high potential to become crops in the future after a domestication process (Van Tassel et al., 2017). The genus belongs to the *Asteraceae* family and is closely related to the well-known sunflower (*Helianthus annuus (*L.); Clevinger & Panero, 2000). Beside silflower (*Silphium integrifolium* Michx.) mainly investigated in north and south America as an oilseed crop, cup plant (*Silphium perfoliatum* L.) is a promising candidate for sustainable biomass production (Van Tassel et al., 2017; Vilela et al., 2018; Wever et al., 2020). In Central Europe, the cultivation of cup plants for biomass has already started on several thousend hectares, for example in Germany on around 10.000 ha (FNR, 2023) have been grown mainly as a substitute for energy maize (*Zea mays* L.). In agricultural practice, *Silphium perfoliatum* is sown directly on the field (Schäfer et al., 2016). In the first year of cultivation the plants form a soilborne rosette without noticable biomass yield (Greve et al., 2023; summarized in Gansberger et al. and 2015 Peni et al., 2020). In the subsequent maximum of 15 years biomass is harvested between August and September, when dry matter (DM) contents of 25–27 % are favorable (Biertümpfel et al., 2018). The reported biomass yield is heterogeneous and can exceed 20 Mg dry matter per ha and is mainly used as substrate for biogas plants or livestock feed (summarized in Gansberger et al., 2015; Peni et al., 2020). However, a process has been developed, whereby silage *Silphium* fibers are extracted prior to utilizing the remainder of the biomass as an energy source (Neis-Beeckmann, 2021). In addition, senescent cup plant biomass can be used for material applications such as pulp and paper production (Höller et al., 2021) or as a substitute for expanded polystyrene (Moll et al., 2022). Later harvests of *Silphium* are always accompanied by lower dry matter yields but might show better nutrient use efficiencies (Ruf & Emmerling 2021; Ruf & Emmerling 2022). Besides yield, the ecological benefits of *Silphium* are a long flowering period (July–September) while producing pollen and nectar, no annual soil preparation, lack of seeding or planting due to a 10–15 years growth phase as a perennial plant, an extensive regrowing root system, which has a positive effect on water and nutrient use efficiencies but also on $CO_2$ sequestration (summarized in Gansberger et al., 2015; Peni et al., 2020; Pimentel et al., 1997; Ruf & Emmerling, 2021). Furthermore, perennials can have an improved ratio of input to output energy while producing similar yields compared to annual crops (Crews et al., 2018; Glover et al., 2010). The combination of perenniality, ecological benefits, comparable yields to common biomass crops and the possibility of using the biomass for feedstock and fuel applications, makes the *Silphium* a promising candidate for becoming a 3rd generation biomass crop in the future (Wever et al., 2020).

The yield heterogeneity of *Silphium perfoliatum* has been described. Most of the heterogeneity in the field and between sites can be explained by the unbred plant population, but a certain amount of the diversity between different plant working groups might occur because different populations of *Silphium* were cultivated. Until today it is uncommon in the literature to provide closer information about the origins of the investigated cu plant material. Wever et al. (2019) analyzed the circulating gene material in Europe, which shows low genetic variance. Only one population from Ukraine showed a larger genetic distance to the other analyzed populations, maybe caused selection processes during breeding attempts in the former Soviet Union. Nevertheless, the plant material available in Europe seems to share a common ancestry. This leads to the assumption that the European accessions originate from the same geographical location (Wever et al., 2019).

To increase the available genetic and phenotypic variation and to get access to the full potential of *Silphium* as a future crop, for new populations across the natural distribution area of *S. perfoliatum* in North America were collected. These populations were cultivated and evaluated for four years in a field trial in Germany (2017–2020). The impact of this genetic resource on quality and quantity of cup plant yield, as well as on quality of biomass for further processing steps, more precisely on paper production was assessed. Furthermore, awareness of the importance of providing closer information about *Silphium* genotypes in future studies should be created.

## 2.2 Material and Methods

### 2.2.1 Plant material

Figure 2.1 and table 2.1 show all accessions used in this study. The wild accessions gathered on a collecting trip in 2016 in the USA cover the natural distribution area of *S. perfoliatum*. These accessions (prefix “SP”) are marked with a black dot on the map (fig. 2.1). The used accession for this study is a part of the whole collection and covers especially the edges of the natural distribution of *Silphium perfoliatum* (fig. 2.1). The seeds from the collection were gathered from open pollinated autochthon populations with a population size of a minimum of 12 individuals. Within the study, only populations from sites with several known herbarium specimens for decades were used. The aim was to gather only wild populations and not plant genotypes from renaturalization programs. Naturally, the obtained seed amounts varied for each population, so that not all populations were included in the field trials. Due to their unknown origin, the currently circulating plant material in Europe (prefix “TLL”; from now on referred to as European accessions) is displayed outside the map (fig. 2.1). This plant material was gathered by the Thüringer Landesanstalt für Landwirtschaft (TLL); Wever et al., 2019). For seed propagation of the European accessions the plants were pollinated by hand with pollen true to each accession and protected against cross pollination by insects. The seeds of the European accessions consisted of populations of 12 individuals for each accession. For seed production, pollen was collected from all individuals of the accession and mixed before pollination.

### 2.2.2 Field trial

The field trial was established in 2017 at *Campus* Klein-Altendorf near Bonn, Germany (Lat: 50.615684, Long: 6.985003). The dominant soil type was haplic luvisol. Long-term mean annual air temperature and precipitation amount were 9.5 °C and 606 mm. The plants for the experimental site were pre-cultivated in the greenhouse for 12 weeks with temperatures between 6–25 °C. Afterwards, the plantlets were planted on 5 and 6 July 2017. The plantlets were irrigated on the day of planting and one week later to support plant establishment. Weed control was carried out manually and mechanically as necessary. The field trial had a randomized block design with three replications. Each plot contained four rows of nine plants. The row distance was 0.5 m and the plant distance within the row was 0.65 m. Resulting to a plot size of 7.8 m² and a plant density of 3.1 plants per m². To avoid border effects the inner two rows without their first and last plants of each plot were used for data collection.

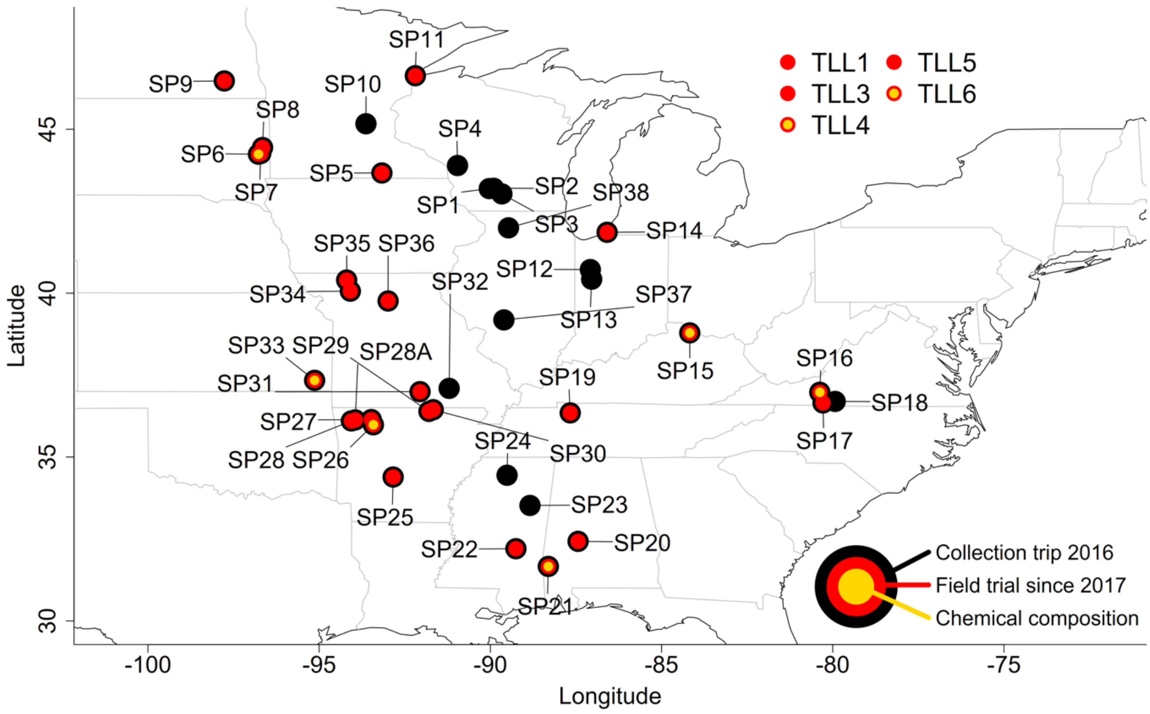

**Figure 2.1: Used accession for yield and biomass analysis. Map of location sites of collected *Silphium perfoliatum* accessions (SP1–SP38) during the collecting trip in the United States of America in 2016, as well as the European plant material (TLL1, TLL3 –TLL6), which are displayed outside the map, because of unknown origination in the natural distribution area. The collection sites are located at roughly equal distances along the borders of the native distribution area in North America. The big black dots mark the collection sites. The medium sized red dots indicate accession which have been established in a field trial at Campus Klein-Altendorf, near Bonn, Germany since 2017. The small yellow dots show populations whose chemical composition was analyzed.**

**Table 2.1: List of available accessions of *Silphium perfoliatum*, their geographic origin in the United States of America and usage for this study.**

| Accession | State | County | Field trial (since 2017) | Chemical Composition |
|---|---|---|---|---|
| SP1 | Wisconsin | Sauk | | |
| SP2 | Wisconsin | Iowa | | |
| SP3 | Wisconsin | Dane | | |
| SP4 | Wisconsin | La Crosse | | |
| SP5 | Minnesota | Freeborn | X | |
| SP6 | South Dakota | Brookings | X | X |
| SP7 | South Dakota | Brookings | X | |
| SP8 | South Dakota | Brookings | X | |
| SP9 | North Dakota | Ransom | X | |
| SP10 | Minnesota | Hennepin | | |
| SP11 | Wisconsin | Douglas | X | |
| SP12 | Indiana | White | | |
| SP13 | Indiana | Tippecanoe | | |
| SP14 | Michigan | Berrien | X | |
| SP15 | Kentucky | Bracken | X | X |
| SP16 | Virginia | Floyd | X | X |
| SP17 | Virginia | Patrick | X | |
| SP18 | Virginia | Henry | | |
| SP19 | Tennessee | Houston | X | |
| SP20 | Alabama | Perry | X | |
| SP21 | Alabama | Washington | X | X |
| SP22 | Mississippi | Jasper | X | |

| Accession | State | County | Field trial (since 2017) | Chemical Composition |
|---|---|---|---|---|
| SP23 | Mississippi | Oktibbeha | | |
| SP24 | Mississippi | Lafayette | | |
| SP25 | Arkansas | Hot Spring | X | |
| SP26 | Arkansas | Newton | X | X |
| SP27 | Arkansas | Carroll | X | |
| SP28 | Arkansas | Washington | X | |
| SP28A | Arkansas | Washington | X | |
| SP29 | Arkansas | Fulton | X | |
| SP30 | Arkansas | Fulton | X | |
| SP31 | Missouri | Howell | X | |
| SP32 | Missouri | Shannon | | |
| SP33 | Kansas | Labette | X | X |
| SP34 | Missouri | Daviess | X | |
| SP35 | Missouri | Harrison | X | |
| SP36 | Missouri | Linn | X | |
| SP37 | Illinois | Montgomery | | |
| SP38 | Illinois | Ogle | | |
| TLL1 | - | - | X | |
| TLL3 | - | - | X | |
| TLL4 | - | - | X | X |
| TLL5 | - | - | X | |
| TLL6 | - | - | X | X |

-: Origination in the native distribution area unknown for the European plant material. X: Accession used for experiment.

### 2.2.3 Biomass yield determination

Due to the plant's rossette-stage during the first year, harvesting of the *Silphium* plants started in 2018 and was replicated annually until 2020. 31 accessions in total, with 26 accessions of the *Silphium* collecting trip and 5 accessions of the European plant material were analyzed (fig. 2.1; tab. 2.1). Two harvests were performed each year. One harvest took place in summer, during the flowering time of most accessions (August/September) and the other one in winter during the plant's dormant stage (November/December). Two plants of each repetition were analyzed at every harvest, resulting in six harvested plants in summer and six harvested plants in winter (except for the winter harvest of 2018, where four plants from each repetition were harvested). For fresh-matter analysis, all shoots of one plant were cut manually at ground level and weighed as a whole. Afterwards, three representative shoots were chosen, for dry matter analysis. The shoots were separated from the leaves and cut into smaller pieces. After that, shoot pieces and leaves were put in a crisp-pac bag each and weighed again. The samples were dried in a drying oven (Venticell, Model 707) at 105 °C until constant weight was reached and weighed again.

### 2.2.4 Grinding and sieving of the raw materials of the winter harvest

The main process steps were grinding/fibrillation and sieving. The raw materials were ground with a cutting mill (Retsch, SM 300). The chosen screen size of the mill was a 1 mm triangle hole recommended by Gil and Arauzo (2014) for a target size of 1 mm for woody and herbaceous plants. According to Blechschmidt et al., 2013, the biomass will consist of fibers, shives and fines after grinding. To boost the pulp quality by increasing the fiber proportion, a sorting and cleaning column (Haldrup, DC-20) was used, dividing biomass in different fractions using air flow. Since the biomass yield of one single plant sample was too low for paper production, the samples of both harvested plants per repetition were mixed.

### 2.2.5 Biomass analysis

*Silphium* internode samples were dried at 50 ˚C until a constant weight was reached. The dried samples were cut into small pieces and ground to powder in a Retsch PM 100 ball mill for 5 minutes at 30 Hz, using 10 ml grinding jars. The alcohol-insoluble residue (AIR) of the *Silphium* biomass was prepared following the method outlined by Jablonowski et al. (2022). Briefly, the pulverized material was washed with 70 % aqueous ethanol, followed by a wash with methanol and chloroform (1:1, v/v) to receive AIR. The obtained lignocellulosic AIR material underwent de-starching by dissolving it with a combination of α-amylase and pullulanase (Sigma-Aldrich). The crystalline cellulose content in the de-starched AIR material was determined as described by Forster et al. (2010b). Briefly, this involved treating the plant material (2 mg) with the Updegraff reagent and discarding the resulting supernatant. The resulting dried pellet was then subjected to a treatment with 72 % aqueous sulfuric acid (Seaman hydrolysis), as per the approach outlined by Saeman et al. (1954). The glucose resulting from the acid hydrolysis was quantified using the anthrone assay. The lignin content of the de-starched AIR material was assessed through the acetyl bromide soluble lignin technique as outlined (Foster et al., 2010a). Briefly, de-starched AIR (1 mg) underwent treatment with a freshly prepared acetyl bromide solution (25 %, v/v, acetyl bromide in glacial acetic acid) at 50 °C for 3 hours. Following neutralization with 2 M NaOH and hydroxylamine hydrochloride, the lignin content was determined by measuring absorbance at 280 nm using a plate reader (SpectraMax® Plus 384 instrument). Kraft-Lignin (0.1–0.6 mg) sourced from Sigma-Aldrich served as the standard.

### 2.2.6 Pulping, paper production and paper testing

Round hand-sheets with a grammage of 80 g/m² and a diameter of 200 mm were produced using a Rapid-Köthen apparatus (Frank-PTI, S95854), according to ISO 5269-1 (2005). The raw material batches were chosen based on their cellulose and lignin content. Three samples with a medium amount of lignin, but differences in cellulose content (tab. 2.2; “High Cellulose”, “Medium Cellulose”, “Low Cellulose”) were chosen, as well as two samples with a medium amount of cellulose, but differences in lignin content (tab. 2.2; “High Lignin”, “Low Lignin”). The resulting paper blends had shares of 75 % pine pulp and 25 % *Silphium* biomass. Hand-sheets of 100 % pine pulp served as control. Before testing, hand-sheets were conditioned for 24 h at 23 °C and 50 % relative humidity according to ISO 187 (1990). Paper thickness according to DIN EN ISO 12625-3 (2014) was determined using Universal Micrometer (FRANK-PTI, S16502) on nine points on each sheet. The first point was located in the center of the sheets, the remaining eight were equally distributed on the sample between the center and the border. Furthermore, tensile index, breaking strain and breaking length according to ISO 12625-4 (2016) were obtained using a Universal Tester Vertical (Frank-PTI, S81838). For this test, one hand-sheet was cut in four samples. Five hand sheets of each batch were analyzed, resulting in 45 measurements of thickness and 11–15 measurements with the universal tester vertical, due to DIN EN ISO 12625-3 (2014), which invalidated some of the measurements. Three more hand-sheets of High Cellulose were analyzed, because samples had a higher rate of invalid measurements at the Universal Tester Vertical (tab. 2.2).

**Table 2.2: Sample description for paper production. Showing the *Silphium* accession used, its chemical composition (cellulose and lignin), its share in the produced paper and sample sizes for the paper tests.**

| | Sample origin | | | Content (µg/mg) | | Share (%) | | Sample size | |
|---|---|---|---|---|---|---|---|---|---|
| | Accession | Repetition number in the field | Year of harvest | Cellulose | Lignin | Pine pulp | *Silphium* biomass | Universal Micrometer | Universal Tester Vertical |
| Control | | | | | | 100 | 0 | 45 | 13 |
| High Cellulose | SP6 | 3 | 2019 | 464.49 | 228.63 | 75 | 25 | 72 | 13 |
| Medium Cellulose | TLL6 | 1 | 2018 | 400.07 | 223.29 | 75 | 25 | 45 | 15 |
| Low Cellulose | SP16 | 1 | 2019 | 344.53 | 255.98 | 75 | 25 | 45 | 14 |
| High Lignin | SP16 | 2 | 2019 | 363.16 | 263.00 | 75 | 25 | 45 | 11 |
| Low Lignin | SP21 | 1 | 2018 | 382.85 | 185.71 | 75 | 25 | 45 | 13 |

### 2.2.7 Statistics

Graphs and statistics were generated using the R programming language version 4.3.1 (R Core Team, 2020). The R package “maps” was used to visualize the collection sites of the *Silphium* accessions on a map (Becker et al., 2022). The “basicPlotteR” library by Crispell (2021) served to put text labels on the map without any overlap. Data with a sample size larger than twenty are displayed as boxplots with notches. These constrictions symbolize the range of their 95 % confidence intervals. If two intervals do not overlap, their difference is interpreted as significant. Data with a sample size of less than twenty are displayed as arithmetic mean with standard deviation.

## 2.3 Results and Discussion

### 2.3.1 Biomass yield

The median and maximum dry matter yields of all *Silphium* accessions (fig. 2.2a) increased over the years of the experiment in both the summer and the winter harvest. The minima remained at the same level close to 0 g per plant or 0 Mg per hectare respectively. In summer the yield increased from about 550 g per plant (about 16.9 Mg/ha) in 2018 to 600 g per plant (about 18.4 Mg/ha) in 2019 and 650 g per plant (about 20 Mg/ha) in 2020. Under high yielding conditions, the harvested dry matter can exceed 20 Mg/ha (Biertümpfel et al., 2013; Pichard, 2012; Siaudinis et al., 2012; Siwek et al., 2019), but as displayed in figure 2.2a, during every harvest in every season, there were individuals yielding more than 20 Mg/ha. In the summer harvest in 2020, about 50 % of the harvested plants exceeded this threshold, leading to the assumption that selection of favorable individuals or populations as first steps in plant breeding offer fast yield improvements during the domestication of *Silphium*. The lower extreme yields close to zero need to be investigated in further research, as it is not clear whether these yields occur due to genetic properties or environmental influences. In terms of annual varying yields, the literature does not indicate any clear trends (Biertümpfel et al., 2013; Pichard et al., 2012; Boe et al., 2019; Siaudinis et al., 2012; Siwek et al., 2019). Thus, the increasing yields in this study from 2018 to 2020 cannot be unrestrictedly confirmed. However, the plant habitus continuously changed from 2018 to 2020, for example, by developing more shoots, which became thinner over growing years. The winter harvest delivered significantly smaller yields every year (about 100 g per plant less than in summer). Stolzenburg & Monkos (2012) already observed decreasing dry matter yields of later harvests in *Silphium*. In early September, they harvested 17.5 Mg/ha and in early October 12.8 Mg/ha. This 4.7 Mg/ha yield difference is of the same magnitude as our data indicate (about 3.1 Mg/ha). Gansberger et al. (2015) mentioned this might be the case due to fallen leaves towards the end of the growing season. In addition to that, the yield reduction might be explained by nutrient resorption to the rhizome for winter.

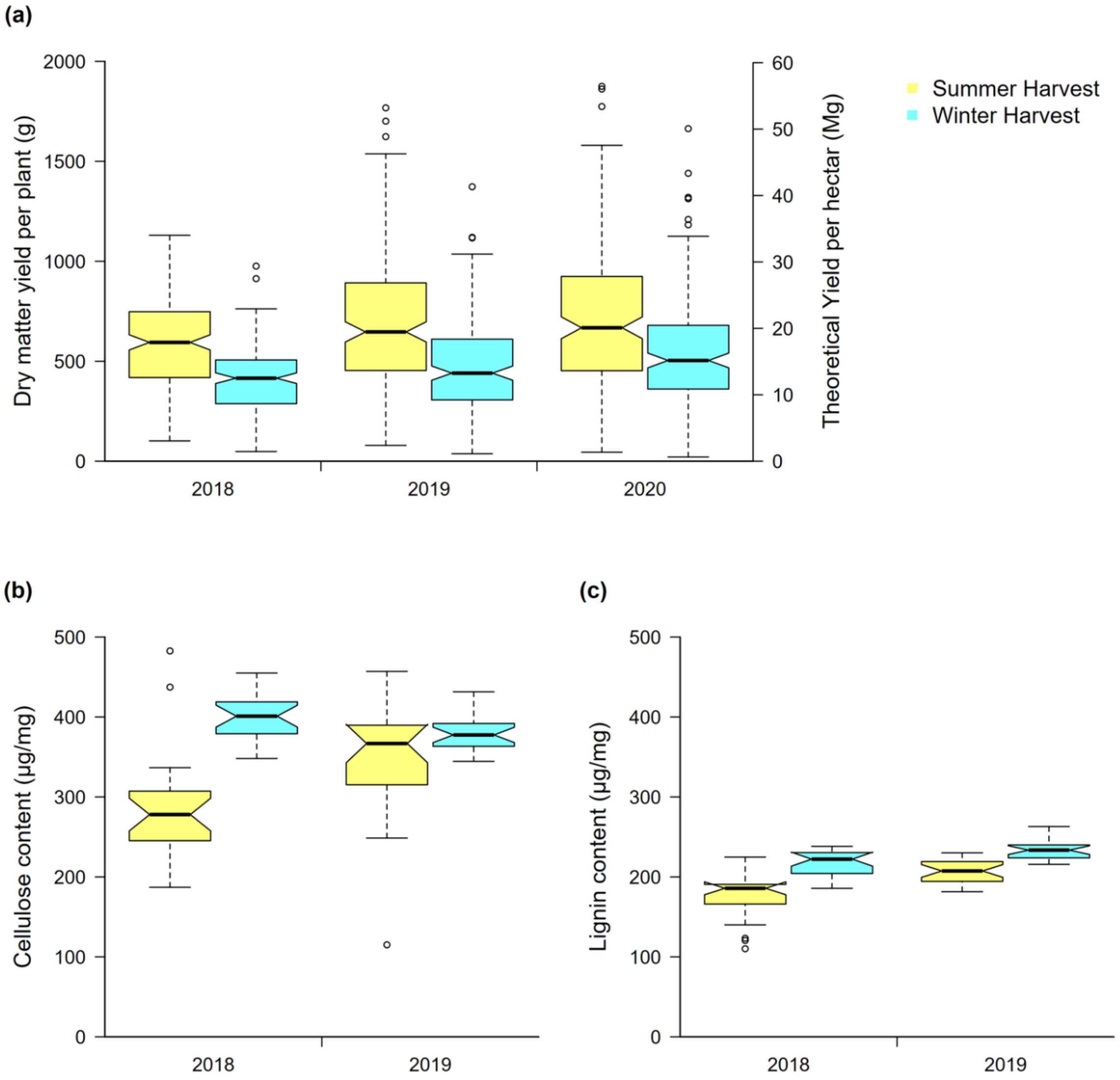

**Figure 2.2: Seasonal and annual comparison of dry matter yields and contents of cellulose and lignin. Boxplots of dry matter yield per plant with n = 167–186 (a), cellulose content with n = 24 (b) and lignin content with n = 24 (c) in the first and second harvesting year (2018, 2019) for chemical composition (b,c) and the first to third harvesting year (2018–2020) for the dry matter yield (a) of all investigated *Silphium* accessions. The data of each variable are separated by year (labels on the x-axis) and season (summer harvest as yellow boxplots on the left; winter harvest as cyan boxplots on the right). The constrictions of the boxplots mark the 95 % confidence intervals of the median. All plants have been established in a field trial at Campus Klein-Altendorf, near Bonn, Germany since 2017.**

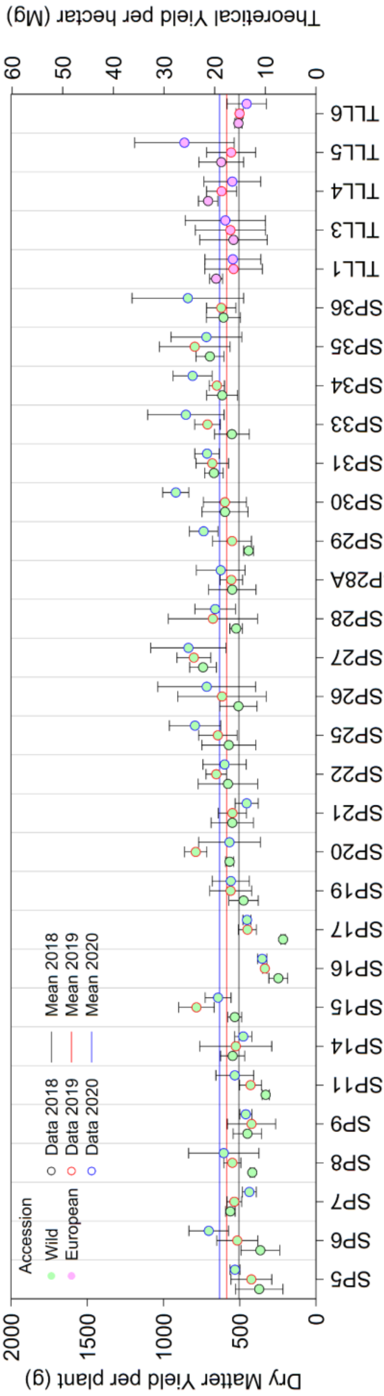

**Figure 2.3: Dry matter yields of the first to third harvesting year (2018–2020) of each cultivated accession of *Silphium perfoliatum*. Mean and standard deviation (n = 3) of dry matter yield per plant. The mean values shown contain data of both summer and winter harvest. The yield data are separated by accession (labels on the x-axis) and year (data points of 2018 presented with black border on the left; data points of 2019 presented with red borders in the middle; data points of 2020 presented with blue borders on the right). The lines passing through the plots from left to right highlight the annual mean of the variable (2018 in black; 2019 in red; 2020 in blue). The green coloring indicates accessions of the collected natural populations, whereas magenta coloring indicates European accessions. All plants have been established in a field trial at Campus Klein-Altendorf, near Bonn, Germany since 2017.**

Figure 2.3 displays the data of figure 2.2a, but now as a function of the different *Silphium* accessions and harvesting years. In general, nearly all accessions show an increasing or constant trend of the dry matter yields for the first three harvesting years, except for the European genotypes TLL1, TLL4, and TLL6, as well as the wild populations SP7, SP14, SP21. These accessions showed decreasing yields in the course of time. The dry matter yields of SP5, SP7– SP14, SP16, SP17, SP19 and SP21 were below average in all years. SP25–SP28 and SP30– SP36 achieved above average biomass yields along the whole sampling period. SP16 reached the least biomass production of about 400 g per plant in 2020, followed by SP5, SP9 and SP17 producing about 500 g per plant. SP27, SP30 as well as SP33 show the highest values (with the smallest standard deviation) with 750–800 g per plant. Furthermore, the mean values of all European accession are above the overall average, whereas the means of the subsequent years are below the annual average. This might be the result of unintended selection of these accessions and raises the importance for multi-annual analyses of this crop. Two exceptions to this pattern are TLL4 in 2019 and TLL5 in 2020. Although TLL4 achieves above average yields in two years, its overall yield is decreasing over time. TLL5 shows one of the highest recorded yields with one of the highest standard deviations, which lowers the reliability of its mean. Determining the yield of single plants is advantageous for breeding, when it comes to selection or when working on relations between yield and other plant traits, but to be able describe the accessions of the collection with more confidence, more field trials at different locations in different years need to be established and investigated. Furthermore, harvesting entire plots might lower the spread of data.

### 2.3.2 Chemical composition of biomass

The cellulose and lignin content were lower in samples harvested in summer compared to winter except the cellulose content in samples of 2019, which remained on the same level (fig. 2.2b/c). The increasing cellulose and lignin content corroborates the findings of a study by Majtkowski et al. (2009), in which lignocellulosic content from the “vegetative phase”, “beginning of flowering” and “beginning of seed setting” were analyzed. The cellulose content in summer samples increased from 2018 to 2019 from a median of about 280 µg/mg to 380 µg/mg, likely due to different environmental growth conditions in the two years. The cellulose content of the winter material remained on the same level, between 390 and 400 µg/mg. The lignin content increased by 20–30 µg/mg from 2018 to 2019, as well as from summer to winter. However, not all accessions show an increase in cellulose content from 2018 to 2019 (fig. 2.4a). SP15 and SP26 reached comparable values in both years. SP16 is the only accession with a decrease in cellulose content. The highest values were achieved by SP26, SP33, TLL4 and TLL6, with their maxima between 380 and 400 µg/mg. SP26 and TLL4 show above average cellulose contents in both years. SP16 reached the lowest cellulose content with about 300 µg/mg in 2019. In contrast, the lignin content of all accessions shows an increase from the 2018 samples compared to 2019 samples. However, the differences between the accessions are not as distinct as for the cellulose content (fig. 2.4b). Taken together, breeding for enhanced cellulose content of *Silphium* biomass has thus more potential than for lignin content. The use of other analytical methods to determine cellulose and lignin content in the field, such as using near-infrared spectroscopy (Blüthner et al., 2016), could be beneficial as they may allow for the analysis of larger sample sizes.

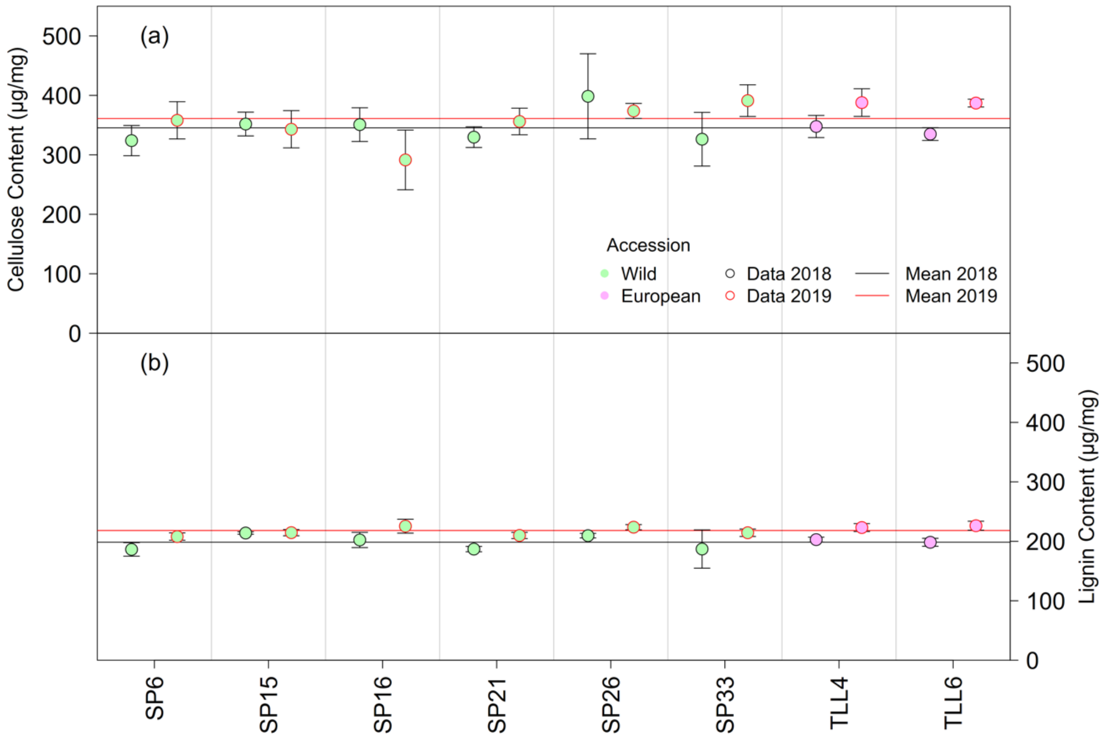

**Figure 2.4: Cellulose and lignin contents of the first and second harvesting year (2018, 2019) of selected *Silphium perfoliatum* accessions. Average and standard deviation (n = 3) of cellulose content (a) and lignin content (b). The mean values shown contain data of both the summer and winter harvest. The data of each variable are separated by accession (labels on the x-axis) and year (data of 2018 presented in black on the left; data of 2019 presented in red in the middle). The lines passing through the plots from left to right highlight the annual mean of the variable (2018 in black; 2019 in red). The green coloring indicates accessions of the plant collecting trip, whereas magenta coloring indicates European accessions. All plants have been established in a field trial at *Campus* Klein-Altendorf, near Bonn, Germany since 2017.**

### 2.3.3 Paper tests

The control sheets with 100 % pine pulp (tab. 2.3) achieved the smallest results in thickness (121.29 µm) as well as the highest tensile index (73.14 Nm/g), breaking strain (3.30 %) and breaking length (7.46 km). The *Silphium* papers about twice as thick (226.2–264.9 µm) show an increasing mechanical attribute trend with decreasing cellulose and lignin contents. The other recorded parameters decrease with decreasing content of cellulose and lignin. Furthermore, the measurements of Medium Cellulose and Low Cellulose are often similar with one exception in the thickness, where the two batches follow the previously mentioned pattern. The tensile index of the hand-sheets with *Silphium* addition is between 44.6 Nm/g and 47.6 Nm/g and the results of the breaking length are distributed around 4.55 km and 4.86 km, which is both about 60 % of the control. The breaking strain of the *Silphium* papers achieves values between 2.34 % and 3.30 %, which is about 75 % of the control. With 5.35 the control's standard deviation of thickness is smaller than the ones of the *Silphium* sheets (22.71–42.23). The standard deviations of tensile index, breaking strain and breaking length are, compared between the five batches, of the same magnitude.

Höller et al. (2021) already observed reduced quality parameter in paper blends with *Silphium* components, whose reported quality reduction is not as high as this study suggests. In addition, the tests by Höller et al. (2021) used chemical pulping, which is not more sustainable compared to the purely mechanical pulping of this work. This might be due to the differences in biomass processing as Höller et al. pulped the biomass after grinding and sieving it. Nevertheless, the reduced quality, especially the increased thickness compared to the control still offer advantages for the cardboard industry, where a high bending stiffness is desirable (Annergren & Hagen, 2009; Höller et al., 2021).

**Table 2.3 Results of paper testing, containing thickness, tensile index breaking strain and breaking length of 5 different samples varying in cellulose and lignin content and a control.**

| | Thickness (µm) | Tensile Index (Nm/g) | Breaking strain (%) | Breaking Length (km) |
|---|---|---|---|---|
| Control | 121.29 ± 5.35 | 73.14 ± 2.79 | 3.30 ± 0.21 | 7.46 ± 0.28 |
| High Cellulose | 236.97 ± 22.71 | 47.64 ± 2.55 | 2.54 ± 0.24 | 4.86 ± 0.26 |
| Medium Cellulose | 240.93 ± 24.56 | 44.89 ± 2.24 | 2.39 ± 0.28 | 4.58 ± 0.23 |
| Low Cellulose | 264.89 ± 42.23 | 44.61 ± 2.15 | 2.49 ± 0.24 | 4.55 ± 0.22 |
| High Lignin | 226.18 ± 32.42 | 46.83 ± 2.09 | 2.65 ± 0.48 | 4.77 ± 0.21 |
| Low Lignin | 248.84 ± 38.02 | 44.73 ± 2.67 | 2.34 ± 0.33 | 4.56 ± 0.27 |

## 2.4 Conclusion

This study introduced new accessions of *Silphium perfoliatum* with known native origins. These accessions underwent a three-year yield analysis when grown in the filed in Germany, showing their increasing yield potential for Central European field conditions. Summer and winter yields of the first harvesting year already exceeded reported biomass production of cup plant found in the literature. Moreover, yield quantity and quality varied between the accessions. Most of the formerly known European accessions show moderate yields with a decreasing trend in the course of time. In contrast, SP27, SP30 and SP33 achieved increasing yields on a high level over the field trial period with a maximum biomass production of 750–800 g per plant in 2020. Even higher harvest yields are also expected in subsequent years. The lowest dry matter yields of 400–500 g per plant in 2020 were reached by SP5, SP9, SP16 and SP17. By showing an expansion of trait expression towards higher and lower yields, the new cup plant accessions add breeding value to the available plant material in Europe. Furthermore, the wild *Silphium* accessions achieved comparable average contents of cellulose and lignin to the European accessions. However, the wild accessions exhibit more variance in their individual populations. After mechanical processing of *Silphium* biomass for pulp production, the impact of cellulose and lignin content on paper quality traits was determined. In general, the use of mechanically processed biomass of *S. perfoliatum* as an additive makes the resulting paper suitable for the cardboard industry. This is substantiated by the increased thickness of the paper and the lower physical paper properties. These effects are higher for biomass with lower contents of cellulose and lignin. Since the contents of cellulose and lignin are lower in biomass harvested in the summer, paper quality is improved by later harvests. In summary, the diversity of *Silphium* accessions pinpoints the importance of knowledge about the origin of plant material and offers the ability to adapt the crop to different purposes of use in future. Both enable new breeding potential for *Silphium perfoliatum*. Due to the high variation within the populations of the new accessions of *Silphium perfoliatum*, selection for biomass yield and increased cellulose and lignin contents could be possible. Further trials could be planned and carried out using seed obtained from the cultivation trial.

# 3 Towards the ideotype of a *Silphium* biomass crop: Agronomical evaluation of phenotypic diversity in *Silphium perfoliatum* L.

This manuscript is still to be submitted:

**Christop A. C. Korte**, Christian Wever, Martin Greve, Martin Höller and Ralf Pude (2024). Towards the ideotype of a *Silphium* biomass crop: Agronomical evaluation of phenotypic diversity in *Silphium perfoliatum* L. Unpublished manuscript.

## 3.1 Introduction

The genus *Silphium* is part of the *Asteraceae* and closely related to the well-known sunflower (*Helianthus annuus* L.) (Clevinger & Panero, 2000). Cup plant (*Silphium perfoliatum* L.) is a promising candidate for sustainable biomass production (Wever et al., 2020; summarized in Gansberger et al., 2015; Peni et al., 2020). Growing cup plant for biomass is done in Middle Europe on several thousand hectares e.g., in Germany on around 10,000 ha (FNR, 2023), mainly as a substitute for energy maize (*Zea mays* L.). In practice, *Silphium perfoliatum* is sown directly on the field (Schäfer et al., 2016). In the first year of cultivation the plants form a soilborne rosette with no worthwhile yield (Greve et al., 2023). In the subsequent years biomass is harvested between August and September, when dry matter (DM) contents of 25–27 % are favorable (Biertümpfel et al., 2018). The reported biomass yield is heterogeneous and can exceed 20 Mg dry matter per hectare (ha), and is mainly used as substrate for biogas reactors or livestock feed (summarized in Gansberger et al., 2015; Peni et al., 2020). Interest is growing in dual usage of silage *Silphium*, since a procedure has been presented that allows for the extraction of the fibers from the biomass before using it as an energy source (Neis-Beeckmann, 2021). On top of that, the biomass of harvested cup plant is reported to be dry enough to store it openly and to utilize it for material applications like pulp and paper production (Höller et al., 2021) or as expanded polystyrene substitute (Moll et al., 2022). Later harvests of *Silphium* are always accompanied by lower dry matter yields but might show better nutrient use efficiencies (Chapter 2; Ruf & Emmerling 2021; Ruf & Emmerling 2022). Besides yield, ecological benefits of *Silphium* are to be mentioned: a long flowering period (July–September) while producing pollen and nectar, no requirements of soil preparation during the 10–15 years as period of use and an extensive regrowing root system, which has a positive effect on water

and nutrient absorption but also on $CO_2$ sequestration (summarized in Gansberger et al., 2015; Peni et al., 2020).
The previously mentioned heterogeneity of *Silphium perfoliatum* can be found within and between studies. Most of the heterogeneity on the field and between locations can be explained by its unbred stage, but a certain amount of the spread between different working groups might occur due to the cultivation of different populations of *Silphium*. Until today, it is uncommon in the literature to provide closer information about the origins of the investigated cup plant material. Wever et al. (2019) analyzed the circulating gen material in Europe, which does not show high genetic variance. Only one population from Ukraine showed a genetic distance to the main gene pool, which may be caused by aimed selection during breeding attempts for this species in the former Soviet Union. Even though the presence of phenotypic and genetic variation within the European plant material (available in Europe) heightens the evidence for an improvement of the overall plant performance via selection or breeding, the single European accessions seem to share their ancestry. This leads to the assumption that the European genotypes originate from the same geographic location (Wever et al., 2019). Recent studies have presented wild plant material of *S. perfoliatum* as a foundation for plant breeding (chapter 2). This was started too recently for a phenotypical description of the collection of wild accessions to be possible yet.

The aim of this study is to assess the diversity of agronomical important plant traits within a collection of wild *Silphium perfoliatum* accessions, as well as to identify connections between these plant traits to direct future breeders in the direction of the ideotype of cup plant. Furthermore, this work should raise the awareness of providing closer information about the origin of plant material in future studies.

## 3.2 Material and Methods

### 3.2.1 Plant material

The map of location sites (fig. 3.1) shows all collected accessions, as well as those used for this study. The wild accessions collected on the hunting trip through the natural distribution area of *S. perfoliatum* in 2016 are marked with the prefix "SP" and a big black dot on the map. The accessions used for this study are indicated by smaller red dots on the map. Some accessions have been left out, but the used selection still covers the whole natural distribution area of *S. perfoliatum*. To indicate its unknown origin, the European plant material (prefix "TLL") is displayed outside the map (fig. 3.1). This plant material was gathered in Europe by the TLL (Thüringer Landesanstalt für Landwirtschaft; since 2019 TLLLR, Thüringer Landesanstalt für Landwirtschaft und Ländlichen Raum).

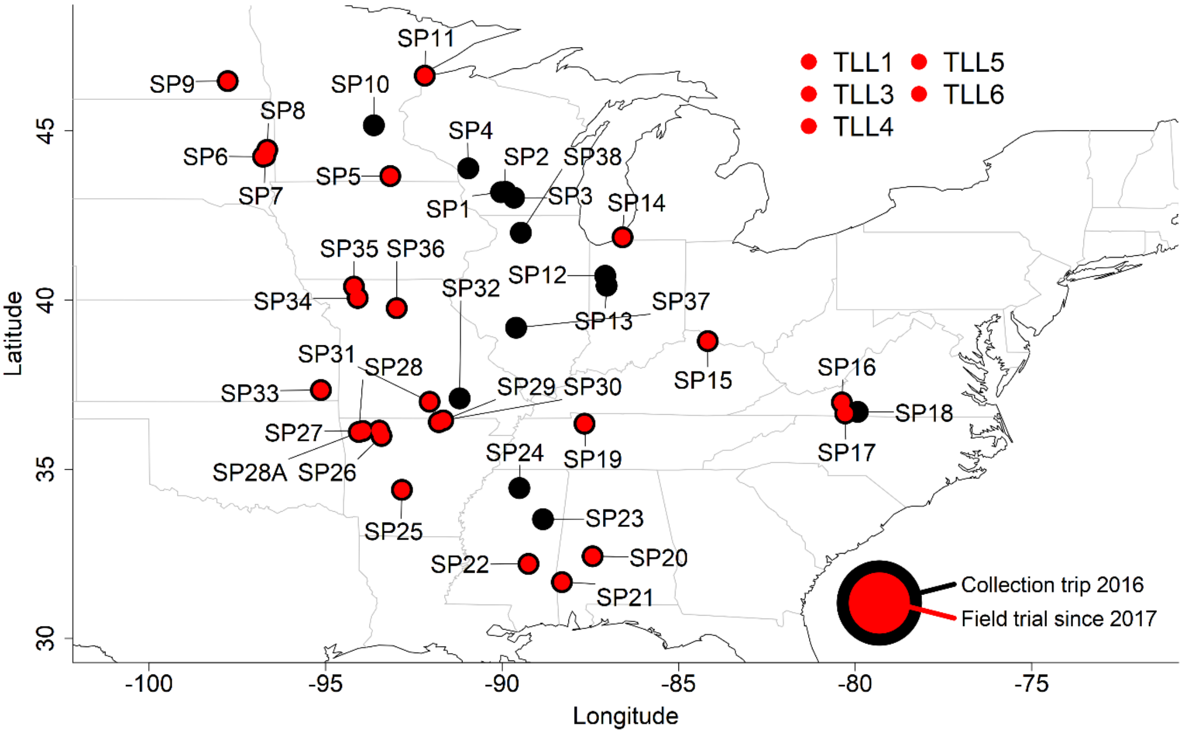

**Figure 3.1: Used accessions for phenotyping. Map of location sites of collected *Silphium perfoliatum* (SP1–SP38) during the hunting trip in 2016. The European plant material (TLL1, TLL3–TLL6) is displayed outside the map, because of unknown origination in the natural distribution area. The natural sites are located equally along the borders of the native distribution area in North America. The big black dots mark the location sites. The small sized red dots indicate natural and European accessions which are established in a field trial at Campus Klein-Altendorf, near Bonn, Germany since 2017 and were investigated from 2018 to 2021.**

### 3.2.2 Field Trial

The investigated field trial was established in 2017 at *Campus* Klein-Altendorf near Bonn, Germany (Lat: 50.615684, Long: 6.985003). The dominant soil type is haplic luvisol. The long-term mean annual air temperature and precipitation amount are 9.5 °C and 606 mm respectively. The plants for the experimental site were pre-cultivated in the greenhouse for 12 weeks, with fluctuating temperatures between 6 and 25 °C. Afterwards, the plantlets were planted on July 5 and 6, 2017. The plantlets were irrigated on the day of planting and one week later to support plant establishment. Weed control was carried out manually and mechanically as necessary. The field trial has a randomized block design with three replications. Each plot contains four rows of nine plants. The row distance is 0.5 m and the plant distance within a row is 0.65 m, resulting in a plot size of 7.8 m² and a plant density of 3.1 plants per m². To bypass border effects, the inner two rows, excluding the first, second and last plants of each plot, were used for data collection.

### 3.2.3 Phenotyping

Due to *Silphium*'s rossette-stage during the first year, phenotyping of the plants began in 2018 and was replicated annually until 2020. The number of shoots was determined once a year mid-July by counting both vital and lethal shoots. Data of plant height, shoot widths and the number of nodes were collected mid/end August every year of phenotyping. Plant height was determined as the parts of the plant above ground, up till the hypsophylls using a leveling staff. Measurements of shoot widths were carried out between the fourth and fifth node with a caliper. The number of nodes were counted. Flowering progress was determined twice a year mid-July and mid/end August by evaluating the flowering stage of the whole plant. Plants were rated with -1 as long as there were no generative plant parts visible. Plants that had developed their first bud were rated with 0. The numbers 1–7 indicate blooming in the uppermost floral rank (compare fig. 3.2). Since lodging does not occur in the second year of growth, the actual data collection started in the third year with one sampling per week. The lodging was recorded based on the procedure for sunflower of the Federal Office of Plant Varieties (Bundessortenamt, 2000). Whole plots were rated on a scale from 1 to 9, where 1, 3, 5, 7, and 9 meant 0, 25, 50, 75, and 100% trait expression, respectively (intervening numbers were used as transitions). Data collection began in mid-October 2019 and ended in mid-December of that year. Lodging was sampled from mid-July to end-October 2020.

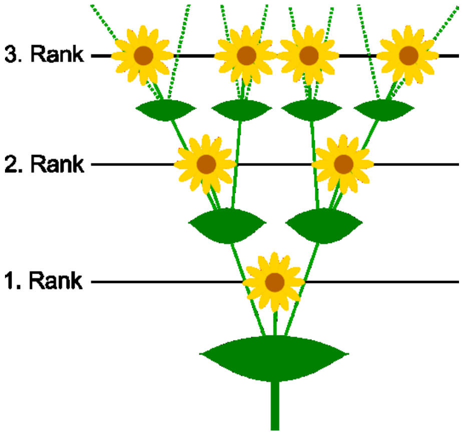

**Figure 3.2: Schematic representation of the different floral ranks in *Silphium perfoliatum*. The constant peaking of the individual inflorescences results in a long flowering period. By integrating the rank number, the flowering progress can be described.**

### 3.2.4 Cup formation

Data collection concerning leaf development started in 2021, with a reduced number of accessions (15) and 6 plants of plot borders. Cups were evaluated along the vegetations period to avoid rating senescent leaves. Leaf pairs were assessed by means a self-created scale of cup formation. The possible scores range from 1 to 7 and are described in table 3.1 and figure 3.3. Cup formation develops along the shoot, starts at 1 in the lowest and end at 7 in the highest node. Relative numbering of nodes along the shoot is also included, starting with the relative node 0 at the lowest and ending with the relative node 1 at the top node, enabling the possibility of comparing individuals with different amounts of nodes.

**Table 3.1: Stagewise description of the self-created scale for evaluating the cup formation of *S. perfoliatum*. Cup formation develops along the shoot, starts at 1 in the lowest and end at 7 in the highest node.**

| Cup Scale | Description |
|---|---|
| 1 | No visible cup formation |
| 3 | Visible cup formation; cup folded |
| 5 | Cup folded; leaf area along the whole petiole |
| 7 | Connate; no visible petiole; maximum cup formation |

The numbers between the stages can be used for transitions (e.g. Stage 2: Visible cup formation; leaf area of cup not folded).

**Figure 3.3: Reference pictures for the self-created cup scale to evaluate the cup formation of *S. perfoliatum*.**

### 3.2.5 Statistics

Graphs and statistics were generated using the R programming language version 4.3.1 (R Core Team, 2020). The R package "maps" was used to visualize the collection sites of the *Silphium* accessions on a map (Becker et al., 2022). The "basicPlotteR" library by Crispell (2021) served to put text labels on the map without any overlap. Data are displayed as boxplots, histograms or line plots. These constrictions of the boxplots symbolize the range of their 95 % confidence intervals. If two intervals do not overlap, their difference is interpreted as significant. Data with a sample size of less than twenty are displayed as arithmetic mean with standard deviation.

## 3.3 Results

The entire collection in figure 3.4a shows significantly lower values in 2018, with an average of 200 cm, compared to those the following years (2019 and 2020), with an average of about 250 cm. The difference of individual populations between 2019 and 2020 turns out to be small and often not significant. This indicates that the plant height of cup plant has already established in 2019 across all accessions. Also significant are the differences between the accessions. SP16 and SP17 show the lowest plant heights, whereas SP27 – SP33 achieve the highest values. All other accessions of the natural range seamlessly fill this difference in plant height. The European accession show values between slightly below to slightly above average, so that the new *Silphium* accessions enrich the available gene pool in both directions.

The shoot widths (fig. 3.4b) show on average a decreasing trend along the sampling years, where the difference between 2018 and 2019 was with about 2.5 mm larger than the difference of 2019 and 2020 (0.5 mm). Particularly exciting are accessions that do not follow this decreasing trend and achieve nearly constant shoot diameter along the whole sampling period (2018–2020). These include SP11, SP25, SP30 and SP33 and can be valuable for further selection as for perennial crops phenotypic stability over the years is an essential factor. The highest shoot widths achieve SP25 and SP30 to SP36. The lowest results are shown by SP5, SP6, SP11 and SP16. Similar to the plant height, the European accessions show neither particularly high nor particularly low values, whereas all accessions but TLL4 achieve below average shoot widths.

Figure 3.4c displays increasing shoot numbers in all accessions over the years, with steadily decreasing differences between the annual averages. However, the spread of the data increases with the median number of shoots. The wild accessions SP5–SP8, SP11, SP14, SP20 and SP22, as well as TLL5 of the European plant material stand out with high numbers of shoots. In contrast to this, SP30–SP34 achieve the lowest numbers of shoots. The remaining European accessions reach average values, so that they are located between the extremes of the wild genotypes.

Figure 3.5a displays the flowering progress sampled in mid-July every year (2018–2020) as histograms. The high values of flowering progress in the accessions SP16 and SP17 clearly show the early onset of flowers in these accessions. The annual modal values of these accession are 4 for SP16 and 3 for SP17. The lowest flowering progress was reached by SP21 and SP25–SP33, where most of the plants did not start flowering in mid-July (indicated by the values 0 and -1). The European accessions, as well as SP5–SP14, show flowering progress in between the early and late flowering populations. Beyond that, TLL1–TLL6 seem to be the most heterogenous accessions, by showing the highest variation in flowering progress. In mid/end-August (fig. 3.5b) SP16 and SP17 were already at the end of their flowering period as the increase of their flowering progress was smaller than in all other accessions. The most individuals to reach 6 floral ranks were in SP16 and SP17. The lowest flowering progress is shown by SP15, SP19–SP30 and SP33. All other accession including the European plant material are distributed in between. Single plants of various accessions did not develop mid/end-August any floral ranks at all.

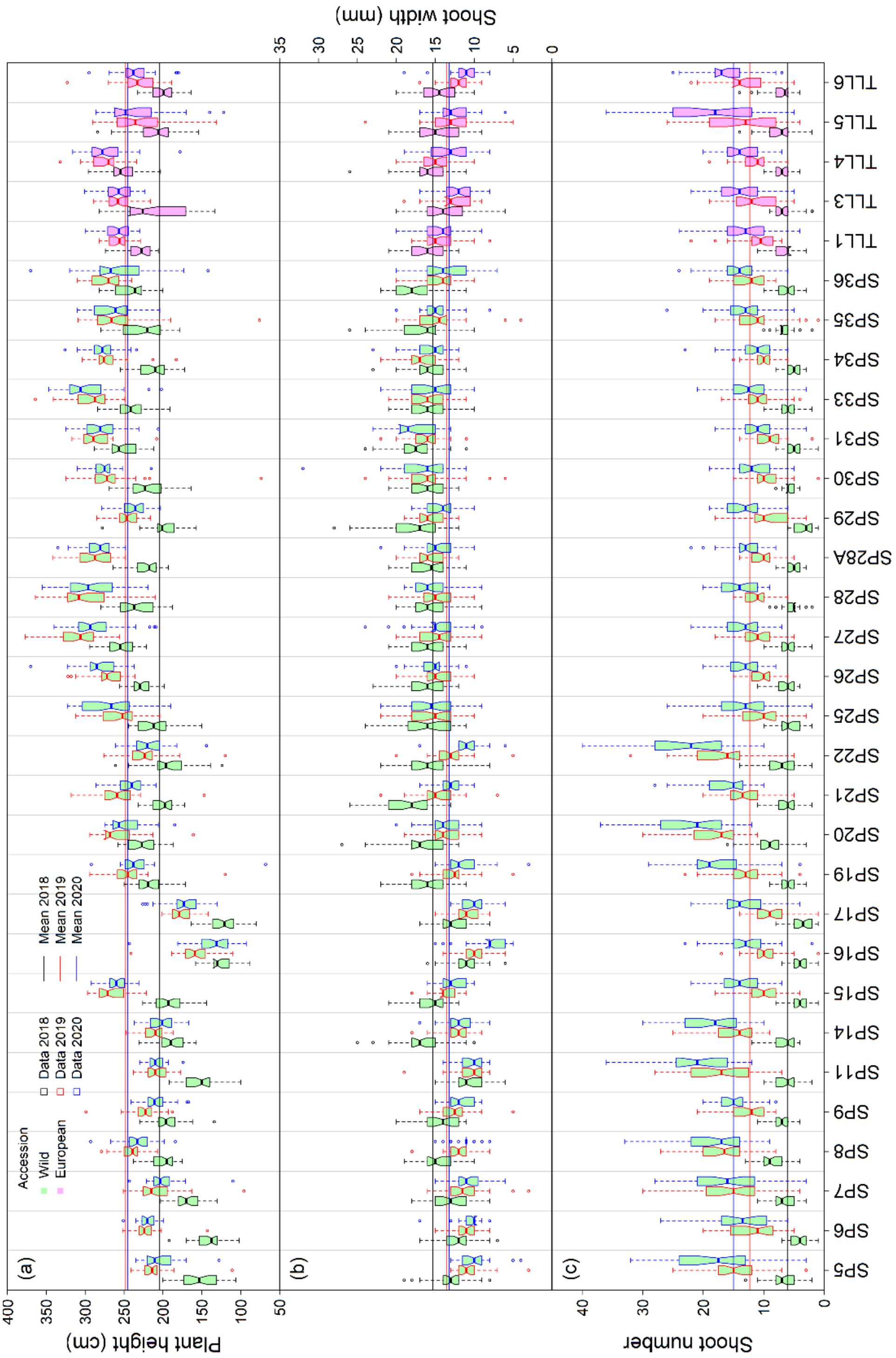

**Figure 3.4: Boxplots with n=28–36 of plant height (a), shoot width (b) and number of shoots (c) of the first three yield years (2018–2020) as a function of the *Silphium perfoliatum* accessions. The constrictions of the boxplots mark the 95%-confidence interval of the median. The black boxplots/histograms show data of 2018, the red ones of 2019 and the blue ones of 2020. The lightgreen coloring indicates wild accessions, the magenta coloring represents the European plant material. The black line is on the level of the overall mean of the parameter of 2018, the red one on the level of the overall mean of 2019 and the blue one on the level of the overall mean of 2020. Plant height is the length of the shoot from the soil to the first flowering stalk (a), the shoot width has been measured between the fourth and fifth node (b), number of shoot and number of nodes have been counted (c,d). All plants have been cultivated since 2017 in the field trial "GEniu*S* II" at Campus Klein-Altendorf, near Bonn, Germany.**

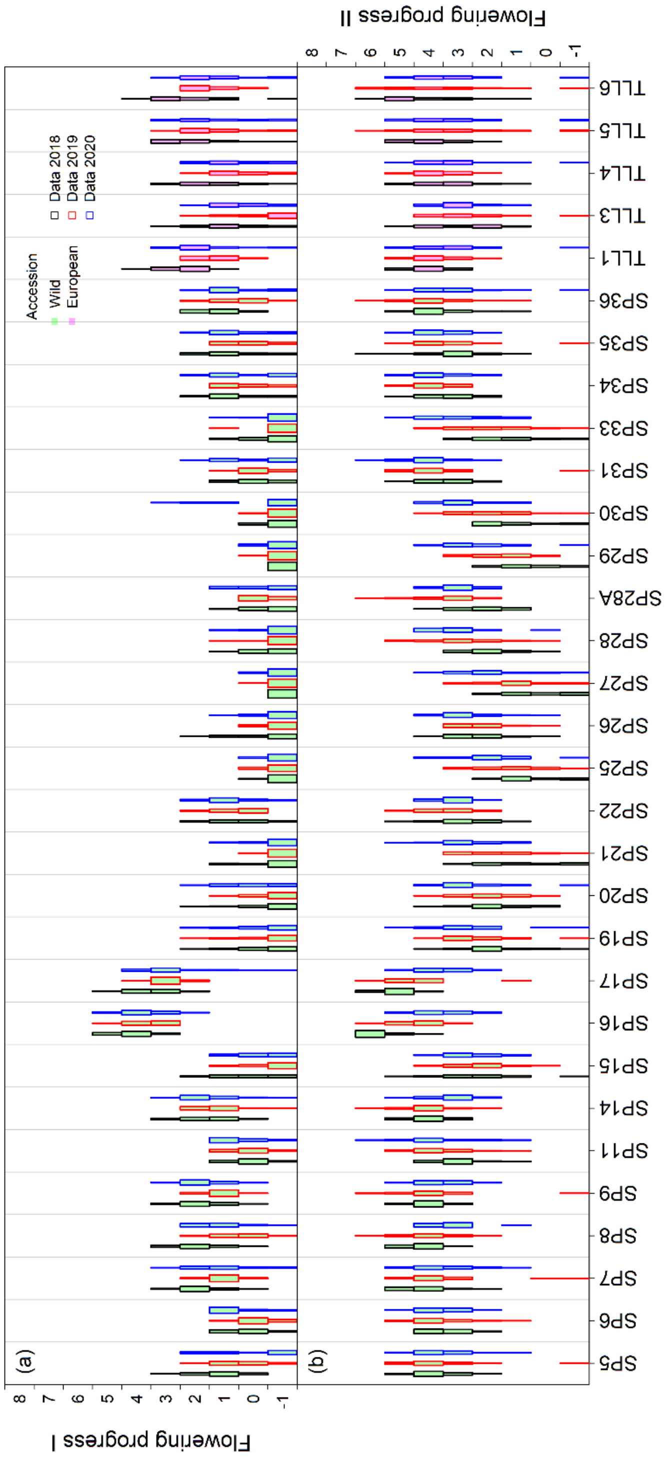

**Figure 3.5: Histograms with n=28–36 of flowering progress I (a) and flowering progress II (b) of the first three yield years (2018–2021) as a function of the *Silphium perfoliatum* accessions. The black histograms show data of 2018, the red ones of 2019 and the blue ones of 2020. The lightgreen coloring indicates wild accessions, the magenta coloring represents the European plant material. The flowering progress have been captured by consideration of the inflorescences, whereby it was distinguished by; plant in vegetative phase (-1), first bud developed (0), flower head of first rank opened (1), flower heads of second rank opened (2), flower head of third rank opened (3), etc. All plants have been cultivated since 2017 in the field trial "GEniu*S* II" at Campus Klein-Altendorf, near Bonn, Germany.**

The detected scores of lodging in figure 3.6 show the performance of each accession in 2019 and 2020. Data of 2018 are not displayed, since the crop had no occurrences of lodging in that year. SP5–SP9, as well as TLL6, (fig. 3.6a) achieved particular high scores in 2019. SP5–SP9 reached the highest frequencies of the score 9 (100% of the plot is lodging), TLL6 shows the highest overall values with the lowest lodging score at 4 and all remaining samples between 7 and 9. The highest frequency of the lowest score of 1 (0% of the plot is lodging) was sampled for SP16, SP17 and SP28A. Still, none of the three accessions was susceptible to lodging until the end of data sampling. SP19 stands out for its low variation, since all data points are between 3 and 5. In 2020 (fig. 3.6b), the sampled lodging scores were low compared to 2019, with SP5, SP6, SP16, SP17, SP28A and SP30 reaching the lowest lodging scores. TLL6 achieved the highest values, since it is the only accession showing scores of 9.

The results of figure 3.7 show that the cup formation in each plant increases along the shoot. In most plants a change from cupless (1) to cup-shaped (5) to connate (7) was observed. Exceptions were the individuals of SP11, whose lowest nodes were evaluated with a score of 2, as well as all plants of SP26, some plants of SP28/SP28A and one plant of SP33, which show a non-connate upper most leaf pair with a score of 6. SP26 and SP28 were the accessions with the slowest leaf development. Up to relative nodes between 0.3 and 0.4 these populations were cupless (1). SP28A is also conspicuous for cuplessness, but not to the extent of the previously mentioned populations. Since four individuals of SP28A had a similar course as SP26 and SP28 and the remaining two plants showed steady cup formation from the beginning, this accession reached the highest variation in cup formation. The fastest cup development along the shoot were reached by SP16 and SP17, which were already connate at a relative node of 0.4–0.5. SP21, SP30, SP33, SP34 and TLL4 stand out due to fast increase of cup formation in the lower leaf layers (relative node 0–0.3), as well as slower cup formation from there on up to the upper most node. The accessions SP6, SP11 SP14 and SP19 show an on average nearly linear increase of cup formation along the shoot.

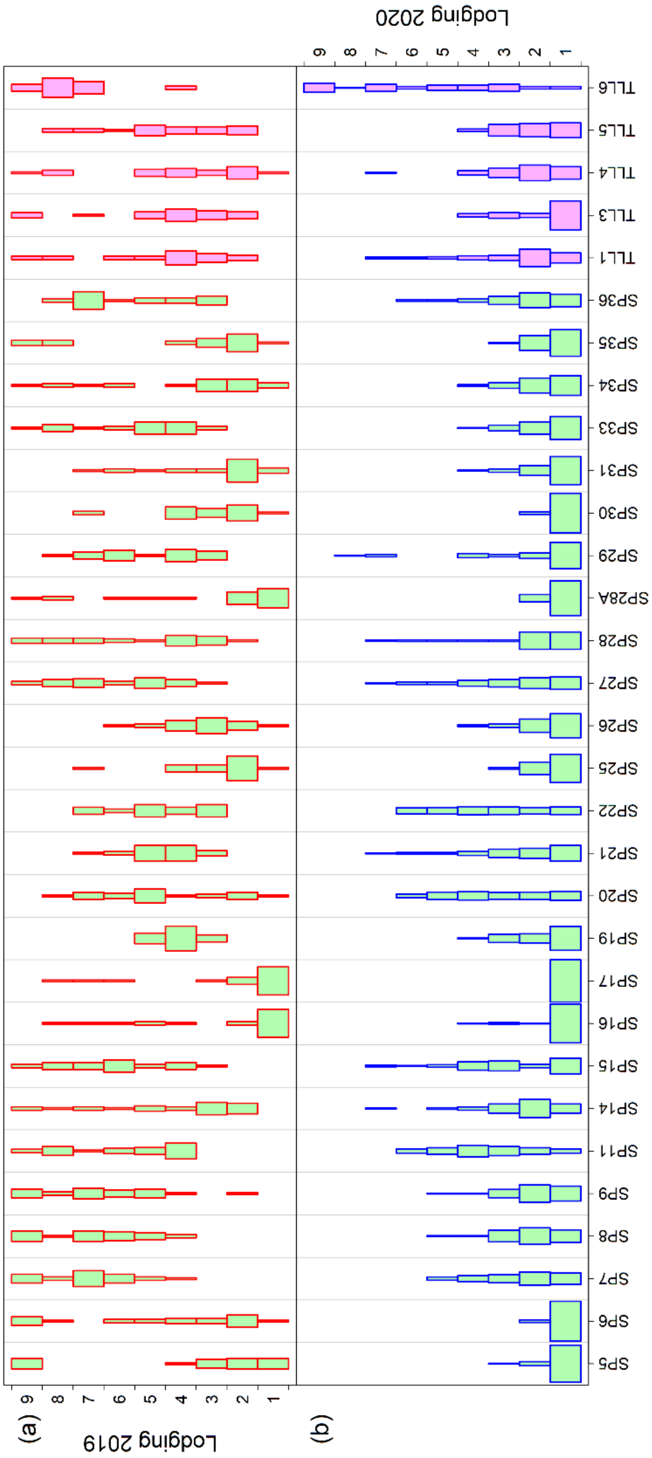

**Figure 3.6: Histograms (a, b) of the detected lodges of 2019 (n=24) and 2020 (n=51) as a function of *Silphium perfoliatum* accessions. The red histograms show the data of 2019 (a) and the blue ones of 2020 (b). The lightgreen coloring indicates wild accessions, the magenta coloring represents the European plant material. The lodge was evaluated plot-wise on a scale between 1 and 9 (0–100%). All plants have been cultivated since 2017 in the field trial “GEniu*S* II” at Campus Klein-Altendorf, near Bonn, Germany.**

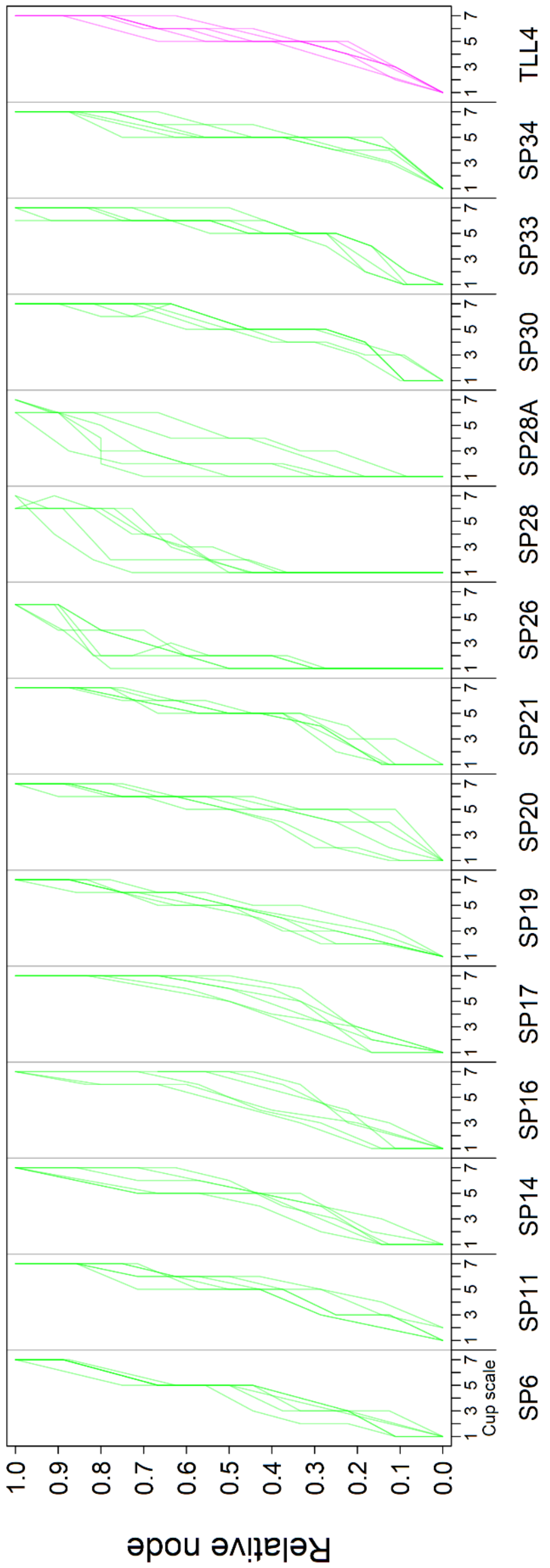

**Figure 3.7: Line diagram of relative nodes as a function of leaf cup development of several *Silphium perfoliatum* accessions. Six plants of each accession have been investigated; every individual is represented as a line. The lightgreen coloring indicates natural accessions, the magenta coloring represents the European plant material. The relative nodes could only be calculated at the end of the vegetation period by setting the first node equal 0, the las node equal 1 and all remaining nodes evenly in between. Detection of leaf cup formation was carried out using the self-created cup scale. All plants have been cultivated since 2017 in the field trial "GEniu*S* II" at Campus Klein-Altendorf, near Bonn, Germany.**

## 3.4 Discussion

Wever et al. (2019) analyzed the performances of the European genotypes in the first harvesting year, with similar results to the ones presented in this study. Average plant height of all accessions was between 200 and 250 cm. The order from the tallest accession (TLL4) to the tiniest accession (TLL6) matched our median plant heights. Shoot width was measured at 10 cm and 130 cm above ground in Wever et al. (2019), whereas for the present study, shoot width was sampled between the fourth and fifth node (about 100 cm above ground). This makes the results not directly comparable. Nevertheless, the results of shoot widths in this study are all situated in between the extremes presented in the results of Wever et al. (2019). The order from accessions with the thickest shoots to accessions with the thinnest shoots presented in this study matches Wever et al.'s for most but not all genotypes. Wever et al. (2019) detected no significant differences of shoot numbers between the European populations with values between 9 and 13. In the present study the differences are non-significant as well, with medians even closer to each other (7–8 shoots per plant), but our data suggest that the European plant material becomes more and more distinct in shoot number over the years. The second trait that is difficult to compare is the flowering progress, due to the unknown sampling period in Wever et al. (2019). However, what the flowering progress in both studies has in common, is that the European plant material does not show much variation. In summary, the study of Wever et al. (2019) confirms the phenotypic findings in the European accessions and therefore raises the confidence in the data of the wild accessions. Unfortunately, this confirmation is only valuable for the data of 2018, since only results from the first harvesting year were published. Compared to the European plant material, the wild accessions cover a wider range of trait expression in plant height, shoot width, shoot number and flowering progress in both directions.

Chapter two of this thesis presented the yield in the same field trial, in the same time period and with the same accessions as this study. By comparing the yield data of chapter two with the phenotypic traits of this study, the impact of these traits on yield can be evaluated. SP5–SP22 are accessions which are more likely to reach lower yields than SP26–SP36. Thus, plant height and shoot width can be classified as positively determining yield, since SP26–SP36 are the highest growing accessions with the thickest shoots. Negatively yield determining are shoot number and flowering progress. This result seems intuitive for plant height, shoot width and flowering progress, since plants with a higher and thicker growth produce more biomass and thus more yield as well as plants with a later flowering onset and therefore a more time in vegetative growth. Unintuitive, is that more shoots reduce the biomass yield. However, this can be explained by the fact that the number of shoots seem to be negative correlated to plant height and shoot width so that the effect of more shoots on yield is canceled out.

Lodging of *S. perfoliatum* has only been investigated in the literature as a possible improvement to be achieved by breeding (Van Tassel et al., 2017). Besides the annual difference between 2019 and 2020, the higher lodging scores in 2019 might occur due the later time period and the accompanied advanced development stages of cup plant. In both years, SP16, SP17 and SP28A were the most lodging resistant accessions of the collection. TLL6 stands out for its lodging susceptibility. For a better understanding of lodging in *Silphium*, closer investigation is needed in future experiments over several growing seasons, with regard to the annual phenotypic differences of the crop and the weather conditions.

Every plant of *Silphium perfoliatum* pass all stages of cup formation along the shoot, from cupless in the lowest node to connate in the highest node. In the wild accessions of cup plant, a variation in cup formation was observed. SP16 and SP17, which belong to the subspecies *Silphium perfoliatum* var. *connatum*, reach the connate cup stage at the lowest nodes. SP26, SP28 and SP28A achieve the cupless stage until relative node 0.4. Therefore, the range of available cup formations is expanded by the collection of wild genotypes. Especially, the "cuplessness" of SP26, SP28 and SP28A is a previously unknown trait of *S. perfoliatum*, and needs to be analyzed more closely in the future. Until today, the function of cups has not been discovered, just as the agronomical impact of this variation of cup formation on the crop. Thus, from a breeding point of view it is not yet clear which phenotype is beneficial. Currently we are working on improvements of the Cup scale, with the aim of creating a "Cup Index" to describe the degree of cup formation more objectively and on a higher level of measurements with a continuous scale. To calculate the "Cup Index", leaf and cup traits must be used. To this end a database of leaf and cup traits of *S. perfoliatum* was created with data from 2020 and 2021.

As already mentioned in chapter 2 of this thesis, further field trials at different locations and environments are needed to raise the confidence in the data and to evaluate the heterogenicity of the crop. To expand knowledge about the ideotype of *Silphium perfoliatum*, future experiments need to assess the phenotypic impact of polyploidization and hybridization on *Silhpium* to find the agronomical optimum of both mechanisms, in order to get closer to the ideotype of the crop.

## 3.5 Conclusion

Compared to the European plant material, the new *Silphium* collection expands the variability of plant traits (plant height, shoot width, shoot number, flowering progress and cup formation) and shows accessions with higher resistances to lodging. Furthermore, the changes in plant height, shoot width and shoot number were evaluated over consecutive years of cultivation. The growth height was established in the second harvesting year and remains constant from then on. Shoot width decreases from year to year, whereas the number of shoots steadily increases. Therefore, constant shoot width along the growing periods of the accessions SP11, SP25, SP30 and SP33 show a previously unknown value in the *Silphium* gene pool by ensuring constant yield and quality of biomass. Cup formation is the most complex plant trait investigated, since it changes throughout the growing season. Although not all accessions of the wild nor of the European *Silphium* collection were analyzed, we assume that the wild genotypes enrich the available variation of cup formation. This is due to fast cup development towards the connate stadium in SP16 and SP17 as well as the long occurrence of the cupless stadium in SP26, SP28 and SP28A.

# 4 First insights into the resistance of *Silphium perfoliatum* L. to *Sclerotinia sclerotiorum* (Lib.) de Bary

This manuscript is still to be submitted:

**Christoph A. C. Korte**, Christian Wever, Martin Greve, Philip Bischoff, Ulrike Steiner and Ralf Pude (2024). First insights into the resistance of *Silphium perfoliatum* L. to *Sclerotinia sclerotiorum* (Lib.) de Bary. Unpublished manuscript.

## 4.1 Introduction

Climate change has an impact on the virulence of pathogens. Even if the full extent of climate change is affected by multiple factors and therefore difficult to determine exactly, “there is limited but increasing evidence suggesting that climate change has a direct impact on pathogen virulence and disease development” (Singh et al., 2023). In addition, agro-political decisions in the European Union (e.g. EU Green Deal, Farm to Fork Strategy), which affect the reduction of chemical plant protection in Europe, raise the importance of breeding for resistances. Therefore, recent *de novo* domestication activities on *Silphium perfoliatum* L. (Greve et al., 2023; Wever et al. 2019) need to include phyto-pathology from the beginning to create a foundation for a sustainable crop in the future. Common pathogens of *Silphium* are *Eucosma giganteana*, *Puccinia silphii* and *Sclerotinia sclerotiorum*. Infestation of *Silphium* with *Sclerotinia* is investigated more closely in this study (Biertümpfel et al. 2018; Turner et al., 2018; Vilela et al., 2020).

The genus *Silphium* is part of the *Asteraceae* family and closely related to the well-known sunflower (Clevinger & Panero, 2000). Beside the oilseed crop silflower (*Silphium integrifolium* Michx.), cup plant (*Silphium perfoliatum* L.) is a promising candidate for sustainable biomass production (Van Tassel et al., 2017; Vilela et al., 2018; Wever et al., 2020). In practice, *Silphium perfoliatum* is sown directly on the field (Schäfer et al., 2016). In the first year of cultivation the plants form a soilborne rosette with no worthwhile yield (Greve et al., 2023) and in the subsequent years biomass is harvested between August and September, at which time dry matter contents of 25–27 % are favorable (Biertümpfel et al., 2018). The reported biomass yield is heterogeneous and can exceed 20 Mg DM per hectare (ha), and is mainly used as substrate for biogas reactors or livestock feed (summarized in Gansberger et al., 2015; Peni et al., 2020). Later harvests of *Silphium* are always accompanied by lower dry matter yields but might show better nutrient use efficiencies (Ruf & Emmerling 2021; Ruf & Emmerling 2022). Besides yield, the ecological benefits of *Silphium* are worth mentioning as well, such as a long flowering period (July–September) while producing pollen and nectar, no requirements of soil preparation due to 10–15 years as period of use and an extensive regrowing root system, which has a positive effect on water and nutrient absorption, but also on $CO_2$ sequestration (summarized in Gansberger et al., 2015; Peni et al., 2020). As an early emerging perennial plant, cup plant is able to use the humidity of winter and spring more efficiently in comparison to annual biomass crops of the second generation (Ruf & Emmerling, 2018; Wever et al., 2020). Growing cup plant for biomass has already been started in Germany on 10,000 hectares (FNR, 2023). *Sclerotinia* infested fields should be harvested as soon as possible to reduce the formation of survival structures (Biertümpfel et al., 2018).

*Sclerotinia sclerotiorum* (Lib.) de Bary is a member of the Ascomycota, causes the disease “White Mold” and is the main pathogen of cup plant in Europe (Biertümpfel et al., 2018; Bolton et al., 2006; Lumsden, 1979). *S. sclerotiorum* has a broad spectrum of plant hosts, including cup plant, sunflower (*Helianthus annuus* L.) and oilseed rape (*Brassica napus* L.; Boland & Hall, 1994; Purdy, 1979). For this reason, it is not advisable to sow cup plant in a field which previously contained sunflower or rapeseed (Biertümpfel et al., 2018). The namesake for *Sclerotinia* is its survival structure called sclerotium. Tribe (1957) suggests that the sclerotia of *S. sclerotiorum* are able to stay viable up to 8 years in field conditions. There are two ways sclerotia are able to germinate. The first of these is the mycelial germination, which is characterized by mycelial growth directly out of the sclerotia and infections at the lower stem or roots. Secondly, there is carpogene germination, forming cup-shaped apothecia, in which asci are located containing haploid ascospores which are produced via meiosis. Released ascospores are carried to their plant hosts by the wind. The infection occurs in both cases by invasion of mycelium using appressoria in plant host tissue. Eventually, *S. sclerotiorum* produces new sclerotia and the life-cycle continues.

In the experiment conducted for this study, various cup plant accessions were infected with several strains of *S. sclerotiorum*. The aim of this study is to identify *Silphium perfoliatum* accessions with natural resistances against the fungus *Sclerotinia sclerotiorum*. These findings should be considered in early stages of cup plant breeding. Furthermore, the susceptible accessions as well as the pathogenicity of different *Sclerotinia sclerotiorum* strains on *Silphium* are evaluated, to form a principal element for upcoming studies.

## 4.2 Material and Methods

### 4.2.1 Plant material

Eleven *Silphium perfoliatum* accessions were used in this study, which are part of the *Silphium* collection described in chapter 2 of this thesis (fig. 4.1). Eight accessions originate in the natural distribution area. The remaining three genotypes are part of the collection that was gathered by the "Thüringer Landesanstalt für Landwirtschaft" (TLL) and are referred from now on as "European" accession, as they present the plant material available in Europe.

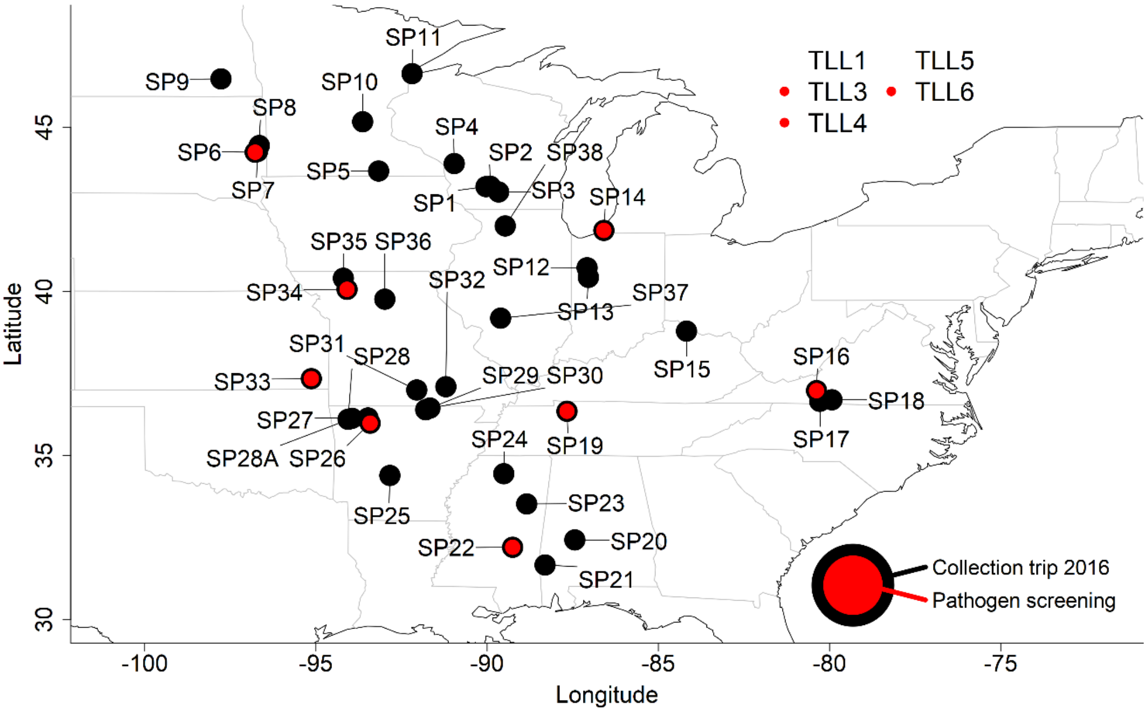

**Figure 4.1: Used accessions for pathogen screening. Map of location sites of collected *Silphium perfoliatum* (SP1–SP38) during the collection trip in 2016, as well as the European plant material (TLL1, TLL3–TLL6), which is displayed outside the map, because of unknown origination in the natural distribution area. The natural sites are located equally along the borders of the native distribution area in North America. The big dots mark the location sites. The small sized green/blue dots indicate natural/European accessions which have been investigated for this study.**

### 4.2.2 Pathogen material

Three different strains of *Sclerotinia sclerotiorum* were used to infect *Silphium* plants. These are named after the corresponding species they were isolated from and are part of the pathogen collection of the Institute of Crop Sciences and Resource Conservation, chair Plant Diseases and Plant protection (University of Bonn).

*Sclerotinia sclerotiorum* ‘*Silphium*’ and *Sclerotinia sclerotiorum* ‘*Helianthus*’ were isolated from cup plant (*Silphium perfoliatum*) and sunflower (*Helianthus annuus*) by PD Dr. Ulrike Steiner (University of Bonn). *Sclerotinia sclerotiorum* ‘*Brassica*’ was isolated from oilseed rape (*Brassica napus*) and provided by the Department of Plant Pathology and Plant protection of the Institute of Crop Sciences (University of Göttingen).

### 4.2.3 Seed propagation

Seed propagation took place in 2020 using plants established in the GEniu*S* II field trial (chapter 2 and 3). First, bags impenetrable to pollinators were put on buds of selected plants, to exclude cross-pollination. With advancing bloom, anthers were collected from the flower heads. This was done for all selected plants of one accession before all anthers were thoroughly mixed. Subsequently, the collected pollen was rubbed on the female flowers. Between accessions, the pollination utensils were cleaned with ethanol, dishwashing detergent and water to prevent cross-pollination by residual pollen. Seeds reached maturity and were harvested after approximately two months, after which they were used for all further experiments.

### 4.2.4 Growing *Silphium* plantlets

Before sowing, the seeds were pretreated in a cold gibberellic acid (GA3) solution ($V_{tot.}$ = 200 ml; 2.5 ml/l ethanol; 0.5 g/l GA3; $H_2O$ ad $V_{tot.}$; approximately 7 °C). Incubation was carried out protected from light in a refrigerator at approximately 7 °C for 12 h. Care was taken to ensure that all seeds were in contact with the GA3 solution during the incubation period. The GA3 solution was then removed and the seeds were rinsed twice with water. Afterwards, seeds were sown in multi-pot pallets using a BRILL PROfessional growing medium. After sowing, the seeds were stratified in a refrigeration chamber without illumination at approximately 6 °C for 14–22 days (tab. 4.1). The germination and cultivation phases took place in a growing chamber at an average temperature of about 27 °C during the day and about 18 °C at night. Illumination was provided for 16 h per day for 50–52 days in total (tab. 4.1). 14 days before the end of the growing phase, the plantlets were transplanted into individual pots with BRILL TYPical substrate.

**Table 4.1: Duration of *Silphium* seed stratification and *Silphium* plantlets cultivation in the growing chamber.**

| | Number of days | |
|---|---|---|
| Repetition | Stratification | Growing chamber |
| 1 | 14 | 52 |
| 2 | 22 | 50 |
| 3 | 21 | 52 |

### 4.2.5 Production of *S. sclerotiorum* inoculates

To obtain sclerotia, maintenance cultures were established in petri dishes, in which fungal cultures were grown on potato dextrose agar (PDA; 1.8 g/l) for 14 days at 20 °C with light-controlled day-night alternation. Grown sclerotia were afterwards harvested and frozen at - 20 °C for storage. To prepare inoculates, stored sclerotia were first cultured on PDA until mycelial growth was observed. Ten circular areas with a diameter of 1 cm were punched out of the fresh mycelium, placed in 500 ml potato dextrose broth (PDB; 24 g/l) and incubated in a buffled flask for eight days on a shaker at 80 rpm. After completion of the cultivation period, the liquid cultures were homogenized using a Waring Blender. Excess nutrient solution was subsequently decanted and the flasks were filled up with distilled water to a total volume of 500 ml. Care was always taken to ensure that the mycelial suspension had a similar degree of turbidity.

### 4.2.6 Pathogen inoculation

The inoculation of the plantlets, as well as the further steps of the experiment, were carried out in the greenhouse. Within the greenhouse, a chamber with transparent foil as walls and an opaque ceiling was built, to ensure optimal growing conditions for *S. sclerotiorum*. Five plantlets of each accession were used per repetition. All present leaves were treated with the mycelial suspension using spray inoculation. The spray bottles were shaken regularly to prevent sedimentation of the mycelium. Each plant was infected with one single strain of the fungus. Before the plantlets were inoculated, the foil chamber was wetted to raise humidity by evaporation. The individuals were randomized and distributed in such a way that none of the leaves touched each other, followed by an incubation period of 72 h. For more details on greenhouse temperatures, see figure 4.2. After incubation, the side walls of the chamber were removed.

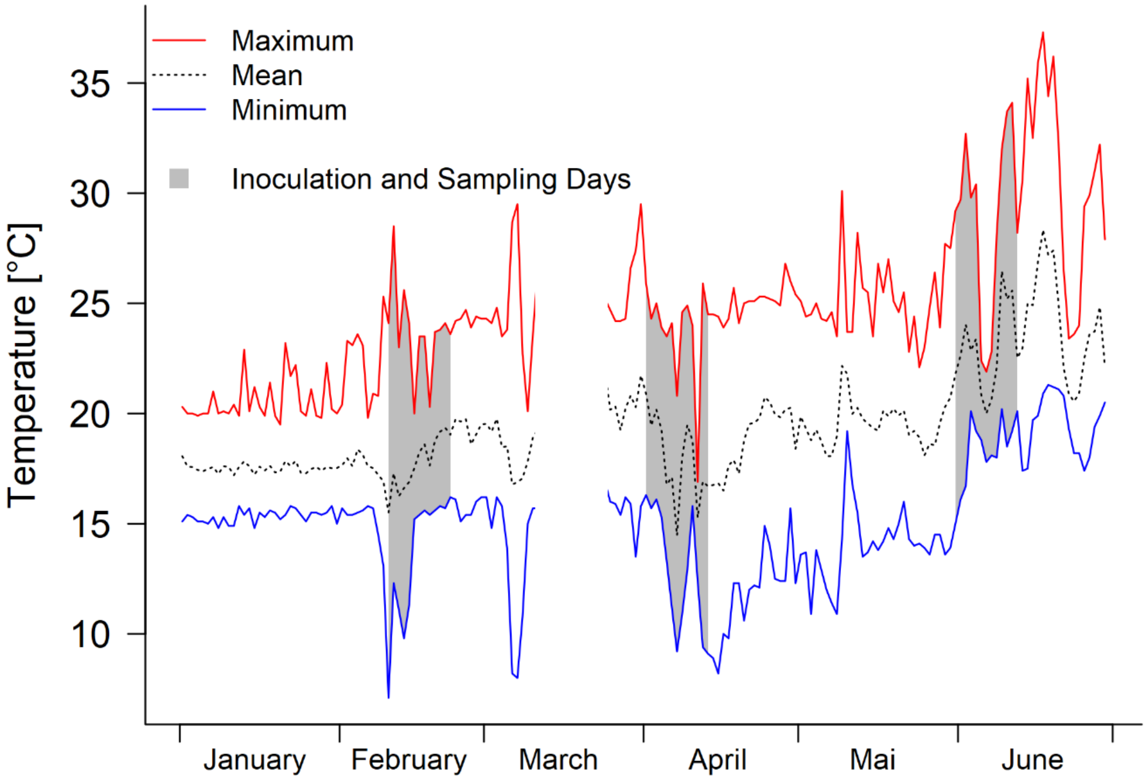

**Figure 4.2: Greenhouse temperature along the inoculation and sampling days between February and June 2021. The daily maximum temperature is displayed as a red line, the daily minimum as a blue line and the daily average as a dotted line. The plantlets were in the greenhouse for 13 days, as marked by the grey area, starting with 3 days of inoculation followed by 10 days of data sampling. Data are missing for about 12 days in March. The gap of missing data does not overlap with the experiment.**

### 4.2.7 Data Sampling

Two resistance-associated parameters were quantified to describe disease progression. First, the relative necrotic leaf area (RNLA) is an estimation of the necrotic area in relation to the individual leaf area (without petiole), where data were in a range of 0 % (no infection) and 100 % (complete necrotic leaf). All infections that were between 0 % and 1 % were titled as 0.1 % to distinguish between infected and not-infected leaves. Dead or fallen leaves were described as 100 %. The second parameter is the relative number of infested leaves, which is the ration of infested- to all leaves of a plantlet. A ten-day daily data sampling of each plantlet was made. Newly formed leaves were added to data sampling at the time of complete leaf unfolding. Due to unequal leaf numbers between the plantlets, a maximum of the oldest three leaves underwent data collection. Data sampling took place at the same time each day.

## 4.3 Results

### 4.3.1 Pathogenicity of *Sclerotinia* inocula for *S. perfoliatum*

The overall means of RNLA on the last day of sampling differed significantly between the used inoculates (fig. 4.3). The lowest pathogen mean of about 5 % was achieved by the *S. sclerotiorum* '*Brassica*' inoculum. Twice as high were the relative necrotic leaf areas of the inocula *S. sclerotiorum* '*Silphium*' and *S. sclerotiorum* '*Helianthus*', with about 10 %, with the strain *S. sclerotiorum* '*Helianthus*' showing a slightly higher, non-significant pathogenicity. On top of the variation between the inocula, the RNLA varied to a significant degree between each experimental repetition for all *Sclerotinia* strains. In all three inocula, RNLA was lowest in the first repetition and had an RNLA of less than one-third in the other two repetitions. For inocula *S. sclerotiorum* '*Brassica*' and *S. sclerotiorum* '*Helianthus*', RNLA increased from the first to the last repetition. Both the minimum RNLA in the first repetition and the maximum RLNA in the second repetition of all RNLA are located in the inoculum *S. sclerotiorum* '*Silphium*'. The significant differences between experimental repetitions suggest that there were factors that affect the measurements despite the same experimental designs.

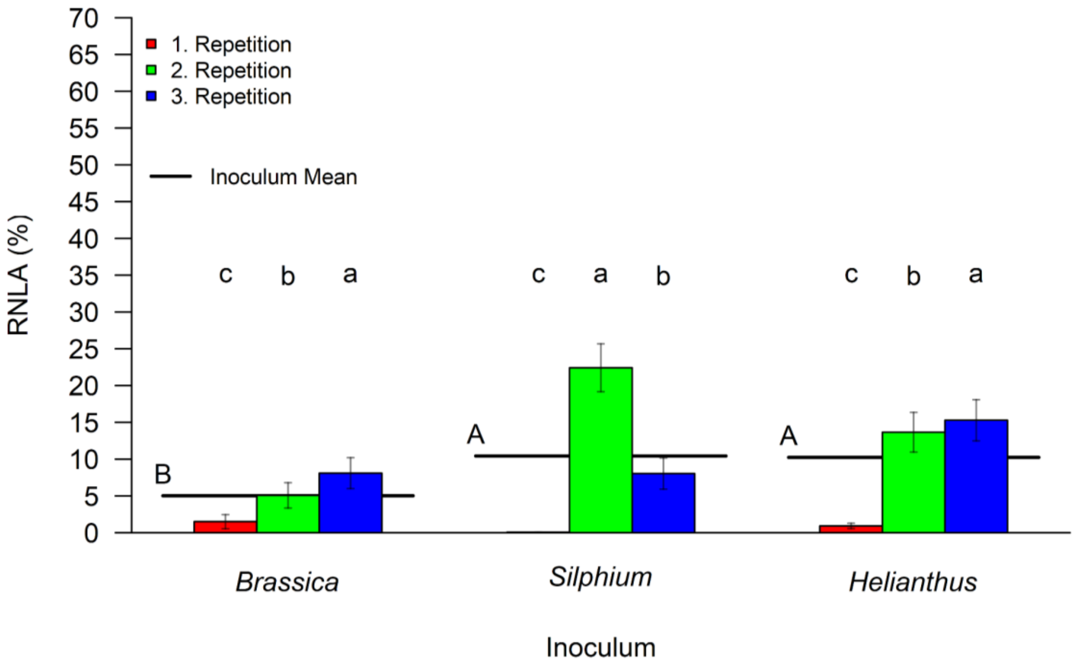

**Figure 4.3: Comparison of elicited relative necrotic leaf area on *Silphium* plantlets between different *Sclerotinia* strains. Leaves of different *Silphium* accessions were infected with one of three different *S. sclerotiorum* strains by spray inoculation. The barplot represents the resulting relative necrotic leaf area for each inoculum of all plantlets from the last sampling day separated by repetition. Red: 1st repetition; green: 2nd repetition; blue: 3rd repetition. The mean value over all three repetitions per inoculum is shown as a horizontal line ("Inoculum mean"). A Kruskal-Wallis test followed by a Bonferroni post-hoc test was used to determine significance. The significance level for both tests was p = 0.05. Significant differences are marked by different letters (a, b and c). The standard error is given as the error indicator.**

### 4.3.2 Infestation process of *S. perfoliatum* accessions after *Sclerotinia* infection

On average, the size of the RNLA increased during the sampling period (fig. 4.4). Furthermore, with increasing RNLA, the standard error increased as well, leading to an uneven grow of necrotic area on the leaves. However, most of the accession infested by *S. sclerotiorum* '*Brassica*' (A) did not show remarkable increase of RNLA along sampling days with values of under 5 %, apart from TLL4, which shows steady growth and the highest RNLA (of more than 20 %) of the *Silphium* collection. SP19, SP26 and TLL6 achieved RNLA close to 0 %. Accessions infested by *S. sclerotiorum* '*Silphium*' (B) which showed high RNLA were SP6, SP16 and SP22. The lowest increase during the sampling days are shown by TLL3, TLL6 and SP14 as well as SP19. Infestation close to 0 % are achieved by SP26 and SP34. Accessions infested by *S. sclerotiorum* '*Helianthus*' showed the highest RNLA. SP26, SP33, TLL4 and TLL6 stand out for small values as well as late and low increase during the sampling period. The highest infestation level with the highest slope of infestation progress is shown by SP6, SP19 and SP34.

In summary of all accessions, Sclerotinia strains and sampling days, SP14, SP26, SP33 and TLL6 show the lowest RNLA. The smallest slopes over the sampling period are achieved by SP14, SP26, TLL3 and TLL6. In contrast, the highest RNLA goes along with the highest slopes for SP6, SP16, SP19, SP22, SP34 and TLL4.

The proportion of infected leaves increased for all accessions in the course of sampling days (fig. 4.5). For inoculum *S. sclerotiorum* '*Brassica*' (A), the difference between the lowest and the highest initial value was about 20 % (SP19, SP22). Between the final values the largest difference was about 40 % (SP16, SP33). The largest increase in proportion of infected leaves during the sampling days was about 60 % (SP33) and the minimum increase was about 10 % (SP16). The minimum and maximum starting value differed in inoculum *S. sclerotiorum* '*Silphium*' (B) by about 40 % (SP6, SP22), the largest and smallest final value by about 25 % (SP22, TLL6). The largest slope is found in SP6 with an increase of about 60 %. The minimum increase was achieved by TLL3 with about 10 %. The largest difference in starting values of the plantlets treated with inoculum *S. sclerotiorum* '*Helianthus*' (C) is about 35 % (TLL4, SP22); the largest difference between the final values is 35 % as well (SP16, SP34). The relative proportion of infected leaved show the largest increase of about 50 % for TLL4 and the smallest of 20 % for SP16. Over all inocula, the lowest initial values of all accessions are found in SP6 and SP19 (natural), as well as in TLL6 (European). The highest initial values are recorded for SP22 (natural) and TLL3 (European). The lowest final values are found for SP19 (natural) and TLL6 (European) and the highest final values are achieved by SP22 (natural) and TLL4 (European). Those accessions with the lowest initial value and the lowest final value are SP19 (natural) and TLL6 (European).

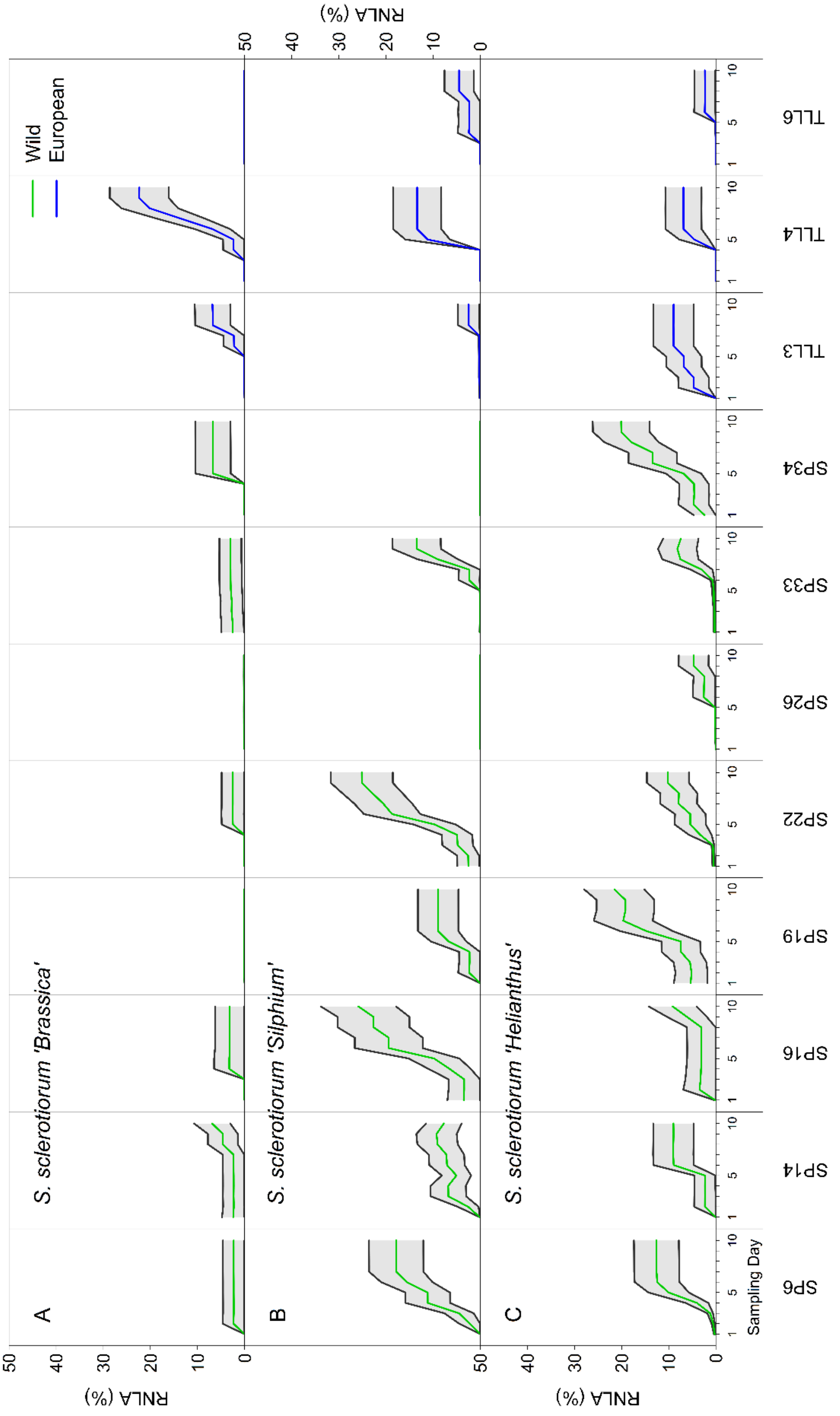

**Figure 4.4: Relative necrotic leaf area of *S. perfoliatum* accessions in the course of time after *Sclerotinia* infection. For each accession, the mean value of the relative necrotic leaf area (RNLA) was calculated per day, per inoculum and over all repetitions. Inocula used: A: *S. sclerotiorum* 'Brassica', B: *S. sclerotiorum* '*Silphium*', C: *S. sclerotiorum* '*Helianthus*'. A time course over ten sampling days was created from means of each day. Colored lines indicate average RNLA. Green lines mark the values of *S. perfoliatum* accessions originating to the natural distribution area (prefix "SP") and blue lines show the values of *S. perfoliatum* accessions available in Europe (prefix "TLL"). The grey area around the average RNLA illustrates the standard errors.**

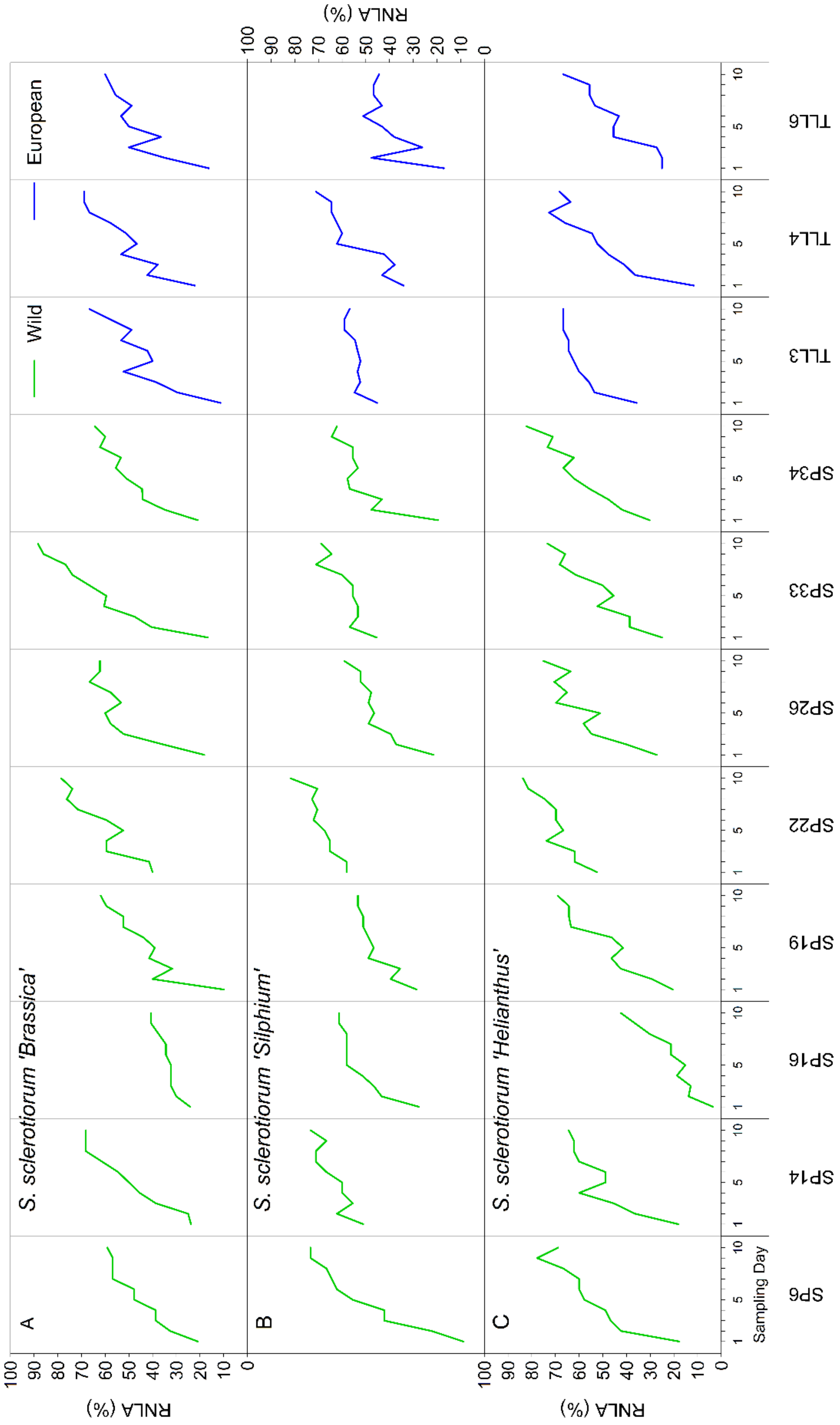

**Figure 4.5: Proportion of infected leaves of *S. perfoliatum* accessions in the course of time after *Sclerotinia* infection. For each accession, the mean value of the proportion of infected leaves was calculated per day, per inoculum and over all repetitions. Inocula used: A: *S. sclerotiorum* 'Brassica', B: *S. sclerotiorum* '*Silphium*', C: *S. sclerotiorum* '*Helianthus*'. A time course over ten sampling days was created from means of each day. Colored lines indicate average proportions. Green lines mark the values of *S. perfoliatum* accessions originating to the natural distribution area (prefix "SP") and blue lines show the values of *S. perfoliatum* accessions available in Europe (prefix "TLL").**

The two estimated values of RNLA 0 % and 0.1 % were sampled most frequently, with frequencies of almost 50 % and 45 % respectively (fig. 4.6). RNLA of 100 % is the third most captured value with a frequency of 5 %. With the exceptions of 45 % RNLA, all other data points range from 0.1 % to 20 %, all with a frequency of under 5 %. It can be determined from the data of figure 4.4 and figure 4.6 that necrosis on the leaves grows throughout the sampling days and that 45 % RNLA was the highest recorded value before the leaves died (100 % RNLA). However, in some cases the leaves did not die and had a maximum RNLA between and including 0 % and 45 % over the sampling period.

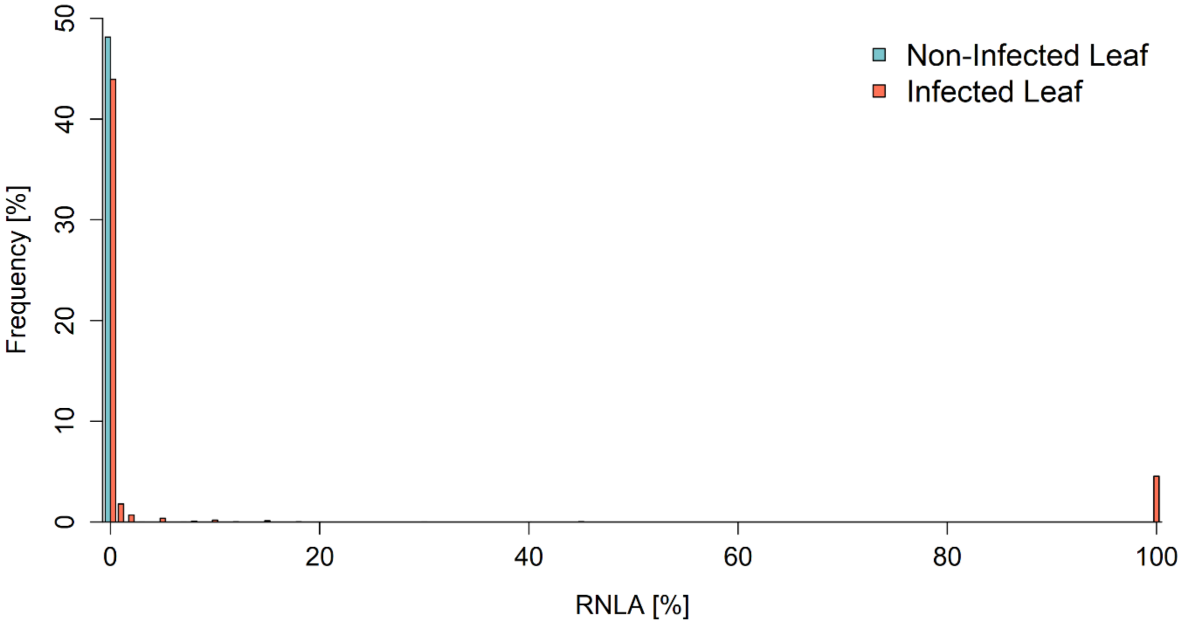

**Figure 4.6: Histogram of relative necrotic leaf areas (RNLA) of *S. perfoliatum* accessions after infection with *S. sclerotiorum* over ten days of sampling. The frequency of the value of 0 % (non-infested) is shown in blue, all data of infested leaves are marked in red.**

## 4.4 Discussion

### 4.4.1 Variability of Pathogenicity in the *S. Sclerotiorum* collection to *S. perfoliatum*

In previous experiments, the pathogenicity of *S. sclerotiorum* was investigated on various crops, such as soybean (*Glycine max*), oilseed rape (*brassica napus*), sunflower (*Helianthus annuus*) or common bean (*Phaseolus vulgaris*). This study is the first one working on *Silphium* (Pascual et al., 2010; Wegulo et al., 1998; Garg et al., 2010a).

The higher pathogenicity of the *Sclerotinia* strains harvested from *Silphium* and sunflower (fig.4.3) might be due to systematics, or the underlying degree of relationship of the plant host species. There is a closer genetic relationship between the two species *Silphium perfoliatum* and *Helianthus annuus*, which both belong to the tribe *Heliantheae*, than between *Brassica napus*, which belongs to the *Brassicaceae*, and *Heliantheae*. Systematics and phylogeny suggest that closely related plant species have more similar genetics, but in some cases also more similar phytochemical and biochemical characteristics, than more distantly related species. Studies from the field of chemotaxonomy suggest that taxonomic classification of plant species is also possible based on metabolite profiles, albeit with certain limitations (Liu et al., 2017; Grayer et al., 1999). Genetic adaptation is widespread among phytopathogenic fungi (Li et al., 2020). Durman et al. (2005) demonstrated that *S. sclerotiourum* populations from different plant hosts showed differences in the production of oxalic acid, among other compounds. On top of that, oxalic acid was identified as one of the major virulence factors of *Sclerotinia* (Kim et al., 2008). Accordingly, it can be hypothesized that an *S. sclerotiourm* strain adapted to the phenotypic and molecular conditions from sunflower and specialized to this host species will be more virulent to *Silphium* than a strain specialized to oilseed rape.

In contrast, other studies suggest that intraspecific genetic variability of *S. sclerotiourum* populations more likely due to genetic recombination as well as gene flow between populations (Kamvar et al., 2017; Aldrich-Wolfe et al., 2015; Atallah et al., 2004). This is illustrated by the fact that differences in intraspecific pathogenicity can also be found in *S. sclerotiorum* populations isolated from a single crop (Ekins et al., 2007). Another reason for variability in oxalic acid production or virulence among the Sclerotinia strains tested could be influenced by their environmental origin. Sexual recombination of *Sclerotinia* is thought to be driven by abiotic environmental factors (Aldrich-Wolfe et al., 2015). In the literature, increased genetic variability has been found in *S. sclerotiorum* populations from sub-tropical regions with average annual temperatures above 20 °C, compared to populations from temperate regions with average annual temperatures of 8 °C (Lehner & Mizubutti, 2017; Carbone & Kohn, 2001). This is explained by an increased carpogenic germination rate under subtropical conditions and confirmed by Huang (1991), who observed exclusively myceliogenic germination when sclerotia were exposed to temperatures below 0 °C. Site-specific influence might be rejected, since all *S. sclerotiorum* strains were collected in a temperate region (Germany), which inhibits genetic recombination to a certain degree.

In the literature, *Sclerotinia* is classified as necrotoph (Amselem et al., 2011; Liang & Rollins, 2018) or as hemibiotroph pathogen (Singh et al., 2020; Kabbage et al., 2013). Based on the data of figure 4.6, *S. sclerotiorum* classifies as hemibiotroph, as a biotroph pathogen it would have shown less infestation and for a necrotrophy pathogen the abundancies would have been more uniformly distributed around the whole spectrum (0–100 %).

In general, the infestation level was low along the three repetitions. This might be partially explained by non-optimal humidity levels in the foil chamber at the time of inoculation. Furthermore, the infestation level varied between each repetition, which could have multiple reasons. One reason may be the temperature of the greenhouse at inoculation. The colder it was, the lower were the resulting necrotic leaf areas. Another reason for the irregular infestation success might be differences in the amount of mycelium applied to each leaf. It is not possible to control this using spray inoculation, especially because the concentration of mycelium in the inocula could not be exactly determined. There is a method of applying a defined amount of ascospores (Young et al., 2004), but since this method is time intensive and a high sample size was investigated, spray inoculation was chosen.

### 4.4.2 Variability of Resistance in *S. perfoliatum* accessions against *S. sclerotiorum*

The accessions showing resistance-associated phenotype differ between relative necrotic leaf area and relative number of infested leaves. Regarding the former, SP26, SP33, SP14 and TLL6 stand out for their late developing small necrotic leaf area. In contrast to that, SP19 and TLL6 showed the smallest number of infested leaves. There are several approaches to explaining the outstanding performance of these accessions.

First, the European plant material offers resistant and susceptible accessions. TLL6, the most resistant one, was subject of a plant breeding program in the former USSR (Wever et al., 2019). It can be assumed that that the resistance of *Silphium* to *S. sclerotiorum* was improved via selection. TLL4, the most susceptible accession, is one of the most widespread (if not the most widespread) accession in Europe due to its high yielding potential. Therefore, the European plant material symbolizes both the opportunity and the obligation to increase the resistance to *S. sclerotiorum* during the breeding process.

Second, based on the widespread and geographically distinct locations of the wild *S. perfoliatum* collection, it seems possible that *Silphium* adapted to different geologic and climatic conditions and evolved certain resistances against *S. sclerotiorum*. Several studies on maize (*Zea mays*), poplar (*Populus tomentosa/beijingensis*), horn clover (*Lotus corniculatus var. japonicus*) and others have demonstrated that different ecotypes are more resistant to specific pathogens (Wu et al., 2013; Li et al., 2019; Bordenave et al., 2013). Combining the geographic origin and RNLA after ten days of the natural accessions (fig. 4.1, fig. 4.4), three clusters are revealed. The clusters with a higher average RNLA are located in the north-west (SP6 and SP34) as well as in the south-east (SP16, SP19, SP22). The third cluster, with more resistant accessions, ranges from central-north (SP14) to central-west (SP26 and SP33). For further evidence, more accessions of the *Silphium* collection need to be investigated.

## 4.5 Conclusion

Even though the infestation success of *Sclerotinia sclerotiorum* strains on different plant hosts varied widely, all strains were able to infest a broad range of *Silphium perfoliatum* accessions. The phylogenetic relation of the plant hosts seems to have the biggest impact on the results. Furthermore, the most resistant *S. perfoliatum* accessions were identified (SP26, SP33, SP14, SP19 and TLL6) as well as the most susceptible ones (SP6, SP22, TLL4). Further research might reveal more accessions with as yet undiscovered potential. Hypotheses for all these findings were formulated and need to be reviewed. Beside knowledge about *Sclerotinia* and its virulence, *Silphium* and its resistance as well as the plant-pathogen-system *Silphium*/*Sclerotinia* are fundamentals that needs to be closer investigated to create a sustainable crop out of *Silphium* in the future.

# 5 Phenotypic variation of seed yield, seed geometry and seed oil traits in wild *Silphium perfoliatum* L. accessions

This manuscript is still to be submitted:

**Christop A. C. Korte**, Christian Wever, Martin Greve, Georg Hölzl, Peter Dörmann and Ralf Pude (2024). Variation of seeds in wild *Silphium perfoliatum* L. accessions: Evaluation of yield, geometry and oil traits. Unpublished manuscript.

## 5.1 Introduction

The genus *Silphium* is part of the *Asteraceae* and closely related to the well-known sunflower (*Helianthus annuus* L.) (Clevinger & Panero, 2000). The perennial cup plant (*Silphium perfoliatum* L.) is a promising candidate for sustainable biomass production (Wever et al., 2020; summarized in Gansberger et al., 2015; Peni et al., 2020). Cup plant Is already cultivated in Middle Europe on several thousand hectares for biomass, e.g., in Germany on around 10,000 ha (FNR, 2023), mainly as a substitute for energy maize (*Zea mays* L.). In the first year of cultivation the plants form a soilborne rosette with no worthwhile yield (Greve et al., 2023). In the subsequent years biomass is harvested between August and September, at which time dry matter (DM) contents of 25–27 % are favorable (Biertümpfel et al., 2018). The reported biomass yield is heterogeneous and can exceed 20 Mg dry matter per hectare (ha), and is mainly used as substrate for biogas reactors or livestock feed (summarized in Gansberger et al., 2015; Peni et al., 2020). Interest is growing in dual usage of silage *Silphium*, since a procedure has been presented that allows the extraction of the fibers from the biomass before using it as an energy source (Neis-Beeckmann, 2021). On top of that, other reported uses are harvesting senescent cup plant biomass and using it for material applications like pulp and paper production (Höller et al., 2021) or like expanded polystyrene substitute (Moll et al., 2022). To reduce costs, *Silphium perfoliatum* is sown directly on the field. Problems of seeders handling *Silphium* seeds are its heterogenicity as well as the small size (Schäfer et al., 2016). Due to its rich flower formation during the long flowering period from July to September (summarized in Gansberger et al., 2015; Peni et al., 2020), *Silphium* is considered as oilseed crop as well. Aside from their use as biomass, seeds of *S. perfoliatum* should also be considered for plant breeding. Increasing the seed size has been one of the first breeding goals that were achieved in many other crops, such as sunflower. Larger seeds show better vigor and emergence rates.

The previously mentioned heterogeneity of *Silphium perfoliatum* seeds can be found within and between studies. Most of the heterogeneity on the field and between locations can be explained by its unbred stage, but a certain amount of the spread between different working groups might occur because different populations of *Silphium* were cultivated. Until today it is uncommon in the literature to provide closer information about the origins of the investigated cup plant material. Wever et al. (2019) analyzed the circulating gen material in Europe, which does not show high genetic variance. Only one population from Ukraine showed a genetic distance to the main gene pool, maybe caused by aimed selection during breeding attempts for this species in the former Soviet Union. Even though the presence of phenotypic and genetic variation within the European plant material (available in Europe) improves the evidence for an improvement of the overall plant performance via selection or breeding, the single European accessions seem to share their ancestry. This leads to the assumption that the European genotypes originate from the same geographic location (Wever et al., 2019). To increase the available variation, wild *S. perfoliatum* populations were gathered on a trip through the plant's native range in North America.

The aim of this study is to describe the variation of seed yield, seed geometric and seed oil traits of the wild *Silphium* collection, as well as to compare the variation to the already available cup plant germplasm in Europe. In addition, seed yield and seed geometric traits are considered in dependence of flowerings ranks. The goal is to create awareness of the urgency of providing accurate information about the origins of plant material itself as well as the analyzed flowering ranks of cup plant for upcoming studies. Beyond that, the results can be useful as a database for future breeding programs.

## 5.2 Material and Methods

### 5.2.1 Plant Material

The map of locations (figure 5.1) shows all accessions used in this study. The wild accessions gathered on a collecting trip through the natural distribution area of *S. perfoliatum* in 2016, are marked with the prefix "SP" and a black dot on the map. Accessions used for seed yield and seed geometric trait analyses are labeled with red dots. The yellow dots show populations utilized for seed oil trait examination. Some accessions have been left out for this study, but those that were used still cover the entire natural distribution area of *S. perfoliatum*. Because of their unknown origin, the European plant material is displayed outside the map. This plant material was gathered by the TLL (Thüringer Landesanstalt für Landwirtschaft) in Europe.

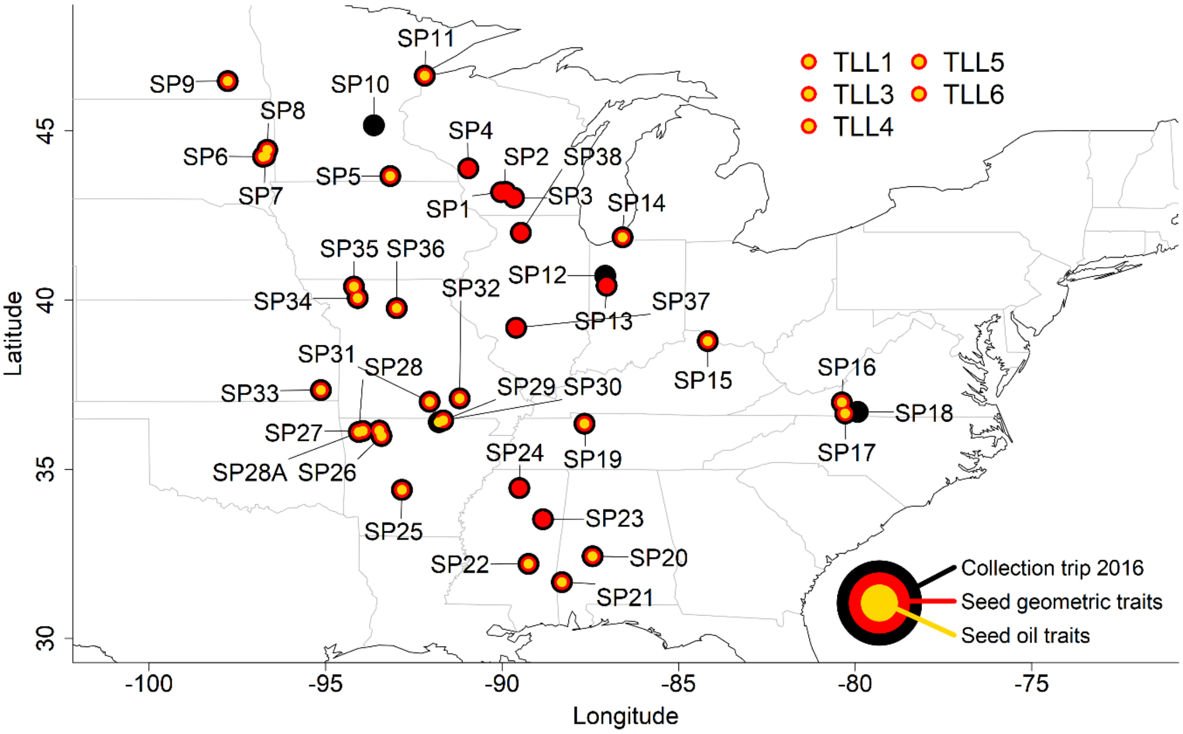

**Figure 5.1: Used accessions for seed geometric, seed yield and seed oil traits. Map of location sites of collected *Silphium perfoliatum* (SP1–SP38) during the hunting trip in 2016, as well as the European plant material (TLL1, TLL3–TLL6), which is displayed outside the map, because of unknown origination in the native range. The natural sites are located equally along the borders of the native distribution area in North America. The big black dots mark the location sites. The medium sized red dots indicate wild/European accessions which have been used in this study for seed yield and seed geometric traits analyses. The small yellow dots represent accessions that were used for the examination of seed oil traits.**

### 5.2.2 Seed material

The seeds for yield, geometry and oil trait analysis were obtained from different field trials at Campus Klein-Altendorf near Bonn, Germany (Lat: 50.615684, Long: 6.985003). The dominating soil type there is haplic luvisol. Long-term mean annual air temperature and precipitation amount are 9.5 °C and 606 mm.

The plants for seed yield and geometry analysis originated from established individuals in the botanical garden of the University of Düsseldorf. The rhizomes of all plants were dug up and divided on March 30, 2021. the next day, these rhizome pieces were planted to establish the field trial “Zuchtgarten” at Campus Klein-Altendorf in accession-wise plots of eight plants with two rows of four individuals each. The space between the plants was 0.7 m in each direction.

The seed-producing plants for seed oil phenotyping were pre-cultivated in the greenhouse for 12 weeks with temperatures fluctuating between 6 and 25 °C. Afterwards, the plantlets for the field trial “GEniu*S* II” were planted, on July 5 and 6, 2017. The plantlets were irrigated on the day of planting and one week later to support plant establishment. Weed control was carried out manually and mechanically as necessary. The field trial had a randomized block design with three replications. Each plot contained four rows of nine plants, with a row distance of 0.5 m and a plant distance within the row of 0.65 m, resulting in a plot size of 7.8 m² and a plant density of 3.1 plants per m². The matured seeds were collected on 29 September 2020 in the second repetition of the field trial without considering either individual plants nor flowering ranks.

### 5.2.3 Data Sampling

For the seed geometry analysis, seeds were collected throughout the flowering period to obtain samples of several flowering ranks of *Silphium perfoliatum*. Six plants of each accession were investigated and one flower head of the flowering ranks 1–6 served as a sample. After inflorescences were openly pollinated, flower heads were covered with bags, in order to catch the seeds and prevent any seeds from scattering in the course of maturation. Not all accessions formed six flowering ranks. Beyond that, shoot buckling and predation caused further reductions in the sample size. The collected seeds of each bag were counted and weighted. The total weight was divided through the number of seeds in order to calculate the average single seed weight. Afterwards, up to 10 seeds of each flower head and a reference were arranged in front of a strong backlight to increase the contrast between seed and background. A photo was taken with a Panasonic camera (DMC-G81M) of the top view. To analyze these images, a program was developed on the basis of the supplementary code of Reinert et al. (2019). First the photo was turned into a negative and afterwards into a gray-scale image, so that the seeds became bright and the background became dark. Using an image-specific threshold for brightness, the photos were transformed into binary images, which contain only black (background) and white (seeds) pixels. Subsequently the area of each seed was determined. Then, the center of mass and the rotation of the seed were determined, by finding the elliptical fit of the seed. Achene length was defined as the length of the line that passes through the center of mass and has the slope of the rotation. Achene width was quantified as the longest line perpendicular to the achene length line. Lastly, the eccentricity was determined by the square root of 1 minus the squared minor axis divided by the squared major axis, using the elliptical fit (Pau et al., 2010).

Since only one flower head per flowering rank was investigated, formulas for the number of theoretical flower heads per rank as well as the sum up to a specific rank were deduced. This allowed for evaluating the potential grain yield per shoot.

A fatty acid methyl ester (FAME) analysis was performed for ten single seeds of each accession in order to identify and quantify the seed oil content and composition. First, seeds were prepared for the analysis by removing the chaff and drying the resulting seeds for five days in an exicator. After seed weight was determined, the seeds were put into a reaction tube along with ceramic beads 600 µl 1N methanolic HCL and 300 µl internal standard (15:0 in methanol; 2 mg/ml), and ground in a Precellys 24 Homogenizer (Bertin) at 6000 rounds per minute. They were ground twice for 30 seconds, with a 60second pause between grinding cycles. Afterwards, the reaction tubes were incubated at 80 °C for 40 minutes. 400 µl 0.9 % NaCl and 400 µl hexane were added to reaction tubes, which were then shaken vigorously and centrifugated for 60 seconds at 21380 g afterwards. Vials were prepared depending on the initial determined seed weight. For samples of seeds with a weight minor to 10 mg, 120 µl of hexane and 30 µl of hexane phase from reaction tube (2$^{nd}$ phase) were put in the vial. For samples of seeds with a weight superior to 10 mg, the ratio of hexane to fatty acid methyl ester solved in hexane was changed to 135 µl hexane and 15 µl of hexane phase from reaction tube, to reduce quantification errors in the subsequent step, where the samples were analyzed using a gas-chromatograph with flame ionization detector (GC-FID; Agilent Technologies, 7890 A). For graphical representation, unplausible measurements have been filtered out (three in total).

### 5.2.4 Data Analysis

Both the program to analyze the seed geometric traits as well as Graphics and Statistics were conducted using the R programming language version 4.3.1 (R Core Team, 2023). The R package “maps” was used to visualize the collection sites of *Silphium* accessions on a map (Becker et al., 2022). The “basicPlotteR” library by Crispell (2021) served to put text labels on the map without any overlap. The program to analyze the photos of seeds was programmed on the basis of the supplementary code of Reinert et al. (2019) and used the package “EBImage” by Pau et al. (2010). An ANOVA, followed by Tukeys HSD-test, was used to perform the statistical grouping of the geometric and yield traits along the flowering ranks ($\alpha = 0.05$). In the figures, data are displayed as arithmetic means with standard deviations for sample sizes below 20; otherwise, boxplots were chosen. The constriction of each boxplots represents the range of its 95 % confidence interval.

## 5.3 Results

The average achene area (tab. 5.1) of the first flowering rank is 64.19 mm² and steadily decreases from there to 48.26 mm² in the sixth flowering rank (a reduction of 18 mm² in total). The differences between the flowering ranks are all significant. The achene length and width follow the same trend and the same magnitude. Both show values along all flowering ranks reduced by 1 mm. The values of achene length decrease from 10.43 mm to 9.24 mm and those of achene width from 7.51 mm to 6.50 mm. With the exception of the fifth and sixth, all flowering ranks differ significantly. The smallest differences of achene area, length and width are between the second and third rank, as well as between the fifth to sixth flowering rank (illustrated by non-significant grouping in achene length and width, respectively). The eccentricity is constant over all flowering ranks with values between 0.72 and 0.74. Seeds per flower head shows the least number of significant differences and a total reduction of 2.5 seeds per flower head along the flowering ranks (from 24.41 to 21.93). The only variable with its maximum not in the first flowering rank is single seed weight. The weights increase from the first (22.13 mg) to second (22.55 mg) flowering rank by 0.42 mg on average. From that point on they follow the decreasing trend to 12.34 mg in the sixth flowering rank, which is a weight loss of about 55 %. The biggest reductions appear after rank number 4. The sample sizes of achene area, achene length, achene width and eccentricity, as well as those of seeds per flowerhead and single seed weight, are identical and decrease along the flowering ranks.

**Table 5.1: Seed geometric and seed yield traits along the flowering ranks. One flower head of each rank (1–6) was analyzed. Phenotyped seed traits are: achene area in mm², achene length in mm, achene width in mm, eccentricity, seeds per flower head and single seed weight in mg. The seeds were harvested in 2021. All plants have been cultivated since 2021 in the field trial "Zuchtgarten" at Campus Klein-Altendorf, near Bonn, Germany.**

| Trait | Rank | Average | | Standard deviation | Statistical grouping | Sample size |
|---|---|---|---|---|---|---|
| Achene area (mm²) | 1 | 64.19 | ± | 15.10 | a | 2336 |
| | 2 | 61.36 | ± | 14.52 | b | 2241 |
| | 3 | 59.79 | ± | 13.79 | c | 2293 |
| | 4 | 56.01 | ± | 13.28 | d | 2180 |
| | 5 | 50.84 | ± | 11.93 | e | 1980 |
| | 6 | 48.26 | ± | 12.34 | f | 850 |
| Achene length (mm) | 1 | 10.43 | ± | 1.28 | a | 2336 |
| | 2 | 10.22 | ± | 1.26 | b | 2241 |
| | 3 | 10.04 | ± | 1.21 | c | 2293 |
| | 4 | 9.74 | ± | 1.21 | d | 2180 |
| | 5 | 9.35 | ± | 1.16 | e | 1980 |
| | 6 | 9.24 | ± | 1.26 | e | 850 |
| Achene width (mm) | 1 | 7.51 | ± | 1.03 | a | 2336 |
| | 2 | 7.39 | ± | 1.05 | b | 2241 |
| | 3 | 7.32 | ± | 1.05 | b | 2293 |
| | 4 | 7.05 | ± | 1.01 | c | 2180 |
| | 5 | 6.74 | ± | 0.99 | d | 1980 |
| | 6 | 6.50 | ± | 1.02 | e | 850 |
| Eccentricity | 1 | 0.73 | ± | 0.09 | ab | 2336 |
| | 2 | 0.72 | ± | 0.09 | bc | 2241 |
| | 3 | 0.72 | ± | 0.10 | c | 2293 |
| | 4 | 0.72 | ± | 0.09 | bc | 2180 |
| | 5 | 0.72 | ± | 0.10 | bc | 1980 |
| | 6 | 0.74 | ± | 0.09 | a | 850 |
| Seeds per flowerhead | 1 | 24.41 | ± | 5.50 | a | 234 |
| | 2 | 23.19 | ± | 5.76 | ab | 224 |
| | 3 | 23.03 | ± | 5.56 | b | 230 |
| | 4 | 23.00 | ± | 4.30 | b | 219 |
| | 5 | 22.29 | ± | 4.30 | b | 198 |
| | 6 | 21.93 | ± | 4.18 | b | 85 |
| Single seed weigth (mg) | 1 | 22.13 | ± | 6.44 | a | 234 |
| | 2 | 22.55 | ± | 6.71 | a | 224 |
| | 3 | 21.64 | ± | 6.66 | a | 230 |
| | 4 | 19.16 | ± | 6.69 | b | 219 |
| | 5 | 14.98 | ± | 6.13 | c | 198 |
| | 6 | 12.34 | ± | 5.63 | d | 85 |

For each natural number $n \geq 1$, let $f(n)$ denote the number of flower heads in rank $n$. Figure 3.2 shows that $f(n) = 2^{n-1}$, as the number of heads doubles in each rank. Therefore, the total number of heads up to a certain rank n reads:

$$F(n) = \sum_{j=1}^{n} 2^{j-1} = 2^n - 1$$

A proof that the last equality holds is found in the Appendix.

Table 5.2 displays the results of the functions f and F up to the sixth flowering rank. The starting point of both is 1. The number of flower heads per rank (f) doubles with each additional rank and reaches 32 in the sixth flowering rank, whereas the sum of flower heads up to a specific rank (F) double and is increased by 1 with each additional rank and achieves 63 in the sixth flowering rank.

**Table 5.2: Theoretical number of flower heads per rank (f) and their sum up to this point (F) of the first six flowering ranks.**

| Flowering rank | f | F |
|---|---|---|
| 1 | 1 | 1 |
| 2 | 2 | 3 |
| 3 | 4 | 7 |
| 4 | 8 | 15 |
| 5 | 16 | 31 |
| 6 | 32 | 63 |

The accessions in figure 5.2a show differences in their median achene areas as well as in their specific spread. The overall average of the achene areas is 65 mm². SP15, SP21 and SP23 are the accessions with the highest medians of 85 mm², 100 mm² and 80 mm², as well as those with the highest recorded achene areas of between 110 and 120 mm². The accessions with the smallest achene areas are SP5, SP11, SP28, SP32 and TLL6, for which the data points are all below the overall average with medians between 40 and 50 mm². The highest spreads are formed in SP23, SP31, SP34, SP36 and TLL3; all cover an interval of about 50 mm² between minimum and maximum achene area. There are certain similarities between the maximum achene area (fig. 5.2a) and the maximum achene length (fig. 5.2b). Again, SP15, SP21, SP23 and SP19 are the accessions achieving the highest results with 12 mm (14 mm for SP21) length. Accessions with the lowest achene lengths are SP5, SP11 with values between 8.5 and 9 mm. The average of all data points is 10.5 mm. The smallest detected achene lengths are around 7 mm by SP17 and SP27. The highest variation within the accessions SP31, SP34, SP36 and TLL3. The achene width (fig. 5.2c) again shows similarities to the achene area (fig. 5.2a) and an average of 8.5 mm. The accessions with the highest values are SP15, SP21, SP22 and SP23 with medians between 8.5 and 9.5 mm. The lowest widths of about 6 mm are achieved by SP5, SP11 and TLL6. The highest spread is shown by SP23, SP31, SP34, SP36, TLL3 and TLL6. The eccentricity (fig. 5.3a) is the seed geometry parameter with the least variation between the accessions. The majority of accession medians are around the overall mean of 0.72. Nevertheless SP9, SP19, SP31 and SP35 stand out for their confidently high values of 0.8 and above. The lowest eccentricity of 0.6 is achieved by SP22. The widest spreads in eccentricity are found in SP16 and SP17, with data between 0.2 and 0.85, as well as in TLL6, which ranges from 0.35 to 0.95. The average seeds per flower head of all accessions (fig. 5.3b) is about 25.

The highest number of seeds was produced by SP32 with an average of 33. Other accessions with above average seed production were SP9, SP13, SP14, SP15, SP23 and SP32, which all produced around 30 seeds per flower head. SP16 and SP17 achieved, with 15 and 10 seeds per flower head, the lowest results in seed setting, followed by TLL6 and SP5, with a seed production of below 20. The highest spreads with standard deviations of greater than 5 were found in SP1, SP3, SP20, SP21, SP25, SP27, SP32, SP35, TLL1 and TLL3. The average weight of single seeds (fig. 5.3c) was 22 mg. The greatest values with 31 mg were achieved by SP15 and SP17. The lightest seeds (12–14 mg) were produced by the accessions SP24, SP25, SP32 and TLL6. The highest spread is shown by SP27, the lowest by SP28.

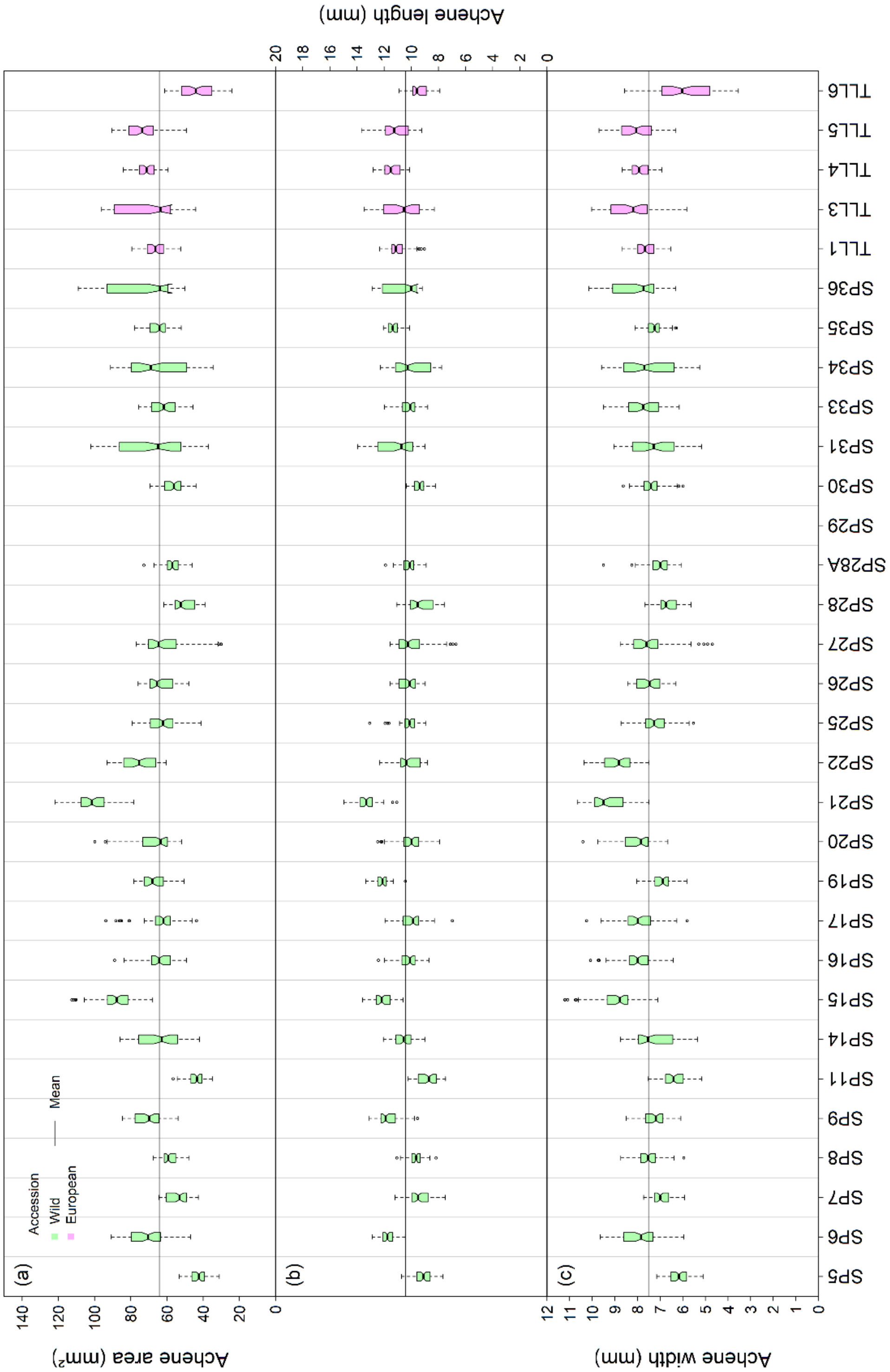

**Figure 5.2: Boxplots (a–c) with n=40–60 of achene area in mm$^2$ (a), achene length in mm (b) and achene width in mm (c) of seeds harvested in 2021 as a function of the *Silphium perfoliatum* accessions. The constrictions of the boxplots (a–c) mark the 95%-confidence interval of the median. The black line is on the level of the overall mean of the parameter. The light-green coloring indicates wild accessions, the magenta coloring represents the European plant material. The achene area is the entire visible surface of a seed (a). The achene length is defined as the line passing through the center of mass and having the slope of the seeds rotation (b). The achene width is the longest perpendicular of the achene length (c). All plants have been cultivated since 2021 in the field trial “Zuchtgarten” at Campus Klein-Altendorf, near Bonn, Germany.**

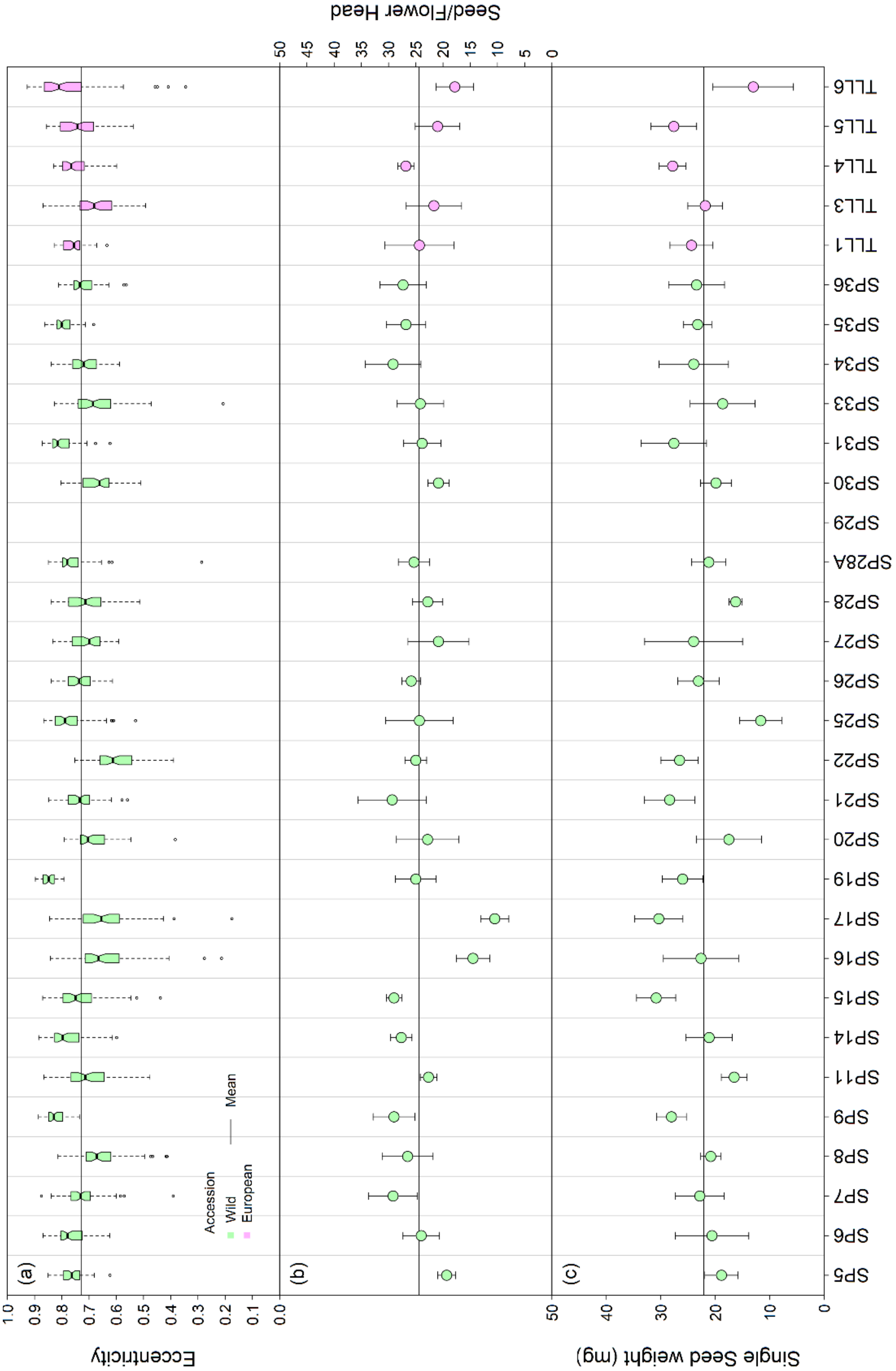

**Figure 5.3: Boxplots (a) with n=40–60 and dot plots (b, c) with n=4–6 of eccentricity (a), seeds per flower head (b) and single seed weight in mg (c) of seeds harvested in 2021 as a function of the *Silphium perfoliatum* accessions. The constrictions of the boxplots (a) mark the 95%-confidence interval of the median. The black line is on the level of the overall mean of the parameter. The light-green coloring indicates wild accessions, the magenta coloring represents the European plant material. Eccentricity was calculated using ellipsoidal fit parameter (a). Seeds per flower head were counted (b). Single seed weight is the average weight of seeds of one flower head (c). All plants have been cultivated since 2021 in the field trial “Zuchtgarten” at Campus Klein-Altendorf, near Bonn, Germany.**

The oil content (fig. 5.4a) reached an average of about 390 mg/g. The accessions with the highest oil contents with 420–440 mg/g were SP25, SP29, SP35 and SP36. In the European collection, TLL3 stood out for its high oil content with 410 mg/g, while all other European accessions were below average. SP17 delivered the lowest oil content (325 mg/g) followed by SP15 (340 mg/g). The accession means of the portion of myristic acid (fig. 5.4b) range between 0.015 mg/g and 0.03 mg/g (0.02 mg/g on average). SP5–SP19 and SP36, as well as SP22 and all European accessions, contained above average portions of 14:0. The highest values were achieved by SP6, whereas the lowest contents were detected in SP20, SP21, SP27 and SP28. The portion of 16:0 (fig. 5.4c) of most accessions was close to the overall average of 0.06 mg/g. SP5 and SP6 stand out for their large contents of 0.065 mg/g, as do SP16 and SP17 with 0.07 mg/g. The lowest palmitic acids accumulation of 0.055 mg/g was found in SP9, SP20 and SP21. The spread and the mean of the portion of 18:0 (fig. 5.5a) seem to be correlated. Above average means have greater standard deviations as well. This indicates that these greater means are achieved by single samples with greater portions of stearic acid. The maximum means of 0.027 were found in SP28 and TLL5. The smallest portion of 18:0 was produced by SP33, followed by SP21, both at the magnitude of 0.01. The overall average was 0.018 mg/g. The average portion of oleic acid (fig. 5.5b) was about 0.16 mg/g. The greatest portions were achieved by TLL4 and TLL5, followed by SP5, SP8, SP9, SP11 and SP20 with values up to 0.20 mg/g. The lowest portion of 18:1 with 0.12 mg/g was shown by SP15, SP27 and SP29. By far the greatest average portion of every fatty acid is shown by 18:2 (fig. 5.5c), with an average of 0.745 mg/g. Again, means and standard deviation seem to be correlated, but in contrast to the results of figure 5.5a, low means are accompanied by wide spreads. TLL4 and TLL5 show the lowest contents of linolic acid (about 69 mg/g), followed by the northern accession SP5–SP11 with values of around 0.70 mg/g. The greatest results (0.77–0.80 mg/g) were achieved by SP15, SP21, SP25, SP27, SP29 and SP30. In addition, all of them have smaller standard deviations than the previously mentioned accessions.

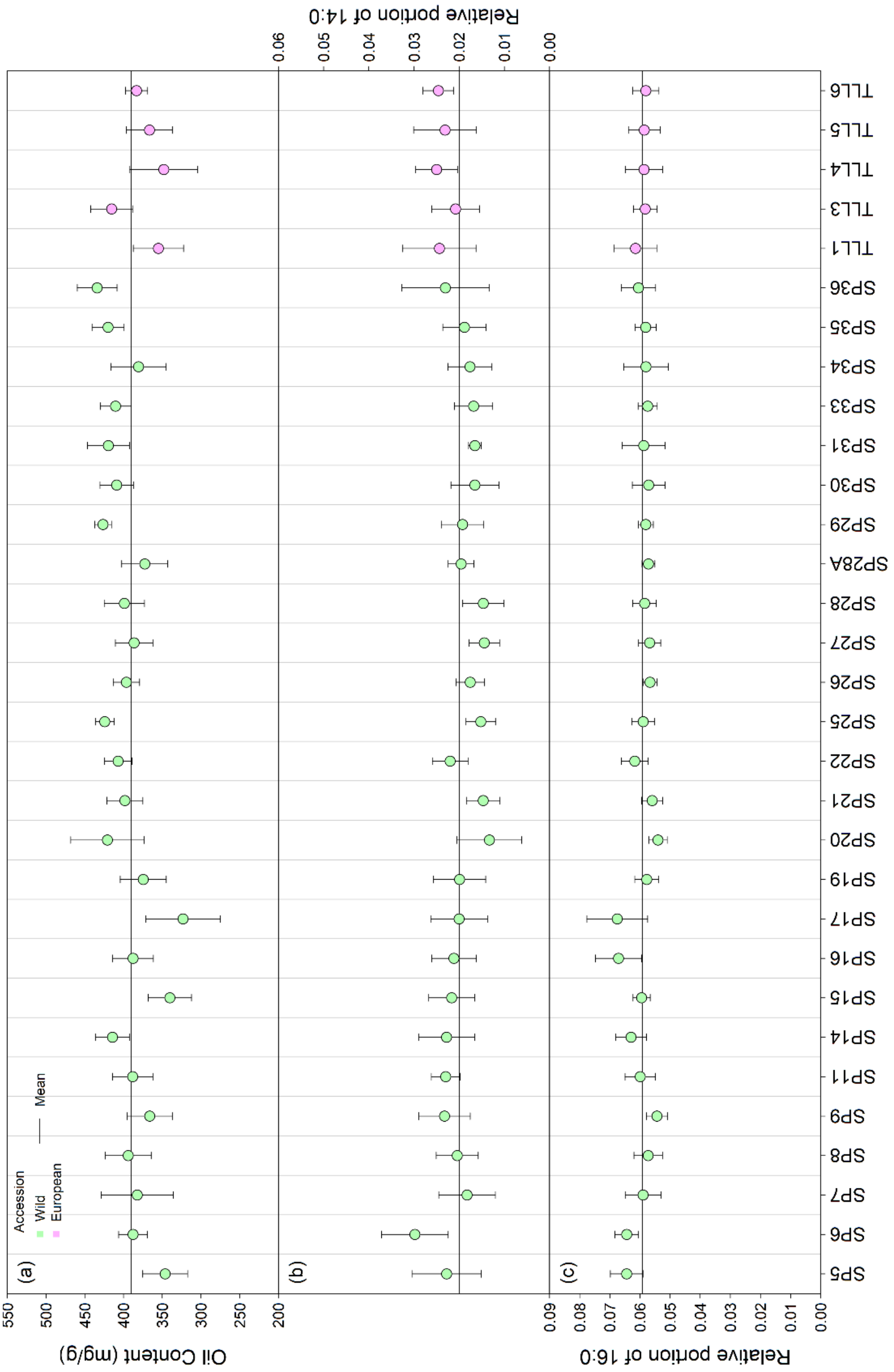

**Figure 5.4: Dot plots (a–c) with n=10 (exceptions: SP5 with n=9 and SP33 with n=14) of oil content (a) as well as the portions of 14:0 (b) and 16:0 (c) of seeds harvested in 2020 as a function of the *Silphium perfoliatum* accessions. The black line is on the level of the overall mean of the parameter. The light-green coloring indicates wild accessions and the magenta coloring represents the European plant material. The oil content was calculated by dividing the total amount of oil by the seed weight (a). The portions of the single fatty acids were calculated by dividing the total amount of the respective fatty acid by the total amount of oil (b, c). All plants have been cultivated since 2017 in the field trial “GEniu*S* II” at Campus Klein-Altendorf, near Bonn, Germany.**

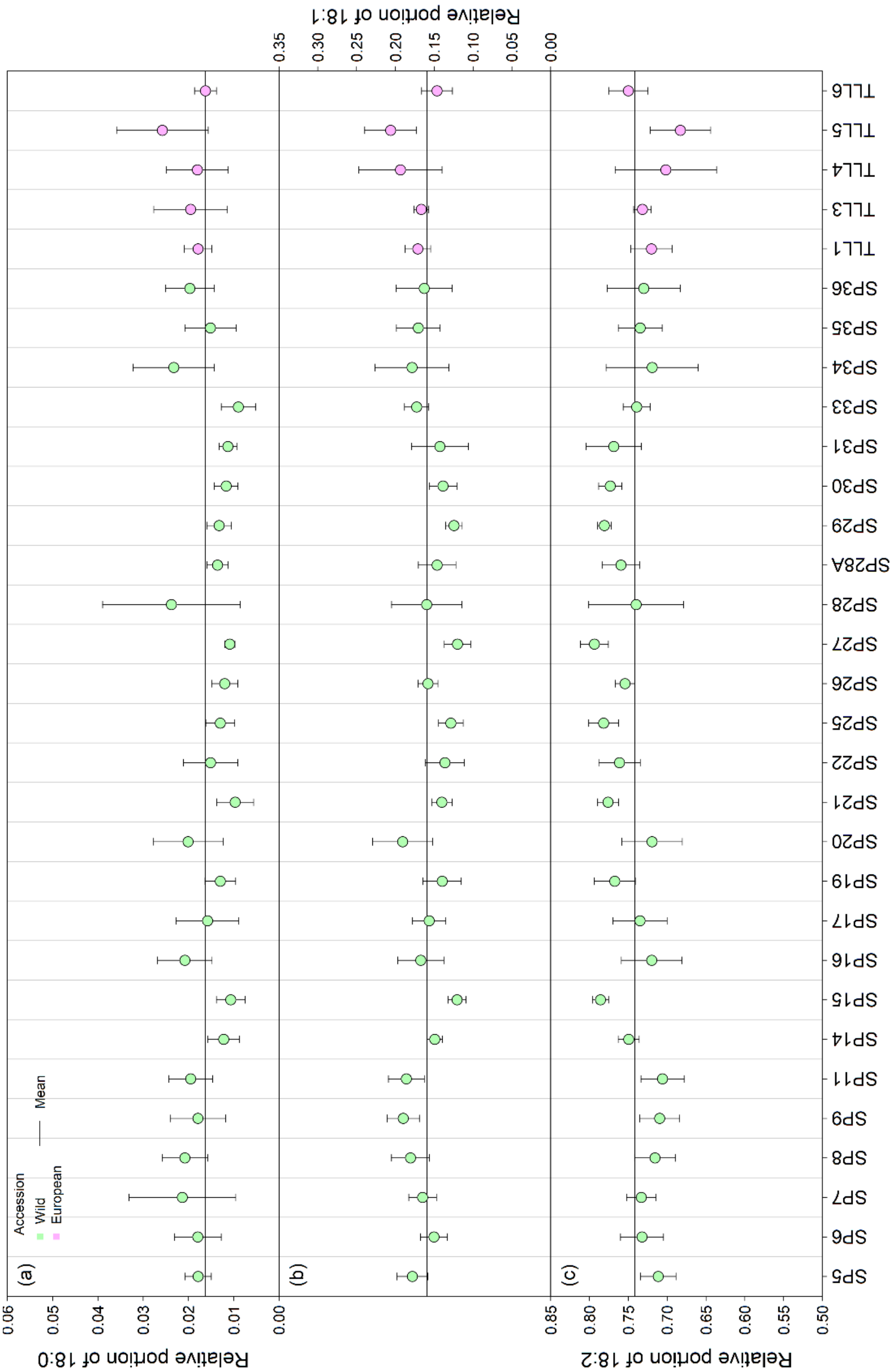

**Figure 5.5: Dot plots (a–c) with n=10 (exceptions: SP5 with n=9 and SP33 with n=14) of the portions of 18:0 (a), 18:1 (b) and 18:2 (c) of seeds harvested in 2020 as a function of the *Silphium perfoliatum* accessions. The black line is on the level of the overall mean of the parameter. The light-green coloring indicates wild accessions and the magenta coloring represents the European plant material. The portions of the single fatty acids were calculated by dividing the total amount of the respective fatty acid by the total amount of oil (a–c). All plants have been cultivated since 2017 in the field trial “GEniu*S* II” at Campus Klein-Altendorf, near Bonn, Germany.**

## 5.4 Discussion

The first thing of note is that all seed geometric traits decrease along the flowering ranks. Assefa et al. (2015) and Schäfer et al. (2018) have reported greater emergence rates and vigor of *Silphium* seedling grown out of seeds with more weight. This might also explain a certain amount of heterogeneity, mentioned by Schäfer et al. (2017). Therefore, flowering ranks should be taken into consideration for upcoming studies, plant breeding and commercial seed propagation. There are single shoots of various accessions which do not show this decreasing trend (data not shown), but the reasons for this may be environmental or related to genotype. From the seed biomass point of view, the decreasing trend of seed traits along the flowering ranks is disproportionate to the exponential increase of the number of flower heads along the ranks (tab. 5.2). Therefore, the potential seed mass of each flowering rank is greater than the yield of the previous rank. Still, more data of each rank are needed for the actual number of flowering heads and the number of unfilled/sterile seeds per flower head, as the theoretical values of table 5.2 are not completely achieved by the plants on the field, especially in the upper flowering ranks (personal observation).

Assefa et al. (2015) observed 33 cup plant half-sibs over two years. The annual average achene lengths were 8.81 mm and 7.03 mm, the achene widths were 6.02 mm and 4.43 mm, the achene weights were 0.015 mg and 0.011 mg. Gansberger (2016) analyzed two different batches of *S. perfoliatum* seeds with average achene lengths of 9.81 mm and 9.46 mm, achene widths of 6.14 mm and 6.35 mm, as well as thousand-seed weights of between 16.99 and 18.62 g. Actual commercial seeds, with mechanically removed wings, have been investigated too, showing achene lengths of 8.39 mm, widths of 4.71 mm, areas of 26.74 mm and thousand-seed weights of 15.6–18.5 g (Schäfer et al., 2017; Schäfer et al., 2018). In comparison of these data with figure 5.2 and figure 5.3, it seems like seeds of the fourth (or even higher) flowering ranks have been analyzed. Regarding the number of seeds yielded per rank (tab. 5.2) this approach appears practical, despite the already mentioned disadvantages of lighter seeds.

As reported for most crops, including sunflower (*Helianthus annuus* L.), and as predicted for *S. intergrifolium*, we assume that seeds of cup plant will grow in the course of domestication (Reinert et al., 2019; Fuller, 2007; summarized by Burke et al., 2002). For further grain yield growth, SP15, SP21 and SP32 should be considered for breeding. SP21 shows the biggest seed shape parameters (achene area, achene length, achene width), SP15 achieves the highest seed weights as well as above average seed shape parameters and the flowerheads of SP32 had the greatest seed set. Schäfer at al. (2018) reported increased viability of seeds with greater opening angles. SP22 showed the lowest eccentricity (the roundest seed shapes), has thus the largest opening angle and might therefore be interesting for upcoming breeding programs. The wild collection expands the available variation of eccentricity and seeds per flower head in both directions. For the plant traits achene area, achene length, achene width and single seed weight, the expansion is only directed towards larger and heavier seeds. In addition, the wild accessions show differences in trait expressions in finer gradations. Further research should target the hull-to-kernel-ratio, to increase the harvestability, the seeding ability and the yield (Reinert et al., 2019).

Our results of chemical composition are comparable to available data in the literature for *S. perfoliatum* and *S. integrifolium* (Kowalski & Wierciński, 2004; Reinert et al., 2019). Slight differences might be explained by the use of different cultivars and climatic conditions. We agree with Reinert er al. (2019) that the fatty acid composition of wild *Silphium* accessions is too heterogenous for direct usages. Nevertheless, oil composition of *Silphium* can still be affected by plant breeding. A certain portion of the heterogeneity can be counteracted through selection and aimed crosses. Especially SP21–SP27 and SP29–SP33 seem to have an oil quality suitable to start breeding for edible oil. These accessions have larger oil contents, below average portions of unsaturated fatty acids (14:0, 16:0 and 18:0) and above average contents of one of the saturated fatty acids (18:1 or 18:2). To aim for a solid fat alternative, SP6 and SP16 seem to have the best conditions with an average in oil content, large quantities of saturated fatty acids and small quantities of unsaturated fatty acids. Furthermore, the application of mutation breeding on *Silphium perfoliatum* appears promising, as the most significant achievements in sunflower-oil-quality breeding, like high oleic, high stearic and high palmitic oil, were mainly reached through mutagenesis (Soldatov, 1976; Ivanov et al., 1988; Osorio er al., 1995).

## 5.5 Conclusion

This study showed decreasing seed yield and seed geometric traits along the flowering ranks of *Silphium perfoliatum*. This was particularly evident in the seed weight, whose values were halved over the ranks. The only constant variable was the seed shape trait eccentricity. In addition, the available variation of various seed traits of a wild cup plant collections was described, highlighting the importance about providing closer information about the origin of accessions and about investigated flowering ranks in upcoming publications. as well as laying another cornerstone for cup plant breeding. Beyond that, first accessions with desired properties were identified. SP15 and SP32 show the best seed yield traits, whereas SP21 and SP22 stand out for their seed geometry. Depending on the designated usage of *Silphium* oil, the accessions SP21–SP27 and SP29–SP33, as well as SP6 and SP16, are starting points for increasing oil quality.

# 6 Evaluation of the Intra- and Interspecific Development of Different Accessions of *Silphium perfoliatum* L. and *Silphium integrifolium* Michx.

This work has been published as:

Martin Greve, **Christoph A. C. Korte**, Johanna Entrup, Hanna Altrogge, Philip Bischoff, Julian Elfers, Christian Wever, Ralf Pude (2023). Evaluation of the Intra- and Interspecific Development of Different Accessions of *Silphium perfoliatum* L. and *Silphium integrifolium* Michx. *Agronomy* 2023, *13*, 1601. https://doi.org/10.3390/agronomy1306160.

The following manuscript has not been modified from the published version.

## 6.1 Introduction

The cultivation of plants as renewable resources for replacing fossil carbon, aiming for a bio-based economy, is growing. After the era of the usage of annual crops for biomass production, a new generation of crops was discussed. These crops are perennial (Sanderson & Adler, 2008) and may be even better as flexible multipurpose third-generation biomass crops (Wever et al., 2020).

At the moment, within the genus *Silphium* are two sister species (Clevinger & Panero, 2000) under evaluation for the development of such a new crop type: cup plant (*Silphium perfoliatum* L.) and silflower (*Silphium integrifolium* Michx.). The genus *Silphium* is widely spread across the eastern part of North America (van Tassel et al., 2017; Clevinger, 2023a; Clevinger 2023b). As both *Silphium* species are distributed over different geographical zones, there is a genetic variance (Albrecht & Goldstein, 1997; Raduski et al., 2021). It can be assumed that different *Silphium* accessions also vary phenotypically from each other (Assefa et al., 2015). According to Wever et al. (2019), an accession is defined as a population from one geographically characterized location. The primary use of *S. perfoliatum* is for energy production, while *S. integrifolium* is under domestication to becoming an oil seed crop (van Tassel et al., 2017; Mayr et al., 2013). Both belong to the *Asteraceae* tribe of *Heliantheae*, and originate from the eastern part of North America (Clevinger, 2004; Cumplido-Marin et al., 2020; Müller & Dauber, 2016; Reinert et al., 2019).

In *S. perfoliatum*, a yield of 15 to 25 Mg of dry matter per hectare is possible depending on soil and water availability (Höller et al., 2021; Peni et al., 2020). In addition to its many agro-ecological benefits, e.g., in supporting biodiversity and as a food source for a variety of insects (Wever et al., 2019; Cumplido-Marin et al., 2020; Müller & Dauber, 2016; Dauber et al., 2016; Gansberger, 2017), *S. perfoliatum* has many interesting characteristics for a potential future non-food-crop with regard to its usability in agriculture, as a fiber plant, as well as in the use of ingredients and metabolites in pharmacy (Cumplido-Marin et al., 2020; Lunze et al., 2021). Furthermore, *S. perfoliatum* biomass can be utilized for multiple purposes (Wever et al., 2020). At the moment, cup plant is mainly used as a biogas substrate, but could also be suitable for the production of fibers, chemical and pharmaceutical substances and insulating materials. Due to this, the agricultural value of *S. perfoliatum* can be versatile, therefore its growing area is increasing (Cumplido-Marin et al., 2020; Gansberger, 2017; Lunze et al., 2021; Kowalski & Kędzia, 2007; Kowalski & Wolski, 2005; Moll et al., 2022). Depending on the type of use, the optimal harvesting time and the expected harvesting quantity will change. An early harvest (22 August; Mast et al., 2014) of *S. perfoliatum* shows a relatively high proportion of quickly convertible carbohydrates, fats and proteins. At later harvest dates (towards the end of the growing season), the fiber, as well as the ash contents, increase (Cumplido-Marin, 2020; Gansberger, 2017; Lunze et al., 2021; Kowalski & Kędzia, 2007; Kowalski & Wolski, 2005).

A plant with a high proportion of quickly convertible carbohydrates is advantageous for the use of energy generation by fermentation in biogas plants (Gansberger, 2017). To an extent, the same applies for the use as forage. *S perfoliatum* shows comparable dry matter yield to alfalfa (*Medicago sativa* L.) and red clover (*Trifolium pratense* L.), with lower nutritional value. This can be optimized by dual harvest management. Thus, the contents of nutritive ingredients change depending on the stage of development or the harvest date (Chiriac et al., 2020; Pichard, 2012).

In the case of silflower, two natural botanic variants are known and described: *S. integriflolium* var. *integrifolium* and *S. integrifolium* var. *laeve* (Clevinger, 2023a). The variant *S. integrifolium* var. *integrifolium* is known to be from the north-eastern part, while *S. integrifolium* var. *laeve* is known to be from the south-western part, of the natural distribution. Both variants of *S. integrifolium*, similar to *S. perfoliatum* as described above, show great environmental benefits in soil, water and biodiversity (Gibson et al., 2019; Grunwald et al., 2020; Prasifka et al., 2022). Interest in the plant, which is largely unknown in Europe, is growing steadily (Reinert et al., 2019).

*S. integrifolium* var. *laeve*, in its pre-domesticated form, can be used as a perennial oilseed crop (Reinert et al., 2019; Kowalski, 2009). In this process, two breeding objectives were pursued: the pistillate ray florets per head were increased (feminization) and the lateral branching of stems was reduced (Prasifka et al., 2022). The oil composition of the seeds of both investigated *Silphium* species is similar to that of sunflower (van Tassel et al., 2017: Reinert et al., 2019; Kowalski & Wierciński, 2009). *S. integrifolium* shows a maximum seed yield of 279.36 g per plant and year, whereby 118 to 253 g of oil can be obtained from 1 kg of seed. In another large-scale field experiment, Schiffner et al. (2020) found that different planting densities, as well as different nitrogen levels in the soil, affect biomass yield. The maximum biomass yields ranged from 8.2 to 15.9 Mg per hectare.

Due to its natural distribution in the prairie habitat of North America, and the complex root system of this perennial crop, the plants are suitable as an oilseed in arid and semi-arid regions (Reinert et al., 2020; Vilela et al., 2018). In addition to their cultivation in Kansas, USA, there are field trials in the north of Patagonia, Argentina. Due to the natural adaptation of *S. integrifolium*, to arid conditions, the amount of water needed can be reduced compared to other oilseeds (Vilela et al., 2018).

Given its high potential as an oilseed crop, *S. integrifolium* seems to be a promising wild plant for domestication (Reinert et al., 2019). A breeding approach was carried out in Kansas, USA (van Tassel et al., 2017; Prasifka et al., 2022).

Due to its missing or low domestication level, *Silphium* accessions show a high phenotypic plasticity. Wever et al. (2019) cultivated five different European *S. perfoliatum* accessions under field conditions at the same location to show differences in phenotypic appearance regarding plant height, stem diameter, number of shoots per plant, internodes per shoot and inflorescence. However, based on these data, the development kinetics of the plants can only be represented indirectly, so quantitative data collection is necessary (Hack et al., 1992).

A BBCH scale is a good tool to translate developmental data into a useful scale and it standardizes the development kinetics of crops and weeds. In this way, it will be possible to exploit the interdependencies that exist today in research, trade, production and services (Meier, 2018). The characteristics of plant development, from germination to senescence, are recorded and divided into ten macro stages. In addition, a smaller-step classification based on ten micro stages is possible to precisely define developmental steps within each macro stage. The structure of the BBCH scale was deliberately based on Zadoks et al. (1974) (Meier, 2018, Zadoks et al., 1974). The BBCH scale always refers to a single plant.

A certain stage is only considered to be given when more than 50% of the examined plants show this stage (Meier, 2018).

For *S. perfoliatum*, a BBCH scale describing the general development of the plant is already available. This BBCH scale divides the development of *S. perfoliatum* into two parts. Thus, it differentiates between the first year (juvenile) and the second year (adult). In the first year, germination, leaf formation and row closure are evaluated. Beginning with the second year, vegetative development phases are assessed in terms of leaf formation and shoot elongation. Generative growth is assessed by bud formation, flowering, seed development, as well as the seed maturity and senescence process as described in Cumplido-Marin et al. (2020).

The aims of this study are to identify the phenotypic plasticity of different *Silphium* species and accessions, the further development of the BBCH scale for *S. perfoliatum* and an adaptation of *S. integrifolium*. In order to describe the genetic variation between accessions in a BBCH scale, it is necessary to investigate different accessions of *S. perfoliatum* and *S. integrifolium*. For the crop management and breeding of both species., developmental stages have to be clearly defined and characterized (Meier, 2018).

## 6.2 Materials and Methods

### 6.2.1 Growing and Climate Conditions

The field trial presented in this study was conducted from April 2020 to November 2021 at the Field Lab Campus Klein-Altendorf near Rheinbach (N 50.617, E 6.983), University of Bonn, Germany. The predominant soil type on the main Rhine terrace is Luvisol, weakly eroded from loess (CKA, 2020a).

The general average climatic conditions are characterized by an average temperature of 9.6 °C and an annual precipitation of 603 mm. Figure 6.1 shows the monthly average temperatures and the corresponding total precipitation. The average temperature in the year of trial establishment was 11.5 °C. The amount of precipitation was 492 mm. In the second year of the trial, the average temperature was 9.8 °C and there was an above-average amount of precipitation of 788 mm (CKA, 2020b).

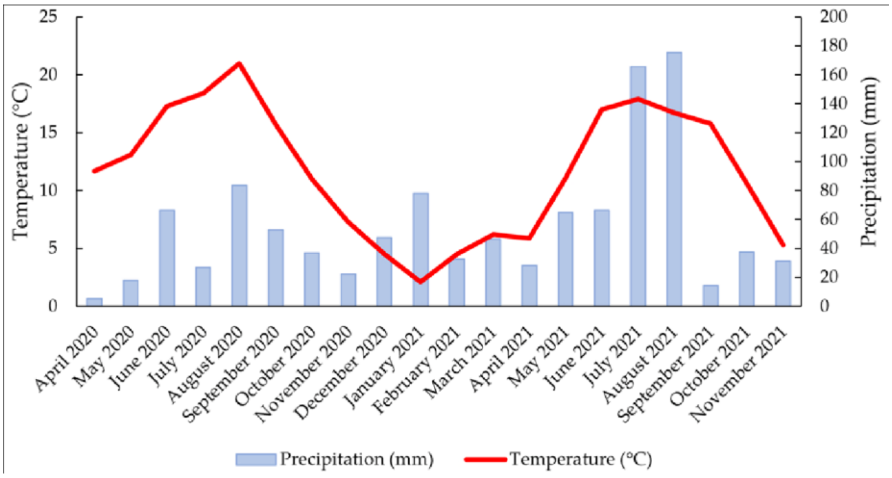

**Figure 6.1: Monthly average temperature and precipitation over the experimental period (CKA, 2020b).**

### 6.2.2 Trial Setup

Two different accessions of each of *Silphium perfoliatum* and *Silphium integrifolium* were used. For this, it was ensured that the accessions were as geographically distinct as possible and had the greatest genetic variance possible. A total of 36 plants per accession were placed in a 6 × 6 plot. Plants were sown at a planting density of four plants per square meter. For this, the seeds were treated in advance with a 0.05 % gibberellic acid (GA3) solution for 12 h at 4 °C to promote even germination (Gansberger, 2017). In order to avoid missing plants due to lack of germination, five seeds of the corresponding accession were sown at each planting plot. Once germination was complete and cotyledons were fully formed, excess plants were mechanically removed.

For the study of *S. perfoliatum*, one accession from the southern (SPS) and one from the northern part (SPN) of the natural range were considered, both undomesticated. To evaluate the development of *S. integrifolium*, an accession from the western part of the native distribution area (Sii), and a pre-domesticated accession originating from the southern part of the native distribution area (Sil), were used (tab. 6.1). Seeds for this trial were produced by a population grown at Campus Klein-Altendorf, (SPN and SPS), the botanical garden of the University of Düsseldorf, Germany (Sii) and The Land Institute in Salina, KS, USA (Sil).

**Table 6.1: Locations of the natural habitat of *Silphium perfoliatum* and *Silphium integrifolium* accessions for this experiment. (* Origin of the accession. A pre-domestication was carried out at the Land Institute in Salina, Kansas, USA).**

| Accession Name | Accession Description | Latitude (N) | Longitude (E) |
|---|---|---|---|
| SPS | *Silphium perfoliatum* south | 32.203 | −89.254 |
| SPN | *Silphium perfoliatum* north | 41.857 | −86.590 |
| Sii | *Silphium integrifolium* var. *integrifolium* | 41.776 | −86.404 |
| Sil | *Silphium integrifolium* var. *laeve* | 39.106 * | −96.576 * |

To avoid border effects and inter-plot competition, an additional two-row border of each accession was added around the whole experimental plot, as well as between the accessions, to reduce possible crowding out effects due to different competitive strengths (Talbot et al., 1995).

During the phase of establishment, irrigation was necessary. Manual weed control procedures were carried out in the first year as well as at the beginning of the second year. Amounts of 50 kg N/ha were given at the beginning of each vegetation phase as maintenance fertilization.

### 6.2.3 Assistance for the Chronology of Incidents

In the evaluation of this experiment, all temporal data were given relative to the sowing date. In order to be able to put this information into a temporal context, table 6.2 shows temporal translations to the day of the year, the Gregorian calendar and to the occurrences in the field trial.

**Table 6.2: Temporal overview of the experimental period with translation into other forms of counting.**

| | Days after Sowing (DAS) | Gregorian Date | Developmental Occurences |
|---|---|---|---|
| First year | 0 | 22 April 2020 | Sowing |
| | 34 | 26 May 2020 | Rosette development |
| | 111 | 11 August 2020 | Shoot development |
| | 146 | 15 September 2020 | Generative stage |
| | 195 | 3 November 2020 | Senescence |
| Second year | 265 | 3 January 2021 | Rosette development |
| | 376 | 3 May 2021 | Shoot development |
| | 426 | 22 June 2021 | Generative stage |
| | 502 | 6 September 2021 | Senescence |
| | 580 | 23 November 2021 | End of experiment |

### 6.2.4 Description of the Germination

To describe the germination of plants, seeds of the accessions from the field trial were observed in rhizotrons. This allowed a precise description of the seed germination and root development of *S. perfoliatum* and *S. integrifolium*.

For this purpose, climatic conditions (day length and temperature profile) of the field trial during germination were replicated in a plant cabinet. Moisture was added as required. Fifty seeds from each accession were considered, which were treated in advance in a 0.05 % GA3 solution for 12 h at 4 °C according to Gansberger et al. (2017) as for the field trial.

### 6.2.5 Data Collection

Data from the germination experiment in the rhizotrons were collected over a period of 30 days. Within the stage of germination, different morphological sub-stages were recorded.

The data collection period of the field trial ranged from 26 May 2020 (34 days after sowing; DAS) to 23 November 2021 (580 DAS), during which the development of the plant was documented weekly. Vegetative growth referred to the counting of nodes on the rosette as well as on the shoot. Here, the node was considered to be fully developed as soon as the corresponding leaves were fully formed. The corresponding data were collected on a pre-selected shoot of each plant. This selection was made at the beginning of the respective growing season and was not changed during the experimental period. In the following, this shoot is referred to as the main shoot. The latest fully developed node was always recorded. Node counts were performed continuously, so a cumulative nodule count of rosette nodes and shoot nodes was used for the evaluation to avoid neglecting node displacement effects, as described by Kadereit et al. (2014). The generative growth was recorded in the form of a rank-by-rank scoring of fully developed buds (fully elongated bud stalk of all buds belonging to the corresponding rank) and composite flowers (complete fertility of all flower heads of the corresponding rank), as well as seed development (seed filling completed in all heads of the corresponding rank, seed coat still green) and their maturity (brown and dry seedpods concerning the flower rank). The respective stage was considered to have been reached as soon as the respective rank had fully completed it. At the end of both growing seasons, the advancing senescence of the plants was estimated as chlorophyll breakdown in the whole plant in percentages. The experiment was terminated after completion of the second vegetation phase (580 DAS).

### 6.2.6 Data Processing

Data for each development stage were cumulated over the respective accession and presented in the form of heat maps. An intraspecies comparison was made between the two *S. perfoliatum* and *S. integrifolium* separately. Furthermore, interspecific development kinetics were evaluated. As soon as a relative frequency within a development characteristic had reached a maximum, a continuous presentation was disregarded. Statistical calculations are based on a 95 % confidence level.

## 6.3 Results

The results of the experiment describe the development of the studied accessions of *Silphium perfoliatum* and *Silphium integrifolium*. The presentation of the results was made chronologically and can be divided into the year of establishment and the second year of development. The development steps occurring in each case, with the associated relative frequencies, are presented in heat maps. Furthermore, the statistically significant developmental differences in intraspecific comparisons were elaborated.

### 6.3.1 Development Description of the Establishment Year

**Germination**

The occurrence of the different development steps for the first 30 days of germination is shown in figure 6.2. In order to be able to follow the underground development steps, germination was carried out separately in an additional experiment under simulated field conditions in a plant cabinet. Initially, both accessions of both species demonstrated seed swelling. Seven days after sowing (DAS), the first seeds of Sil showed radicle emergence, while the other accessions lagged two to three days behind. The other developmental characteristics displayed the same pattern. The elongation of the radicle, the breaking through of the seed coat, the breaking through of the soil surface, as well as the development of cotyledons occurred, on average, three days earlier in Sil. Furthermore, it is noticeable that the germination of *S. perfoliatum*, in the late phase of the experimental period, had higher variance compared with *S. integrifolium*. Thus, it can be seen that, in a certain proportion of young seedlings, development stagnated during seed coat breakthrough or soil surface breakthrough. Furthermore, it showed a certain percentage of seeds in all accessions that did not progress beyond seed swelling (SPS: 16 %; SPN: 36 %; Sii: 22 %; Sil: 10 %). After 28 days of the experiment, the studied accessions reached the maximum germination rate (SPS: 52 %; SPN: 42 %; Sii: 54 %; Sil: 70 %).

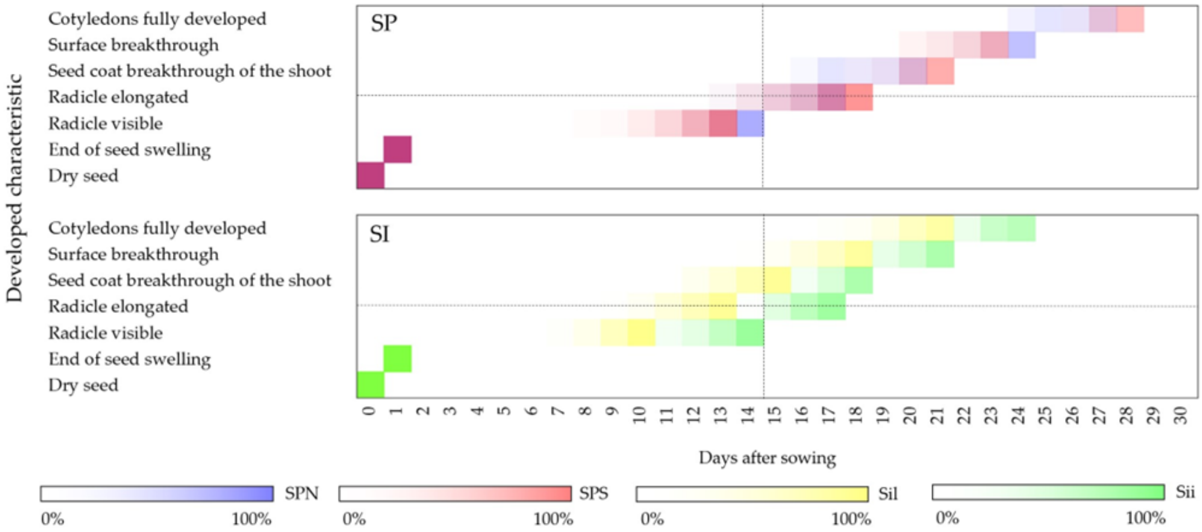

**Figure 6.2: Heat map of *Silphium perfoliatum* (SP) and *Silphium integrifolium* (SI) germination in a rhizotron system over a period of 30 days. Heat map SP shows the germination behavior of both accessions of *Silphium perfoliatum* (SPN and SPS); heat map SI shows the equivalent of both *Silphium integrifolium* accessions (Sii and SiI) (n = 50). The intensity of the coloration shows the respective relative frequency (0–100 %) of the complete expression of certain characteristics. After the achievement of the maximum level of development, the trait value will no longer be displayed. The climatic conditions were adapted from the corresponding climate during the field trial. The dashed lines serve as an orientation aid.**

## Rosette Development

The development of the rosette of *S. perfoliatum* (SP) and *S. integrifolium* (SI), in the first year after sowing, is shown in figure 6.3. In general, *S. integrifolium* showed a slightly faster development than *S. perfoliatum*. SiI formed a maximum of 20, Sii, SPS and SPN 14 nodes. The development of the individual plants of each accession becomes more heterogeneous over time.

Within *S. perfoliatum*, both accessions underwent a similar development. SPN was more inhomogeneous over time than SPS, so that the maximum frequencies of each fully developed rosette node were reached later. On two dates (139 and 160 DAS), a significant difference could be observed regarding the average number of nodes between the SPN and SPS accessions. Due to the relatively high p-values (p = 0.041) at these time points, and the fact that there were no other differences between the studied accessions, no pattern can be identified, thus a random difference can be assumed.

The *S. integrifolium* accessions showed, equivalent to *S. perfoliatum*, a similar course in the first half of the growing period, with some significant differences at the beginning of plant growth. The development of Sii stagnated almost completely after 125 DAS, with a maximum of 14 nodes. In the second half of the developmental course, SiI showed progressive node formation, moving significantly steadily farther away from Sii. After 125

DAS, Sii showed an average of 10.26 ± 1.42 and Sil 10.91 ± 1.81 formed nodes ($p = 0.016$). After 216 DAS, there was no change in Sii, whereas Sil developed further and produced an average of 15.06 ± 4.53 nodes, making the difference between the studied accessions more significant ($p = 2 \times 10{-}8$). Compared with this, *S. perfoliatum* showed an average of 7.52 ± 0.93 nodes after 126 DAS and 11.31 ± 2.66 nodes after 216 DAS.

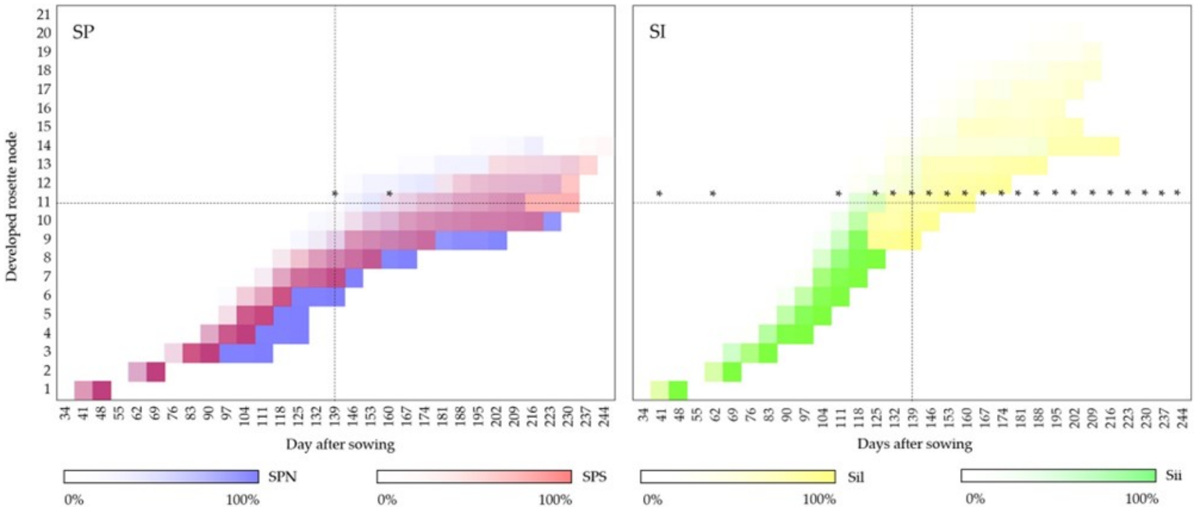

**Figure 6.3: Heat map of rosette node development in the year of establishment of *Silphium perfoliatum* (SP) and *Silphium integrifolium* (SI) from 34 to 244 days after sowing. Heat map SP shows the rosette development of the first year of both accessions of *Silphium perfoliatum* (SPN and SPS); heat map SI shows the equivalent of both *Silphium integrifolium* accessions (Sii and Sil) (n = 36). The intensity of the coloration shows the respective relative frequency (0–100 %) of the completely developed rosette node. After the achievement of the maximum level of development, the trait value will no longer be displayed. The star-shaped markings (*) indicate a significant difference in the average number of nodes between the accessions shown at the respective time point, with a confidence level of 95 %. The dashed lines serve as an orientation aid.**

### Shoot Development

The shoot growth of the establishment year is shown in figure 6.4, which is plotted with sequential numbering from figure 6.3. In general, *S. integrifolium* shows a distinctly earlier shoot growth than *S. perfoliatum*. In *S. integrifolium*, the first shoot node could be detected after 118 DAS and in *S. perfoliatum* after 139 DAS. *S. perfoliatum* had a low tendency to form shoots in the accession SPS, as 22 % of the plants formed rudimentary shoot growth in the first year. In SPN, there appeared no shoot formation. *S. integrifolium* showed shoot formation in both accessions. In Sii, 25 % of the plants developed 25 cumulative shoot nodes; Sil achieved 27 cumulative shoot nodes on about 3 % of the plants, after an experimental period of 265 DAS. The studied accessions of *S. perfoliatum* showed a significant difference for the first time after 160 DAS. SPS had an average of 1.06 shoot nodes ($p = 0.038$) at this time, while SPN did not form any shoot nodes. The studied accessions of *S. perfoliatum* showed a significant difference for the first time after 160 DAS.

SPS had an average of 1.06 ± 2.14 nodes (p = 0.038) at this time, while SPN did not form any shoot nodes. Over time, shoot node development continued in SPS so that, after 265 DAS, an average of 1.82 ± 3.43 shoot nodes had been formed and a significance increase (p = 0.015) was seen. The studied accessions of *S. integrifolium* showed a significant difference in the average number of shoot nodes from the beginning of shoot development. After 160 DAS, Sii had developed an average of 10.66 ± 4.57 shoot nodes and Sil 3.31 ± 5.8 shoot nodes (p = 4.1 × 10−7). At 265 DAS, Sil had formed an average of 12.81 ± 5.33 and Sil had formed 4.63 ± 6.99 shoot nodes. The p-value increased marginally to 1.7 × 10−6 at this time point.

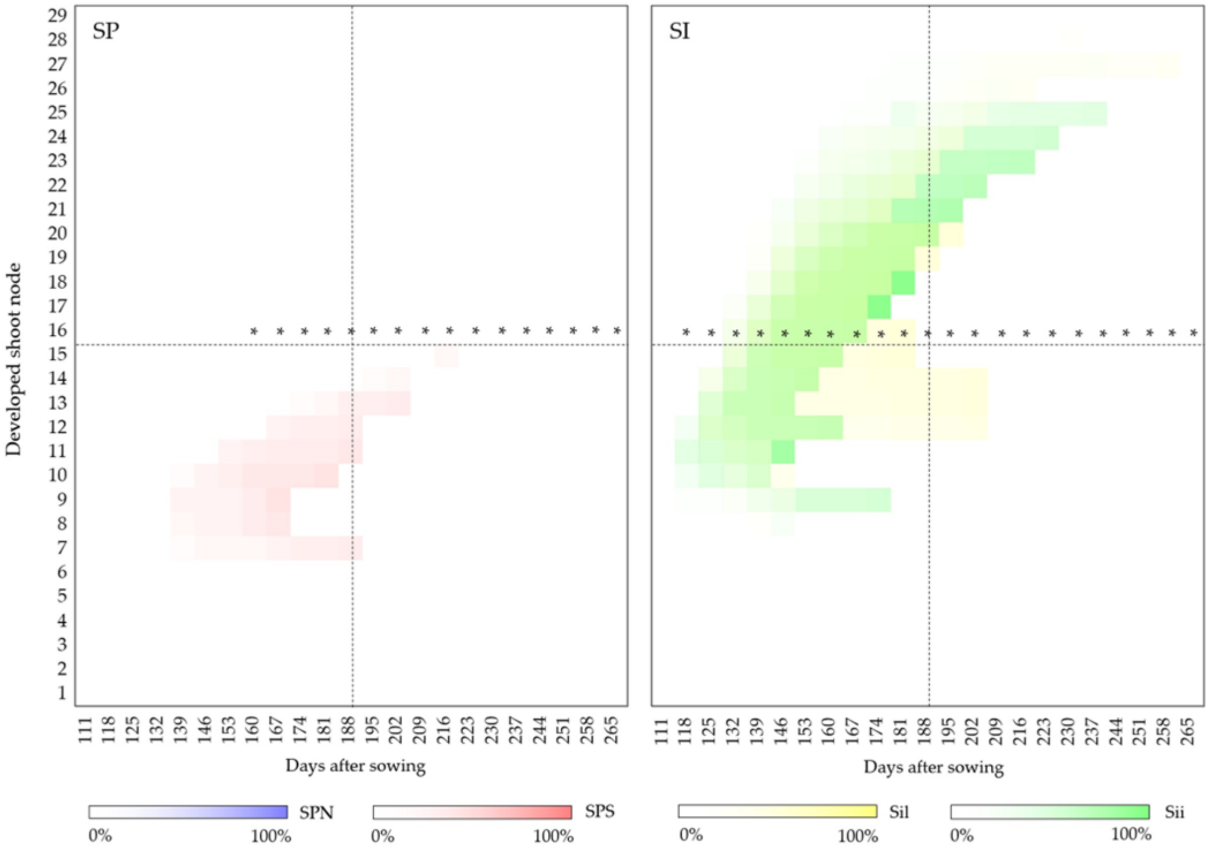

**Figure 6.4: Heat map of shoot node development of *Silphium perfoliatum* (SP) and *Silphium integrifolium* (SI) from 111 to 265 days after sowing. Heat map SP shows the shoot development of the first year of both accessions of *Silphium perfoliatum* (SPN and SPS); heat map SI shows the equivalent of both *Silphium integrifolium* accessions (Sii and Sil) (n = 36). The intensity of the coloration shows the respective relative frequency (0–100 %) of the completely developed shoot node. After the achievement of the maximum level of development, the trait value will no longer be displayed. The star-shaped markings (*) indicate a significant difference in the average number of nodes between the accessions shown at the respective time point, with a confidence level of 95 %. The dashed lines serve as an orientation aid.**

## Generative Stage

The generative development of the year of establishment is shown in figure 6.5. *S. perfoliatum* showed highly reduced generative growth in the first year of development. SPS showed first rudimentary bud development after 174 DAS. After 209 DAS, first rank buds were formed in 11 % of the plants. From this point on, a significant difference was present between SPS and SPN ($p = 0.04$). Further generative growth was not detected in *S. perfoliatum*.

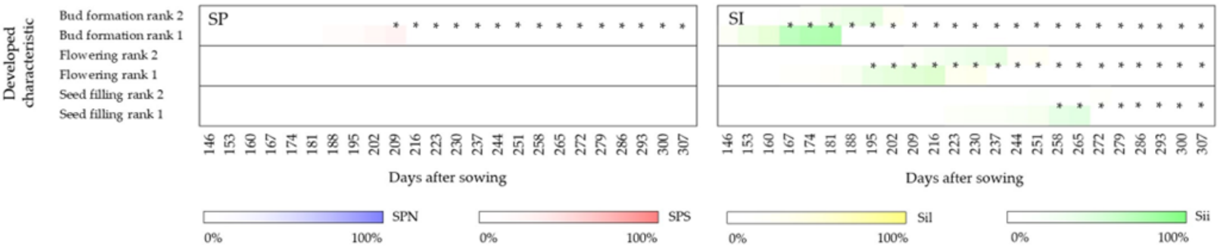

**Figure 6.5: Heat map of the period of generative development of *Silphium perfoliatum* (SP) and *Silphium integrifolium* (SI) from 146 to 307 days after sowing. Heat map SP shows the generative development of the first year of both accessions of *Silphium perfoliatum* (SPN and SPS); heat map SI shows the equivalent of both *Silphium integrifolium* accessions (Sii and Sil) divided into bud formation, flowering and seed filling (n = 36). The intensity of the coloration shows the respective relative frequency (0–100 %) of the completed development stage. After the achievement of the maximum level of development, the trait value will no longer be displayed. The star-shaped markings (*) indicate a significant difference in the average number of nodes between the accessions shown at the respective time point, with a confidence level of 95 %.**

*S. integrifolium* reached generative growth in both accessions studied. Both variants showed 146 DAS initial buds of the first rank. In Sil, 14 % of the plants showed bud formation in the first and 9 % in the second rank. An equivalent pattern arose during flower formation. Seed filling, in the first and second flowering rank, was completed in 6 % and 3 % of the plants, respectively. Bud development was reached in Sii of the first rank in 62 % of the plants and in 34 % of the second rank. Flowering was achieved in the first rank in 50 % of the plants. In the second rank, 34 % of plants attained this stage. Complete seed filling occurred in 21 % of the first rank, and in 3 % of the second rank, in Sii. The first significant differences in bud formation were seen after 167 DAS. On average, Sii had formed 0.47 ± 0.55 and Sil 0.14 ± 0.35 bud ranks at this time ($p = 0.003$). After completion of bud development after 202 DAS, an average of 0.86 ± 0.85 and 0.22 ± 0.58 bud ranks were formed by Sii and Sil, respectively. The difference at this time point also had a highly significant p-value of $5 \times 10^{-4}$. The first significant differences with respect to flower formation were evident after 195 DAS. At this time, an average of 0.28 ± 0.45 in Sii and 0.06 ± 0.23 in Sil flowering ranks were formed ($p = 0.011$). After the completion of flower formation after 251 DAS, significant differences between the studied accessions were still present with a p-value of 0.0016. At this time point, an average of 0.75 ± 0.89 and 0.17 ± 0.55 flowering ranks were formed in Sii and Sil, respectively. The first significant differences between the studied accessions were present after 258 DAS. At this time, Sii showed an average of 0.19 ± 0.46 filled seed ranks per plant in Sii and 0.06 ± 0.23 in Sil. At this point, a p-value of 0.0016 was evident, which did not change later in the time course. Seed maturity did not occur in any accession.

### Senescence

The course of senescence at the end of the vegetation phase of the first year is described in figure 6.6. Senescence of the investigated plants was first detected after 195 DAS. The investigated accessions of *S. perfoliatum* showed a temporal offset, so that the senescence process in SPN ended after 300 DAS. SPS reached complete senescence in 81 % of the examined plants after 307 DAS. Over the entire observation period, *S. perfoliatum* accessions showed a significant difference with an average p-value of 0.003.

The course of senescence of *S. integrifolium* was comparable referring to the two investigated accessions. The complete development of senescence occurred in Sii after 307 DAS and after 300 DAS for Sil. In the first half of the observation period, significant differences were present between the two studied accessions. Thus, Sii, after 195 DAS, showed an average senescence of 11.94 % ± 3.95 % and Sil 16.7 % ± 0.7 % with a p-value of $9.6 \times 10^{-4}$. As the course of senescence proceeded, the differences between the accessions became smaller. Thus, after 244 DAS, the average senescence for Sii was 65.83 % ± 15.7 % and for Sil 75.28 % ± 17.56 %, respectively, with a resulting p-value of 0.0204.

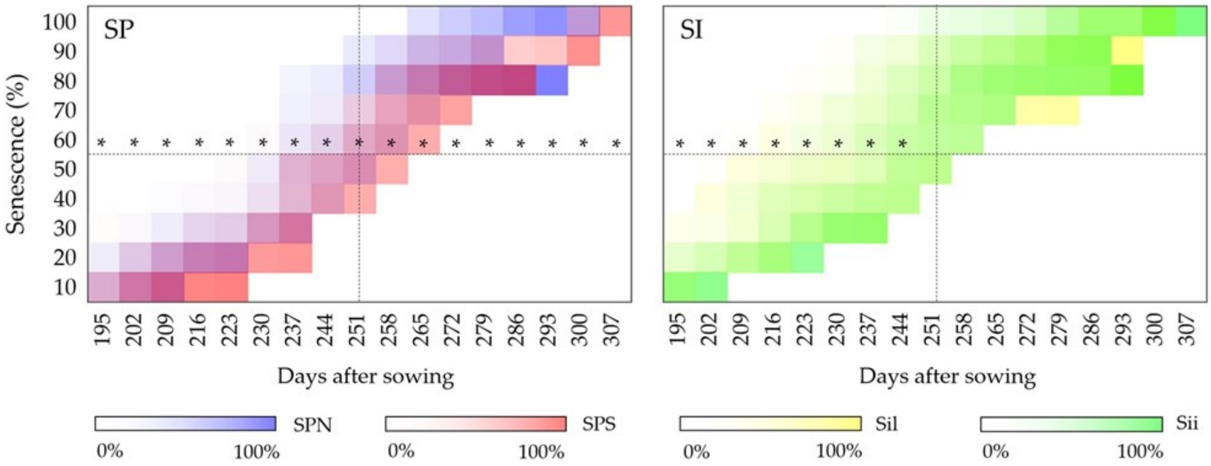

**Figure 6.6: Heat map of the course of senescence progress of *Silphium perfoliatum* (SP) and *Silphium integrifolium* (SI) from 195 to 307 days after sowing. Heat map SP shows the senescence course of both accessions of *Silphium perfoliatum* (SPN and SPS) of the first year; heat map SI shows the equivalent of both *Silphium integrifolium* accessions (Sii and SiI) (n = 30). The intensity of the coloration shows the respective relative frequency (0–100 %) of different senescence levels. After the achievement of the maximum level of development, the trait value will no longer be displayed. The star-shaped markings (*) indicate a significant difference in the average number of nodes between the accessions shown at the respective time point, with a confidence level of 95 %. The dashed lines serve as an orientation aid.**

### 6.3.2 Development Description of the Second Year of Development

#### Rosette Development

The development of rosette nodes in the second year is shown in figure 6.7. The regrowth of the investigated plants started after 265 DAS. In general, the rosette node development in the second year of *S. perfoliatum* and *S. integrifolium* were comparable, because a similar progression of rosette formation occurred and it was terminated simultaneously in all accessions after 376 DAS. At the end of the observation period (384 DAS), SPS and SPN had formed a maximum of 9 and 11 rosette nodes, respectively. At the same time point, Sii and SiI formed a maximum of 10 and 13 rosette nodes, respectively.

Over the time course, *S. perfoliatum* showed significant differences in the average rosette node number from 307 DAS to the end of the observation period (384 DAS). Thus, an average of 1.64 ± 0.67 rosette nodes was formed in SPS after 307 DAS, and an average of 2.27 ± 0.61 rosette nodes were formed in SPN. After 384 DAS, SPS had formed an average of 6.25 ± 1.23 and SPN an average of 7.97 ± 1.07 rosette nodes. As a result, the p-value increased from an initial $8.5 \times 10^{-5}$ to 0.0037 over time. The significant differences between 279 and 386 DAS showed no pattern and are therefore negligible.

*S. integrifolium* fulfilled a rather comparable development between the studied accessions. Significant differences between Sii and SiI were present between 286 DAS and 351 DAS.

On average, Sii showed 0.22 ± 0.48 and Sil 0.61 ± 0.68 nodes after 286 DAS (p = 0.0071). After 351 DAS, Sii had formed an average of 4.84 ± 0.7 and Sil 5.42 ± 1.16 nodes. At this point, there was a p-value of 0.0096. At the end of the observation period, Sii showed an average of 7.06 ± 1.13 and Sil 8.03 ± 1.64 rosette nodes, respectively. There is no significant difference at this point.

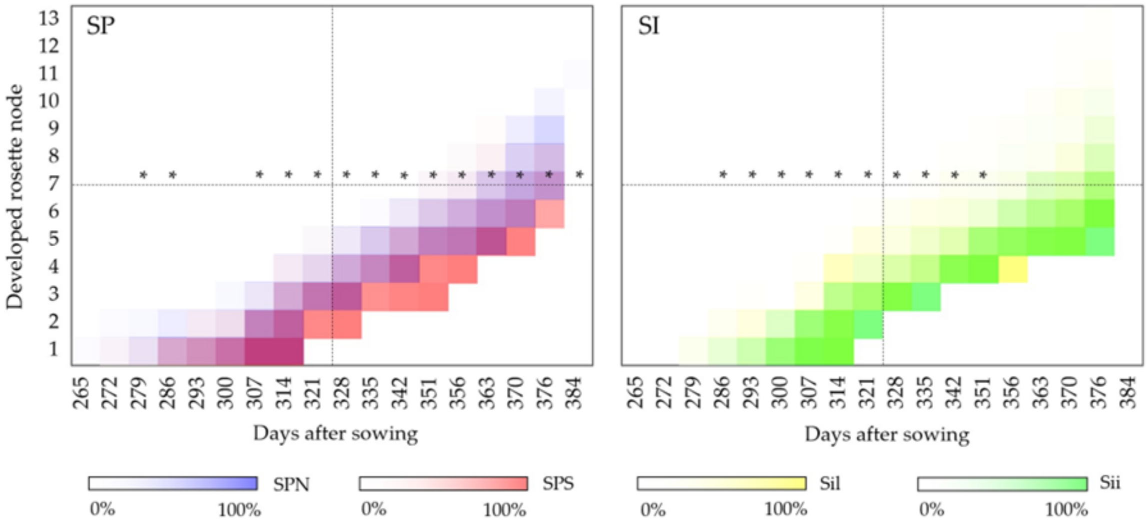

**Figure 6.7: Heat map of the course of rosette node development of *Silphium perfoliatum* (SP) and *Silphium integrifolium* (SI) from 265 to 384 days after sowing. Heat map SP shows rosette development of both accessions of *Silphium perfoliatum* (SPN and SPS) of the second year; heat map SI shows the equivalent of both *Silphium integrifolium* accessions (Sii and Sil) (n = 36). The intensity of the coloration shows the respective relative frequency (0–100 %) of the completely developed rosette node. After the achievement of the maximum level of development, the trait value will no longer be displayed. The star-shaped markings (*) indicate a significant difference in the average number of nodes between the accessions shown at the respective time point, with a confidence level of 95 %. The dashed lines serve as an orientation aid.**

## Shoot Development

The shoot growth of the second year of development is shown in figure 6.8, which is plotted with sequential numbering from figure 6.7. The considered accessions of *S. perfoliatum* demonstrated a comparable developmental course. The first shoot nodes became visible after 376 DAS. After 446 DAS, no further shoot nodes were formed. At this point, SPN reached a maximum of 17 shoot nodes, while SPS formed 16 shoot nodes at the peak. *S. integrifolium* showed a comparable initial phase of shoot development between the two accessions which was slightly earlier than the development of *S. perfoliatum*. Both accessions developed first shoot growth after 376 DAS. A maximum of 24 nodes was counted in Sii after 446 DAS. At the same time point, Sil reached up to 33 shoot nodes.

Shoot development in *S. perfoliatum* is subject to widely significant differences among the studied accessions. These can be detected for the first time after 391 DAS. At this time, SPS showed an average of 2.94 ± 0.62 and SPN an average of 3.72 ± 1.1 shoot nodes. This resulted in a p-value of $5 \times 10^{-4}$. At the end of the observation period, SPS produced an average of 9.0 ± 1.13 and SPN 9.94 ± 1.1 shoot nodes, resulting in a p-value of $7.3 \times 10^{-4}$. *S. integrifolium* showed sporadic significant differences between the studied accessions in the first half of the observation period, which do not seem to be subject to any pattern and are negligible. In the second half of the shoot development period, coherent significant differences were present among the studied accessions. Thus, after 412 DAS, Sii showed an average of 10.64 ± 1.75 and Sil 12.2 ± 2.71 shoot nodes, resulting in a p-value of 0.0057. After 446 DAS, Sii formed 16.55 ± 2.33 and Sil 19.64 ± 4.39 shoot nodes. This resulted in a p-value of $4.6 \times 10^{-4}$, which corresponded to a significant increase.

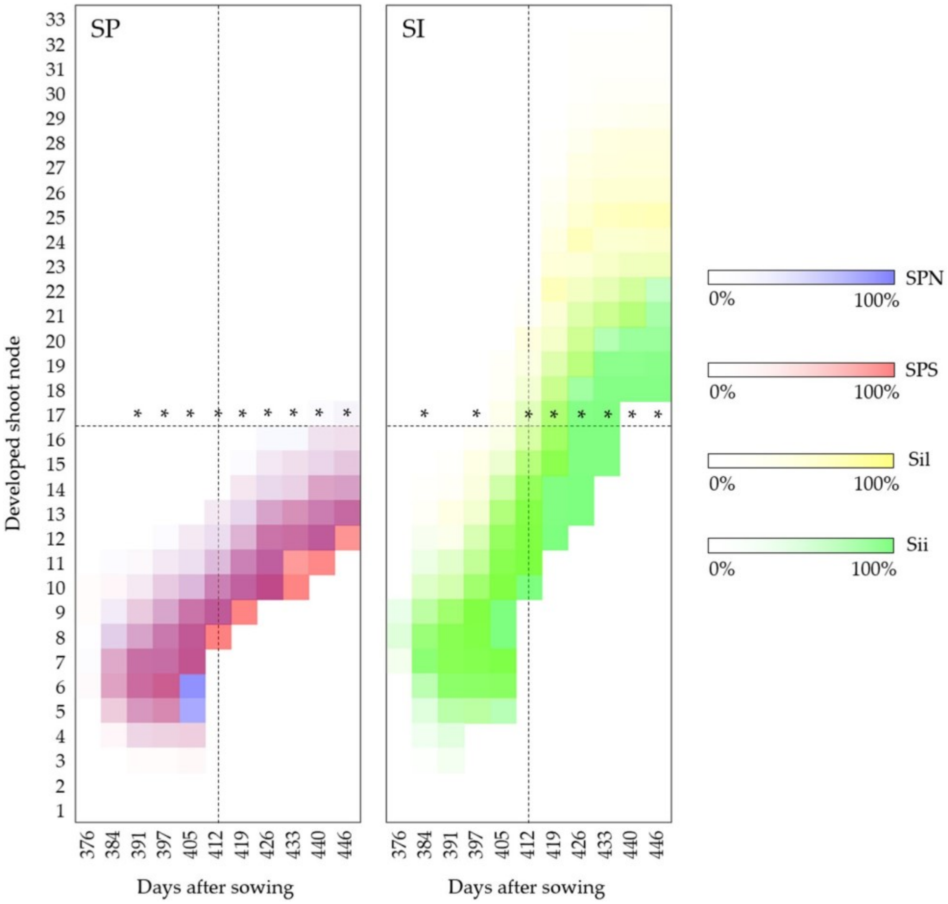

**Figure 6.8: Heat map of the course of shoot node development (main shoot) of *Silphium perfoliatum* (SP) and *Silphium integrifolium* (SI) from 376 to 446 days after sowing. Heat map SP shows the shoot development of both accessions of *Silphium perfoliatum* (SPN and SPS) of the second year; heat map SI shows the equivalent of both *Silphium integrifolium* accessions (Sii and Sil) (n = 36). The intensity of the coloration shows the respective relative frequency (0–100 %) of the completely developed shoot node. After the achievement of the maximum level of development, the trait value will no longer be displayed. The star-shaped markings (*) indicate a significant difference in the average number of nodes between the accessions shown at the respective time point, with a confidence level of 95 %. The dashed lines serve as an orientation aid.**

## Generative Stage

The course of the generative development phase of *S. perfoliatum* and *S. integrifolium* divided into bud formation, flower formation, seed filling and seed ripening, in rank-wise presentation, is shown in figure 6.9. In essence, *S. perfoliatum* and *S. integrifolium* show a generative phase in which the individual developmental steps build on each other in a mutually dependent manner. In general, the time offset between bud development, flowering and the seed filling phase is less than that for seed ripening.

The bud formation in *S. perfoliatum* ranged up to 8 bud ranks in SPS and up to 6 bud ranks in SPN, respectively. On average, at the end of the observation period, SPS showed 6.5 ± 0.73 and SPN 5.75 ± 0.76 bud ranks. Between 440 and 482 DAS, there was a significant difference between the two accessions, with an average p-value of $9 \times 10^{-4}$. In *S. integrifolium*, Sii showed a maximum of 8 and Sil showed a maximum of 6 bud ranks at the end of the evaluation period. On average, 6.72 ± 0.61 bud ranks were formed in Sii and 5.82 ± 1.19 in Sil at this time. Except for 461, 469 and 482 DAS, there was a significant difference between the sampled accessions over the entire observation period. Since the non-significant time points did not reveal a pattern, these could be neglected. There was a resulting average p-value of 0.0032.

*S. perfoliatum* showed up to 7 flowering ranks during flowering in SPS. SPN flowered in a maximum of 6 ranks. At the end of the observation period, SPS had an average of 5.43 ± 0.72 and SPN 5.22 ± 0.77 flowering ranks. Over the flowering period, there was mostly a significant difference between the studied accessions. No significant difference was present at 497 and 502 DAS, which is negligible due to non-detectable patterns. An average p-value of 0.0035 was present over the period. The flowering of *S. integrifolium* is shown in Sii up to 7 formed flowering ranks. Sil flowered in up to 6 ranks. On average, Sii flowered in 5.65 ± 0.64 flowering ranks and Sil in 4.8 ± 0.62 flowering ranks. Significant differences between the two accessions were at the end of flowering, due to flower development being more tapered in Sil than in Sii. No other significant differences were evident.

The seed filling phase in *S. perfoliatum* shows a maximum of 7 filled seed ranks in SPS. In SPN, up to 6 seed ranks were filled at the end of the observation period. On average, the number of filled seed strands in SPS was 5.19 ± 0.63 and in SPN was 5.22 ± 0.76. Significant differences with an average p-value of 0.0028 were consistently present between the studied accessions over the observation period. In *S. integrifolium* up to 7 and, in Sil, up to 6 seed ranks were filled. On average, there were 5.5 ± 0.66 filled seed ranks in Sii and 4.72 ± 0.64 in Sil. Significant differences among the studied accessions were present at 490, 509 and 516 DAS. As no pattern was discernible, it could be assumed at this point that the alleged significant differences were negligible.

In the last part of the generative phase, *S. perfoliatum* in SPS showed up to 7 ripened seed ranks. In SPN, up to 6 seed strands had fully ripened. On average, in SPS 5.47 ± 0.73 and, in SPN, 5.28 ± 0.77 seed heads were fully matured. Between 482 and 552 DAS there were significant differences with an average p-value of $9 \times 10^{-6}$. The ripening characteristics of *S. integrifolium* showed a maximum of 7 fully ripened seed ranks in Sii and 6 fully ripened seed ranks in SiI. On average, 5.75 ± 0.6 and 4.63 ± 0.59 seed ranks were ripened in Sii and SiI, respectively. From 539 to 573 DAS, significant differences were observed between the studied accessions. An average p-value of 0.0025 was present. A single significant difference after 482 DAS could be neglected due to a missed pattern.

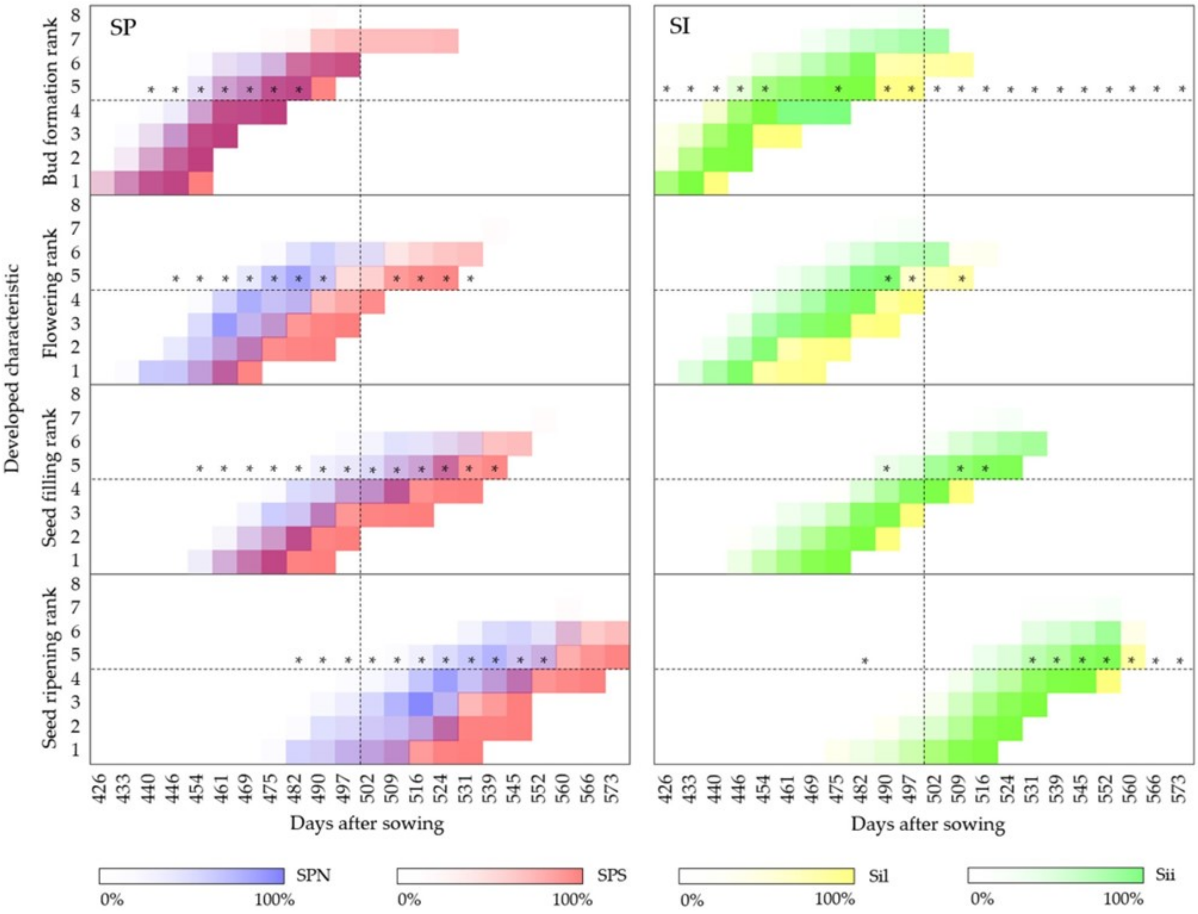

**Figure 6.9: Heat map of the period of generative development of *Silphium perfoliatum* (SP) and *Silphium integrifolium* (SI) from 426 to 573 days after sowing. Heat map SP shows the generative development of the first year of both accessions of *Silphium perfoliatum* (SPN and SPS); heat map SI shows the equivalent of both *Silphium integrifolium* accessions (Sii and SiI) divided into bud formation, flowering and seed filling. (n = 36). The intensity of the coloration shows the respective relative frequency (0–100 %) of the completed development stage. After the achievement of the maximum level of development, the trait value will no longer be displayed. The star-shaped markings (*) indicate a significant difference in the average number of nodes between the accessions shown at the respective time point, with a confidence level of 95 %.**

### Senescence

The course of senescence after the end of the vegetation phase of the first year is described in figure 6.10. The senescence evaluation began at 502 DAS. In general, the senescence progression of the two accessions of *S. integrifolium* (Sii and Sil) and SPN is comparable. The senescence process of SPS is successively delayed over the observation period after the same onset. Thus, complete senescence in SPN is reached after 566 DAS. Sii and Sil reach this state already after 560 DAS. SPS is completely senescent after 580 DAS.

In the intraspecific comparison, *S. perfoliatum* and *S. integrifolium* showed a significant difference between the studied accessions over the major part of the observation period. Thus, *S. perfoliatum* shows an average p-value of 0.0077 and *S. integrifolium* shows a p-value of 0.013 on average over this period. At the end of the experiment, the differences became non-significant due to the fact that complete senescence occurred in all accessions.

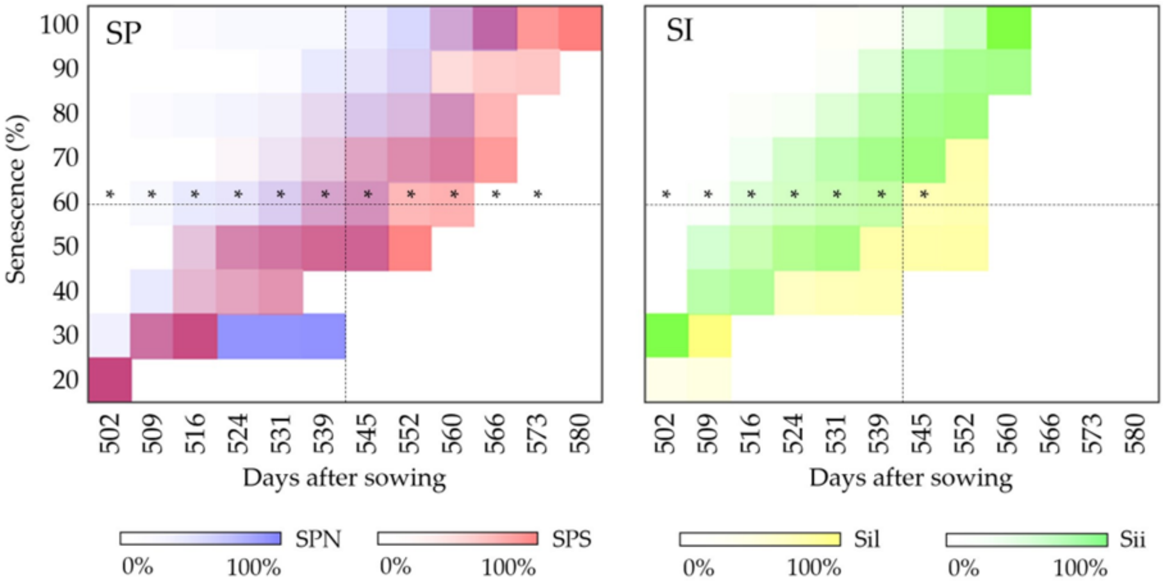

**Figure 6.10: Heat map of the course of senescence progress of *Silphium perfoliatum* (SP) and *Silphium integrifolium* (SI) from 502 to 580 days after sowing. Heat map SP shows the senescence course of both accessions of *Silphium perfoliatum* (SPN and SPS) of the second year; heat map SI shows the equivalent of both *Silphium integrifolium* accessions (Sii and Sil) (n = 36). The intensity of the coloration shows the respective relative frequency (0–100 %) of different senescence levels. After the achievement of the maximum level of development, the trait value will no longer be displayed. The star-shaped markings (*) indicate a significant difference in the average number of nodes between the accessions shown at the respective time point, with a confidence level of 95 %. The dashed lines serve as an orientation aid.**

### 6.3.3 BBCH-Coding of the Phenological Development Stages of *Silphium perfoliatum* and *Silphium integrifolium*

In the following, an adaptation of the collected data to a BBCH scale, according to Hack et al. (1992) and Meier (2018), was carried out for *Silphium perfoliatum* and *Silphium integrifolium* (tab. 6.3–tab. 6.7). For this purpose, only those stages that occurred on more than 50% of the examined plants were included (Hack et al., 1992; Meier, 2018). Accordingly, the possible BBCH stages occurring for both species are shown below, with a brief description with the respective cumulative relative frequencies determined, in order to define the relevant stages for the establishment of a BBCH scale of both investigated accessions. Additionally, illustrations of *S. perfoliatum* and *S. integrifolium* of selected BBCH stages are presented (fig. 6.11–fig. 6.15).

- BBCH Macro Stage 0—Germination

**Table 6.3: BBCH macro stage 0—Seed germination. Present stages of the different phases of seed germination, with the corresponding relative frequencies of each germination characteristic of *Silphium perfoliatum* and *Silphium integrifolium*, based on the collected data from the germination trial. (n = 36).**

| Code | | Description | 1. Year | | 2. Year | |
|---|---|---|---|---|---|---|
| | | | SP | SI | SP | SI |
| 0 | 0 | Dry seed | 1.00 | 1.00 | - | - |
| 0 | 3 | End of seed swelling | 1.00 | 1.00 | - | - |
| 0 | 5 | Radicle visible | 0.84 | 0.90 | - | - |
| 0 | 6 | Radicle elongated | 0.82 | 0.82 | - | - |
| 0 | 7 | Seed coat breakthrough of the cotyledons | 0.64 | 0.82 | - | - |
| 0 | 8 | Surface breaktrough | 0.52 | 0.76 | - | - |
| 0 | 9 | Cotyledons fully developed | 0.52 | 0.70 | - | - |

*Silphium perfoliatum*
BBCH **0 0**

*Silphium integrifolium*
BBCH **0 0**

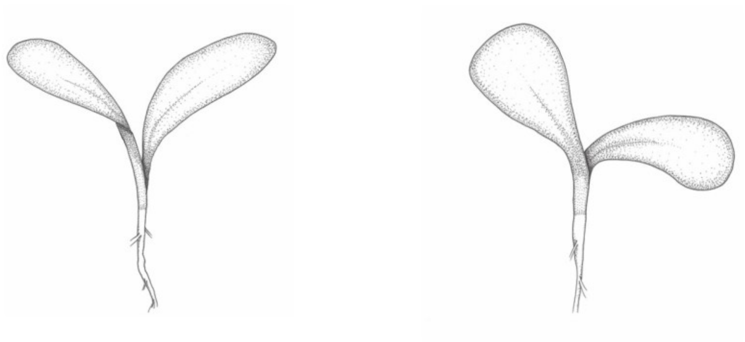

*Silphium perfoliatum*
BBCH **0 9**

*Silphium integrifolium*
BBCH **0 9**

**Figure 6.11: BBCH macro stage 0—Illustration of dry seeds and young seedlings of *Silphium* spp.**

- BBCH Macro Stage 1—Rosette Development

**Table 6.4: BBCH macro stage 1—Leave and rosette development. Present stages of rosette development based on rosette nodes or leaf pairs with the corresponding relative frequencies for the first, as well as the second, year of development of *Silphium perfoliatum* and *Silphium integrifolium* based on the collected data from the field trial. (n = 36).**

| Code | | Description | 1. Year | | 2. Year | |
|---|---|---|---|---|---|---|
| | | | SP | SI | SP | SI |
| 1 | 1 | 1st rosette node/1st pair of leaves fully developed | 1.00 | 1.00 | 1.00 | 1.00 |
| 1 | 2 | 2nd rosette node/2nd pair of leaves fully developed | 1.00 | 1.00 | 1.00 | 1.00 |
| 1 | 3 | 3rd rosette node/3rd pair of leaves fully developed | 0.97 | 1.00 | 1.00 | 1.00 |
| 1 | 4 | 4th rosette node/4th pair of leaves fully developed | 0.97 | 1.00 | 1.00 | 1.00 |
| 1 | 5 | 5th rosette node/5th pair of leaves fully developed | 0.94 | 1.00 | 1.00 | 1.00 |
| 1 | 6 | 6th rosette node/6th pair of leaves fully developed | 0.83 | 1.00 | 1.00 | 1.00 |
| 1 | 7 | 7th rosette node/7th pair of leaves fully developed | 0.63 | 1.00 | 0.92 | 0.83 |
| 1 | 8 | 8th rosette node/8th pair of leaves fully developed | - | 1.00 | 0.67 | 0.53 |
| 1 | 9 | 9th rosette node/9th pair of leaves fully developed | - | 0.91 | - | - |
| 1 | 9 | 10th rosette node/10th pair of leaves fully developed | - | 0.83 | - | - |
| 1 | 9 | 11th rosette node/11th pair of leaves fully developed | - | 0.83 | - | - |
| 1 | 9 | 12th rosette node/12th pair of leaves fully developed | - | 0.77 | - | - |
| 1 | 9 | 13th rosette node/13th pair of leaves fully developed | - | 0.71 | - | - |
| 1 | 9 | 14th rosette node/14th pair of leaves fully developed | - | 0.66 | - | - |
| 1 | 9 | 15th rosette node/15th pair of leaves fully developed | - | 0.54 | - | - |

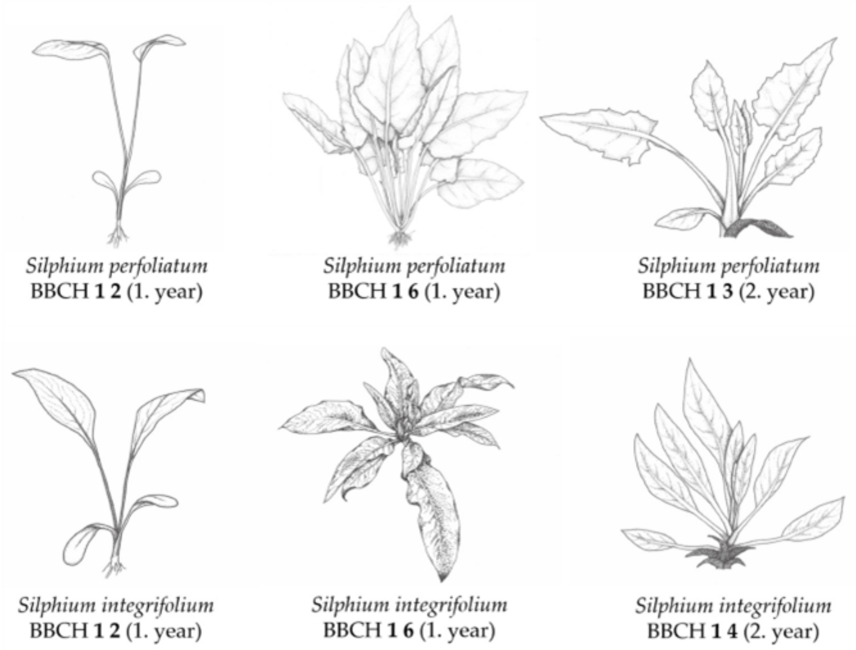

*Silphium perfoliatum*
BBCH **1 2** (1. year)

*Silphium perfoliatum*
BBCH **1 6** (1. year)

*Silphium perfoliatum*
BBCH **1 3** (2. year)

*Silphium integrifolium*
BBCH **1 2** (1. year)

*Silphium integrifolium*
BBCH **1 6** (1. year)

*Silphium integrifolium*
BBCH **1 4** (2. year)

**Figure 6.12: BBCH macro stage 1—Illustration of rosette development of *Silphium* spp.**

- BBCH Macro Stage 3—Shoot Development

**Table 6.5: BBCH macro stage 3—Shoot development (main shoot). Present stages of shoot development on the basis of shoot nodes or leaf pairs with the corresponding relative frequencies for the first, as well as the second, year of development of *Silphium perfoliatum* and *Silphium integrifolium* based on the collected data from the field trial. The consecutive numbering is to be understood as the subtracted respective rosette nodes. (n = 36).**

| Code | | Description | 1. Year | | 2. Year | |
|---|---|---|---|---|---|---|
| | | | SP | SI | SP | SI |
| 3 | 1-x | 1st shoot node/corresponding leaves fully developed | - | - | - | - |
| 3 | 2-x | 2nd shoot node/corresponding leaves fully developed | - | - | - | - |
| 3 | 3-x | 3rd shoot node/corresponding leaves fully developed | - | - | - | - |
| 3 | 4-x | 4th shoot node/corresponding leaves fully developed | - | - | - | - |
| 3 | 5-x | 5th shoot node/corresponding leaves fully developed | - | - | 0.67 | 0.56 |
| 3 | 6-x | 6th shoot node/corresponding leaves fully developed | - | - | 0.86 | 0.92 |
| 3 | 7-x | 7th shoot node/corresponding leaves fully developed | - | - | 0.94 | 1.00 |
| 3 | 8-x | 8th shoot node/corresponding leaves fully developed | - | - | 0.97 | 1.00 |
| 3 | 9-x | 9th shoot node/corresponding leaves fully developed | - | - | 1.00 | 1.00 |
| 3 | 9-x | 10th shoot node/corresponding leaves fully developed | - | 0.57 | 1.00 | 1.00 |
| 3 | 9-x | 11th shoot node/corresponding leaves fully developed | - | 0.71 | 1.00 | 1.00 |
| 3 | 9-x | 12th shoot node/corresponding leaves fully developed | - | 0.89 | 1.00 | 1.00 |
| 3 | 9-x | 13th shoot node/corresponding leaves fully developed | - | 0.89 | 0.89 | 1.00 |
| 3 | 9-x | 14th shoot node/corresponding leaves fully developed | - | 0.89 | 0.61 | 1.00 |
| 3 | 9-x | 15th shoot node/corresponding leaves fully developed | - | 0.89 | - | 0.97 |
| 3 | 9-x | 16th shoot node/corresponding leaves fully developed | - | 0.89 | - | 0.97 |
| 3 | 9-x | 17th shoot node/corresponding leaves fully developed | - | 0.89 | - | 0.97 |
| 3 | 9-x | 18th shoot node/corresponding leaves fully developed | - | 0.89 | - | 0.94 |
| 3 | 9-x | 19th shoot node/corresponding leaves fully developed | - | 0.89 | - | 0.94 |
| 3 | 9-x | 20th shoot node/corresponding leaves fully developed | - | 0.89 | - | 0.94 |
| 3 | 9-x | 21st shoot node/corresponding leaves fully developed | - | 0.63 | - | 0.94 |
| 3 | 9-x | 22nd shoot node/corresponding leaves fully developed | - | 0.54 | - | 0.86 |
| 3 | 9-x | 23rd shoot node/corresponding leaves fully developed | - | 0.51 | - | 0.81 |
| 3 | 9-x | 24th shoot node/corresponding leaves fully developed | - | - | - | 0.75 |
| 3 | 9-x | 25th shoot node/corresponding leaves fully developed | - | - | - | 0.56 |

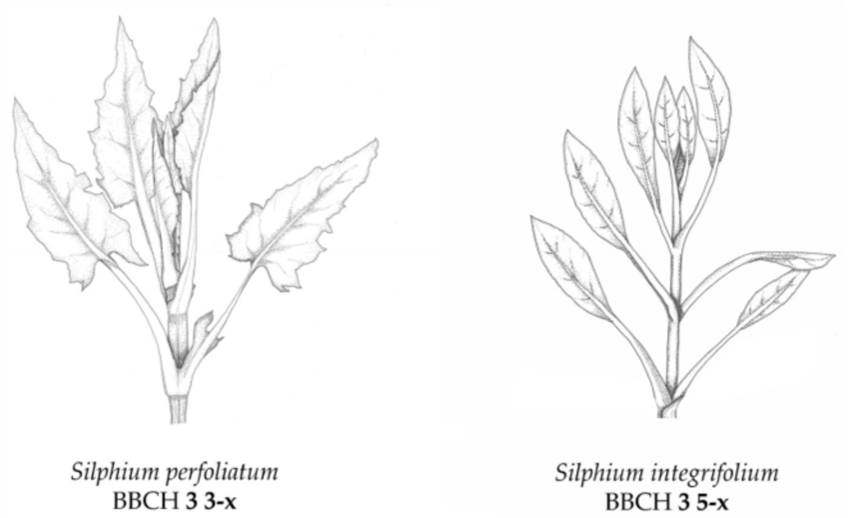

*Silphium perfoliatum*
BBCH **3 3-x**

*Silphium integrifolium*
BBCH **3 5-x**

**Figure 6.13: BBCH macro stage 3—Illustration of shoot and leaf development of *Silphium* spp.**

- BBCH Macro Stage 5–8—Generative Stage

As the generative phase of *S. perfoliatum* or *S. integrifolium* occurs rank-wise and independently nested, several BBCH stages occur in parallel. It is therefore recommended to define all occurring BBCH stages.

**Table 6.6: BBCH macro stage 5–8—Generative development. Present stages of the generative phase based on bud and flower development as well as seed filling and ripening with the corresponding relative frequencies for the first as well as the second year of development of *Silphium perfoliatum* and *Silphium integrifolium*. (n = 36).**

| Code | | Description | 1. Year | | 2. Year | |
|---|---|---|---|---|---|---|
| | | | SP | SI | SP | SI |
| | | Macro Stage 5—Bud formation | | | | |
| 5 | 1 | 1st rank: bud fully developed | - | 0.63 | 1.00 | 1.00 |
| 5 | 2 | 2nd rank: buds fully developed | - | - | 1.00 | 1.00 |
| 5 | 3 | 3rd rank: buds fully developed | - | - | 1.00 | 1.00 |
| 5 | 4 | 4th rank: buds fully developed | - | - | 1.00 | 1.00 |
| 5 | 5 | 5th rank: buds fully developed | - | - | 1.00 | 1.00 |
| 5 | 6 | 6th rank: buds fully developed | - | - | 0.94 | 0.97 |
| 5 | 7 | 7th rank: buds fully developed | - | - | 0.56 | 0.69 |
| | | Macro Stage 6—Flowering | | | | |
| 6 | 1 | 1st rank: Flower fully developed | - | 0.50 | 1.00 | 0.97 |
| 6 | 2 | 2nd rank: Flowers fully developed | - | - | 0.97 | 0.94 |
| 6 | 3 | 3nd rank: Flowers fully developed | - | - | 1.00 | 1.00 |
| 6 | 4 | 4th rank: Flowers fully developed | - | - | 0.97 | 1.00 |
| 6 | 5 | 5th rank: Flowers fully developed | - | - | 0.92 | 0.97 |
| 6 | 6 | 6th rank: Flowers fully developed | - | - | 0.50 | 0.61 |
| | | Macro Stage 7—Seed filling | | | | |
| 7 | 1 | 1st rank: Seed filling fully completed | - | - | 1.00 | 1.00 |
| 7 | 2 | 2nd rank: Seed filling fully completed | - | - | 1.00 | 1.00 |
| 7 | 3 | 3rd rank: Seed filling fully completed | - | - | 1.00 | 1.00 |
| 7 | 4 | 4th rank: Seed filling fully completed | - | - | 1.00 | 1.00 |
| 7 | 5 | 5th rank: Seed filling fully completed | - | - | 0.92 | 0.97 |
| 7 | 6 | 6th rank: Seed filling fully completed | - | - | 0.53 | 0.69 |

| Code | | Description | 1. Year | | 2. Year | |
|---|---|---|---|---|---|---|
| | | | SP | SI | SP | SI |
| | | Macro Stage 8—Seed filling | | | | |
| 8 | 1 | 1st rank: Seed ripening completed | - | - | 1.00 | 1.00 |
| 8 | 2 | 2nd rank: Seed ripening completed | - | - | 1.00 | 1.00 |
| 8 | 3 | 3rd rank: Seed ripening completed | - | - | 1.00 | 1.00 |
| 8 | 4 | 4th rank: Seed ripening completed | - | - | 1.00 | 1.00 |
| 8 | 5 | 5th rank: Seed ripening completed | - | - | 0.94 | 0.97 |
| 8 | 6 | 6th rank: Seed ripening completed | - | - | 0.53 | 0.72 |

*Silphium perfoliatum* BBCH **5 1**

*Silphium perfoliatum* BBCH **5 3**

*Silphium perfoliatum* BBCH **6 1/5 3**

*Silphium perfoliatum* BBCH **8 1/7 3/5 4**

*Silphium integrifolium* BBCH **5 1**

*Silphium integrifolium* BBCH **5 3**

*Silphium integrifolium* BBCH **7 1/6 2/7 4**

*Silphium integrifolium* BBCH **8 1/7 3/5 4**

**Figure 6.14: BBCH macro stage 5–8—Illustration of generative development of *Silphium* spp.**

- BBCH Macro Stage 9—Senescence

**Table 6.7: BBCH macro stage 9—Senescence. Present stages of senescence with the corresponding relative frequencies for the first, as well as the second, year of development of *Silphium perfoliatum* and *Silphium integrifolium* (n = 36).**

| Code | | Description | 1. Year | | 2. Year | |
|---|---|---|---|---|---|---|
| | | | SP | SI | SP | SI |
| 9 | 1 | 10 % of aboveground plant parts are senescent | 0.97 | 0.86 | - | - |
| 9 | 2 | % of aboveground plant parts are senescent | 0.89 | 0.78 | 1.00 | - |
| 9 | 3 | % of aboveground plant parts are senescent | 0.75 | 0.81 | 0.97 | 1.00 |
| 9 | 4 | % of aboveground plant parts are senescent | 0.64 | 0.72 | 0.61 | 0.61 |
| 9 | 5 | % of aboveground plant parts are senescent | 0.64 | 0.75 | 0.94 | 0.69 |
| 9 | 6 | % of aboveground plant parts are senescent | 0.64 | 0.58 | 0.61 | 0.60 |
| 9 | 7 | Leaves completely senescent | 0.72 | 0.72 | 0.78 | 0.75 |
| 9 | 9 | Fully senescent aboveground plant parts | 1.00 | 1.00 | 1.00 | 1.00 |

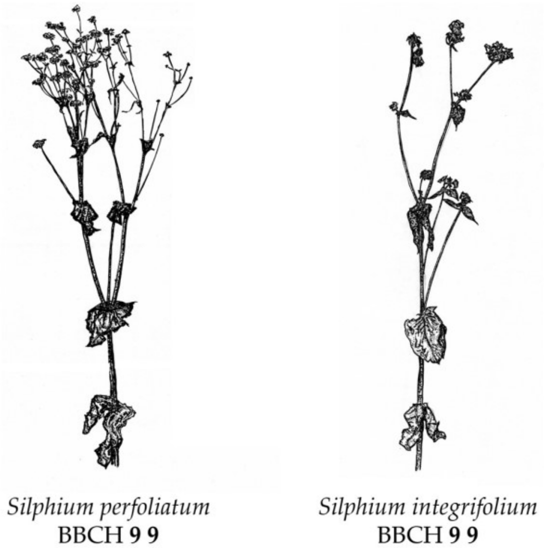

**Figure 6.15: BBCH macro stage 9—Illustration of senescence of *Silphium* spp.**

## 6.4 Discussion

In the present experiment, *Silphium perfoliatum* and *Silphium integrifolium*, each species with two different geographic accessions, were investigated with regard to their development kinetics. The aim was to identify the phenotypic plasticity for both species regarding agricultural traits. It was noticed that there are differences between, as well as within, the investigated species and accessions. In a further step, possibilities for the further development of the BBCH scale for *S. perfoliatum* of Cumplido-Marin et al. (2020) will be discussed. In addition, an adaptation for *S. integrifolium* will be carried out.

### 6.4.1 Germination Kinetics of Both *Silphium* Species

The emergence rate of Sil was distinctly higher than the emergence rates of the other *Silphium* accessions, which occurred due to unintended selection during the domestication process (Wang et al., 2018), as is well known from serval crops of lower domestication level (Pickersgill, 2007). Furthermore, it is worth mentioning that the southern accessions of both species behaved comparably with respect to the higher emergence rate compared to the western/northern variants. This can be projected accordingly to the results from the overall germination kinetics in the interspecific comparison. The *S. integrifolium* accessions show a higher relative frequency of the respective trait in all described developmental stages. Especially in Sil, this domestication syndrome was detectable, which showed up in the form of a higher germination rate (Allaby, 2014). Intraspecific differences in germination and emergence characteristics are visible between the southern and northern variants of *S. perfoliatum* within all developmental stages. They become more pronounced with increasing growth stages. In contrast, a decrease in the differences of germination characteristics between the southern and the western accession can be observed in *S. integrifolium* over time.

Based on established methods, and in order to exclude possible influencing factors, the seeds were selected by hand and underwent a 0,05 % gibberellic acid treatment. Compared to untreated or pelleted seed, this method achieved significantly higher and faster field emergence in *S. perfoliatum* than in previous studies (Gansberger et al., 2014). The omission of a seed treatment by means of light and dark phases, as well as a temperature change during the swelling phase, in combination with a wet stratification of seven days at 0 °C can be seen as a weak point of this study; however, this does not limit the validity of the observations. However, Gansberger et al. (2017) showed that a significant increase in emergence rates can be achieved with this combination of methods used. This being said, the same study shows relatively high standard deviations in the mentioned factors of 20 % to 30 %, which can support the relatively low germination rate of SPN. Transferred to the establishment of *S. perfoliatum* in field conditions, further research is needed with regard to emergence rates (Gansberger, 2017). Regarding the germination behavior of *S. integrifolium*, a study was conducted by Reinert et al. (2018) whereby different pretreatments were carried out on a chemical and thermal basis. Among other results, a treatment with Ethephon and potassium nitrate in combination with a drying process showed significant increases in the germination rate of different *S. integrifolium* accessions. Since these treatment options are also applied to sunflowers (Nasreen et al., 2015), it can be assumed that the same treatments would also be a useful instrument for *Silphium*.

### Adaption to BBCH Code—Macro Stage 0 (Meier, 2018)

In accordance to the phenotyping results, the interspecific comparison clearly shows that the *S. integrifolium* accessions tend to reach a higher degree of formation (%) at all micro stages (BBCH 0 0 to 0 9). Additionally, it can be stated that, on both studied species, the achievement of successive micro stages decreases with the increasing degree of formation. Intraspecific differences in the germination and emergence process are visible between the southern and western/northern accessions of *S. perfoliatum* and *S. integrifolium* within all micro stages, which increase with progressing growth stages. Regarding germination traits, both accessions of *S. perfoliatum* showed a high conformity with the BBCH scale established by Cumplido-Marin et al. (2020). Furthermore, an adaptation to the BBCH scale for Miscanthus × giganteus, according to Pude (1998), was omitted at this point, since resprouting in the second year of development could be clearly described on the basis of leaf formation (BBCH macro stage 1 (leaf formation)). A differentiation within this macro stage between actual seed germination and resprouting, as was carried out for the BBCH scale of *Sida hermaphrodita* L., was, accordingly, omitted (Jablonowski et al., 2017).

### 6.4.2 Rosette Development

**Year of Establishment**

Rosette development was defined by the fully developed node, contrary to the method used in the literature of considering the single leaf, since each node usually expresses two opposite leaves (Kowalski, 2004; Stanford, 1992). The descriptions in the literature differ from the data collected from the phenotyping conducted in this experiment, but tend to accurately describe the difference between *S. perfoliatum* and *S. integrifolium*. Accordingly, a formation of an average of 26 leaves (13 rosette nodes), rather than 12–17 foliage leaves (Schäfer, 2019), was observed in *S. perfoliatum* during this field experiment. In *S. integrifolium*, an average of 34 leaves (17 rosette nodes) was counted instead of 32 deciduous leaves (Kowalski, 2004; Schäfer, 2019). An adaptation to the environmental conditions regarding the leaf and root architecture, biochemical pathways and defense mechanisms of the respective origin seem clear here (van Tassel et al., 2017).

Franzaring et al. (2014) show that the results from a greenhouse experiment in which *S. perfoliatum* accessions from different geographic origins were evaluated for foliage number up to three months after sowing were also exceeded. After an experimental period of 106 days, an average of 7.1 leaves per plant were observed. The data underlying this study show a mean rosette node number of 5.67 ± 0.67 at a comparable time point (104 DAS) for *S. perfoliatum*. Thus, a mean leaf number of 10 to 12 leaves per plant can be assumed. Projected on *S. integrifolium*, Sii and SiI showed an average of 8.1 ± 1.08 rosette nodes which is equal to 16–18 rosette leaves.

**Second Year of Development**

The phenotyping in the context of rosette node development shows that all accessions formed fewer rosette nodes, so that shoot formation occurred distinctly earlier than in the previous year. The fact that SiI developed the most rosette nodes compared to all other accessions could be related to a domestication syndrome that occurred incidentally due to breeding activity on this accession (Allaby, 2014). Whether this was a breeding goal, or arose incidentally, remains to be seen. The temporal divergence between SiI and Sii is less pronounced than in the *S. perfoliatum* accessions studied. After 376 DAS, all accessions showed an end of rosette formation. From this time on, shoot formation started.

**Adaption to BBCH Code—Macro Stage 1 (Meier, 2018)**

Using the BBCH code of *S. perfoliatum* according to Cumplido-Marin et al. (2020), the evaluation was also conducted up to the 9th nodes or 18th leaf. Accompanying the higher number of fully developed nodes by the *S. integrifolium* accessions, a higher number of micro stages, as well as higher proportions of fully developed micro stages, could be scored on them using the modified BBCH macro stage "leaf development". Since the development of *Silphium* is continuous at this point, a progressive description of more than nine nodes (18 true leaves) is not absolutely necessary, provided that a node-dependent counting method is available. With respect to rosette development, a maximum BBCH-stage of 1 9, describing 9 or more rosette nodes, results for both species studied.

### 6.4.3 General Shoot Development

The shoot forms the largest part of the total yield in the biomass-oriented culture of *S. perfoliatum*. At the end of the growing period, the biomass in the leaves amounts to 30.94 % of the total biomass. After the completion of senescence, this percentage is reduced to 8.14 % (Titei, 2017). The relative proportion of biomass formed in the shoot behaves accordingly. Depending on the intended use and the expected biomass yield, the ratio of shoot to leaf biomass can be varied considerably by adjusting the harvest date. The biomass uses of *S. integrifolium* are to be assessed as secondary, since the main focus here is on its use as a perennial oilseed (van Tassel et al., 2017; Vilela et al., 2018). Accordingly, less importance is attributed to shoot formation. However, the shoot development of both species will be discussed below, as it is important for the general plant development.

The shoot development of *S. perfoliatum* and *S. integrifolium* is generally characterized by the shoot tip forming a shoot through the formation of elongated internodes and internode elongation within the already-formed rosette. A simultaneous longitudinal growth allows the rapid shoot formation (Kadereit et al., 2014). Thus, supposedly, rosette-bearing nodes become shoot-bearing nodes. Retrospectively, originally rosette-bearing nodes can be identified on the shoot by the lack of cupped leaf formation. Due to this fact, it is necessary to count continuously for nodes in the rosette and nodes on the shoot.

### Year of Establishment

Contrary to the statement of Gansberger et al. (2015), *S. perfoliatum* showed a sporadically developed shoot formation in the field trial conducted in the first year of cultivation. The tendency of *S. integrifolium* for shoot formation is in agreement with the statements of Kowalski (2004), who noted that *S. integrifolium* can reach a growth height of 20 to 69 cm in the first year. In a previous field experiment conducted by Conrad and Biertümpfel (2010), the influence of shoot formation on individual plants in the first growing season was observed with an unfavorable growth behavior of *S. perfoliatum* in the following year, so that only 0.853 Mg dry matter yield per hectare could be harvested. Accordingly, it can be assumed that differences between the previous year's shoot-forming and nonshoot-forming plants could also occur in this field trial, in the second growing season, with regard to stand closure, shoot formation as well as stand stability. As shown in the previous chapter, "Rosette development—Year of establishment", *S. perfoliatum* accessions tended to differ less than the *S. integrifolium* accessions studied with respect to rosette formation. However, SPN was the only accession characterized by a lower emergence rate and by slower emergence kinetics compared to the other *Silphium* accessions. Thus, SPN tended to show slower germination kinetics and delayed rosette development by about 21 days, which may result in failure to shoot. Other factors may also have an influence on this result (Conrad & Biertümpfel, 2010). Furthermore, *S. perfoliatum* and *S. integrifolium* showed large morphological differences (Kowalski, 2004). For instance, the average fresh mass yield of *S. integrifolium* fluctuated at 345 g per plant in the first year (Kowalski, 2004). *S. perfoliatum* formed about 50 % more biomass in the first year with an average of 519 g per plant (Kowalski, 2004; Kowalski & Wolski, 2001).

### Second Year of Development

After the simultaneous start of shoot formation in all analyzed plants, phenotypic differences were observed between and within both species. Thus, the difference regarding shoot node development in the intraspecific comparison between the studied *S. perfoliatum* accessions was characterized by a slight temporal divergence. *S. integrifolium* showed, in addition to a larger temporal discrepancy, a much larger number of formed nodes on the shoot. SiI formed significantly more nodes than Sii. Sii showed comparable results to other studies (Kowalski, 2004). Due to breeding progress and divergent parent material, SiI showed a higher number of nodes and, at this point, was apparently subject to a domestication syndrome (Allaby, 2014). *S. perfoliatum* showed a comparable number of nodes within the shoot formation of European accessions in a previous study under the same field conditions

(Wever et al., 2019). In contrast to the first year of development, a similar picture tends to be seen in the *S. integrifolium* accessions studied, with all plants now showing shoot growth. Based on the fact that shoot growth is a necessary step for generative growth in *Silphium*, it can be shown that this has also been observed elsewhere (Schiffner et al., 2021). In *S. perfoliatum*, this picture is clearer, since, in the first year of cultivation, the proportion of shooting plants was lower than or completely absent in the *S. integrifolium* accessions studied. This allows for the hypothesis that *S. perfoliatum* is more dependent on vernalization than *S. integrifolium* or that both species show different strategies for generative propagation (Pichard, 2012; Schiffner et al., 2021).

### Adaption to BBCH Code—Macro Stage 3 (Meier, 2018)

In the context of this study, only the development of a predefined main shoot of the respective plant was described, since the development of the secondary shoots occurs in parallel and these were equal. Accordingly, the BBCH macro stage 2 (side shoot formation) postulated by Meier (2018) was omitted. A description of crop closure at BBCH macro stage 2, which was carried out here for *S. perfoliatum*, in the first year (Cumplido-Marin et al., 2020), and *Sida hermaphrodita* (Jablonowski et al., 2017), is not provided in the extended BBCH scale according to Meier (2018).

After the shoot development phase was completed, the generative phase of *S. perfoliatum* and *S. integrifolium* was initiated. An overlapping of shoot growth and generative growth did not occur on the individual plant.

Delayed internode elongation (Kadereit et al., 2014) in the rosette leads to a shift in shoot node numbering. As mentioned above, this leads to a subtraction of the remaining rosette nodes and results in an optional extension of the BBCH scale. Thus, for BBCH macro stage 3, the result is an indication from 3 1−x to 3 9−x, where the sequential number describes the micro stages present and the variable x describes the nodes remaining in the rosette. Here, BBCH 3 9−x defines 9 or more fully formed shoot nodes, less the nodes remaining in the rosette. The classification of micro stages, as performed according to Cumplido-Marin et al. (2020), using the relative proportions of final shoot height as the determining measure, may present difficulties, as this can only be carried out retrospectively. Furthermore, macro stage 4 (development of vegetative plant parts), as postulated by Meier (2018), was also not included, as this stage also did not occur in the actual sense.

### 6.4.4 Generative Phase

#### Year of Establishment

Generative growth was not documented in the first year of cultivation of *S. perfoliatum* by another study. Equally, no generative development of *S. perfoliatum* is described in the summary of the literature (Gansberger et al., 2015; Titei, 2017). Contrary to these statements, some of the *S. perfoliatum* cultivated during this field experiment showed a generative growth phase in the first year. In terms of further development, neither the development of a flower, nor the formation of seeds, occurred. Another possible reason could be that the plants received on-demand irrigation at the beginning of their development and, in combination with the excellent soils and climatic conditions, partial flower induction occurred in SPS. This hypothesis is clear, but is not described in the literature. SPN, corresponding to the absence of shoot formation in the first year, showed no tendency towards generative growth. *S. integrifolium* showed a tendency to enter a generative phase of development equivalent to shoot formation in both accessions studied. Kowalski et al. (2004) documented no generative development in the first year in their developmental description of *S. integrifolium*. Contrary to this, Schiffner et al. (2021) describes that *S. integrifolium* also shows generative development depending on the sowing date, and the available development time, until the end of the vegetative phase of the first year. Sil shows a higher tendency towards generative growth than Sii whereas, in both accessions, the seed filling phase no longer occurred completely. Since these developmental steps occurred distinctly later than usual (Gansberger et al., 2015), it can be assumed that the performance of pollinating insects was diminished because of the flowering in winter.

#### Second Year of Development

In the second year of the field experiment, all plants showed full generative growth. The same was reported in other studies (Kowalski, 2004; Stanford, 1992; Schäfer, 2019). The first buds were visible in all accessions 426 DAS and, in the course of generative growth, an intraspecific variation of the respective accessions developed. This was more evident in *S. perfoliatum* and increased over the entire generative development, so that the seed ripening of SPN of each flowering rank occurred 21 days earlier than SPS. *S. integrifolium* did not show this behavior, so that a more comparable development of the generative phase in both accessions was present. Conspicuous were the far larger flowers appearing in Sil, due to the breeding activity and feminization. This increases the number of seeds formed in each flower (Prasifka et al., 2022).

Across both *Silphium* species, all investigated accessions were showed at the last flower rank just at the bud stage. A further development of the last rank in each case did not occur.

**Adaption to BBCH Code—Macro Stage 5–8 (Meier, 2018)**

A classification in the BBCH scale according to Meyer et al. (2018) is possible in the macro stage 5 to 8, which describes the generative development phase of the plant. Within the existing BBCH scale, a methodology is used giving the most precise description possible (Cumplido-Marin et al., 2020). A difficulty to be considered is that, especially in the higher ranks, there are certain shifts in the individual inflorescences in each stage, which makes it impossible to give an accurate description of the plant as a whole. One possibility to describe the inflorescence would be by using a percentage of the advanced inflorescence, as it was established within the BBCH scale of rape seed (*Brassica napus* L.; Meier, 2018). As the number of inflorescences multiplies with increasing rank, this method can be misleading, because of the problems in estimating the exact global developmental stage of the plant. A rank-by rank assessment of progressive flowering seems to be the most appropriate method. The number of flowers per rank is fixed, and each rank has a distinct designation.

## 6.4.5 Senescence

### Year of Establishment

Senescence occurred but was delayed in the first year of cultivation. Complete senescence in all accessions was seen after 307 DAS. This was probably due to the extremely mild climatic conditions until then. A cold period in the end of January provided the onset of complete senescence. *S. perfoliatum* showed a general offset of the senescence progress, so that SPN, in general, had a head start of one week, which was due to the climatic conditions of the place of origin in the northern part of the distribution area. This adaptation to climatic conditions was also found in European wild types of *Arabidopsis thaliana* (Debieu et al., 2013). Thus, it can be assumed that the southern accession (SPS) goes through a longer vegetative phase, due to its natural habitat, than a northern accession (SPN), and thus reaches full senescence later. Since the studied accessions of *S. integrifolium* originate from similar latitudes, divergence, with respect to the senescence progression between them, is not likely. Furthermore, the senescence of individual plants of *S. integrifolium* is more inhomogeneous than within the accessions of *S. perfoliatum*, as both accessions show a greater dispersion of the senescence degrees.

### Second Year of Development

The development of senescence in the second year is more differentiated in *S. perfoliatum* than in the first year. Equivalent to the first year, this behavior can be explained by the different climatic conditions of the natural origin (Debieu et al., 2013).

The *S. integrifolium* accessions studied showed a much similar senescence behavior. A tendency of earlier onset of senescence of Sii showed no influence on the achievement of complete senescence. Both accessions studied showed complete senescence at 560 DAS, which was due to the similar latitude of the origin.

### Adaption to BBCH Code—Macro Stage 9 (Meier, 2018)

A classification in the BBCH scale according to Meyer et al. (2018) is possible in macro stage 9. An initial classification in percentage terms is given, up to a degree of senescence of 60 %. The use of the BBCH scale according to Cumplido-Marin et al. (2020) is only of partial use at this point, since senescence may not proceed in the order indicated. The foliage of the plants located at the lower part of the shoot had already become necrotic while the plant was still in the generative phase, because the light intensity there was no longer sufficient. This had already occurred after about 461 DAS (no data shown). However, actual senescence was not detected until 502 DAS. Since the course of senescence is simultaneous on almost all plant parts, a percentage representation of the expression of senescence up to and including BBCH 9 6 is reasonable. BBCH 9 7 describes the complete senescence of the foliage. BBCH 9 9 describes the complete senescence of the aboveground emergence of the plants (Cumplido-Marin et al., 2020).

### 6.4.6 Classification of Phenotypic Traits and Use

Harvesting, as well as utilization, of any kind, in the first year of cultivation, should generally be avoided due to low yields and possible damage to the plants. A versatile usage of the second-year biomass is possible (Wever et al., 2019; Moll et al., 2022; Gansberger et al., 2015). Often, the time of harvest and the associated developmental stage or maturity is crucial for the use (Gansberger, 2017; Moll et al., 2022).

Here, the agronomic usability of *Silphium* maturing at different rates is an important aspect. Depending on the site conditions and climate, it makes sense to select a suitable accession. The results show that SPN may be of interest for use in the case of large weed pressure, because it is characterized by a high growth rate in rosette development in the second year of emergence in the first stages. It develops many leaves quickly and thus can take light away from competing weeds more quickly than other *Silphium* accessions through early stand closure. Soil type can also be a criterion for selecting a certain *Silphium* accession. A high clay and fine silt content, along with high water content, provide difficult conditions for trafficability as well as soil compaction (Lorenz et al., 2016). Thus, in terms of harvest timing, which accession is chosen and when it matures may be critical for a specific use. Since SPS finished maturing over two weeks later than SPN in the trial, this should be taken into consideration when choosing an accession.

With regard to economic use, the harvesting times should be clearly defined. Harvesting times should generally distinguish between green biomass and dry biomass. For practical use, it is useful to label the harvest time in BBCH scales and to map the associated dry matter content. A common classification of maturity dates for corn are the FAO numbers. These represent a use-specific maturity number that considers dry matter contents. The intended use defines the stage of maturity and, respectively, the harvest date (DMK, 2024).

Green *Silphium* biomass is mainly harvested for energy use in biogas plants (Gansberger et al., 2015; Peni et al., 2022). Plants used for fiber production for the packaging industry also have the same maturity period as those for energy use, since a cascade use is possible here (Metzler & Brodmann Saaten GmbH, 2022). The plants should be cut for harvest when the stems are not fully lignified. An advanced or even shot down lignification of the fibers is also detrimental with respect to convertibility in biogas production (Cater et al., 2014). To maximize methane yield, a harvest in summer at the end of flowering in BBCH 6 6 is envisaged. Dry matter should then range from 20 % to 25 % (Gansberger et al., 2015; Peni et al., 2022). If *Silphium* is to be harvested together with maize (*Zea mays* L.), a late-maturing accession, such as SPS, would be suitable here. If necessary, an early-maturing maize should be used here to generate a further convergence of the harvest date (Cater et al., 2014).

If the plant is to be used as a building material, the aim is to achieve a dry matter content as high as possible, and lignification that is preferably high, so that the plant is not harvested until BBCH 9 9. This development stage occurs at the end of the vegetation period. Harvesting in winter reduces the moisture content. After 596 DAS, a harvest of aboveground biomass was conducted. A mean dry matter content of 63.65 % ± 12.73 % was determined. Longer maturity in the field would suggest higher dry matter contents. It may be necessary to consider the amounts of different structures or the contents of different carbohydrates in the respective harvested material. Moll et al. (2022) found that certain *Silphium* accessions had different ratios of cortex to parenchyma, which could imply different benefits of biomass.

*S. integrifolium* can also be harvested as a biomass crop from mid-June to mid-August. Schiffner et al. (2020) described a dual use of *S. integrifolium*. Due to the different maturation dates of biomass and seeds, and the resulting discrepancy between the optimal harvest dates, an adaptation of the optimal harvest date should be carried out. Therefore, a differentiation should be made between its use for animal feed and use for oilseeds. Accessions with a safe maturity are critical for yield in oilseed use. Late *Silphium* accessions cannot realize their high yield potential in Central European climatic conditions. A higher yield can thus be generated at early harvesting times (Vilela et al., 2020). For oilseed use, the studied pre-domesticated accession Sil is the most promising. Thus, the average number of seeds per flower was distinctly increased (van Tassel et al., 2017). Since *Silphium* still shows natural seed shattering, the seeds drop out as soon as a complete maturation of the seed pod occurs. As maturation progresses continuously across the different flower ranks, an optimal harvest date must be found to ensure the highest possible yield with the best quality possible. The utilization of biomass in late spring requires high forage quality. However, the seed yield from the regrowing biomass is reduced by up to 45 %, which is equivalent to a utilization gap (Vilela et al., 2020). Furthermore, an adaptation of the ripening behavior to that of forage maize would be advisable, as a simultaneous harvest would offer great economic advantages.

The harvesting technique and the silage process for both crops are almost identical (von Cossel et al., 2020).

## 6.5 Conclusions

Different genotypes of *Silphium integrifolium* and *Silphium perfoliatum* were investigated, with two accessions each, during their establishment phase and the second year of their cultivation. Both the interspecific and intraspecific variations in the quantitative phenotypic traits and growth kinetics were analyzed. *S. integrifolium* shows distinctly more developed nodes, and a stronger tendency towards flower formation, than *S. perfoliatum* in the first year. In the second year of cultivation, the geographical difference of the places of origin of the two *S. perfoliatum* accessions studied becomes apparent by a discrepancy that increases over the course of development. *S. integrifolium* shows this to a lesser extent.

Furthermore, a BBCH scale based on genotypes with high genetic distance was developed within this study and was adapted to *S. integrifolium*. In addition, botanical drawings of the growing parts of the plant were made to provide references for exemplary developmental stages.

The suitability of differently developing accessions of *S. perfoliatum* and *S. integrifolium* were discussed. Here, different forms of usage and corresponding harvesting times were addressed. The genus *Silphium* represents two species that are good alternatives to conventional annual crops for industries of many kinds. The usage of this plant family for oil and biomass production has been intensively researched in the recent years and, for *S. integrifolium*, domestication has already started. The phenotypic variation within the exploited accessions is still at a high level, which affects the uniformity of the crop in the field. Breeding for varieties with specific uses would be crucial for further crop development and would accelerate the domestication process in both species.

# 7 Cup Plant (*Silphium perfoliatum* L.) Biomass as Substitute for Expanded Polystrene in Bonded Leveling Compounds

This work has been published as:

Lüders Moll, Martin Höller, Charlotte Hubert, **Christoph A. C. Korte**, Georg Völkering, Christian Wever, Ralf Pude (2022). Cup Plant (*Silphium perfoliatum* L.) Biomass as Substitute for Expanded Polystyrene in Bonded Leveling Compounds. *Agronomy* 2022, *12*, 178. https://doi.org/10.3390/agronomy12010178.

The following manuscript has not been modified from the published version.

## 7.1 Introduction

Building and construction materials are responsible for 11 % of global annual greenhouse gas emissions, and actually building operations are adding a further 28 % (United Nations, 2009). Therefore, this industrial sector becomes an integral element of battling climate change. Construction materials, for example, could be used as long-term storage for $CO_2$ (Churkina et al., 2020). Atmospheric carbon can be trapped using technical solutions such as carbon capture and storage (Mikunda, 2021), or through the photosynthesis of plants (Terrer et al., 2021; Di Vita et al., 2017). Compared to annual plants, perennial crops allow a more sustainable biomass production due to lower nutrient requirements and increased stability against volatile climatic conditions (van Tassel et al., 2010; Crews et al., 2018; Bai et al., 2012; McLaughlin & Walsh, 1998; Schoo et al., 2017; Wever et al., 2019).

Cup plant (*Silphium perfoliatum* L.) is an undomesticated wild crop (van Tassel et al., 2017) with a dry matter yield of 14–25 Mg $ha^{-1}$ $y^{-1}$ (Bury et al., 2020), if harvested in August for biogas production or of 8.4–14.3 Mg $ha^{-1}$ $y^{-1}$ in case of harvesting in December as a raw material for building materials (Wever et al., 2019). This perennial crop can be harvested annually for a period of 15–20 years. Furthermore, cup plant presents several ecological benefits like pollen, nectar and soil health regulation resulting in an increase in biodiversity and minimization of soil erosion (Schorpp et al., 2016; Cumplido-Marin et al., 2020; Ruf & Emmerling, 2021). It is also discussed as a high-yielding bioenergy plant for problematic areas such as periodically waterlogged cropland (Ruf et al., 2019). Furthermore, cup plant has been found to substitute silage maize in biomass yield and quality (Grunwald et al., 2020). Due to these factors, and their high amounts of carbohydrates and proteins, cup plant is currently being used for biogas and fodder (van Tassel et al., 2017; Siwek et al., 2019; Wever et al., 2020; Gansberger et al., 2015). Among other biomasses, cup plant is under investigation as a potential greenhouse gas remedy through the production of biofuels (Cumplido-Marin et al., 2020). However, ecological improvement necessitates a biomass feedstock that is procured in a manner that allows an overall increase in sustainability (McLauglhlin & Walsh, 1998; Ruf & Emmerling, 2021; Lunze et al., 2020; Jami et al., 2019). To take full advantage of the ecological benefits, a late harvest with the least possible agronomical input is necessary (Ruf & Emmerling, 2021). In contrast to biogas applications, late harvests take place after the end of the flowering period so the full pollen and nectar supply is available to pollinators (Schorpp et al., 2016).

Furthermore, non-wooden perennial biomass has already been examined as a replacement for woody biomass in the paper industry (Höller et al., 2021) and particleboard manufacturing (Klimek et al., 2016; Klimek et al., 2021). Plant-based materials could play another key role in $CO_2$ fixation and sustainable construction (Bozsaky, 2019; Ljungberg, 2007). Due to its positive environmental impact, biomass is suggested as a possible substitute for traditional insulation (Bozsaky, 2019; Latif et al., 2015; Rojas et al., 2019). Schulte et al. (2021) shows that the perennial grass *Miscanthus* may compete with expanded polystyrene (EPS) for insulation applications. Other applications include light concretes or foam concrete systems. Those are investigated to improve the building materials $CO_2$ and ecological balance by substituting scarce sand, reducing the compound weight, and improving thermal insulation properties (Ramamurthy et al., 2009). Integration of natural aggregates in lightweight concrete (Pude et al., 2004; Pude et al., 2005), concrete (Acikel, 2011; Vo & Navard, 2016) and foamed concrete has been studied as reinforcements (Castillo-Lara et al., 2020). A partial substitution may be a step towards the development of implemented biomass concretes.

The physical performance of this building material substituted with cup plant may suggest different selection criteria for specific applications. Due to visual similarities of the cup plant parenchyma and EPS we assume similar insulating performance for building materials. So, the goal of the study was to investigate if cup plant can be used as lightweight aggregate and partially substitute EPS in bonded leveling compound.

## 7.2 Materials and Methods

### 7.2.1 Study Design

The parenchyma contents of several European cup plant accessions were analyzed as quality traits for insulation purposes. Bonded leveling compound served as test application. Its insulation properties and moderate strengths requirements are ideal to analyze the effect of the biomass substitution. The lightweight aggregate constitutes the high-volume compound of the BLC to reduce the overall weight. It was examined if EPS can be substituted by cup plant aggregates and if adverse biomass effects can be reduced by changing the binder. We increased the biomass (0–45 vol%) and thus decreased the EPS share along with the use of two different mineral binders. The thermal conductivity was determined by guarded hot plate analysis and the strength was determined at 20 % sample compression.

### 7.2.2 Plant Material

The cup plant biomass was grown at the Field Lab Campus Klein-Altendorf (Rheinbach, Germany). The cup plant biomass used for the BLC samples was obtained from a plot resembling the commercially available feedstock. The field trial was established by planting of plantlets in 2014 (N.L. Chrestensen Erfurter Samen und Pflanzenanzucht GmbH, Erfurt, Germany).

The plant material for the comparison of different European accessions derived from the Thüringer Landesamt für Landwirtschaft und Ländlichen Raum (TLLLR). The plants were established at the Campus Klein-Altendorf in 2016. The accessions ‘USA’, ‘Germany’, ‘Russia’, ‘Northern Europe’ and ‘Ukraine’, described by Wever et al. (2019), were used for the parenchyma quality trait. The annual mean temperature was 9.4 °C with a mean precipitation of 603 mm. The growing season included 165–170 days.

### 7.2.3 Biomass Preparation for the Construction Material Trial

The harvest of the cup plant biomass for the BLC samples was carried out in December 2016 (Champion 1200, Maschinenfabrik Kemper GmbH & Co.KG, Breul, Germany,). At this time the relocation of nutrients from the stems into the rhizomes was completed and the plants were senescent. The harvested biomass had a water content of 46 % which was reduced to 15 % after drying on a drying trailer. To produce a vegetal lightweight aggregate with a similar size distribution comparable EPS the biomass was ground with a hammer mill (BHS 100, Th. Buschhoff GmbH & Co., Ahlen, Germany) equipped with a 10 mm grinding screen. The sieve fraction used for the BLC was 1–6 mm, produced on an oscillating screen (ASM 100, S&F GmbH, Grünkraut, Germany). After sieving no further biomass processing was performed (fig. 7.1).

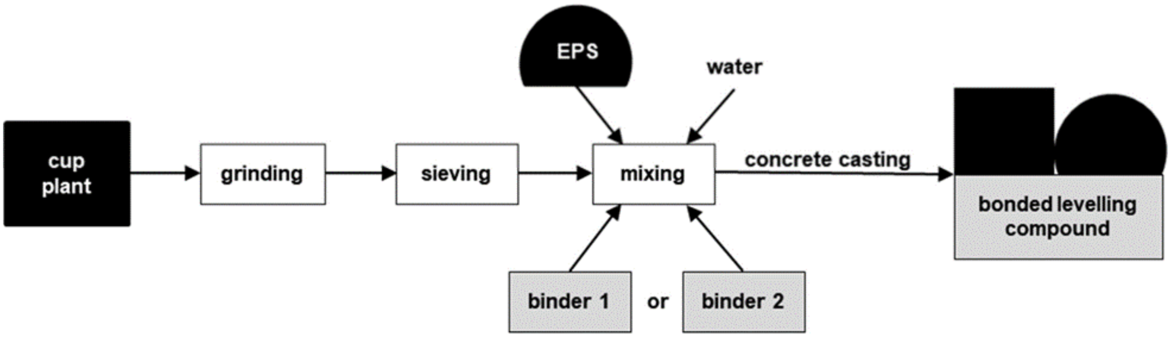

**Figure 7.1: Schematic depiction of the study design. Grinding and sieving of the cup plant biomass, followed by mixing with expanded polystyrene (EPS), water, and one of the binders.**

### 7.2.4 Parenchyma Analysis

The biomass used for the determination of the parenchyma content was harvested after senescence in November 2021. The stems were cut 10 cm above ground at the cut height of a field chopper. The inflorescence and remaining leaves were removed. The water content of the stems was 49 %. The stems were dried for 24 h at 105 °C to mass stability. Three internodes at different stem heights were used as segments for the parenchyma determination. The low segment was defined as the lowest intact internode above the cut, the high segment was the highest internode, and the third segment was the respective middle internode. From each internode a central segment of 5 cm length was sawed out and the width of each specific stem segment was recorded.

The mass ratio of cortex to parenchyma was established by longitudinal sectioning of the segments and scraping the parenchyma from the cortex pieces. Afterwards both cortex and parenchyma were weighed separately (ME 54TE, Mettler Toledo, Columbus, OH, USA).

For the estimation of the parenchyma density the cortex was removed from the lower segments and the size of the parenchyma cuboids was measured. The raw density was estimated by the individual mass of the parenchyma cuboids and their truncated volume (n = 10).

### 7.2.5 Binder Systems

Binder 1 was extracted from a commercial bonded leveling compound (Fermacell, Bonded Leveling Compound) by sieving. Binder 2 (Otterbein, PROMPT Fix) was chosen for its high compatibility with biomass aggregates as demonstrated for hempcrete (Neufert & Neff, 1997). The binder systems cannot be compared directly, as Binder 1 is a ready-mix of a cementitious quick setting binder with EPS lightweight aggregates. In contrast, Binder 2 is a highly hydraulic lime cement powder with high early strength development.

### 7.2.6 Lightweight Aggregates and Concrete Specimens

The original lightweight aggregates (EPS) of the commercial bonded leveling compound (BLC) were separated by sieving over a 1 mm sieve. The mass ratio in the commercial BLC was recorded at 80 % binder and 20 % EPS. The compositions for the substitution of EPS by cup plant aggregates were measured volumetrically. The biomass ratio ranged between 0–45 vol%, thus the EPS partition shifted between 100–55 vol%. The final list of the lightweight compositions is shown in table 7.1.

**Table 7.1: Volumetric compositions and bulk densities of the lightweight aggregate mixtures containing cup plant (CP) and expanded polystyrene (EPS).**

| | Sample Composition [%] | | | | |
|---|---|---|---|---|---|
| Lightweight component | CP 0 | CP 15 | CP 30 | CP45 | CP 100* |
| Bullk density (g cm$^{-3}$) | 0.045 | 0.050 | 0.060 | 0.070 | 0.100 |
| EPS (mL) | 6500 | 5525 | 4550 | 3575 | - |
| Cup plant (mL) | - | 975 | 1950 | 2925 | - |

*CP 100 was used as a reference for pure biomass.

All samples were produced using the same weight ratio between binder and aggregate (8:1) according to the commercial BLC. Each sample batch had ~500–600 g (6.5 L) lightweight aggregates and 2–2.2 kg mineral binder sufficient material for 4 slabs (15 × 15 × 3 cm) and 6 prisms (4 × 4 × 16 cm). The Binder 1 samples were produced by mixing 10 wt% lightweight aggregate, containing 0–45 % cup plant with 80 wt% mineral Binder 1, and water to a w/c of 0.45–0.50. The Binder 1 sample with 0 % cup plant (CP 0) was the commercial product and served as control. The Binder 2 samples were produced likewise, but with Binder 2 and ascorbic acid (8 g L$^{-1}$) as a setting delay agent, according to the manual (Neufert & Neff, 1997), and water, to a w/c of 0.76. To measure the direct substitution potential of cup plant aggregates, the mix-water was given as determined by the product manuals, and no additional water was given to treat the water uptake of the biomass. The lightweight aggregates were mixed and then wetted with 75 % of the water. Subsequently, the binder and the residual water were added and mixed for 5 min. The molds for the sample slabs and prisms were filled and compacted by manual agitation. The samples for the compression strength were produced in triplet prism molds, cured at room temperature for 7 days, and finally sawn into cubes (4 cm edge) for compression testing. The compression tests were carried out on a Hess TMN 10 (Richard Hess MBV GmbH, Sonsbeck, Germany) with compression plates at 10 mm $s^{-1}$. For those tests, a preload of 5 N was used and the force was recorded at 20 % sample compression. The slabs for the thermal conductance were cast into slabs, cured for 7 days at room temperature, and sanded flush. The slabs were dried in an oven at 60 °C. During the testing procedure, the slabs were wrapped in cling film to eliminate humidity uptake. The thermal conductance measurements were carried out at an average of 10 °C with 15 K temperature difference using a guarded hot plate apparatus of the type Lambdameter EP500e (Lambda-Meßtechnik GmbH, Dresden, Germany).

### 7.2.7 Lightweight Aggregate Analysis

Random samples of the lightweight aggregate mixtures CP 0–CP 45 and the raw biomass CP 100 were homogenized on a sample divider (Retsch, PT 100, Haan, Germany). The analysis of the aggregate sizes was carried out using dynamic image analysis on a Camsizer P4 (Retsch). The shape parameters included in the analysis are Xarea (radius of an equivalent circle), FeMax (length according to Feret), and FeMin (width according to Feret). The width to length ratio (W/L) and sphericity index (SPHT) were calculated from the shape parameters (Chaloupkocá & Ivanova, 2019). The water uptake was performed as cyclic water immersion, while the weight was recorded on the universal testing machine (TMN 10, Richard Hess MBV GmbH, Sonsbeck, Germany). After preliminary experiments, the machine was programmed to hold both extreme positions (immersed, well above water) for 30 s, to traverse the Z-axis at 10 mm $s^{-1}$, and to repeat the immersion process 20 times. Samples for the scanning electron microscope (SEM) were prepared from extracted cup plant parenchyma and EPS by drying in a desiccator for 24 h. The microscopes used were a Phenom ProX (Phenom, Thermo Fisher Scientific, Waltham, MA, USA) and a VHX-7000 (Keyence, Osaka, Japan). The pore size measurements were performed using ImageJ software (v 1.52. URL:https://imagej.nih.gov/ij/download.html, accessed on 1 May 2021).

### 7.2.8 Statistics

Data analysis was conducted in R (R Core Team, 2021) under Version 4.1.0 (18 May 2021). R: A language and environment for statistical computing. R Foundation for Statistical Computing, Vienna, Austria. URL: https://www.R-project.org/, (accessed on 18 May 2021). The used packages were: (Bentgsson, 2021; Graves et al., 2019; Signorell et al., 2021; Wickham & Hester, 2020; Wickham et al., 2019; Lenth, 2021; Gibb & Stimmer, 2012). A one-way ANOVA was performed to compare the effect of biomass ratio on the compression strength and the effect of biomass ratio on the thermal conductivity. The ANOVA was followed by Tukey HSD for homogeneous groupings. The calculations were performed on 6 repetitions for the compression strength values and on 4 repetitions for the thermal conductivity while normal distribution was assumed. The correlation coefficient of thermal conductivity vs. density was determined by the Pearson method.

## 7.3 Results and Discussion

### 7.3.1 Cup Plant Parenchyma

Due to its foamlike structure, parenchyma seems to be a suitable feedstock for insulation materials. Scanning electron microscopy (SEM) of EPS and cup plant parenchyma cells showed that the macropore diameters range the same order of magnitude for both materials as can be seen in figure 7.2. The cell size of the cup plant material (fig. 7.2a) varies between 141–217 µm and the shape is rectangular. In comparison, the EPS reveals rounded cells with size variations between 44–140 µm in figure 7.2b. Neroth & Vollenschaar (2011) assume that pores have to be closed and as small as possible for low thermal conductivity. Therefore, the pore size similarity of EPS and cup plant parenchyma suggest similar thermal conductivities.

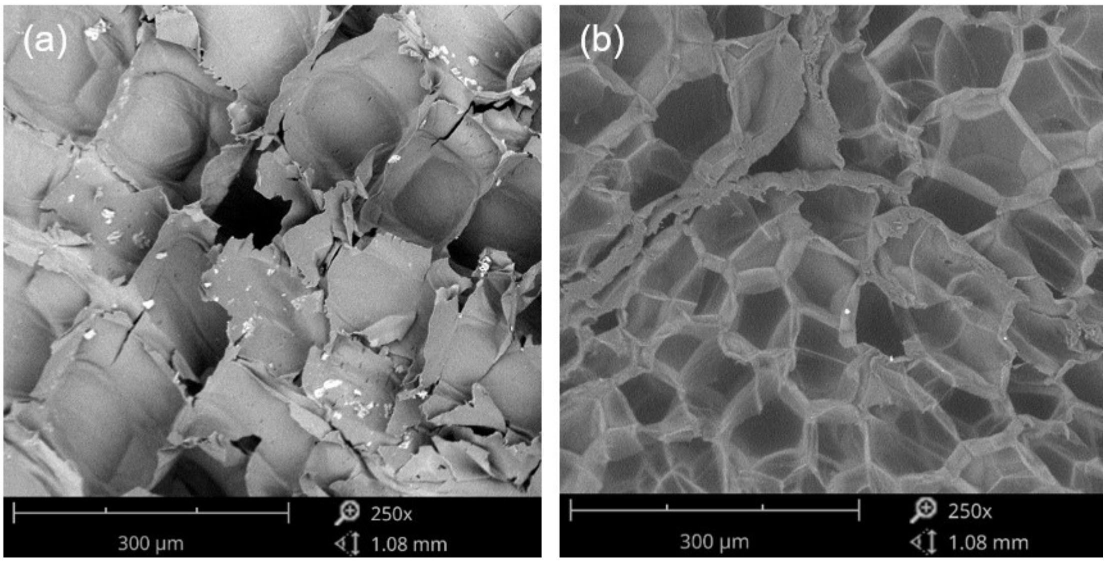

**Figure 7.2: Structural similarities of (a) cup plant parenchyma, (b) EPS granules under scanning electron microscopy with 250× magnification [10 kV, 60 Pa, image scalebar = 300 µm].**

The cross section of the cup plant stem shows the outer cortex as pink tissue after reaction with Wiesner stain and the inner non lignified parenchyma tissue (fig. 7.3). Cross-sections of the stem display a parenchyma area of approximately 44 %. Cup plant shows a high volumetric amount of parenchyma throughout the plant stem. The estimated density of parenchyma at 0.041 mg/mm$^{-3}$ is in the order of magnitude of EPS with 0.01–0.03 mg mm$^{-3}$.

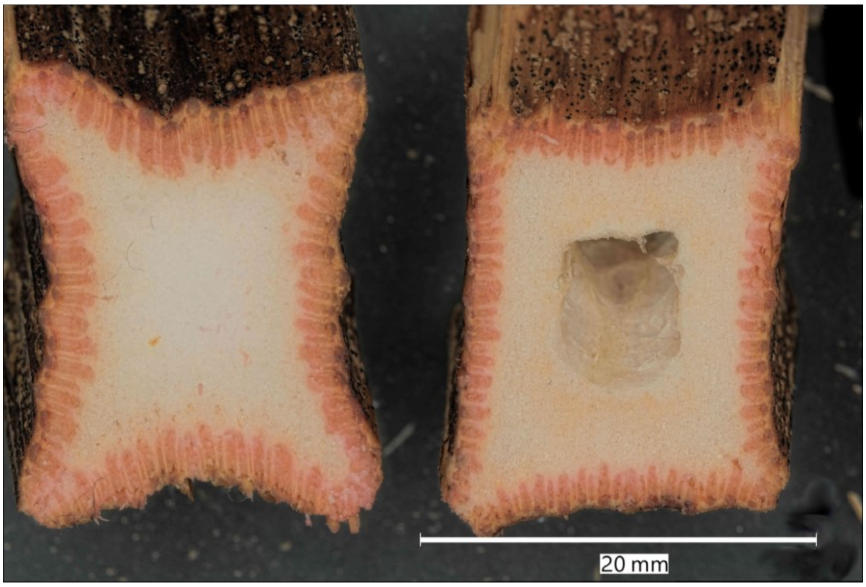

**Figure 7.3: Cross-sections of commercial cup plant stems with visible parenchyma and cortex, Wiesner staining of the lignified cortex, under 20× magnification [image scalebar= 20 mm].**

As all cup plants, the shoots, from the N.L. Chrestensen plots display a decreasing stem diameter at increasing stem heights. The stem diameter decreases up to 53 % from the bottom to top. The absolute gravimetric amount of parenchyma decreases to 38 % as shown in table 7.2. Due to the low parenchyma density an approximately tenfold amount of cortex is observed. The high standard deviation of stem width and mass is likely caused by the phenotypic variation of the N.L. Chrestensen genotypes. Due to the fact, that the commercially available seed materials (N.L. Chrestensen) is a mixture of several European accessions.

**Table 7.2: Biomass qualities of commercially available cup plant material (N.L. Chrestensen) at three different stem heights [n = 32].**

| | Diameter (mm) | Weight cortex (g) | Weight Parenchyma (g) | Cortex to Parenchyma |
|---|---|---|---|---|
| High | 6.8 ± 2.8 | 0.60 ± 0.34 | 0.05 ± 0.03 | 12 |
| Mid | 10.1 ± 3.3 | 0.93 ± 0.49 | 0.09 ± 0.06 | 10.3 |
| Low | 12.8 ± 2.8 | 1.63 ± 0.87 | 0.12 ± 0.08 | 13.6 |

The European cup plant accessions were analyzed for biomass quality in terms of parenchyma quantity. Of the five cup plant accessions displayed in figure 7.4a ‘Russia’ displayed a significantly larger parenchyma weight. With 0.121 g the parenchyma weight of ‘Russia’ is 104 % higher than the accession with the lowest parenchyma weight ‘Northern

Europe' (0.059 g). This agrees with the previous findings where 'Russia' showed the highest stem thickness (Wever et al., 2019). However, the highest annual dry matter yield is reported for 'Northern Europe' (Wever et al., 2019). Due to the high phenotypic variation of 104 % for parenchyma yield, this trait offers the possibility to develop adapted cultivars focusing on a material use of the cup plant biomass.

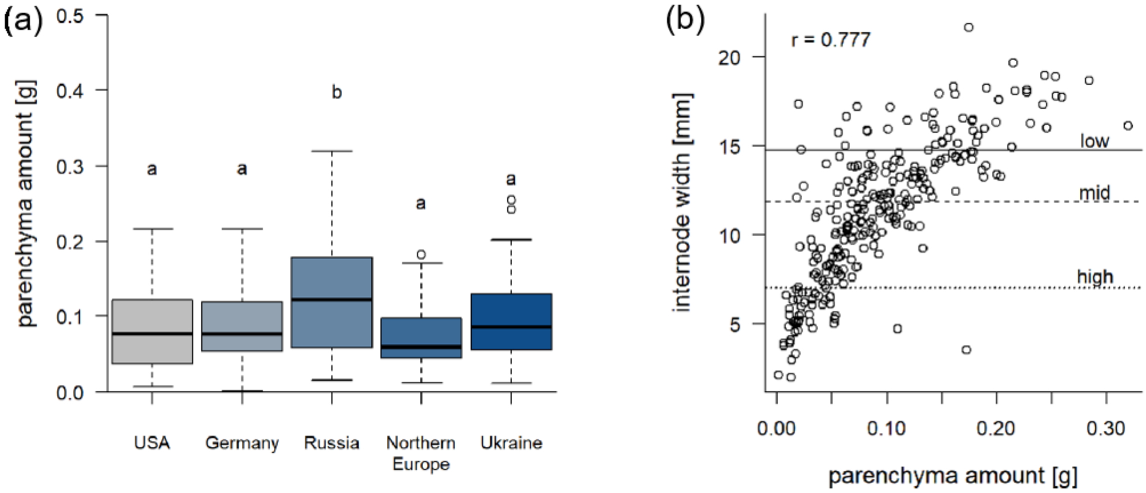

**Figure 7.4: Qualities of different European cup plant accessions. The data presented were acquired by surveying internode segments of 5 cm length. Three internodes in different heights (high, mid, low) were examined per stem. In total five accession ('USA', 'Germany', 'Russia', 'Northern Europe', 'Ukraine') with 18 stems each were analyzed. (a) Boxplots (n = 54) of parenchyma amounts as a function of their accession. The letters above represent homogenous groupings, calculated via ANOVA with following post hoc test (Tukey-HSD). Different letters indicate significance at $p < 0.05$. (b) Scatterplot of internode width against parenchyma amount (n = 270). The correlation coefficient of both parameters equals 0.777 over all five accessions. Horizontal lines display the arithmetic means of internode widths on different positions on the shoot (independent of accession).**

The parenchyma weight and stem diameter show a correlation coefficient of 0.777 over all height levels and all accessions (fig. 7.4b). Therefore, cultivating cup plant accessions with increased shoot diameters define a new cup plant ideal type for material use. The variance of biomass quality in the European gene pool shows that various accessions could be differently suited as feedstock for materials production.

### 7.3.2 Aggregate Analysis

To substitute cup plant in the BLC the shape parameters need to match the original EPS aggregates. The observed cup plant aggregates exist mainly as rod-like shapes of different aspect ratios. Elongated aggregates with low aspect ratios appear to be dominated by the outer section of the cortex. In contrast, the shorter aggregates contain more parenchyma. The resulting biomass is a wide spread of rod-like larger aggregates and more granulated smaller aggregates. In comparison, the EPS used in this study consists of mainly spherical aggregates.

Figure 7.5a shows the high volumetric parenchyma content in the native stem. Shredding of the plant during harvest and processing in the hammer mill causes losses, which can be observed in figure 7.5a. The overall size of the cup plant aggregates (CP 100) obtained by milling and sieving comparable to the expanded polystyrene (CP 0) separated from the concrete mix. However, the shape of the cup plant aggregates is inhomogeneous with mainly rod-like aggregates (fig. 7.5a) in contrast to the round EPS (fig. 7.5b).

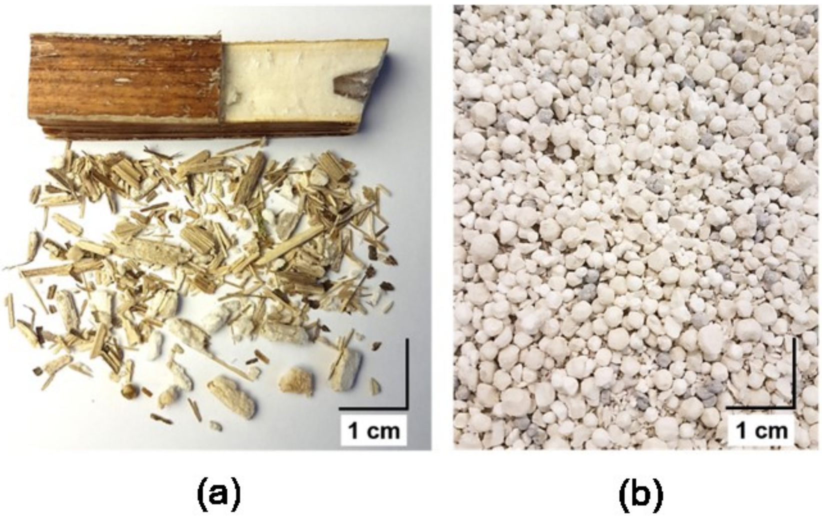

**Figure 7.5: Lightweight aggregate examples (a) Cup plant stem and milled sieve fraction; (b) Expanded polystyrene aggregates (sieve fraction: 1–6 mm) [Scalebar = 1 cm].**

The composition of the lightweight aggregates shows distinct differences in size (fig. 7.5 and fig. 7.6) and shape distributions for EPS (CP 0; fig. 7.6a), the mixture of cup plant aggregates and EPS (CP 45; fig. 7.6b), as well as pure milled cup plant (CP 100; fig. 7.6c). The aggregate size as cumulative share (Q) of the total distribution allows to represent the influence of the amount of different aggregate sizes on the total composition of the mixtures. The shape of the EPS (CP 0) curves (fig. 7.6a) is approximately a parallel sigmoidal curve in all measured shape parameters. This indicates relatively uniform aggregate shape and aspect ratios. The distinct sigmoid shape also shows a sharp aggregate size cut-off, where 10 % of the aggregates have a width or equivalent radius below 3 mm. Aggregates above 6 mm have nearly no contribution. The same behavior is observable for the aggregate length but shifted to a size interval of 4–7 mm. In the case of CP 100 (fig. 7.6c), the sigmoid for the length distribution (FeMax) displays a decreasing slope with increasing aggregate size compared to both other parameters. The size range of the pure biomass up to 3 mm width spans 85 %, while it reaches 75 % at a length up to 7 mm. For the mixtures of biomass and EPS (CP 45), the overall shape of all sigmoid curves shows an increased presence of small aggregates (fig. 7.6b). A shift towards smaller aggregate girths (FeMin) raises the number of aggregates below 3 mm to 25 %. The length span of the aggregates is slightly increased (FeMax) from 3–8 mm.

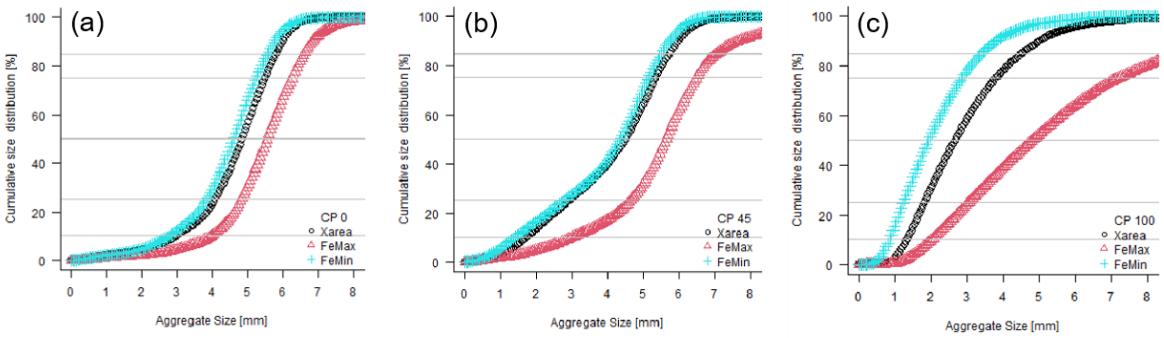

**Figure 7.6: Average development of aggregate shape parameters with increasing cup plant ratio (CP) as cumulative size distribution Q. (a) CP 0: EPS extracted from the commercial mix; (b) CP 45: mix composition of 45 vol% milled cup plant aggregates and 55 vol% extracted EPS; (c) CP 100: cup plant aggregates obtained by milling and sieving. The parameters are: Feret minimal diameter (FeMin) as width; equivalent circle radius (Xarea); Feret maximal diameter (FeMax) as length [n = 4].**

Considering the change in general shape parameters such as the width to length ratio (W/L) and sphericity (SPHT) in table 7.3 at the cumulative readout Q, the influence of the biomass in the mixtures CP 15–CP 45 of up to 85 % is minor for the main amounts of the aggregates. The size and shape characteristics are still dominated by the EPS for most aggregates in all lightweight aggregate mixtures used in this study. In order to substitute EPS with an alternative feedstock, this similarity of shapes is necessary to ensure similar workability as rheology and compaction are influenced by the granulometry (Van der Putten et al., 2016; Glas et al., 2015). Otherwise, a reconstitution of an optimized mixture by predictions methods such as the Andreasen and Andersen model may be necessary (Glas et al., 2015).

Partial substitution of EPS by cup plant biomass is thus possible, as long as the found feedstock shape parameters are considered.

**Table 7.3: Development of aggregate size [mm], aspect ratio (W/L) and sphericity (SPHT, normalized) with increasing cumulative size distribution (Q [%]) of aggregate size (equivalent circle radius) at CP levels increasing from CP 0 (pure EPS) to CP 100 (pure cup plant) [n = 4].**

| | Q (%) | 10 | 25 | 50 | 75 | 85 |
|---|---|---|---|---|---|---|
| CP 0 | size | 3.0 | 4.0 | 4.8 | 5.5 | 5.8 |
| | W/L | 0.64 | 0.76 | 0.81 | 0.81 | 0.83 |
| | SPHT | 0.74 | 0.82 | 0.86 | 0.85 | 0.85 |
| CP 15 | size | 2.2 | 3.7 | 4.7 | 5.4 | 5.7 |
| | W/L | 0.45 | 0.64 | 0.76 | 0.81 | 0.80 |
| | SPHT | 0.58 | 0.74 | 0.82 | 0.84 | 0.84 |
| CP 30 | size | 1.9 | 3.3 | 4.6 | 5.4 | 5.7 |
| | W/L | 0.37 | 0.54 | 0.73 | 0.77 | 0.80 |
| | SPHT | 0.51 | 0.65 | 0.79 | 0.81 | 0.82 |
| CP 45 | size | 1.7 | 2.9 | 4.5 | 5.3 | 5.7 |
| | W/L | 0.34 | 0.45 | 0.70 | 0.76 | 0.75 |
| | SPHT | 0.50 | 0.59 | 0.76 | 0.81 | 0.79 |
| CP 100 | size | 1.3 | 1.8 | 2.7 | 3.8 | 4.6 |
| | W/L | 0.34 | 0.34 | 0.37 | 0.38 | 0.38 |
| | SPHT | 0.51 | 0.49 | 0.48 | 0.47 | 0.43 |

### 7.3.3 Early Onset Water Absorption of Cup Plant Raw Material

The water immersion cycles of cup plant biomass can be seen in figure 7.7. The individual measurement (fig. 7.7a) consists of 3 cycle stages where 0 N corresponds to the immersed sample, followed by the oversaturated peak, and the wet saturation plateau.

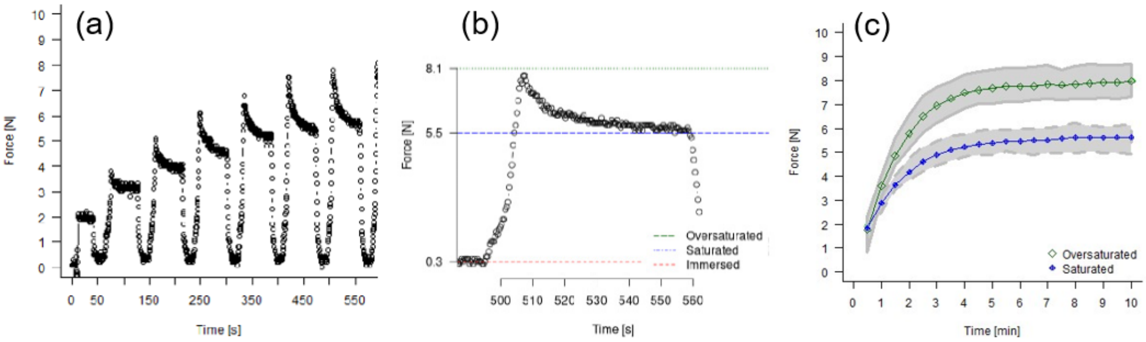

**Figure 7.7: Increasing water uptake as function over time at short wetting intervals. (a) Force against time of cyclic wetting; (b) individual force in dependence of time result of a single soaking cycle. The horizontal lines represent the three stages of soaking in water followed by dripping of adsorbed water until the wet aggregates are saturated with absorbed water; (c) force against time result as mean values of the oversaturated and saturated values. The grey area represents the value range of all samples [n = 6].**

The oversaturated peak and wet saturated plateau increase asymptotically and reach a stable value within 5 min of cumulative soaking time as seen in figure 7.7c. Pude et al. (2004) concluded that the most relevant water absorption appears in the first minutes, and presoaking of biomass is often performed in practical applications (Neufert & Neff, 1997; Kochova et al., 2016; Doudart de la Grée et al., 2019).

Water uptake of the biomass has previously been identified as a relevant parameter (Pude et al., 2004; Pude et al., 2005; Yu et al., 2013; Boix et al., 2016; Moll et al., 2020; Doudart de la Grée et al., 2021). However, water absorption is no simple linear process, as physical and chemical absorption processes are contributors as well (Doudart de la Grée et al., 2019; Brouard et al., 2018). The stable water uptake from figure 7.7c is ≈200 wt% of the biomass (300 %) for the saturation and ≈300 wt% of the biomass (400 %) for the oversaturated state.

The oversaturated state is of relevance for this application. Water that is superficially adsorbed may disturb the w/c ratio if it is desorbed during the mixing of the concrete. Table 7.4 with its recalculated w/c values was generated under the assumption that the biomass absorbed sufficient water to reach the saturation plateau during mixing of the wet concrete.

Disregarding further water competition between binder and biomass the water availability for concrete during mixing was recalculated.

**Table 7.4: Recalculated w/c for each CP level and theoretical water demand of increasing biomass substitution levels from CP 0 (pure EPS) to CP 45 (EPS 55%, cup plant 45%).**

| | CP 0 | CP 15 | CP 30 | CP 45 |
|---|---|---|---|---|
| Binder 1 w/c | 0.45 | 0.36 | 0.26 | 0.20 |
| Binder 2 w/c | 0.76 | 0.62 | 0.59 | 0.56 |
| Water demand (mL) | - | 200 | 400 | 600 |

The w/c for Binder 1 starts at a normal level of 0.45 at CP 0 but decreases rapidly (0.36–0.20) with biomass addition. The same behavior for Binder 2 causes a transition from a high w/c (0.76) to a more usual w/c ratio (0.56) with increasing biomass content.

### 7.3.4 Compression Strength

The compression strength did not display an increase over time in the measured intervals. This is likely caused by the quick-setting nature of both binders and the overall low strength of the BLC. The sample structure consists of the binder covered lightweight aggregates and gas cavities as displayed in figure 7.8.

**Figure 7.8: Samples of bonded leveling compound (a) CP 0 in Binder 1; (b) CP 30 in Binder 2.**

According to the commercial information (James Hardie Europe GmbH, 2021), Binder 1 is designed to solidify after 6 h and should reach the final compression strength of 0.4–0.5 N mm$^{-2}$ after 28 days. Binder 2 on the other hand is an inherently quick setting binder and is designed to lower a final compression strength above 0.3 N mm$^{-2}$ with biomass, according to the commercial information (Neufert & Neff, 1997). The compression strength of the control (Binder 1, CP 0) fluctuated between 0.73 and 0.86 N mm$^{-2}$ at an average of 0.79 N mm$^{-2}$. With an increase of the cup plant aggregates, the compressive strength of Binder 1 diminished from an average of 0.79 N mm$^{-2}$ (CP 0) to 0.40 N mm$^{-2}$ (CP 15) and, respectively, further to 0.38 and 0.25 N mm$^{-2}$ for CP 30 and CP 45 (fig. 7.9a). The compression strength is in the same order of magnitude as other biomass containing concretes such as *Miscanthus* concretes from Pude et al. (0.28–0.75 N mm$^{-2}$; 2004), waterproofed EPS based lightweight aggregate concretes (0.42–0.47 N mm$^{-2}$; Li & Li, 2014), Hemp lime systems from Benfratello et al. (0.09–0.46 N mm$^{-2}$; 2013) but considerably lower than the higher density (1160–1520 kg m$^{-3}$) systems with strength values ranging from 2–28 N mm$^{-2}$ reached by Chen et al. (2020).

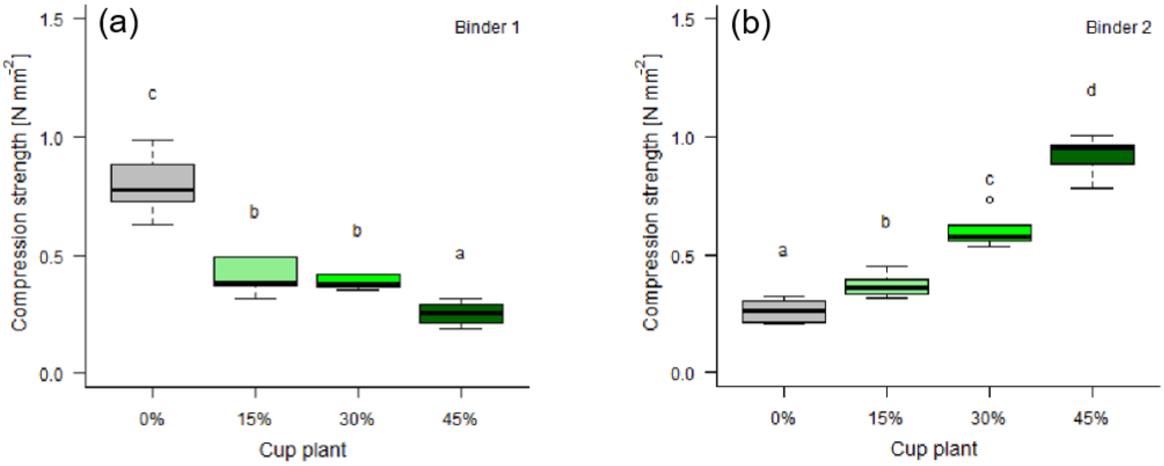

**Figure 7.9: Compression strength values [N mm$^{-2}$] at 20 % compression after 28 days. Samples with 0–45 % cup plant mixed with Binder 1 (a) or Binder 2 (b). [The letters a–d represent homogeneous subsets of the 28 days strength averages according to Tukey HSD, n = 6].**

Investigations of the interaction of concrete with biomass extractives have shown that concrete setting will be retarded by different organic species (Peschard et al., 2006; Le Ngoc Huyen et al., 2011; Diguélou et al., 2015; Doudart de la Grée et al., 2015; Kochova et al., 2017; Ye et al., 2018). The effective water to binder ratio w/c is also a factor that determines the compressive strength via concrete hydration (Pude et al., 2005; Glas et al., 2015; Yu et al., 2013; Le Ngoc Huyen et al., 2011). Even though the binders are setting quickly, the retardation effect should not be dominating since the biomass and the binder systems are still in strong competition for the available water (Caprai et al., 2018).

When compared to Binder 1, the mixture for Binder 2 is especially adapted for biomass aggregates by an increased water amount.

For Binder 2 the compressive strength behavior is reversed. The CP 0 mixture shows the lowest compressive strength at 0.26 N mm$^{-2}$. With an increased biomass ratio, the compressive strength increases from 0.37 N mm$^{-2}$ to 0.60 N mm$^{-2}$, and a maximum of 0.92 N mm$^{-2}$ (CP 45; fig. 7.9b). The samples CP 30 and CP 45, therefore, reach the desired strength values above 0.5 N mm$^{-2}$ of the product. The most likely reason for the strength increase is the initial water excess, causing a weakened matrix which is offset by increased water uptake by the biomass. The decrease in w/c is accompanied by a change in workability and mechanical properties as lower w/c ratios correspond to a higher cement stiffness (Tayossi et al., 1999). An increasing water uptake by the biomass may be the main explanation for both the increased compression strength at higher substitution levels in Binder 2, as well as the inverted strength behavior between Binder 1 and Binder 2. The Binder 2 sample is formed with a concrete mix that is made with an initially higher w/c ratio of 0.76 compared to w/c of 0.45 in Binder 1. The highest compression strengths of 0.79 N mm$^{-2}$ and 0.92 N mm$^{-2}$ are reached for CP 0 at w/c of 0.46 in Binder 1 and CP 45 at w/c at 0.76 in Binder 2. Both results correspond to the highest reached density (tab. 7.5) in their respective sets.

**Table 7.5: Density values of the compression prism samples for both binder systems at the light aggregates compositions from CP 0 (pure EPS) to CP 45 (EPS 55%, cup plant 45%).**

| Density (kg m$^{-3}$) | CP 0 | CP 15 | CP 30 | CP 45 |
|---|---|---|---|---|
| Binder 1 | 604 ± 36 | 457 ± 39 | 516 ± 22 | 466 ± 33 |
| Binder 2 | 339 ± 37 | 426 ± 32 | 564 ± 27 | 701 ± 47 |

### 7.3.5 Thermal Conductivity

The thermal conductivity for Binder 1 shows two distinct groups with CP 0 around 117 mW $m^{-1}$ $K^{-1}$ and ≈82–95 mW $m^{-1}$ $K^{-1}$ for all other biomass samples, which is shown in figure 7.10a. A drop in density of the same fashion can be seen in figure 7.11, as evidenced by the values from 565 ± 36 kg $m^{-3}$ (CP 0) to 431 ± 48 kg $m^{-3}$ (CP 45). The reduction of the density with biomass addition in Binder 1 cannot be caused by the inherent density of the lightweight aggregates, as the cup plant biomass displays a higher bulk density than the EPS as it is referenced in table 7.1. Hence, the biomass must influence the compaction of the system indirectly.

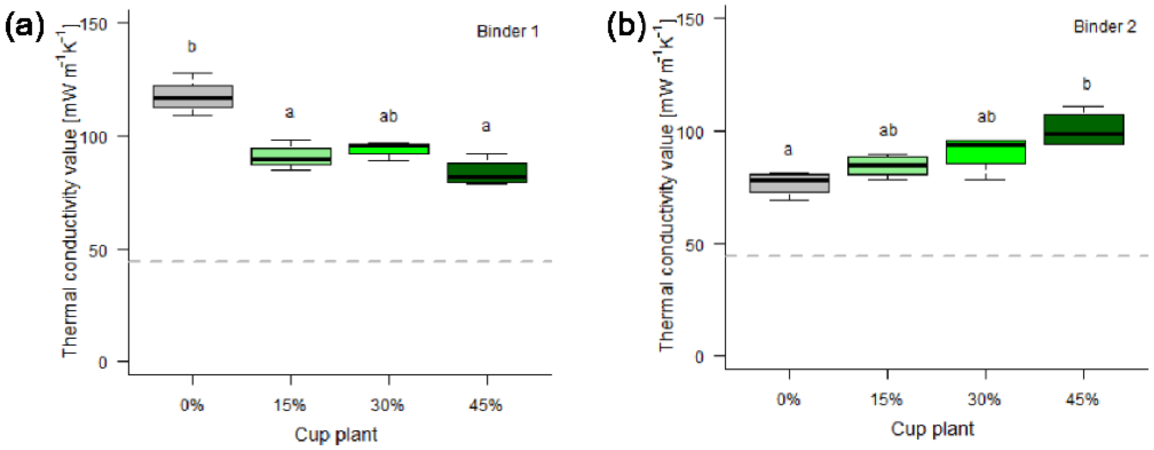

**Figure 7.10: Boxplot of the thermal conductivities [mW m−1 K−1] of bonded leveling compound slabs produced with cup plant ratios of 0–45%. The grey lines represent reference values of the pure EPS control (45 mW m−1 K−1) [69]. (a) Thermal conductivity values of Binder 1 (b); Thermal conductivity values of Binder 2; differences in values followed by a different letter for each batch are statistically significant at $p < 0.05$ [(Tukey grouping), n = 4].**

In Binder 2, the density and thermal conductivity both increase with biomass content from 78 to 99 mW $m^{-1}$ $K^{-1}$ and 359 ± 28 kg $m^{-3}$ to 506 ± 107 kg $m^{-3}$ for CP 0 and CP 45, respectively, figure 7.10b as well as figure 7.11. The resulting thermal conductivities for both binders are in the same order of magnitude as other insulation concretes found in literature such as hemp lime biocomposite with 83 mW $m^{-1}$ $K^{-1}$ at 231 kg $m^{-3}$ (Benfratello et al., 2013), or ultra-lightweight concrete from *Miscanthus* fiber and expanded glass with 90 mW $m^{-1}$ $K^{-1}$ at 554 kg $m^{-3}$ (Chen et al., 2020). A strong correlation (r = 0.86) between the thermal conductivity and the density can be found in figure 7.11. These results are in accordance with the generally accepted theoretical framework as insulation materials tend to show lower thermal conductivity with lower density values (Freymuth et al., 2002).

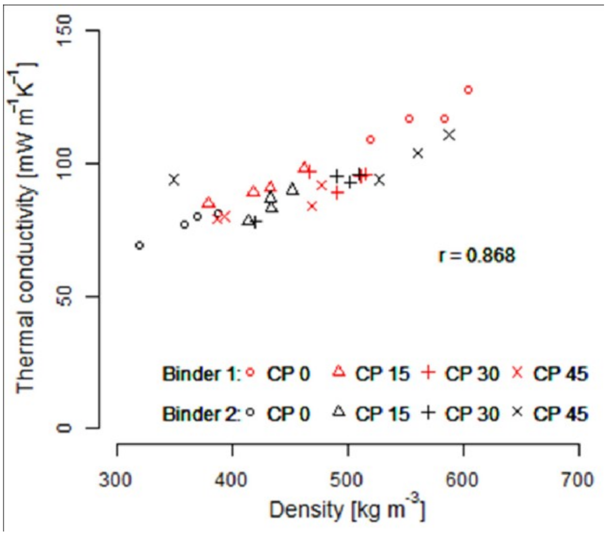

**Figure 7.11: Scatterplot of sample density against thermal conductivity values for both Binders at different ratios of cup plant biomass and EPS [n = 4, r = 0.868, p = 1.245 × $10^{-10}$].**

In combination with the apparent reversed density effect due to cup plant addition, it must be concluded that compatibility is the main factor determining the thermal conductivity, as is generally the case for insulation concrete (Samson et al., 2016). However, the span of thermal conductivities for the obtained specimen is sufficient when compared with the commercial reference (120 mW $m^{-1}$ $K^{-1}$), and follows the same behavior relations as foamed concretes as reported by Samson et al. (Samson et al., 2016).

The flow behavior and packing density of concretes have been shown to depend on both the water availability and the shape characteristics of the aggregates (Van der Putten et al., 2016). Therefore, the difference in water availability by the addition of cup plant biomass impedes the flow behavior and the compaction. Both factors leading to an inhomogeneous density.

The thermal conductivity of the composite material is thus a complex function of the lightweight aggregates, the binder system, and the w/c. Future studies of this kind of biomass systems should entail porosity and permeability tests in relation to the parenchyma content of the concrete, as well as a quantification of rheological behavior against bioaggregate granulometry.

## 7.4 Conclusions

Cup plant could change the balance of $CO_2$ emissions for certain construction materials. The local production of the low-density cup plant biomass could be ecologically beneficial compared to the production and transport of petro- or mineral-based lightweight aggregates. The influence of biomass quality traits on the performance of the materials should be further researched. The phenotypic variation of parenchyma content in the European accessions offers the possibility to develop product-adapted cultivars. Long-term breeding goals for materials applications could be derived from the relation of biomass quality and materials performance. Increased stem thickness and the correlated parenchyma increase could be used as selection criteria.

To ensure a sustainable contribution of cup plant use in construction materials the following topics need to be addressed:

- Land use competition between food and biomass production;
- Life cycle analysis of cup plant as industrial raw material;
- Industrial scalability of processing and production of bio-based building materials.

The results indicate that late harvested cup plant biomass could be a biobased substitute for EPS in bonded leveling compounds. The resulting compression strength of 0.92 N $mm^{-2}$ and thermal conductivity of 99 mW $m^{-1}$ $K^{-1}$, of the sample with 45 % cup plant, are within the original product specification. Hence, the biobased samples allow the same applications as the reference product if the binder system is adapted. At the current state, the maximum cup plant content of ≈45 % is limited by the w/c ratio and the rheology of the mix. The short-term biomass water uptake of 200 % and the water to concrete (w/c) ratio are the determining factors of the sample density. The density governs both thermal conductivity and compression strength. To obtain a better understanding of the complex insulation system, the porosity of the resulting overall system needs to be determined. The effect of the comminution on the granulometry of the aggregates must be investigated. The resulting changes in rheology must be analyzed so that optimized mixtures can be designed.

Experimental studies for the w/c need to be performed to enhance either the thermal conductivity or the compression strength. For practical applications, solid guidelines for the handling of the biomass aggregate and the casting BLC, especially the adjustment of the water to binder ratio, must be implemented. Further studies must address fire behavior, water vapor diffusion, and alternatives to the cement binder, which continues to be the main $CO_2$ emitter.

# 8 General Discussion

To evaluate the diversitiy of the available European and wild *Silphium* plant material (research question I), the phenotypic data shown in Chapter 2–5 can be combined using a principal component analysis (PCA; fig. 8.1), containing all variables for which the most accessions of both collections were phenotyped. The PCA includes points of 25 wild (green) and 5 European (blue) *Silphium* accessions as well as the convex hulls of both collections as polygons in the same colors with a certain amount of transparency. Loadings of accession means of variables are displayed as red arrows of dry matter yield (DMY), plant height (PH), shoot width (SHW), shoot number (SHN), flowering progress 1 & 2 (FP1, FP2), lodging susceptibility (LS), oil content (OC), fatty acid portions of myristic acid (14:0), palmitic acid (16:0), stearic acid (18:0), oelic acid (18:1) and linolic acid (18:2), as well as achene area (AA), achene length (AL), achene width (AW), seed number (SN) and seed weight (SW) of the first flowering rank.

The position of points can be interpreted as a function of similarity. Closer points are more similar than distant ones. The origin is the average of all variables. To compare the trait expression of the accessions, the respective points need to be projected in a right angle on the arrow. The more the projection crosses the arrow in the direction it is pointing at, the higher the achieved values of the accessions. To compare variables with each other, the angle between the arrows needs to be considered. Arrows pointing in the same direction are positively correlated, whereas arrows pointing in the opposite directions are negatively correlated. Right angles between the loading vectors indicate uncorrelated relations. The length of arrows indicates the portion of the variables total variance that is explained through this specific projection. Overall, the principal component analysis explains 50.6 % of the variation in the data. 32.9 % are explained by principal component (PC) 1 and 17.7 % by PC 2.

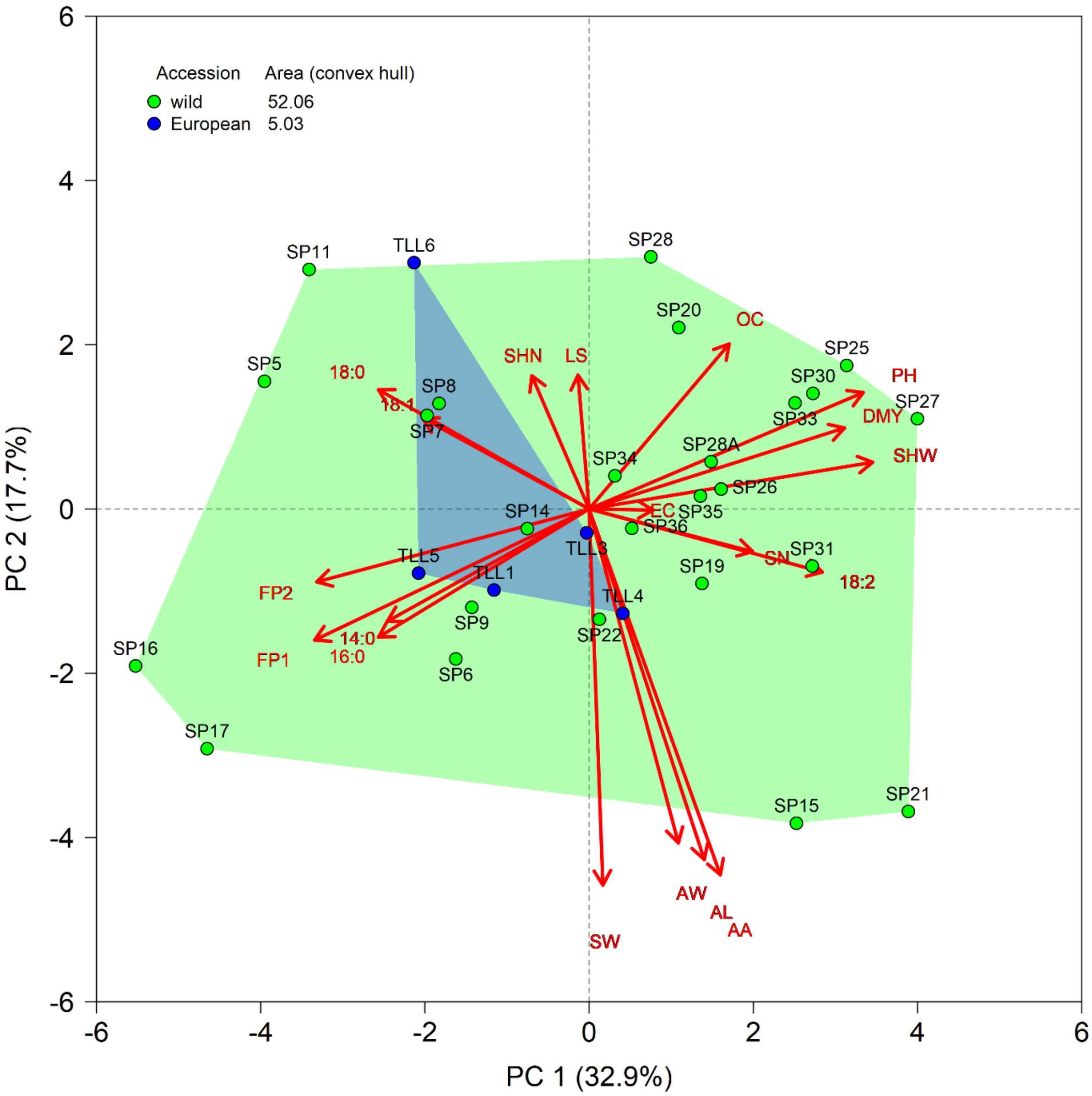

**Figure 8.1: Principal component analysis of the wild and European collection. The 25 green dots indicate wild *Silphium perfoliatum* accessions and the blue ones represent European genotypes. The green (wild accessions) and blue (European accession) polygons display the convex hulls of both collections. The area of each polygon is shown in the top-left corner. The loadings of the variables are displayed as arrows. All plant traits of chapter 2–5 for which all accessions of both collections were phenotyped are included: dry matter yield (DMY), plant height (PH), shoot width (SHW), shoot number (SHN), flowering progress 1 & 2 (FP1, FP2), lodging susceptibility (LS), oil content (OC), fatty acid portions of myristic acid (14:0), palmitic acid (16:0), stearic acid (18:0), oleic acid (18:1) and linoleic acid (18:2) as well as achene area (AA), achene length (AL), achene width (AW), seed number (SN) and seed weight (SW) of the first floral rank. The first and second principal components (PC) are included as x- and y-axis, explaining 32.9 % and 17.7 % (50.6 % in total). All plants were cultivated at Campus Klein-Altendorf, near Bonn, Germany.**

The green convex hull of the wild accessions (52.06) in figure 8.1 is about 10 times the size of the blue convex hull of the European genotypes (5.03). Therefore, the variation in the wild collection is larger than the diversity in the European collection. The new accessions expand the variability in all directions. This expansion is the lowest towards the top left. This direction is mostly associated with high shoot numbers and lodging susceptibility as well as a low achene area, achene length, achene width and seed weights. The blue convex hull of the European accessions reaches out from slightly below the average (origin) towards the previously mentioned top-left direction and to a lower extent to the bottom-left. The bottom-left direction is associated with early flowering plants with high portions of 14:0 and 16:0, as well as plants with low dry matter yields, plant heights, shoot widths and oil contents. Regarding the five European accessions, the reported genetic distance of TLL6 to TLL1–TLL5 can be confirmed based on phenotypic data (Wever et al., 2019). The analysis of cup formation (fig. 3.7) includes only parts of the collections, but it can still be shown, that the wild accessions enrich the available diversity towards directions of slower cup development (cupless to relative node 0.5) as well as faster cup development (connate at relative node 0.4). Another reduced collection was evaluated for its *Sclerotinia* susceptibility (fig. 4.4) in which neither more susceptible nor more resistant accessions were found, compared to the European genotypes, in which both resistant and susceptible accessions are represented. Nevertheless, this thesis has not determined whether the resistance or susceptibility of different accessions rely on distinct genes. This needs to be investigated in future studies. In addition, the cellulose and lignin contents of shoot biomass harvested in winter of parts of the collections were analyzed (fig. 2.4), showing almost no differences between the accessions, which means that the wild populations do not directly enrich the available diversity.

To carry out the assessment of breeding suitability of the wild *Silphium* accessions (research question II), figure 8.1 is taken into consideration again. The accessions which are more to the right than TLL4 already outperform the European genotypes concerning dry matter yield in their unbred stage. The highest yielding accessions are SP25, SP27, SP30 and SP33. Through selection of these wild populations, breeding success is expected within a few generations, with yields continuously rising. In addition, SP25, SP30 and SP33 show constant shoot widths along different years of cultivation (fig. 3.4), allowing harvested biomass to be more consistent in quantity and quality. There are accessions which show favorable and unfavorable trait expressions. SP15 and SP21 produce lower dry matter yields while forming the biggest seeds (seed weight, achene area, achene length and achene width). These genotypes can be important for aimed crosses with higher yielding populations in long-term breeding programs, to further increase seed size. On top of that, the ideotype of *S. perfoliatum* as biomass crop needs to be investigated more closely. Plant height, shoot width and flowering progress are the biomass variables that are highly associated to dry matter yield. The first and second trait are positively correlated to DMY, this connection has already been reported for the plant height (Ende et al., 2021; Dauber et al., 2015; Biertümpfel et al., 2013). The flowering progress is negatively correlated to DMY, which was to be expected, since the plant's generative growth inhibits its vegetative growth. Shoot number and lodging susceptibility are not correlated to the yield, but positively correlated to each other. This indicates that both traits have a rather low impact on biomass production of the crop, as it has already been reported by Ende et al. (2021) for shoot number. Furthermore, there might be a link between shoot number and lodging susceptibility, but no direct statement can be made about causation between the two plant traits on the basis of these data, though, so this relation needs to be investigated more closely in the course of the breeding process. To improve the biomass quality through cellulose and lignin contents, the identification of specific individuals or mutagenesis is necessary, since no meaningful differences between the accessions were found. The first step in oil quality breeding should be to reduce the heterogenicity of the fatty acids (chapter 5; Reinert et al., 2019), focusing on either saturated or unsaturated fatty acids. The easiest fatty acid for this purpose is the polyunsaturated linoleic acid (18:2), since larger portions are associated with accessions showing higher dry matter yield, yield determining variables (plant height, shoot width), seed number per flower head and oil content, as well as lower portions of saturated fatty acids (14:0, 16:0 and 18:0). Therefore, breeding cup plant for biomass and oil production should not necessarily be mutually exclusive. Nevertheless, greater breeding successes are necessary in oil production than in biomass production, so that cup plant can keep up with its competitors. In addition, to achieve a full value substitute for sunflower oil, mutagenesis might be a significant area of investigation (Soldatov, 1976; Ivanov et al., 1988; Osorio er al., 1995). Independent of which plant parts are used, cup formation trait of *S. perfoliatum* is enriched by the wild accessions (fig. 3.7). SP16 and SP17 show faster leaf development towards connate formation, whereas, SP26, SP27, SP28 and SP28A produce connate leaves at later nodes (no data for SP27 available; personal observation). However, the breeding value of different cup formations still needs to be determined. For this, the evolutionary advantages of cups, as well as the impact of different cup formations on large scale field trials need to be evaluated first. Based on the experiments of this thesis, the resistance of the European *Silphium perfoliatum* genotypes to *Sclerotinia sclerotiorum* is not expanded by the wild accessions (fig. 4.4). SP26 and TLL6 are the most resistant populations. However, since SP26 shows more favorable trait expressions than TLL6 (fig.8.1), SP26 is more suitable for a beginning in resistance breeding. Nevertheless, genes and mechanisms behind the resistances and susceptibilities needs to be investigated more closely, since discovering new resistances is fundamental for sustainable plant protection against further evolving pathogens. Furthermore, experiments with other inoculation methods should be conducted, as they might reveal more accessions with increased resistance. On top of that, *S. sclerotiorum* is one of cup plant's most important pathogens in Europe (Biertümpfel et al., 2018). However, from a global perspective *S. sclerotiorum* is only one of many pathogens that need to be considered (Turner et al., 2018; Vilela et al., 2020). As phenotyping of *Silphium* continues, as yet undetected plant traits might reveal further accessions carrying favorable expressions. Undetected plant traits may fall under one of the three following categories: first, plant parts that have not yet been investigated, like roots, rhizome and trichomes; second, other methods of trait detection using sensors for phenotyping, for example; third, taking developmental stages into consideration, which may be facilitated by the BBCH-scale (chapter 6). Plant development itself is an undetected plant trait., but traits of cup plant put into context of its respective developmental stage were not yet carried out. In addition, the BBCH-scale enables an increase of the comparability between studies. Through creation of a reference genome of cup plant, all accessions become interesting for domestication, since, aside from the desired trait expressions, the undesired ones are also helpful for identifying of the genes responsible for the respective traits. Therefore, the generally greater convex hull of the wild collection is an enrichment for plant breeding. Further, yield- and habitus-changing mechanisms like polyploidization and hybridization need to be analyzed in future projects (Van Tassel et al., 2017). Like every crop, *Silphium* has an agronomical optimum of its ploidy level, which needs to be determined, as does extensive information about the heterosis effect of the crop. First trials in crossing accessions have already led to remarkably vigorous and vital plants (personal observation; no data available). To realize large scale hybridization in a breeding program, screening for pollen sterility is essential. In addition, it may be important to share breeding successes of *S. perfoliatum* with breeders of *S. integrifolium* and *vice versa*, since Reinert et al. (2020b) demonstrated that interspecific hybrids were fertile, so that genes and thereby traits can be transferred between the species. Especially the reported higher seed production of silflower (Reinert et al., 2020b) as well as constant seed sizes along the flowering ranks (no data shown) might be interesting for cup plant breeding.

The third objective of this thesis (research question III) is to evaluate late harvested biomass of *Silphium perfoliatum* as a resource for material uses with increased nutrient use efficiencies. There are three possible applications of *Silphium* biomass as a feedstock for material use presented in this thesis: paper industry (chapter 2), insulation material (chapter 7) and oil (chapter 5). To use fibers of cup plant for pulp production is not a novelty. Höller et al. (2021) already achieved high quality paper blends, by using birch- and *Silphium* pulp of late harvested biomass with a share of 50 % each. Another method, which is already performed in practice, accesses the fibers of cup plant using steam explosion on biomass harvested in summer (Neis-Beeckmann, 2021). These fibers are then used for paper production. The study presented in this thesis (chapter 2) is the first one using *Silphium* biomass as an additive (25 %) to conventional pulp (75 %). In addition, various additive samples with different cellulose and lignin contents were analyzed. Showing improved paper quality traits along with increasing cellulose and lignin contents, breeding for raised contents of these polymers might be meaningful, in which the focus should be on cellulose content, since lignin inhibits fiber to fiber bonding in paper production (Andreasson et al., 2009). In Chapter 7, late harvested *Silphium* biomass was discussed as an expanded polystyrene (EPS) substitute for bonded leveling compound. Compression strength and thermal conductivity are within the common product specification, indicating that it could be a biobased full value substitute. Still further research is needed to optimize the bonded leveling compound. Through plant breeding, the biomass can become more suitable for an EPS substitute, by increasing the parenchyma contents in the shoots. This means breeding for thicker shoots, which, according to fig. 8.1, can happen by increasing the biomass yield. On top of that, parenchyma quality might become an interesting plant trait in the future, since pore size affects the insulation properties of the biomass. An alternative to improving process qualities proposed by Höller (2022) might be the separation of cortex and parenchyma of cup plant biomass. The cortex could then be used for pulp production and the parenchyma as insulation material, since the cortex should have a better cellulose to lignin ratio (Zhai & Lee, 2006) and the parenchyma are the cells showing similarities to expanded polystyrene (chapter 7). The material applications of *Silphium* oil will be, due do similarities, oriented to those of sunflower, including use in biodiesel, lubricants, paints, cosmetics, detergents, varnishes, agrichemicals, adhesives, plastics, fabric softeners and coatings. The respective applications are determined by the fatty acid pattern of the oil. Generally, the larger the proportion of saturated fatty acids, the lower the melting point is. In addition, polyunsaturated fatty acids have a lower thermo-oxidative stability than monounsaturated fatty acids (Garcés et al., 2009; Gupta, 2014). In contrast to the performed material uses of cup plant biomass, there are many possible applications of the oil (including human consumption). To use the oil for these applications, progress in the previously discussed fatty acid pattern, in grain yield and oil content, as well as in harvestability of *Silphium* seeds has to be made first. If this succeeds, cup plant can become a third generation crop, by producing both biomass and food, as the market situation dictates (Wever et al., 2020).

# 9 General Conclusion

In summary, the plant hunting trip across the native range of *Silphium perfoliatum* has been able to enrich our understanding of the plant's suitability for biomass production. The collection of wild *Silphium perfoliatum* accessions expands the available diversity of the most agronomical important plant traits in both directions (more and less trait expression). Exceptions are shoot number, lodging, seed geometric traits and *Sclerotinia* susceptibility as well as cellulose and lignin contents. For the first three of these traits, the expansion of variation is only directed towards lower shoot numbers, lower lodging susceptibility and larger seed geometric traits. Regarding the *Sclerotinia* pathogenicity, susceptible and resistant genotypes are already available in the European collection. Almost no differences were found in cellulose and lignin contents in the accessions of both collections.

Furthermore, the new collection is suitable for upcoming breeding programs. There are available accessions which already outperform the European genotypes in biomass production. Through selection of these accessions, further breeding successes within only a few generations are expected. Due to the high level of variation within the collection of wild accessions, plant material for long-term breeding programs has now been made available. There are plant traits in *Silphium* that are not completely understood yet (shoot number, lodging susceptibility, cup formation, *Sclerotinia* susceptibility) or that have not yet been analyzed (plant development, rhizome, etc.), all of which need closer investigation. To raise the importance of accessions with undesired trait expressions for domestication, more knowledge about the *S. perfoliatum* is needed (for example regarding the reference genome). Polyploidization and intraspecific hybridization are interesting mechanisms for cup plant breeding, which are also not yet understood and still need preparatory work. Interspecific hybridization of *Silphium perfoliatum* with *Silphium integrifolium* allows for sharing breeding successes outside the primary gene pool.

Late harvested biomass of *Silphium perfoliatum* can be used for material use. This applies especially to uses as an additive for the pulp and paper industry and as a substitute for expanded polystyrene in bonded leveling compounds. The results suggest that these applications might become sustainable alternatives in the future. The use of *Silphium* oil as a platform chemical is not recommended at the current state of knowledge. Nevertheless, the realization of this application seems possible. In general, increasing the usability of biomass increases its value stability. Additionally, working on new ways of using biomass leads to new breeding demands of the crop. Due to the early stage of *Silphium* breeding, these demands are easier to implement and facilitate the realization of unconventional usages of cup plant biomass.

# References

Acikel, H. (2011). The use of *miscanthus* (Giganteus) as a plant fiber in concrete production. *Scientific Research and Essays*, *6*(13), 2660-2667.

Albrecht, K. A., & Goldstein, W. (1997). *Silphium perfoliatum*: A North American Prairie Plant with Potential as A Forage Crop. Conference June 8-19 Conference Year, Winnipeg, 167-168.

Aldrich-Wolfe, L., Travers, S., & Nelson, B. D., Jr. (2015). Genetic Variation of *Sclerotinia sclerotiorum* from Multiple Crops in the North Central United States. *PLoS One*, *10*(9), e0139188. https://doi.org/10.1371/journal.pone.0139188

Allaby, R. G. (2014). Domestication Syndrome in Plants. In *Encyclopedia of Global Archaeology* (pp. 2182–2184). Springer.

Amselem, J., Cuomo, C. A., van Kan, J. A., Viaud, M., Benito, E. P., Couloux, A., Coutinho, P. M., de Vries, R. P., Dyer, P. S., Fillinger, S., Fournier, E., Gout, L., Hahn, M., Kohn, L., Lapalu, N., Plummer, K. M., Pradier, J. M., Quevillon, E., Sharon, A., Simon, A., ten Have, A., Tudzynski, B., Tudzynski, P., Wincker, P., Andrew, M., Anthouard, V., Beever, R. E., Beffa, R., Benoit, I., Bouzid, O., Brault, B., Chen, Z., Choquer, M., Collemare, J., Cotton, P., Danchin, E. G., Da Silva, C., Gautier, A., Giraud, C., Giraud, T., Gonzalez, C., Grossetete, S., Guldener, U., Henrissat, B., Howlett, B. J., Kodira, C., Kretschmer, M., Lappartient, A., Leroch, M., Levis, C., Mauceli, E., Neuveglise, C., Oeser, B., Pearson, M., Poulain, J., Poussereau, N., Quesneville, H., Rascle, C., Schumacher, J., Segurens, B., Sexton, A., Silva, E., Sirven, C., Soanes, D. M., Talbot, N. J., Templeton, M., Yandava, C., Yarden, O., Zeng, Q., Rollins, J. A., Lebrun, M. H., & Dickman, M. (2011). Genomic analysis of the necrotrophic fungal pathogens *Sclerotinia sclerotiorum* and *Botrytis cinerea*. *PLoS Genet*, *7*(8), e1002230. https://doi.org/10.1371/journal.pgen.1002230

Annegren, G., & Hagen, N. (2009). Industrial Beating/Refining. In *Paper Chemistry and Technology* (Vol. 3). De Gruyter. https://doi.org/10.1515/9783110213447

Assefa, T., Wu, J., Albrecht, K. A., Johnson, P. J., & Boe, A. (2015). Genetic Variation for Biomass and Related Morphological Traits in Cup Plant (*Silphium perfoliatum* L.). *American Journal of Plant Sciences*, *06*(08), 1098-1108. https://doi.org/10.4236/ajps.2015.68114

Atallah, Z. K., Larget, B., Chen, X., & .Johnson, D. A. (2004). High Genetic Diversity, Phenotypic Uniformity, and Evidence of Outcrossing in *Sclerotinia Sclerotiorum* in the Columbia Basin of Washington State. *Phytopathology*, *94*(7), 737-742. https://doi.org/10.1094/PHYTO.2004.94.7.737

Bai, C., Alverson, W. S., Follansbee, A., & Waller, D. M. (2012). New reports of nuclear DNA content for 407 vascular plant taxa from the United States. *Ann Bot*, *110*(8), 1623-1629. https://doi.org/10.1093/aob/mcs222

Becker, R. A., Wilks, A. R., Brownrigg, R., Minka, T. P., & Deckmyn, A. (2022). *maps: Draw Geographical Maps. R package version 3.3.0* https://CRAN.R-project.org/package=maps

Benfratello, S., Capitano, C., Peri, G., Rizzo, G., Scaccianoce, G., & Sorrentino, G. (2013). Thermal and structural properties of a hemp–lime biocomposite. *Construction and Building Materials*, *48*, 745-754. https://doi.org/10.1016/j.conbuildmat.2013.07.096

Bengtsson, H. (2021). *matrixStats: Functions that Apply to Rows and Columns of Matrices (and to Vectors). R package version 0.60.0.* https://CRAN.R-project.org/package=matrixStats

Biermann, C. J. (1993). *Essentials of Pulpiing and Papermaking*. Academic Press Inc.

Biertümpfel, A., & Conrad, M. (2013). *Verbundvorhaben: Erhöhung des Leistungspotenzials und der Konkurrenzfähigkeit der Durchwachsenen Silphie als Energiepflanze durch Züchtung und Optimierung des Anbauverfahrens Teilvorhaben 2: Optimierung des Anbauverfahrens und Bereitstellung von Selektionsmaterial. Fachagentur Nachwachsende Rohstoffe e. V. (FNR).* https://www.fnr.de/ftp/pdf/berichte/22012809.pdf

Biertümpfel, A., Köhler, J., Reinhold, G., Götz, R., & Zorn, W. (2018). *Leitlinie zur effizienten und umweltverträglichen Erzeugung von Durchwachsener Silphie. Thüringer Landesanstalt für Landwirtschaft*. https://nbn-resolving.org/urn:nbn:de:gbv:27-dbt-20191018-083557-002

Blechschmidt, J., Heinemann, S., Putz, H.-J., & Duffy, G. G. (2013). Fibrous Materials for Paper and Board Manufacture. In *Handbook of Paper and Board, H. Holik (Ed.)*. https://doi.org/10.1002/9783527652495.ch2

Blüthner, W.-D., Krähmer, A. & Hänsch K.-T. (2016). Züchterische Verbesserung der Silphie – erste Schritte. *Journal für Kulturpflanzen*, *68*(12), 392-398. https://doi.org/10.1399/JfK.2016.12.09

Boe, A., Albrecht, K. A., Johnson, P. J., & Wu, J. (2019). Biomass Production of Cup Plant (*Silphium perfoliatum* L.) in Response to Variation in Plant Population Density in the North Central USA. *American Journal of Plant Sciences*, *10*(06), 904-910. https://doi.org/10.4236/ajps.2019.106065

Boix, E., Georgi, F., & Navard, P. (2016). Influence of alkali and Si-based treatments on the physical and chemical characteristics of *miscanthus* stem fragments. *Industrial Crops and Products*, *91*, 6-14. https://doi.org/10.1016/j.indcrop.2016.06.030

Boland, G. J., & Hall, R. (1994). Index of plant hosts of *Sclerotinia sclerotiorum*. *Canadian Journal of Plant Pathology*, *16*(2), 93-108. https://doi.org/10.1080/07060669409500766

Bolton, M. D., Thomma, B. P., & Nelson, B. D. (2006). *Sclerotinia sclerotiorum* (Lib.) de Bary: biology and molecular traits of a cosmopolitan pathogen. *Mol Plant Pathol*, *7*(1), 1-16. https://doi.org/10.1111/j.1364-3703.2005.00316.x

Bordenave, C. D., Escaray, F. J., Menendez, A. B., Serna, E., Carrasco, P., Ruiz, O. A., & Garriz, A. (2013). Defense responses in two ecotypes of *Lotus japonicus* against non-pathogenic *Pseudomonas syringae*. *PLoS One*, *8*(12), e83199. https://doi.org/10.1371/journal.pone.0083199

Bozsaky, D. (2019). Nature-Based Thermal Insulation Materials From Renewable Resources – A State-Of-The-Art Review. *Slovak Journal of Civil Engineering*, *27*(1), 52-59. https://doi.org/10.2478/sjce-2019-0008

Brouard, Y., Belayachi, N., Hoxha, D., Ranganathan, N., & Méo, S. (2018). Mechanical and hygrothermal behavior of clay – Sunflower (*Helianthus annuus*) and rape straw (*Brassica napus*) plaster bio-composites for building insulation. *Construction and Building Materials*, *161*, 196-207. https://doi.org/10.1016/j.conbuildmat.2017.11.140

Bundessortenamt (2000). Richtlinien für die Durchführung von landwirtschaftlichen Wertprüfungen und Sortenversuchen. Bundessortenamt. Landbuch Verlag, Hannover.

Burke, J. M., Shunxue, T., Steven, J. K., & Riesenberg, L. H. (2002). Genetic Analysis of Sunflower Domestication. *Genetics*, *161*, 1257-1267. https://doi.org/10.1093/genetics/

Bury, M., Możdżer, E., Kitczak, T., Siwek, H., & Włodarczyk, M. (2020). Yields, Calorific Value and Chemical Properties of Cup Plant *Silphium perfoliatum* L. Biomass, Depending on the Method of Establishing the Plantation. *Agronomy*, *10*(6). https://doi.org/10.3390/agronomy10060851

Caprai, V., Gauvin, F., Schollbach, K., & Brouwers, H. J. H. (2018). Influence of the spruce strands hygroscopic behaviour on the performances of wood-cement composites. *Construction and Building Materials*, *166*, 522-530. https://doi.org/10.1016/j.conbuildmat.2018.01.162

Carbone, I., & Kohn, L. M. (2001). A microbial population−species interface: nested cladistic and coalescent inference with multilocus data. *Molecular Ecology*, *10*, 947-964. https://doi.org/10.1046/j.1365-294X.2001.01244.x

Castillo-Lara, J. F., Flores-Johnson, E. A., Valadez-Gonzalez, A., Herrera-Franco, P. J., Carrillo, J. G., Gonzalez-Chi, P. I., & Li, Q. M. (2020). Mechanical Properties of Natural Fiber Reinforced Foamed Concrete. *Materials (Basel)*, *13*(14). https://doi.org/10.3390/ma13143060

Čater, M., Zorec, M., & Logar, R. M. (2014). Methods for Improving Anaerobic Lignocellulosic Substrates Degradation for Enhanced Biogas Production. *Springer Science Reviews*, *2*(1-2), 51-61. https://doi.org/10.1007/s40362-014-0019-x

Chaloupková, V., Ivanova, T., & Krepl, V. (2019). Particle size and shape characterization of feedstock material for biofuel production. *Agronomy Research*, *117*(5), 1861-1873. https://doi.org/10.15159/AR.19.152

Chen, Y. X., Wu, F., Yu, Q., & Brouwers, H. J. H. (2020). Bio-based ultra-lightweight concrete applying *miscanthus* fibers: Acoustic absorption and thermal insulation. *Cement and Concrete Composites*, *114*. https://doi.org/10.1016/j.cemconcomp.2020.103829

Chiriac, E. R., Chiţescu, C. L., Sandru, C., Geană, E.-I., Lupoae, M., Dobre, M., Borda, D., Gird, C. E., & Boscencu, R. (2020). Comparative Study of the Bioactive Properties and Elemental Composition of Red Clover (*Trifolium pratense*) and Alfalfa (*Medicago sativa*) Sprouts during Germination. *Applied Sciences*, *10*(20). https://doi.org/10.3390/app10207249

Churkina, G., Organschi, A., Reyer, C. P. O., Ruff, A., Vinke, K., Liu, Z., Reck, B. K., Graedel, T. E., & Schellnhuber, H. J. (2020). Buildings as a global carbon sink. *Nature Sustainability*, *3*(4), 269-276. https://doi.org/10.1038/s41893-019-0462-4

CKA. (2024). *Informationen zum Standort*. Campus Klein-Altendorf. Retrieved 09.03.2024 from https://www.aussenlabore.uni-bonn.de/cka/de/standort/copy_of_standortbeschreibung

CKA. (2024). *Wetterdaten*. Campus Klein-Altendorf. Retrieved 09.03.2024 from https://www.aussenlabore.uni-bonn.de/cka/de/standort/wetterdaten

Clevinger, J. A. (2004). New Combination in *Silphium* (Asteraceae: *Heliantheae*). *Novon*, *14*(3), 275-277.

Clevinger, J. A. (2020). *Silphium Integrifolium Michaux*. Flora of North America Association. Retrieved 09.03.2024 from http://floranorthamerica.org/Silphium_integrifolium

Clevinger, J. A. (2020). *Silphium perfoliatum Linnaeus*. Flora of North America Association. Retrieved 09.03.2024 from http://floranorthamerica.org/Silphium_perfoliatum

Clevinger, J. A., & Panero, J. L. (2000). Phylogenetic analysis of *Silphium* and subtribe *Engelmanniinae* (Asteraceae: *Heliantheae*) based on ITS and ETS sequence data. *American Journal of Botany*, *87*(4), 565-572. https://doi.org/10.2307/2656600

Conrad, M., Biertümpfel, A., & Vetter, A. (2010). *Optimierung des Anbauverfahrens für Durchwachsene Silphie (Silphium perfoliatum) als Kofermentpflanze in Biogasanlagen sowie Überführung in die landwirtschaftliche Praxis*. https://www.fnr.de/index.php?id=11150&fkz=22004307

Crews, T. E., Carton, W., & Olsson, L. (2018). Is the future of agriculture perennial? Imperatives and opportunities to reinvent agriculture by shifting from annual monocultures to perennial polycultures. *Global Sustainability*, *1*. https://doi.org/10.1017/sus.2018.11

Crispell, J. (2021). *basicPlotteR*. GitHub. GitHub repository. Retrieved 09.03.2024 from https://github.com/JosephCrispell/basicPlotteR#basicplotter

Cumplido-Marin, L., Graves, A. R., Burgess, P. J., Morhart, C., Paris, P., Jablonowski, N. D., Facciotto, G., Bury, M., Martens, R., & Nahm, M. (2020). Two Novel Energy Crops: *Sida hermaphrodita* (L.) Rusby and *Silphium perfoliatum* L.—State of Knowledge. *Agronomy*, *10*(7). https://doi.org/10.3390/agronomy10070928

D'Agnone, U. (2016). *Faserstoffzusammensetzung/Fibrous Composition/Composition de Matière Fibreuse* (EP 2 825 699 B1). European Patent Office. https://worldwide.espacenet.com/patent/search/family/049160273/publication/EP2825699B1?q=EP2825699B1&search_type=patents

Dauber, J., Müller, A. L., Schnittenhelm, S., Schoo, B., Schorpp, Q., Schrader, S., & Schroetter, S. (2015). *Agrarökologische Bewertung der Durchwachsenen Silphie (Silphium perfoliatum L.) als eine Biomassepflanze der Zukunft. Fachagentur Nachwachsende Rohstoffe e. V. (FNR)*. https://www.fnr.de/ftp/pdf/berichte/22004411.pdf

Debieu, M., Tang, C., Stich, B., Sikosek, T., Effgen, S., Josephs, E., Schmitt, J., Nordborg, M., Koornneef, M., & de Meaux, J. (2013). Co-variation between seed dormancy, growth rate and flowering time changes with latitude in *Arabidopsis thaliana*. *PLoS One*, *8*(5), e61075. https://doi.org/10.1371/journal.pone.0061075

Di Vita, G., Pilato, M., Pecorino, B., Brun, F., & D'Amico, M. (2017). A Review of the Role of Vegetal Ecosystems in $CO_2$ Capture. *Sustainability*, *9*(10). https://doi.org/10.3390/su9101840

DIN EN ISO 12625-3, 2005. Tissue Paper and tissue products - Part 3: Determination of Thickness, Bulking Thickness and Apparent Bulk Density. International Organization for Standardization, Geneva, Switzerland

Diquélou, Y., Gourlay, E., Arnaud, L., & Kurek, B. (2015). Impact of hemp shiv on cement setting and hardening: Influence of the extracted components from the aggregates and study of the interfaces with the inorganic matrix. *Cement and Concrete Composites*, *55*, 112-121. https://doi.org/10.1016/j.cemconcomp.2014.09.004

DMK (2024). *Bestimmung Reifezahl*. Deutsches Maiskomitee e. V. Retrieved 09.03.2024 from https://www.maiskomitee.de/Produktion/Sorten/Bestimmung-Reifezahl

Domínguez-Muñoz, F., Anderson, B., Cejudo-López, J. M., & Carrillo-Andrés, A. (2010). Uncertainty in the thermal conductivity of insulation materials. *Energy and Buildings*, *42*(11), 2159-2168. https://doi.org/10.1016/j.enbuild.2010.07.006

Doudart de la Grée, G. C. H., Caprai, V., van Dam, J. E. G., van As, H., Brouwers, H. J. H., & Yu, Q. L. (2019). Ionic interaction and liquid absorption by wood in lignocellulose inorganic mineral binder composites. *Journal of Cleaner Production*, *206*, 808-818. https://doi.org/10.1016/j.jclepro.2018.09.220

Doudart de la Grée, G. C. H., Yu, Q. L., & Brouwers, H. J. H. (2014). Wood-wool cement board : optimized inorganic coating. Proceedings of the 14th International Inorganic-Bonded Fiber Composites Conference (IIBCC), 15-19 September 2014, Da Nang, Vietnam.

Doudart de la Grée, G. C. H., Yu, Q. L., & Brouwers, H. J. H. (2015). The effect of glucose on the hydration kinetics of Ordinary Portland Cement. *Academic Journal of Civil Engineering*, *33*(2), 126-131. https://doi.org/10.26168/icbbm2015.19

Durman, S., Menendez, A., & Godeas, A. (2005). Variation in oxalic acid production and mycelial compatibility within field populations of. *Soil Biology and Biochemistry*, *37*(12), 2180-2184. https://doi.org/10.1016/j.soilbio.2005.03.017

Ekins, M. G., Aitken, E. A. B., & Goulter, K. C. (2007). Aggressiveness among isolates of *Sclerotinia sclerotiorum* from sunflower. *Australasian Plant Pathology*, *36*, 580-586. https://doi.org/https://doi.org/10.1071/AP07062

Ende, L. M., Knöllinger, K., Keil, M., Fiedler, A. J., & Lauerer, M. (2021). Possibly Invasive New Bioenergy Crop Silphium perfoliatum: Growth and Reproduction Are Promoted in Moist Soil. *Agriculture*, *11*(1). https://doi.org/10.3390/agriculture11010024

FNR (2023). *Anbau. Table, Anbaufläche nachwachsender Rohstoffe in Deutschland nach Kulturarten 2020-2022*. Fachagentur Nachwachsende Rohstoffe e. V. (FNR). Retrieved 09.03.2024 from https://www.fnr.de/nachwachsende-rohstoffe/anbau

Foster, C. E., Martin, T. M., & Pauly, M. (2010a). Comprehensive compositional analysis of plant cell walls (Lignocellulosic biomass) part I: lignin. *J Vis Exp*(37). https://doi.org/10.3791/1745

Foster, C. E., Martin, T. M., & Pauly, M. (2010b). Comprehensive compositional analysis of plant cell walls (lignocellulosic biomass) part II: carbohydrates. *J Vis Exp*(37). https://doi.org/10.3791/1837

Franklin Inst (1835). Straw Paper. *Journal of the Franklin Institute*, *19*(4), 292. https://doi.org/10.1016/s0016-0032(35)91752-5

Franzaring, J., Schmid, I., Bäuerle, L., Gensheimer, G., & Fangmeier, A. (2013). Investigations on plant functional traits, epidermal structures and the ecophysiology of the novel bioenergy species *Sida hermaphrodita* Rusby and *Silphium perfoliatum* L. *Journal of Applied Botany and Food Quality*, *87*, 36-45. https://doi.org/10.5073/JABFQ.2014.087.006

Freymuth, H., Jenisch, R., Klopfer, H., Petzold, K., Strohrer, M., Fischer, H.-M., & Richter, E. (2002). *Lehrbuch der Bauphysik: Schall-Wärme-Feuchte-Licht-Brand-Klima*. Vieweg+Teubner Verlag.

Fuller, D. Q. (2007). Contrasting patterns in crop domestication and domestication rates: recent archaeobotanical insights from the Old World. *Ann Bot*, *100*(5), 903-924. https://doi.org/10.1093/aob/mcm048

Gansberger, M. (2016). Samenmorphologie, Keimprozess, Saatgutaufbereitung und Bestimmung der Lebensfähigkeit von *Silphium perfoliatum* L. Samen. *Journal für Kulturpflanzen*, *68*(12), 363-366. https://doi.org/10.1399/JfK.2016.12.03

Gansberger, M., Montgomery, L. F. R., & Liebhard, P. (2015). Botanical characteristics, crop management and potential of *Silphium perfoliatum* L. as a renewable resource for biogas production: A review. *Industrial Crops and Products*, *63*, 362-372. https://doi.org/10.1016/j.indcrop.2014.09.047

Gansberger, M., Stüger, H.-P., Weinhappel, M., Moder, K., Liebhard, P., von Gehren, P., Mayr, J., & Ratzenböck, A. (2017). Germination characteristic of *Silphium perfoliatum* L. seeds. *Die Bodenkultur: Journal of Land Management, Food and Environment*, *68*(2), 73-79. https://doi.org/10.1515/boku-2017-0007

Gansberger, M., Weinhappel, M., von Gehren, P., Ratzenböck, A., Liebhard, P., & Mayr, J. (2014). Seed germination in Silphium perfoliatum L. & Sida hermaphrodita L. and technological measures for its improvement. Tagung der Vereinigung der Pflanzenzüchter und Saatgutkaufleute Österreichs, 19-21 November 2014, Raumberg-Gumpenstein, Irding, Austria.

Garcés, R., Martínez-Force, E., Salas, J. J., & Venegas-Calerón, M. (2009). Current advances in sunflower oil and its applications. *Lipid Technology*, *21*(4), 79-82. https://doi.org/10.1002/lite.200900016

Garg, H., Kohn, L. M., Andrew, M., Li, H., Sivasithamparam, K., & Barbetti, M. J. (2009). Pathogenicity of morphologically different isolates of *Sclerotinia sclerotiorum* with *Brassica napus* and *B. juncea* genotypes. *European Journal of Plant Pathology*, *126*(3), 305-315. https://doi.org/10.1007/s10658-009-9547-7

Gibb, S., & Strimmer, K. (2012). MALDIquant: a versatile R package for the analysis of mass spectrometry data. *Bioinformatics*, *28*(17), 2270-2271. https://doi.org/10.1093/bioinformatics/bts447

Gibson, D. R., Rowe, L., Isaacs, R., & Landis, D. A. (2019). Screening Drought-Tolerant Native Plants for Attractiveness to Arthropod Natural Enemies in the U.S. Great Lakes Region. *Environ Entomol*, *48*(6), 1469-1480. https://doi.org/10.1093/ee/nvz134

Gil, M., & Arauzo, I. (2014). Hammer mill operating and biomass physical conditions effects on particle size distribution of solid pulverized biofuels. *Fuel Processing Technology*, *127*, 80-87. https://doi.org/10.1016/j.fuproc.2014.06.016

Glas, D. J., Yu, Q. L., Spiesz, P. R., & Brouwers, H. J. H. (2015). Structural lightweight aggregates concrete. IBAUSIL, 19. Internationale Baustofftagung, 16-18 September 2015, Weimar, Germany.

Glover, J. D., Culman, S. W., DuPont, S. T., Broussard, W., Young, L., Mangan, M. E., Mai, J. G., Crews, T. E., DeHaan, L. R., & Buckley, D. H. (2010). Harvested perennial grasslands provide ecological benchmarks for agricultural sustainability. *Agriculture, Ecosystems & Environment*, *137*(1-2), 3-12. https://doi.org/10.1016/j.agee.2009.11.001

Graves, S., Piepho, H. P., Selzer, L., & Dorai-Raj, S. (2019). multcompView: Visualizations of Paired Comparisons. R Package Version 0.1-8. https://CRAN.R-project.org/package=multcompView

Grayer, R. J., Chase, M. W., & Simmonds, S. J. (1999). A comparison between chemical and molecular characters for the determination of phylogenetic relationships among plant families: An appreciation of Hegnauer’s "Chemotaxonomie der Pflanzen". *Biochemical Systematics and Ecology*, *27*, 369-393.

Greve, M., Korte, C. A. C., Entrup, J., Altrogge, H., Bischoff, P., Elfers, J., Wever, C., & Pude, R. (2023). Evaluation of the Intra- and Interspecific Development of Different Accessions of *Silphium perfoliatum* L. and *Silphium integrifolium* Michx. *Agronomy*, *13*(6). https://doi.org/10.3390/agronomy13061601

Grunwald, D., Panten, K., Schwarz, A., Bischoff, W. A., & Schittenhelm, S. (2020). Comparison of maize, permanent cup plant and a perennial grass mixture with regard to soil and water protection. *GCB Bioenergy*, *12*(9), 694-705. https://doi.org/10.1111/gcbb.12719

Gupta, M. K. (2014). Sunflower oil and its applications. *Lipid Technology*, *26*(11-12), 260-263. https://doi.org/10.1002/lite.201400068

Hack, H., Bleiholder, H., Buhr, L., Meier, U., Schnock-Fricke, E., Weber, E., & Witzenberger, A. (1992). Einheitliche Codierung der phänologischen Entwicklungsstadien mono- und dikotyler Pflanzen.–Erweiterte BBCH-Skala, Allgemein–. *Nachrichtenbl. Deut. Pflanzenschutzd.*, *44*(12), 265-270.

Höller, M. (2022). *Phenotypic analysis of different Silphium perfoliatum L. accessions and evaluation as a renewable resource for material use* [Dissertation, Rheinische Friedrich-Wilhelms-Universtität Bonn].

Höller, M., Lunze, A., Wever, C., Deutschle, A. L., Stücker, A., Frase, N., Pestsova, E., Spiess, A. C., Westhoff, P., & Pude, R. (2021). Meadow hay, *Sida hermaphrodita* (L.) Rusby and *Silphium perfoliatum* L. as potential non-wood raw materials for the pulp and paper industry. *Industrial Crops and Products*, *167*. https://doi.org/10.1016/j.indcrop.2021.113548

Huang, H. C. (1991). Induction of myceliogenic germination of sclerotia of *Sclerotinia sclerotiorum* by exposure to sub-freezing temperatures. *Plant Pathology*, *40*, 621-625. https://doi.org/10.1111/j.1365-3059.1991.tb02427.x

Huovila, P., Ala-Juusela, M., Melchert, L., Pouffary, S., Cheng, C.-C., Ürge-Vorsatz, D., Koeppel, S., Svenningsten, N., & Graham, P. (2009). *Buildings and Climate Change: Summary for Decision-Makers*. United Nations Environment Programme.

ISO 12625-4, 2016. Tissue paper and tissue products - Part 4: Determination of tensile strength strech at maximum force and tensile energy absorption. International Organization for Standardization, Geneva, Switzerland

ISO 187, 1990. Paper, board and pulps - Standard atmosphere for conditioning and testing and procedure for monitoring the atmosphere and conditioning of samples. International Organization for Standardization, Geneva, Switzerland

ISO 5269-1, 2005. Pulps; Preparation of labortatory sheets for physical testing - Part 1: Conventional sheetformer method. International Organization for Standardization, Geneva, Switzerland

Ivanov, P., Petakov, V., Nikolova, E., & Pentchev, E. (1988). Sunflower breeding for high palmitic acid content in the oil. 12th Int. Sunflower Conf., Novi Sad, Yugoslavia.

Jablonowski, N. D., Pauly, M., & Dama, M. (2021). Microwave Assisted Pretreatment of Szarvasi (Agropyron elongatum) Biomass to Enhance Enzymatic Saccharification and Direct Glucose Production. *Front Plant Sci*, *12*, 767254. https://doi.org/10.3389/fpls.2021.767254

James Hardie Europe GmbH (2024). *fermacell$^{TM}$ Gebundene Schüttung T*. Retrieved 09.03.2024 from https://jameshardieeurope.my.salesforce.com/sfc/p/#200000000AOI/a/0J000000cQCx/Tv9_RSrXx0XB3LvTmXs_T1gH4O_3A3ThimkaxqQAAt0

Jami, T., Karade, S. R., & Singh, L. P. (2019). A review of the properties of hemp concrete for green building applications. *Journal of Cleaner Production*, *239*. https://doi.org/10.1016/j.jclepro.2019.117852

Kabbage, M., Williams, B., & Dickman, M. B. (2013). Cell death control: the interplay of apoptosis and autophagy in the pathogenicity of *Sclerotinia sclerotiorum*. *PLoS Pathog*, *9*(4), e1003287. https://doi.org/10.1371/journal.ppat.1003287

Kamoga, O. L. M., Byaruhanga, J. K., & Kirabira, J. B. (2013). A Review on Pulp Manufacture from Non Wood Plant Materials. *International Journal of Chemical Engineering and Applications*, 144-148. https://doi.org/10.7763/ijcea.2013.V4.281

Kamvar, Z. N., Amaradasa, B. S., Jhala, R., McCoy, S., Steadman, J. R., & Everhart, S. E. (2017). Population structure and phenotypic variation of *Sclerotinia sclerotiorum* from dry bean (Phaseolus vulgaris) in the United States. *PeerJ*, *5*, e4152. https://doi.org/10.7717/peerj.4152

Kim, K. S., Min, J.-Y., & Dickman, M. B. (2008). Oxalic Acid Is an Elicitor of Plant Programmed Cell Death during *Sclerotinia sclerotiorum* Disease Development. *MPMI*, *21*(5), 605-612. https://doi.org/10.1094/MPMI-21-5-0605

Klímek, P., Meinlschmidt, P., Wimmer, R., Plinke, B., & Schirp, A. (2016). Using sunflower (*Helianthus annuus* L.), topinambour (*Helianthus tuberosus* L.) and cup-plant (*Silphium perfoliatum* L.) stalks as alternative raw materials for particleboards. *Industrial Crops and Products*, *92*, 157-164. https://doi.org/10.1016/j.indcrop.2016.08.004

Klímek, P., Wimmer, R., & Meinlschmidt, P. (2021). TOF-SIMS Molecular Imaging and Properties of pMDI-Bonded Particleboards Made from Cup-Plant and Wood. *Applied Sciences*, *11*(4). https://doi.org/10.3390/app11041604

Kochova, K., Schollbach, K., & Brouwers, H. J. H. (2016). Use of alternative organic fibres in cement composites. 4th International Conference on Sustainable Solid Waste Management, 23-25 June 2016, Lymasol, Cyprus.

Kochova, K., Schollbach, K., Gauvin, F., & Brouwers, H. J. H. (2017). Effect of saccharides on the hydration of ordinary Portland cement. *Construction and Building Materials*, *150*, 268-275. https://doi.org/10.1016/j.conbuildmat.2017.05.149

Kowalska, G., Baj, T., Kowalski, R., & Hanif, M. A. (2022). Characteristics of Selected *Silphium* Species as Alternative Plants for Cultivation and Industry with Particular Emphasis on Research Conducted in Poland: A Review. *Sustainability*, *14*(9). https://doi.org/10.3390/su14095092

Kowalska, G., Pankiewicz, U., & Kowalski, R. (2020). Evaluation of Chemical Composition of Some *Silphium* L. Species as Alternative Raw Materials. *Agriculture*, *10*(4). https://doi.org/10.3390/agriculture10040132

Kowalski, R. (2004). Growth and development of *Silphium integrifolium* in the first 3 years of cultivation. *New Zealand Journal of Crop and Horticultural Science*, *32*(4), 389-395. https://doi.org/10.1080/01140671.2004.9514320

Kowalski, R. (2009). *Silphium* L. extracts – composition and protective effect on fatty acids content in sunflower oil subjected to heating and storage. *Food Chemistry*, *112*(4), 820-830. https://doi.org/10.1016/j.foodchem.2008.06.038

Kowalski, R., & Kędzia, B. (2008). Antibacterial Activity of *Silphium perfoliatum*. Extracts. *Pharmaceutical Biology*, *45*(6), 494-500. https://doi.org/10.1080/13880200701389409

Kowalski, R., & Wiercinski, J. (2004). Evaluation of chemical composition of some *Silphium perfoliatum* L. species seeds as alternative foodstuff raw materials. *Polish Journal of Food and Nutrition Sciences*, *54*(4), 349-354.

Kowalski, R., & Wolski, T. (2001). Characteristics of Growth and Development of *Silphium perfoliatum* L. in the First Years of Cultivation. *Ann. Univ. M.C.S.*, *9*, 311-317.

Kowalski, R., & Wolski, T. (2005). The chemical composition of essential oils of *Silphium perfoliatum* L. *Flavour and Fragrance Journal*, *20*(3), 306-310. https://doi.org/10.1002/ffj.1418

Kumar, P., Barrett, D. M., Delwiche, M. J., & Stroeve, P. (2009). Methods for Pretreatment of Lignocellulosic Biomass for Efficient Hydrolysis and Biofuel Production. *Ind. Eng. Chem. Res.*, *48*, 3713-3729. https://doi.org/10.1021/ie801542g

Lamberg, J.-A., Ojala, J., Peltoniemi, M., & Särkkä, T. (2012). *The Evolution of Global Paper Industry 1800-2050: A Comparative Analysis*. Springer.

Latif, E., Ciupala, M. A., Tucker, S., Wijeyesekera, D. C., & Newport, D. J. (2015). Hygrothermal performance of wood-hemp insulation in timber frame wall panels with and without a vapour barrier. *Building and Environment*, *92*, 122-134. https://doi.org/10.1016/j.buildenv.2015.04.025

Le Ngoc Huyen, T., Queneudec T'kint, M., Remond, C., Chabbert, B., & Dheilly, R. M. (2011). Saccharification of *Miscanthus* x *giganteus*, incorporation of lignocellulosic by-product in cementitious matrix. *C R Biol*, *334*(11), 837 e831-837 e811. https://doi.org/10.1016/j.crvi.2011.07.008

Lehner, M. S., & Mizubuti, E. S. G. (2017). Are *Sclerotinia sclerotiorum* populations from the tropics more variable than those from subtropical and temperate zones? *Tropical Plant Pathology*, *42*(2), 61-69. https://doi.org/10.1007/s40858-016-0125-1

Lenth, V. R. (2021). Emmeans: Estimated Marginal Means, Aka Least-Squares Means. R Package Version 1.7.0. https://CRAN.R-project.org/package=emmeans

Li, J., & Li, G. Z. (2014). Study on the Waterproofing Properties of Cement-Based Composite Thermal Insulation Materials. *Applied Mechanics and Materials*, *711*, 166-169. https://doi.org/10.4028/www.scientific.net/AMM.711.166

Li, J., Cornelissen, B., & Rep, M. (2020). Host-specificity factors in plant pathogenic fungi. *Fungal Genet Biol*, *144*, 103447. https://doi.org/10.1016/j.fgb.2020.103447

Li, Y., Feng, Y., Lu, Q., Yan, D., Liu, Z., & Zhang, X. (2019). Comparative Proteomic Analysis of Plant-Pathogen Interactions in Resistant and Susceptible Poplar Ecotypes Infected with Botryosphaeria dothidea. *Phytopathology*, *109*(12), 2009-2021. https://doi.org/10.1094/PHYTO-12-18-0452-R

Liang, X., & Rollins, J. A. (2018). Mechanisms of Broad Host Range Necrotrophic Pathogenesis in *Sclerotinia sclerotiorum*. *Phytopathology*, *108*(10), 1128-1140. https://doi.org/10.1094/PHYTO-06-18-0197-RVW

Liu, K., Abdullah, A. A., Huang, M., Nishioka, T., Altaf-Ul-Amin, M., & Kanaya, S. (2017). Novel Approach to Classify Plants Based on Metabolite-Content Similarity. *Biomed Res Int*, *2017*, 5296729. https://doi.org/10.1155/2017/5296729

Ljungberg, L. Y. (2007). Materials selection and design for development of sustainable products. *Materials & Design*, *28*(2), 466-479. https://doi.org/10.1016/j.matdes.2005.09.006

Lorenz, M., Brunotte, J., Vorderbrügge, T., Brandhuber, R., Koch, H.-J., Senger, M., Fröba, N., & Löpmeier, F.-J. (2016). Anpassung der Lasteinträge landwirtschaftlicher Maschinen an die Verdichtungsempfindlichkeit des Bodens – Grundlagen für ein bodenschonendes Befahren von Ackerland. *Appl Agric Forestry Res*, *2*(66), 101-144. https://doi.org/10.3220/LBF1473334823000

Lumsden, R. D. (1979). Histology and Physiology of Pathogenesis in Plant Diseases Caused by *Scleotinia* Species. *Phytopathology*, *69*, 890-896. https://doi.org/10.1094/Phyto-69-8909-890

Lunze, A., Heyman, B., Chammakhi, Y., Eichhorn, M., Büchs, J., Anders, N., & Spiess, A. C. (2020). Investigation of *Silphium perfoliatum* as Feedstock for a Liquid Hot Water–Based Biorefinery Process Towards 2,3-Butanediol. *BioEnergy Research*, *14*(3), 799-814. https://doi.org/10.1007/s12155-020-10194-9

Majtkowski, W., Piłat, J., & Szulc, P. M. (2009). Perspektywy uprawy i wykorzystania w Polsce rożnika przerośniętego (*Silphium perfoliatum* L.). Prospects of cultivation and utilization of Silphium perfoliatum L. in Poland. *IHAR*, *251*, 283-291.

Mast, B., Lemmer, A., Oechsner, H., Reinhardt-Hanisch, A., Claupein, W., & Graeff-Hönninger, S. (2014). Methane yield potential of novel perennial biogas crops influenced by harvest date. *Industrial Crops and Products*, *58*, 194-203. https://doi.org/10.1016/j.indcrop.2014.04.017

Mayr, J., Gansberger, M., Leonhardt, C., Moosbeckhofer, R., & Liebhard, P. (2013). Durchwachsene Silphie (*Silphium perfoliatum* L.) a new biomass plant in Austria. 68. ALVA-Tagung, Klosterneuburg, Austria.

McLaughlin, S. B., & Walsh, M. E. (1998). Evaluating enviromental consequences of producing herbaceous crops for bioenergy. *Biomass and Bioenergy*, *14*, 317-324.

Medvedev, P. F. (1940). New Fibrous Crop in the USSR: Sel’khozgiz.

Meier, U. (2018). *BBCH Monografie: Entwicklungsstadien mono- und dikotyler Pflanzen*. https://doi.org/10.5073/20180906-075119

Mejouyo, P. W. H., Nkemaja, E. D., Beching, O. R., Tagne, N. R. S., Kana'a, T., & Njeugna, E. (2020). Physical and Tensile Properties of Handmade *Sida rhombifolia* Paper. *Int J Biomater*, *2020*, 3967641. https://doi.org/10.1155/2020/3967641

Metzler & Brodmann Saaten GmbH (2022). *Das Silphiefaserprojekt*. Donau Silphie. Retrieved 06.11.2022 from https://www.donau-silphie.de/faserprojekt/faserprojekt-1

Mikunda, T., Santos, S., Helseth, J., & Leger, H. S. (2013). *$CO_2$ Capture and Storage (CCS) in energy-intensive industries: An indispensable route to an EU low-carbon economy. Zero emissions platform (ZEP)*. https://zeroemissionsplatform.eu/wp-content/uploads/ZEP-report_-CCS-in-industry-1.pdf

Moll, L., Höller, M., Hubert, C., Korte, C. A. C., Völkering, G., Wever, C., & Pude, R. (2022). Cup Plant (*Silphium perfoliatum* L.) Biomass as Substitute for Expanded Polystyrene in Bonded Leveling Compounds. *Agronomy*, *12*(1). https://doi.org/10.3390/agronomy12010178

Moll, L., Wever, C., Völkering, G., & Pude, R. (2020). Increase of *Miscanthus* Cultivation with New Roles in Materials Production—A Review. *Agronomy*, *10*(2). https://doi.org/10.3390/agronomy10020308

Müller, A. L., & Dauber, J. (2016). Hoverflies (Diptera: *Syrphidae*) benefit from a cultivation of the bioenergy crop *Silphium perfoliatum* L. (*Asteraceae*) depending on larval feeding type, landscape composition and crop management. *Agricultural and Forest Entomology*, *18*(4), 419-431. https://doi.org/10.1111/afe.12175

Nasreen, S., Khan, M. A., Zia, M., Ishaque, M., Uddin, S., Arshad, M., & Rizvi, Z. F. (2015). Response of sunflower to various pre-germination techniques for breaking seed dormancy. *Pakistan Journal of Botany*, *47*(2), 413-416.

Neis-Beeckmann, P. (2021). *Paper production from plant fibres. In one cycle: ecopaper, energy and fertiliser made from Silphium perfoliatum*. Bioeconomy Baden-Württemberg. Retrieved 09.03.2024 from https://www.biooekonomie-bw.de/en/articles/news/one-cycle-ecopaper-energy-and-fertiliser-made-silphium-perfoliatum

Neroth, G., & Vollenschaar, D. (2011). *Wendehorst Baustoffkunde*. Vieweg+Teubner Verlag.

Neufert, P., & Neff, L. (1997). Ökologisches Bauen. In *Gekonnt planen - richtig bauen* (pp. 25-27). Vieweg+Teubner Verlag. https://doi.org/10.1007/978-3-322-96920-0_8

Osorio, J., Fernández-Martínez, J., Mancha, M., & Garcés, R. (1995). Mutant Sunflowers with High Concentration of Saturated Fatty Acids in the Oil. *Crop Sci.*, *35*, 739-742.

Pascual, A., Campa, A., & Pérez-Vega, E. (2010). Screening Common Bean for Resistance to Four *Sclerotinia sclerotiorum* Isolates Collected in Northern Spain. *Plant Disease*, *94*(7), 885-890. https://doi.org/10.1094/PDIS-94-7-0885

Pau, G., Fuchs, F., Sklyar, O., Boutros, M., & Huber, W. (2010). EBImage—an R package for image processing with applications to cellular phenotypes. *Bioinformatics*, *26*(7), 979-981. https://doi.org/10.1093/bioinformatics/btq046

Pauly, M., & Keegstra, K. (2008). Cell-wall carbohydrates and their modification as a resource for biofuels. *Plant J*, *54*(4), 559-568. https://doi.org/10.1111/j.1365-313X.2008.03463.x

Peni, D., Dębowski, M., & Stolarski, M. J. (2022). Influence of the Fertilization Method on the *Silphium perfoliatum* Biomass Composition and Methane Fermentation Efficiency. *Energies*, *15*(3). https://doi.org/10.3390/en15030927

Peni, D., Stolarski, M. J., Bordiean, A., Krzyżaniak, M., & Dębowski, M. (2020). *Silphium perfoliatum*—A Herbaceous Crop with Increased Interest in Recent Years for Multi-Purpose Use. *Agriculture*, *10*(12). https://doi.org/10.3390/agriculture10120640

Peschard, A., Govin, A., Pourchez, J., Fredon, E., Bertrand, L., Maximilien, S., & Guilhot, B. (2006). Effect of polysaccharides on the hydration of cement suspension. *Journal of the European Ceramic Society*, *26*(8), 1439-1445. https://doi.org/10.1016/j.jeurceramsoc.2005.02.005

Pichard, G. (2012). Management, production, and nutritional characteristics of cup-plant (*Silphium perfoliatum*) in temperate climates of southern Chile. *Cien. Inv. Agr.*, *39*(1), 61-77.

Pickersgill, B. (2007). Domestication of plants in the Americas: insights from Mendelian and molecular genetics. *Ann Bot*, *100*(5), 925-940. https://doi.org/10.1093/aob/mcm193

Pimentel, D., Wilson, C., McCullum, C., Huang, R., Dwen, P., Flack, J., Tran, Q., Saltman, T., & Cliff, B. (1997). Economic and Environmental Benefits of Biodiversity. *BioScience*, *47*(11), 747-757. https://doi.org/10.2307/1313097

Prasifka, J. R., Peterson, K., Mallinger, R. E., & Van Tassel, D. L. (2022). Changes to architecture of *Silphium integrifolium* Michx. during domestication reveal new trade-offs for yield. *Crop Science*, *62*(3), 1060-1068. https://doi.org/10.1002/csc2.20737

Pude, R. (1997). *Die Winterfestigkeit von Miscanthus in der Etablierungsphase* [Dissertation, Rheinische Friedrich-Wilhelms-Universtität Bonn]. Verl. M. Wehle.

Pude, R., Banaszuk, P., Trettin, R., & Noga, G. (2005). Suitability of Phragmites for leightweight concrete. *Journal of Applied Botany and Food Quality*, *79*(2), 141-146.

Pude, R., Treseler, C.-H., & Noga, G. (2004). Morphological, chemical and technical parameters of *Miscanthus* genotypes. *Journal of Applied Botany and Food Quality*, *78*(1), 58-63.

Purdy, L. H. (1979). *Sclerotinia sclerotiorum*: History, Diseases and Symptomatology, Host Range, Geographic Distribution, and Impact. *Phytopathology*, *68*, 875-880. https://doi.org/10.1094/Phyto-69-875

R Core Team (2020). *R: A language and environment for statistical computing. R Foundation for Statistical Computing. R version 3.6.3.* https://www.R-project.org/

Raduski, A. R., Herman, A., Pogoda, C., Dorn, K. M., Van Tassel, D. L., Kane, N., & Brandvain, Y. (2021). Patterns of genetic variation in a prairie wildflower, *Silphium integrifolium*, suggest a non-prairie origin and locally adaptive variation. *Am J Bot*, *108*(1), 145-158. https://doi.org/10.1002/ajb2.1603

Ramamurthy, K., Kunhanandan Nambiar, E. K., & Indu Siva Ranjani, G. (2009). A classification of studies on properties of foam concrete. *Cement and Concrete Composites*, *31*(6), 388-396. https://doi.org/10.1016/j.cemconcomp.2009.04.006

Reinert, S., Hulke, B. S., & Prasifka, J. R. (2020a). Pest potential of *Neotephritis finalis* (Loew) on *Silphium integrifolium* Michx., Silphium perfoliatum L., and interspecific hybrids. *Agronomy Journal*, *112*(2), 1462-1465. https://doi.org/10.1002/agj2.20078

Reinert, S., Money, K. L., Rockstad, G. B. G., Kane, N. C., Van Tassel, D. L., & Hulke, B. S. (2018). Two contrasting laboratory methods improve *Silphium integrifolium* Michx. germination rate to agronomically acceptable levels. *Euphytica*, *214*(9). https://doi.org/10.1007/s10681-018-2236-x

Reinert, S., Price, J. H., Smart, B. C., Pogoda, C. S., Kane, N. C., Van Tassel, D. L., & Hulke, B. S. (2020b). Mating compatibility and fertility studies in an herbaceous perennial Aster undergoing de novo domestication to enhance agroecosystems. *Agronomy for Sustainable Development*, *40*(4). https://doi.org/10.1007/s13593-020-00632-5

Reinert, S., Van Tassel, D. L., Schlautman, B., Kane, N. C., & Hulke, B. S. (2019). Assessment of the biogeographical variation of seed size and seed oil traits in wild *Silphium integrifolium* Michx. genotypes. *Plant Genetic Resources: Characterization and Utilization*, *17*(5), 427-436. https://doi.org/10.1017/s1479262119000248

Rojas, C., Cea, M., Iriarte, A., Valdés, G., Navia, R., & Cárdenas-R, J. P. (2019). Thermal insulation materials based on agricultural residual wheat straw and corn husk biomass, for application in sustainable buildings. *Sustainable Materials and Technologies*, *20*. https://doi.org/10.1016/j.susmat.2019.e00102

Ruf, T., & Emmerling, C. (2018). Site-adapted production of bioenergy feedstocks on poorly drained cropland through the cultivation of perennial crops. A feasibility study on biomass yield and biochemical methane potential. *Biomass and Bioenergy*, *119*, 429-435. https://doi.org/10.1016/j.biombioe.2018.10.007

Ruf, T., & Emmerling, C. (2021). Different life-form strategies of perennial energy crops and related nutrient exports require a differentiating view specifically concerning a sustainable cultivation on marginal land. *GCB Bioenergy*, *13*(6), 893-904. https://doi.org/10.1111/gcbb.12830

Ruf, T., & Emmerling, C. (2022). Biomass partitioning and nutrient fluxes in Silphium perfoliatum and silage maize cropping systems. *Nutr Cycl Agroecosyst*, *124*(3), 389-405. https://doi.org/10.1007/s10705-022-10242-0

Ruf, T., Audu, V., Holzhauser, K., & Emmerling, C. (2019). Bioenergy from Periodically Waterlogged Cropland in Europe: A First Assessment of the Potential of Five Perennial Energy Crops to Provide Biomass and Their Interactions with Soil. *Agronomy*, *9*(7). https://doi.org/10.3390/agronomy9070374

Saeman, J. F., Moore, W. E., Mitchell, R. L., & Millet, M. A. (1954). Techniques for the determination of pulp constituents by quantitative paper chromatography. *Technical Association of the the Paper Pulp Industry Journal*, *37*(8), 336-343.

Samson, G., Phelipot-Mardelé, A., & Lanos, C. (2016). Thermal and mechanical properties of gypsum–cement foam concrete: effects of surfactant. *European Journal of Environmental and Civil Engineering*, 1-20. https://doi.org/10.1080/19648189.2016.1177601

Sanderson, M. A., & Adler, P. R. (2008). Perennial forages as second generation bioenergy crops. *Int J Mol Sci*, *9*(5), 768-788. https://doi.org/10.3390/ijms9050768

Schäfer, A. (2019). *Verfahrenstechnische Optimierung der Bestandesetablierung von Durchwachsener Silphie (Silphium perfoliatum L.) mittels Einzelkornsätechnik unter Berücksichtigung der Korngeometrie* [Dissertation, Rheinische Friedrich-Wilhelms-Universtität Bonn].

Schäfer, A., Damerow, L., & Schulze Lammers, P. (2016). Durchwachsene Silphie: Bestandesetablierung mittels Aussaat. *Journal für Kulturpflanzen*, *68*(12), 367-371. https://doi.org/10.1399/JfK.2016.12.04

Schäfer, A., Damerow, L., & Schulze Lammers, P. (2017). Bestimmung der Korngeometrie der Durchwachsenen Silphie als Voraussetzung für die Einzelkornsaat. *Landtechnik*, *72*(3), 122-129. https://doi.org/10.15150/lt.2017.3159

Schäfer, A., Leder, A., Maximilian, G., Damerow, L., & Schulze Lammers, P. (2018). Vermessung und Sortierung von Saatkörnern der Durchwachsenen Silphie zur Optimierung der Bestandesetablierung. *Landtechnik*, *73*(4), 97-105. https://doi.org/10.15150/lt.2018.3186

Schiffner, S., Jungers, J. M., Hulke, B. S., Van Tassel, D. L., Smith, K. P., & Sheaffer, C. C. (2020). Silflower seed and biomass responses to plant density and nitrogen fertilization. *Agrosystems, Geosciences & Environment*, *3*(1). https://doi.org/10.1002/agg2.20118

Schiffner, S., Jungers, J. M., van Tassel, D., Smith, K. P., & C., S. C. (2021). Seeding date affects seed and biomass yield of *Silphium integrifolium* Michx. (silflower). *Native Plants Journal*, *22*(1), 30-44. https://doi.org/10.3368/npj.22.1.30

Schoo, B., Wittich, K. P., Böttcher, U., Kage, H., & Schittenhelm, S. (2016). Drought Tolerance and Water-Use Efficiency of Biogas Crops: A Comparison of Cup Plant, Maize and Lucerne-Grass. *Journal of Agronomy and Crop Science*, *203*(2), 117-130. https://doi.org/10.1111/jac.12173

Schorpp, Q., Müller, A. L., Schrader, S., & Dauber, J. (2016). Agrarökologisches Potential der Durchwachsenen Silphie (*Silphium perfoliatum* L.) aus Sicht biologischer Vielfalt. *Journal für Kulturpflanzen*, *68*(12), 412-422. https://doi.org/10.1399/JfK.2016.12.12

Schulte, M., Lewandowski, I., Pude, R., & Wagner, M. (2021). Comparative life cycle assessment of bio-based insulation materials: Environmental and economic performances. *GCB Bioenergy*, *13*(6), 979-998. https://doi.org/10.1111/gcbb.12825

Siaudinis, G., Jasinskas, A., Slepetiene, A., & Kacauskiene, D. (2012). The evaluation of biomass and energy productivity of common mugwort (*Artemisia vulgaris* L.) and cup plant (*Silphium perfoliatum* L.) in Albeluvisol. *Zemdirbyste Agriculture*, *99*(4), 357-362.

Signorell, A., Aho, K., Alfons, A., Anderegg, N., & Aragon, T. (2021). DescTools: Tools for Descriptive Statistics. R Package Version 0.99.40. https://CRAN.R-project.org/package=DescTools

Singh, B. K., Delgado-Baquerizo, M., Egidi, E., Guirado, E., Leach, J. E., Liu, H., & Trivedi, P. (2023). Climate change impacts on plant pathogens, food security and paths forward. *Nat Rev Microbiol*, *21*(10), 640-656. https://doi.org/10.1038/s41579-023-00900-7

Singh, M., Avtar, R., Pal, A., Punia, R., Singh, V. K., Bishnoi, M., Singh, A., Choudhary, R. R., & Mandhania, S. (2020). Genotype-Specific Antioxidant Responses and Assessment of Resistance Against *Sclerotinia sclerotiorum* Causing Sclerotinia Rot in Indian Mustard. *Pathogens*, *9*(11). https://doi.org/10.3390/pathogens9110892

Siwek, Włodarczyk, Możdżer, Bury, & Kitczak. (2019). Chemical Composition and Biogas Formation potential of *Sida hermaphrodita* and *Silphium perfoliatum*. *Applied Sciences*, *9*(19). https://doi.org/10.3390/app9194016

Soldatov, K. I. (1976). Chemical mutagenesis in sunflower breeding. 7th Int Sunflower Conf, Krasnodar, USSR.

Stanford, G. (1990). *Silphium perfoliatum* (cup-plant) as a new forage. 12th North American Prairie Conference.

Stanford, G. (1992). *Silphium perfoliatum (Cup-Plant)*. Retrieved 11.06.2023 from https://images.library.wisc.edu/EcoNatRes/EFacs/NAPC/NAPC12/reference/econatres.napc12.gstanford.pdf

Stolzenburg, K., & Monkos, A. (2012). *Erste Versuchsergebnisse mit der Durchwachsenen Silphie (Silphium perfoliatum L.) in Baden-Württemberg. Landwirtschaftliches Technologiezentrum Augustenberg*. https://lw.landwirtschaft-bw.de/site/pbs-bw-mlr-root/get/documents_E545218469/MLR.LEL/PB5Documents/ltz_ka/Arbeitsfelder/Nachwachsende%20Rohstoffe/Kulturinformationen/Silphie_DL/Erste%20Versuchsergebnisse%20mit%20der%20Durchwachsenen%20Silphie%20in%20Baden-W%C3%BCrttemberg%20aktualisiert%202012-08.pdf?attachment=true

Strasburger, E., Kadereit, J. W., Körner, C., Kost, B., & Sonnewald, U. (2014). *Strasburger–Lehrbuch der Pflanzenwissenschaften*. Springer.

Taherzadeh, M. J., & Karimi, K. (2008). Pretreatment of lignocellulosic wastes to improve ethanol and biogas production: a review. *Int J Mol Sci*, *9*, 1621-1651. https://doi.org/10.3390/ijms9091621

Talbot, M., Milner, A. D., Nutkins, M. A. E., & Law, J. R. (1995). Effect of interference between plots on yield perfomance in crop variety trials. *Journal of Agricultural Scinece*, *124*, 335-342.

Tavossi, H. M., Tittmann, B. R., & Cohen-Tenoudji, F. (1999). Ultrasonice Characterization of Cement and Concrete.

Terrer, C., Phillips, R. P., Hungate, B. A., Rosende, J., Pett-Ridge, J., Craig, M. E., van Groenigen, K. J., Keenan, T. F., Sulman, B. N., Stocker, B. D., Reich, P. B., Pellegrini, A. F. A., Pendall, E., Zhang, H., Evans, R. D., Carrillo, Y., Fisher, J. B., Van Sundert, K., Vicca, S., & Jackson, R. B. (2021). A trade-off between plant and soil carbon storage under elevated $CO_2$. *Nature*, *591*(7851), 599-603. https://doi.org/10.1038/s41586-021-03306-8

Tîtei, V. (2017). The evaluation of biomass of the *Sida hermaphrodita* and *Silphium perfoliatum* for renewable energy in Moldova. *Scientific Paper. Series A. Agronomy*, *60*.

Tîtei, V., Cîrlig, N., & Gutu, A. (2020). Some biological peculiarities and economic value of the cultivation of cup plant, *Silphium perfoliatum* L. *Biologie*, *136*, 79-82.

Tribe, H. T. (1957). ON THE PARASITISM OF *SCLEROTINIA TRIFOLIORUM* BY CONIOTHYRIUM MINITANS. *Transactions of the British Microbiological Society*, *40*, 489-499. https://doi.org/10.1016/S0007-1536(57)80055-2

Turner, M., Ravetta, D., & Van Tassel, D. (2018). Effect of *Puccinia silphii* on Yield Components and Leaf Physiology in Silphium integrifolium: Lessons for the Domestication of a Perennial Oilseed Crop. *Sustainability*, *10*(3). https://doi.org/10.3390/su10030696

USDA (2024). *Silphium perfoliatum L. - cup plant*. United States Department of Agriculture. Natural Resources Conservation Service. Retrieved 09.03.2024 from https://plants.sc.egov.usda.gov/home/plantProfile?symbol=SIPE2

Van der Putten, J., Lesage, K., & De Schutter, G. (2016). Influence of the particle shape on the packing density and pumpability of UHPC. International Symposium on Ultra High Performance Concrete.

Van Tassel, D. L., Albrecht, K. A., Bever, J. D., Boe, A. A., Brandvain, Y., Crews, T. E., Gansberger, M., Gerstberger, P., González-Paleo, L., Hulke, B. S., Kane, N. C., Johnson, P. J., Pestsova, E. G., Picasso Risso, V. D., Prasifka, J. R., Ravetta, D. A., Schlautman, B., Sheaffer, C. C., Smith, K. P., Speranza, P. R., Turner, M. K., Vilela, A. E., von Gehren, P., & Wever, C. (2017). Accelerating *Silphium* Domestication: An Opportunity to Develop New Crop Ideotypes and Breeding Strategies Informed by Multiple Disciplines. *Crop Science*, *57*(3), 1274-1284. https://doi.org/10.2135/cropsci2016.10.0834

Van Tassel, D. L., DeHaan, L. R., & Cox, T. S. (2010). Missing domesticated plant forms: can artificial selection fill the gap? *Evol Appl*, *3*(5-6), 434-452. https://doi.org/10.1111/j.1752-4571.2010.00132.x

Vilela, A. E., González-Paleo, L., Ravetta, D. A., Murrell, E. G., & Van Tassel, D. L. (2020). Balancing Forage Production, Seed Yield, and Pest Management in the Perennial Sunflower *Silphium integrifolium* (*Asteraceae*). *Agronomy*, *10*(10). https://doi.org/10.3390/agronomy10101471

Vilela, A., González-Paleo, L., Turner, K., Peterson, K., Ravetta, D., Crews, T., & Van Tassel, D. (2018). Progress and Bottlenecks in the Early Domestication of the Perennial Oilseed *Silphium integrifolium*, a Sunflower Substitute. *Sustainability*, *10*(3). https://doi.org/10.3390/su10030638

Vo, L. T. T., & Navard, P. (2016). Treatments of plant biomass for cementitious building materials – A review. *Construction and Building Materials*, *121*, 161-176. https://doi.org/10.1016/j.conbuildmat.2016.05.125

von Cossel, M., Amarysti, C., Wilhelm, H., Priya, N., Winkler, B., & Hoerner, L. (2020). The replacement of maize (*Zea mays* L.) by cup plant (*Silphium perfoliatum* L.) as biogas substrate and its implications for the energy and material flows of a large biogas plant. *Biofuels, Bioproducts and Biorefining*, *14*(2), 152-179. https://doi.org/10.1002/bbb.2084

Wang, M., Li, W., Fang, C., Xu, F., Liu, Y., Wang, Z., Yang, R., Zhang, M., Liu, S., Lu, S., Lin, T., Tang, J., Wang, Y., Wang, H., Lin, H., Zhu, B., Chen, M., Kong, F., Liu, B., Zeng, D., Jackson, S. A., Chu, C., & Tian, Z. (2018). Parallel selection on a dormancy gene during domestication of crops from multiple families. *Nat Genet*, *50*(10), 1435-1441. https://doi.org/10.1038/s41588-018-0229-2

Wegulo, S. N., Yang, X. B., & Martinson, C. A. (1998). Soybean Cultivar Responses to *Sclerotinia sclerotiorum* in Field and Controlled Environment Studies. *Plant Disease*, *82*(11), 1264-1270. https://doi.org/10.1094/PDIS.1998.82.11.1264

Werling, B. P., Dickson, T. L., Isaacs, R., Gaines, H., Gratton, C., Gross, K. L., Liere, H., Malmstrom, C. M., Meehan, T. D., Ruan, L., Robertson, B. A., Robertson, G. P., Schmidt, T. M., Schrotenboer, A. C., Teal, T. K., Wilson, J. K., & Landis, D. A. (2014). Perennial grasslands enhance biodiversity and multiple ecosystem services in bioenergy landscapes. *Proc Natl Acad Sci U S A*, *111*(4), 1652-1657. https://doi.org/10.1073/pnas.1309492111

Wever, C., Höller, M., Becker, L., Biertümpfel, A., Köhler, J., van Inghelandt, D., Westhoff, P., Pude, R., & Pestsova, E. (2019). Towards high-biomass yielding bioenergy crop *Silphium perfoliatum* L.: phenotypic and genotypic evaluation of five cultivated populations. *Biomass and Bioenergy*, *124*, 102-113. https://doi.org/10.1016/j.biombioe.2019.03.016

Wever, C., Van Tassel, D. L., & Pude, R. (2020). Third-Generation Biomass Crops in the New Era of De Novo Domestication. *Agronomy*, *10*(9). https://doi.org/10.3390/agronomy10091322

Wickham, H., & Hester, J. (2020). Readr: Read Rectangular Text Data. R Package Version 1.4.0. https://CRAN.R-project.org/package=readr

Wickham, H., Averick, M., Bryan, J., Chang, W., McGowan, L., François, R., Grolemund, G., Hayes, A., Henry, L., Hester, J., Kuhn, M., Pedersen, T., Miller, E., Bache, S., Müller, K., Ooms, J., Robinson, D., Seidel, D., Spinu, V., Takahashi, K., Vaughan, D., Wilke, C., Woo, K., & Yutani, H. (2019). Welcome to the Tidyverse. *Journal of Open Source Software*, *4*(43). https://doi.org/10.21105/joss.01686

Wu, L., Han, Z., Wang, S., Wang, X., Sun, A., Zu, X., & Chen, Y. (2013). Comparative proteomic analysis of the plant-virus interaction in resistant and susceptible ecotypes of maize infected with sugarcane mosaic virus. *J Proteomics*, *89*, 124-140. https://doi.org/10.1016/j.jprot.2013.06.005

Ye, H., Zhang, Y., Yu, Z., & Mu, J. (2018). Effects of cellulose, hemicellulose, and lignin on the morphology and mechanical properties of metakaolin-based geopolymer. *Construction and Building Materials*, *173*, 10-16. https://doi.org/10.1016/j.conbuildmat.2018.04.028

Young, C. S., Clarkson, J. P., Smith, J. A., Watling, M., Phelps, K., & Whipps, J. M. (2004). Environmental conditions influencing *Sclerotinia sclerotiorum* infection and disease development in lettuce. *Plant Pathology*, *53*(4), 387-397. https://doi.org/10.1111/j.1365-3059.2004.01018.x

Yu, Q. L., Spiesz, P., & Brouwers, H. J. H. (2013). Development of cement-based lightweight composites – Part 1: Mix design methodology and hardened properties. *Cement and Concrete Composites*, *44*, 17-29. https://doi.org/10.1016/j.cemconcomp.2013.03.030

Zadoks, J. C., Chang, T. T., & F., K. C. (1974). A decimal code for growth stages of cereals. *Weed Research*, *14*, 415-421.

Zhai, H. M., & Lee, Z. Z. (1989). Ultrastructure and Topochemistry of Delignification in Alkaline Pulping of Wheat Straw. *Journal of Wood Chemistry and Technology*, *9*(3), 387-406. https://doi.org/10.1080/02773818908050306

# Appendix

Prove that for all $n \geq 1$, $\sum_{j=1}^{n} 2^{j-1} = 2^n - 1$ using mathematical induction (chapter 5.3; page 59):

Base Case: Considering $n = 1$

$$\begin{aligned} \sum_{j=1}^{1} 2^{j-1} &= 2^1 - 1 \\ 2^{1-1} &= 2^1 - 1 \\ 2^0 &= 2 - 1 \\ 1 &= 1 \end{aligned}$$

Inductive Hypothesis: Suppose that for some $n \geq 1$ we have

$$\sum_{j=1}^{n} 2^{j-1} = 2^n - 1$$

Induction Step: Considering $n = n + 1$

$$\begin{aligned} \sum_{j=1}^{n+1} 2^{j-1} &= 2^{n+1} - 1 \\ \sum_{j=1}^{n} 2^{j-1} + 2^{(n+1)-1} &= 2^{n+1} - 1 \\ 2^n - 1 + 2^n &= 2^{n+1} - 1 \qquad \text{(by the Inductive Hypothesis)} \\ 2 \times 2^n - 1 &= 2^{n+1} - 1 \\ 2^{n+1} - 1 &= 2^{n+1} - 1 \end{aligned}$$

If the equation holds for $n$, it also holds for $n + 1$. By induction, it must be true for any $n \geq 1$, since the statement is true for $n = 1$.

# Danksagung

An dieser Stelle möchte ich mich bei allen bedanken, die mich im Verlauf meiner Promotion unterstützt und gefördert haben.

Zunächst bedanke ich mich bei der Fachagentur Nachwachsende Rohstoffe e.V., die mir mit der Förderung des Projektes „GEniu*S*“ die Möglichkeit zur Promotion gaben.

Mein besonderer Dank gilt Prof. Dr. Ralf Pude für die Begutachtung meiner Arbeit, sowie für die wissenschaftliche Betreuung und der persönlichen Unterstützung der letzten Jahre.

Bei Prof. Dr. Annaliese Mason bedanke ich mich für die Übernahme des Korreferats meiner Dissertation sowie für die fachliche Betreuung im Rahmen der Graduiertenschule.

Ich danke Prof. Dr. Peter Westhoff für die Übernahme des fachnahen Mitglieds sowie für die konstruktive Kritik meiner Arbeit im Zuge zahlreicher Projekttreffen.

Vielen Dank an Dr. Christian Wever für die erfolgreiche Zusammenarbeit, das Vertrauen und die wissenschaftliche Begleitung bis zum Schluss.

Ich bedanke mich bei Dr. Martin Greve für den starken Zusammenhalt, der maßgeblich für den Erfolg meiner Promotion war.

Darüber hinaus danke ich allen Mitarbeitern des Campus Klein-Altendorf und des INRES – Nachwachsende Rohstoffe, ohne deren tatkräftigen Unterstützung es nicht zu dieser Arbeit gekommen wäre.

Des Weiteren gilt mein Dank den Doktorandinnen und Doktoranden des INRES – Nachwachsende Rohstoffe die durch ständigen Austausch und Feedback zu dieser Arbeit beitrugen.

Ebenso bedanke ich mich bei Frau PD Dr. Ulrike Steiner für das Bereitstellen der *Sclerotinia*-Inokulate sowie der fachlichen Unterstützung bei der Durchführung und der Auswertung der Versuche.

Außerdem bedanke ich mich bei Prof. Dr. Peter Dörmann und Dr. Georg Hölzl, die mir die Möglichkeit und die nötige Unterstützung gaben, Samen der Durchwachsenen Silphie auf Ölgehalt und Fettsäuremuster in ihren Laboren zu untersuchen.

Ein besonderer Dank gilt meinen Freunden, vor allem Philip Bischoff und Micha Strauch, die mir uneingeschränkt mit ihren jeweiligen Expertisen zur Seite standen.

Abschließend bedanke ich mich bei meinen Eltern Hedda und Wilhelm, sowie meinen Geschwistern Anne, Wilhelm und Johannes, die mir in den letzten Jahren bedingungslos den nötigen Rückhalt zum verfassen dieser Arbeit gaben.